DESIGN, CONSTRUCTION, AND VISUALIZATION OF TRANSPARENT FULL SCALE HIGH PRESSURE TEST FACILITY FOR ELECTRONIC SUBMERSIBLE PUMPS

A Thesis

by

JOSEPH MICHAEL MARCHETTI

Submitted to the Office of Graduate and Professional Studies of
Texas A&M University
in partial fulfillment of the requirements for the degree of

MASTER OF SCIENCE

Chair of Committee,	Gerald Morrison
Committee Members,	Robert Randall
	Devesh Ranjan
Head of Department,	Andreas Polycarpou

December 2013

Major Subject: Mechanical Engineering

Copyright 2013 Joseph Michael Marchetti

ABSTRACT

With the advent of aging oilfields and extraction in extreme conditions, artificial lift has become a necessity to make certain fields technically and economically feasible. One artificial lift method which has high throughput and can be adapted to a variety of production situations is electric submersible pumps. One issue with these pumps is their natural inability to handle two phase gas-liquid flow without considerable loss or failure in performance. A pump, the Baker Hughes Centrilift G470 multi-vane pump (MVP) was developed to handle two phase flow. To understand the flow patterns and phenomena that occur in the pump over a variety of conditions, a full scale, full speed, moderate pressure, and transparent pump was designed and constructed at the Texas A&M University Turbomachinery Laboratory. The closed loop test facility then provides a means for flow visualization of predicted recirculation, bubble coalescence, and stagnation. The pump was designed and constructed using the SLA manufacturing process with a polycarbonate casing for optimal clarity and safety. High speed photography with lighting sources allowed visualization through the eye of the impeller and in the channels of the diffuser. Recirculation between the blades of the impeller was observed. Within the diffuser, large recirculation zones on the suction side of the vane were observed blocking up to 75% of the diffuser channel outlet. Further analysis using advanced flow velocity measurements such as PIV or DGV will more fully characterize the pump. This will allow improvement of CFD simulations and even pump design.

DEDICATION

Ad Majorem Dei Gloriam

"For the greater glory of God"

ACKNOWLEDGEMENTS

I wish to express my profound gratitude, respect, and most importantly thanks to a man who has greatly impacted my life: Dr. Gerald Morrison. Besides being an advisor in research and the lab, he always amazed me with his ability to speak on a plethora of non-related subjects. I know that typically you lose certain aspects of respect for employers and advisors as you work for them longer, but with Dr. Morrison, my respect and the impact he had on me increased with time. He always put his family and students first; education and care for us was always front and center for him. Often times when talking, I would leave the conversation with the next step in research as well as a good book, movie, or article to read for personal growth and enjoyment. On critical steps in research, he was always working right beside us to ensure that we would get the job done with the best quality and efficiency; I have found few things that I respect more from an advisor or employer.

Dr. Randall and Dr. Ranjan, thank you for being members of the thesis committee. I have always known both of you as professors who give great time and consideration for the good of their students. Thanks also for the attention, curiosity, and support through the defense process.

I want to express a large thanks to all the members, past and present from the Turbomachinery Lab. I would like to write a paragraph for all of you, but time and space are limited. Certainly I would like to thank the „old crew‟: Scott Chien, Sahand Pirouzpanah, Nicolas Carvajal, Abhay Patil, Emanuel Marsis, Klayton Kirkland, Sujan

Reddy Gudigopuram, Ramy Saleh, Daniel Cihak and Shankar Narayanan. I would also like to thank all the new recruits: Daniel Steck, Daniel Zheng, Ted Hatch, Wenfei Zhang, Burak Erdogan, Yi Chen, Yong Zhang, Peng Liu, Muhammet Cevik, Mustafa Karabacak, Yusuf Turhan, Nick Mass, Chase Dube, Andrew Crisafulli, Chokote Kamdeu, and Srinivas Ragavan. Thank you for helping keep me motivated in times of struggle, and working hard to aid me in finishing my work. I also thank each of you for your friendship that we have developed through this process. I know that each friendship is different and each special. I have been blessed with the ability to know, learn and grow from each one of you in a positive way. I hope that my contribution to the friendship was as fruitful. I hope to keep up as time goes by and our memories from here fade. Those memories of struggling, working, and learning together are priceless and will dim but not be forgotten.

I would also like to thank all of the other Turbolab researchers and their friendship and support. Thanks to Ray Matthews for improving my skills, both in the shop in machining and construction, and also for the training in improving cleanliness and order in shop work.

Finally, I would like to thank my mother, father, brothers, and sister for their unfailing love and support through the sometimes strenuous and frustrating, but always rewarding graduated process. The support of family and friends is necessary to successfully completing a work such as this. From the vantage point that I now have, I see how much my parents and family taught and formed me. More and more I contemplate why I have the goals, morals, and traits that I do. I think of the good ones

and where and when I learned them. Most of them are from my parents and family; I do not understand necessarily how I acquired them and how they so effectively taught them, but I thank them and am in awe of them.

Most importantly, I would like to thank the Good Lord, One God in Three for everything.

NOMENCLATURE

ANSI	American National Standards Institute
ASME	American Society of Mechanical Engineers
B&PV	Boiler and Pressure Vessel
BEP	Best Efficiency Point
BPD	Barrels Per Day
CFD	Computational Fluid Dynamics
CNC	Computer Numerical Control
ESP	Electric Submersible Pump
FEA	Finite Element Analysis
FLA	Fully Loaded Amps
FN	Force or Shrink Fit
FOS	Factor of Safety
FPS	Frames Per Second
FS	Flow Structure
GVF	Gas Volume Fraction
ID	Inner Diameter
LC	Locational Clearance Fit
MAWP	Maximum Allowable Working Pressure (at a given temperature)

MTR	Mill Test Report
MVP	Multi-vane Pump
NDE	Non-destructive Examination
OD	Outer Diameter
OSHA	Occupational, Safety, and Health Administration
P&ID	Piping and Instrumentation Diagram
PC	Polycarbonate
PI	Proportional Integrator (Controller)
PMMA	Poly(Methyl Methacrylate)
PPE	Personal Protective Equipment
RPM	Rotations/ Revolutions per Minute
SCF/H	Standard Cubic Feet per Hour
SCFM	Standard Cubic Feet per Minute
SLA	Stereolithography
SOP	Standard Operating Procedure
TEFC	Totally Enclosed Fan Cooled
VFD	Variable Frequency Drive
VI	Virtual Instrument

TABLE OF CONTENTS

LIST OF FIGURES

LIST OF TABLES

1 INTRODUCTION

1.1 Motivation

In the continual quest for energy, fuels, and materials in the form of oil and natural gas, exploration and production is increasingly moving to far flung geographical locations where extreme conditions both at the surface and in the well are prevalent. Also of importance is the focus on enhanced oil production in aging fields where naturally flowing wells no longer produce oil unaided by mechanical or artificial production methods. As these challenges have developed, the technical community has kept the pace with advanced drilling, stimulation, and production technologies. In the area of enhanced oil production, a variety of artificial lift methods have been developed for two primary purposes: 1) to increase production capacity and throughput in key asset areas and 2) to improve recovery and utilize more of the reservoir in once naturally flowing wells, also known as enhanced oil recovery. Enhanced oil recovery describes the goal of obtaining 60 to 70 percent production of a reservoir as compared to the 20 to 30 percent recovery from naturally flowing wells. To work toward achieving that end, many production technologies have been implemented, but one of considerable importance is artificial lift.

1.2 Introduction to Artificial Lift

Artificial lift is employed when the flowing pressure in the production zone of a well is less than the pressure loss from the production zone to the wellhead at a given desired throughput, Economides [1]. Thus, it is used when either the production flowing pressure drops below the pressure losses in the pipe to the surface, or when the pressure losses in the pipe become larger than the production flowing pressure, Takacs [2]. Two typical types of lift are gas lift, and mechanical lift, which includes positive displacement and dynamic displacement pumps.

1.2.1 Gas Lift

The general method of gas lift follows from its name; gas, typically natural gas or methane, is injected at one or more locations along the production casing. This primarily reduces the density of the production fluid. The lowered average density of the well fluid drastically reduces the static pressure head in the tubing, which effectively reduces the pressure loss along the production piping. Thus, a lesser flowing well pressure is required to maintain a desirable pressure at the wellhead. One drawback of the method is large separation surface facilities required to handle the large GVF of the well fluids. There is also a limit where more gas injection will not lower the total pressure losses in the pipe because frictional pressure losses dominate instead of static pressure losses, Economides [1]. An example of a well fitted with gas lift is shown in Figure 1.

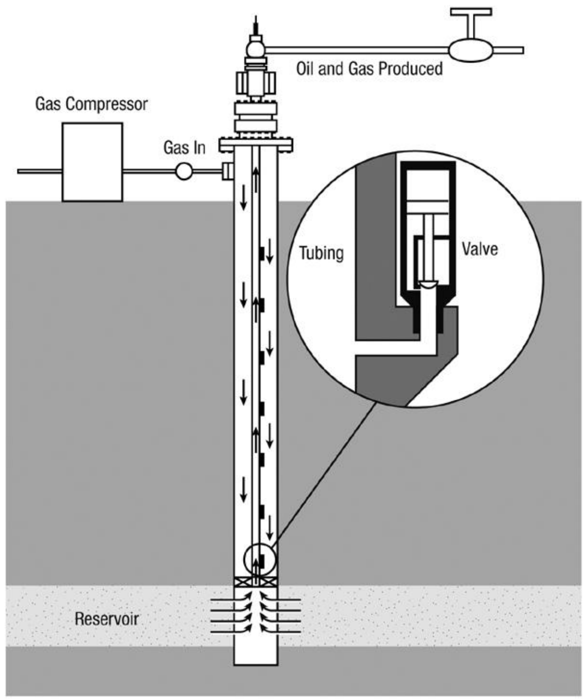

Figure 1 Example gas lift application, Economides [1]

1.2.2 Mechanical Lift

Mechanical lift approaches the problem by increasing the pressure in the well to combat pressure losses due to friction. Two common pump types are positive displacement pumps and dynamic displacement pumps (ESPs). Positive displacement pumps include sucker rod pumps, progressive cavity pumps, as well as twin screw pumps. A sucker rod pump uses a barrel with a one way valve on the top and a traveling valve that draws a slug of fluid up. As the traveling valves moves down after delivering its fluid, the top valve checks the slug of fluid preventing backflow. This pump has a relatively low throughput and requires a large walking beam actuator on the surface, shown in Figure 2. Progressive cavity pumps and twin screw pumps operate by moving a finite volume of fluid up the pipeline. Progressive cavity pumps move a fixed volume of fluid between a spiral shaped rotor and a polymer stator, Economides [1]. Twin screw pumps move the volume up in cavities formed by two intermeshing screw rotors. Dynamic displacement pumps accelerate the fluid with an impeller and convert the kinetic energy to head in the pump through the diffuser. The most common type of dynamic displacement pumps are submersible pumps. Electric submersible pumps are advantageous and used over other types of artificial lift for many reasons. One primary benefit of ESPs is the high throughput capacity of typical ESPs. They also may be used in highly deviated wells, since the pump does not require a rod to transfer energy from the surface emplacement. The ESP completion also has an extremely small surface footprint and can be used where space is costly, like in urban situations and offshore completions. Typical conventional ESPs can naturally handle about 5% GVF, but after that head degradation greatly limits production capacity and can even lead to gas lock rendering the ESP ineffective. Gas lock occurs when liquid is „locked" out of the impeller and no liquid is produced. Some issues with ESPs are the need for high voltage available electricity and a VFD to allow adjustments of the rotational speed of the motor to allow the ESP to be tuned to meet the changing production demands of a well. Also, repairs are difficult and complicated and the work over costs to pull and re-run an ESP are expensive. Finally, ESPs do not handle high viscosity fluids well and their temperature limits are conventionally about 250 ^{0}F and with special construction about 400 ^{0}F, Takacs [2]. A typical ESP completion is shown in Figure 2. Subsurface completions include an ESP motor hung below the pump, followed by a motor seal or protector and the inlet. After the inlet of the pump is the pump itself which contains the impellers and diffusers necessary to provide the desired pressure rise. The pumped fluid exits directly into the production tubing hangar and to the wellhead. An electrical cable is run from the source and VFD on the surface to power the motor. This all occurs in a cased section of the well.

A typical ESP impeller and diffuser set for one stage of the pump is shown in the center of Figure 3. The impeller is connected to a driving shaft and imparts kinetic energy through centrifugal acceleration through the blades. This kinetic energy is then transferred to head as it decelerates through the vanes of the diffuser.

1.3 Two Phase Pumping Issues

Further discussion of two phase pumping issues and phenomena in ESPs are warranted since it is the primary driver of this work. When free gas is introduced into the inlet stream to an ESP, the physics of the pump immediately change. Since ESPs are dynamic displacement pumps, the driving principle is the acceleration of the fluid in the impeller and its subsequent deceleration in the diffuser developing a pressure head. This acceleration is primarily centrifugal acceleration for centrifugal pumps and is effective because of the high density of water. When gas, which has a density that is orders of magnitude less than that of liquid, enters the impeller, the centrifugal acceleration is much less. Thus head degradation increases as GVF increases in the pump. At a certain point, the flow reaches an unstable point known as surging where the flow rate and pressures rise fluctuate continuously. This often leads to ESP shutdowns because of surging in electrical power to the motor from the VFD. As even more gas is introduced to the pump, gas lock occurs where the pump is filled only with gas and fluid pumping stops. A general plot of these phenomena is shown in Figure 4.

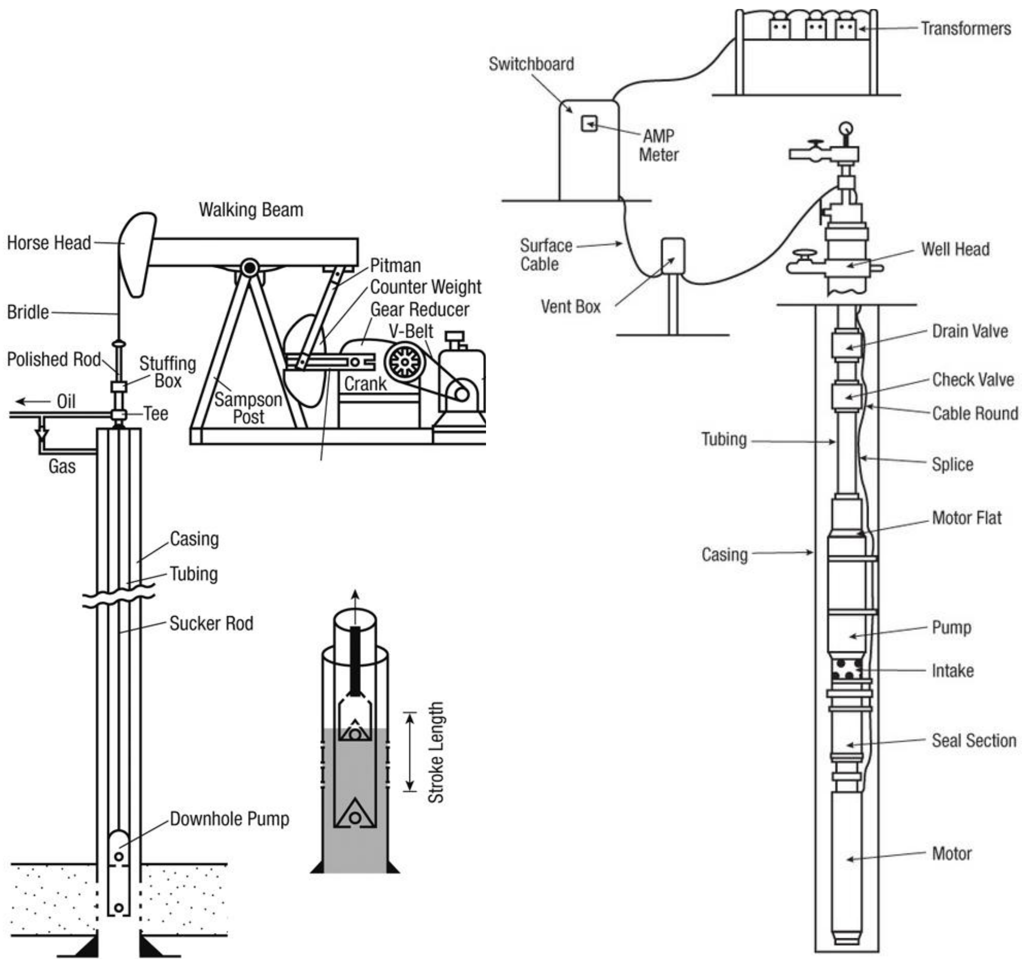

Figure 2 Example of sucker rod pump completion (left) and typical ESP completion (right), Economides [1]

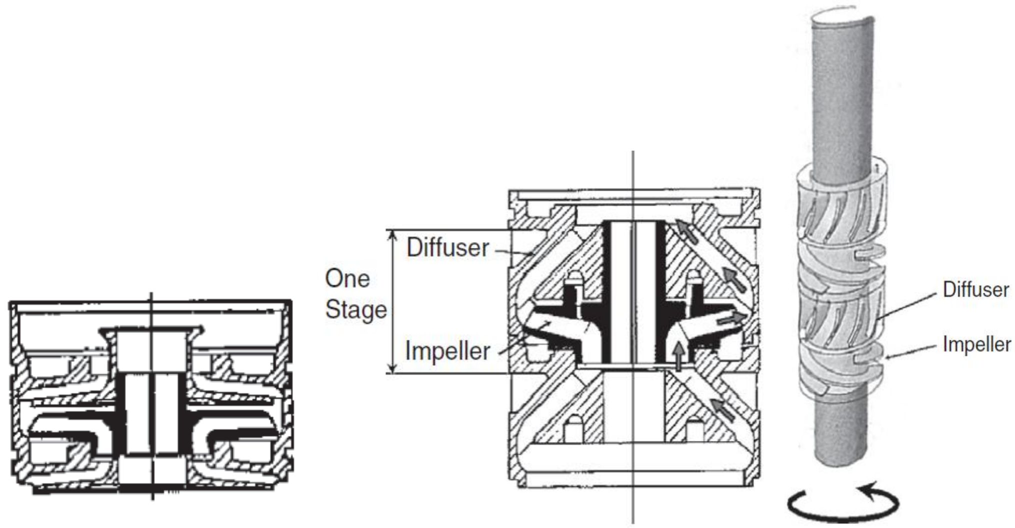

Figure 3 ESP pump comparison: radial pump (left), mixed flow pump (center), axial pump (right), Takacs [2]

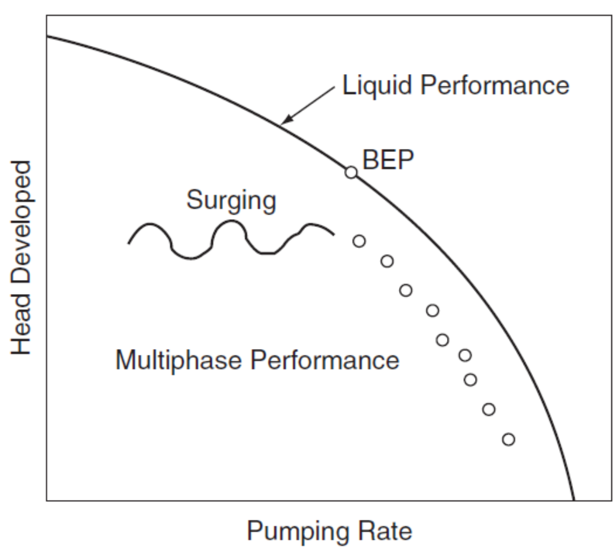

Figure 4 Two phase versus single phase pump performance, Takacs [2]

Studies into the phenomena of two phase pumping, surging, and gas lock direct the cause of these issues to the impeller. As the impeller turns, gravity and centrifugal forces serve to separate the phases, while turbulence chops the bubbles and promotes homogeneous mixing. When the gas phase is in the form of small homogenized bubbles, the head degradation is limited. Otherwise, the gas separates from the liquid and accumulates on the suction side of the blades. This leads to surging and eventually gas lock. The factors which affect mixing are: impeller geometry, bubble size, phase density difference, liquid viscosity, and pump speed. Phase density difference and liquid viscosity cannot be controlled by the operator, but must be considered in design. As the phase density difference decreases and the liquid viscosity increases, mixing becomes more favorable. Drag forces on the bubbles pulls them along with the liquid, but buoyancy forces attempt to separate the phases which would cause head degradation. Thus, small bubbly homogenized flow is optimum. The rotational speed of the pump causes larger centrifugal forces, but aids with large turbulent mixing. Higher rotational speeds decrease head degradation in the pump. Finally, the geometry of the impeller affects the performance of the pump. Since pumps whose only driving force is centrifugal acceleration are severely degraded by two phase flow, radial flow centrifugal pumps fare worst under two phase flow. Mixed flow pumps handle two phase flow better, and axial flow pumps fare the best since very little centrifugal acceleration occurs. Radial (right), mixed (middle), and axial flow (left) pumps are shown in Figure 3 for comparison, Takacs [2].

1.4 Goals and Objectives

With the challenge and prevalence of two phase pumping presented, much work is being done to understand and handle the associated issues. The goals of this work are to design, construct, and complete preliminary visualization on a test facility to allow flow visualization of the impeller and diffuser of a mixed flow pump designed to handle considerable amounts of GVF at the inlet. The objectives are that the pump be full sized, and the flow rates, rotational speeds, and inlet pressures are the same as those in industrial applications. The design conditions are shown in Table 1. From there, the final goals of the project are to characterize the pump with head-flow rate curves and observe the flow structures developed in the pump at various gas volume fractions. The objectives are to observe any recirculation zones, or gas stagnation bubbles in the flow.

Table 1 Test facility design parameters

Parameter	Unit	Minimum Design Value	Maximum Design Value
Rotational Speed	RPM	1800	3600
Inlet Pressure	psig	0	200
Flow rate	BPD	5100	36000
GVF	%	0	40

1.5 Organization of the Work

This document is arranged in the format of a typical technical paper or thesis. It begins with the introduction which explains the motivation and background information about the work. Then an extensive review of previous work pertinent to the research completed, which includes test facility construction and flow or pump visualization studies. There then is a comprehensive discussion of the design and construction of the transparent pump testing facility. For the benefit of all subsequent work on this test facility, the next section is the testing methodology and finally visualization and performance results. The work ends with a conclusion and appendices containing pertinent technical information.

2 LITERATURE REVIEW

This work concentrates on both the construction and validation of the clear MVP testing facility and the visualization of bubble coalescence, stagnation, and recirculation within the pump. Previous work on both test facilities constructed for pump visualization and observation are presented as well as studies, both physical and theoretical on bubble stagnation and coagulation within pumps.

2.1 Early Two Phase Flow Visualization

Early studies on two phase flow visualization were much more technically difficult due to less developed testing equipment, materials and manufacturing methods. An in depth study was completed by Minemura and Murakami [3] on bubble flow within radial centrifugal pumps. This study was focused on the flow of small volumes of air introduced into a system as well as vapor bubbles caused by cavitation. The investigators first developed equations of motion for bubble flow in a centrifugal pump in a coordinate system describing a bladed impeller. These were done with basic physics principles. Then visualization was completed on the inlet pipe and impeller to validate the results. The pump implemented was a radial open impeller pump with a low specific speed. The pump included a 5 bladed impeller with a maximum operating speed of 1750 rpm, a head of 27 psig, and a flow rate of 240 gpm, with an inlet pressure maintained to at most 8 psig. To allow visualization, the casing or volute and inlet piping was replaced with a clear transparent material. For the flow visualization, a 16mm camera with a frame rate of 3000 fps was used. Due to luminous power limitations, a maximum pump speed of 1300 rpm and GVF of 1.5% was used for visualization when air was introduced into the system. Figure 5 shows the view through the clear casing of the impeller in operation. In this figure, silk threads are attached to the surface of the impeller channel to visualize the streamlines of the pure liquid flow.

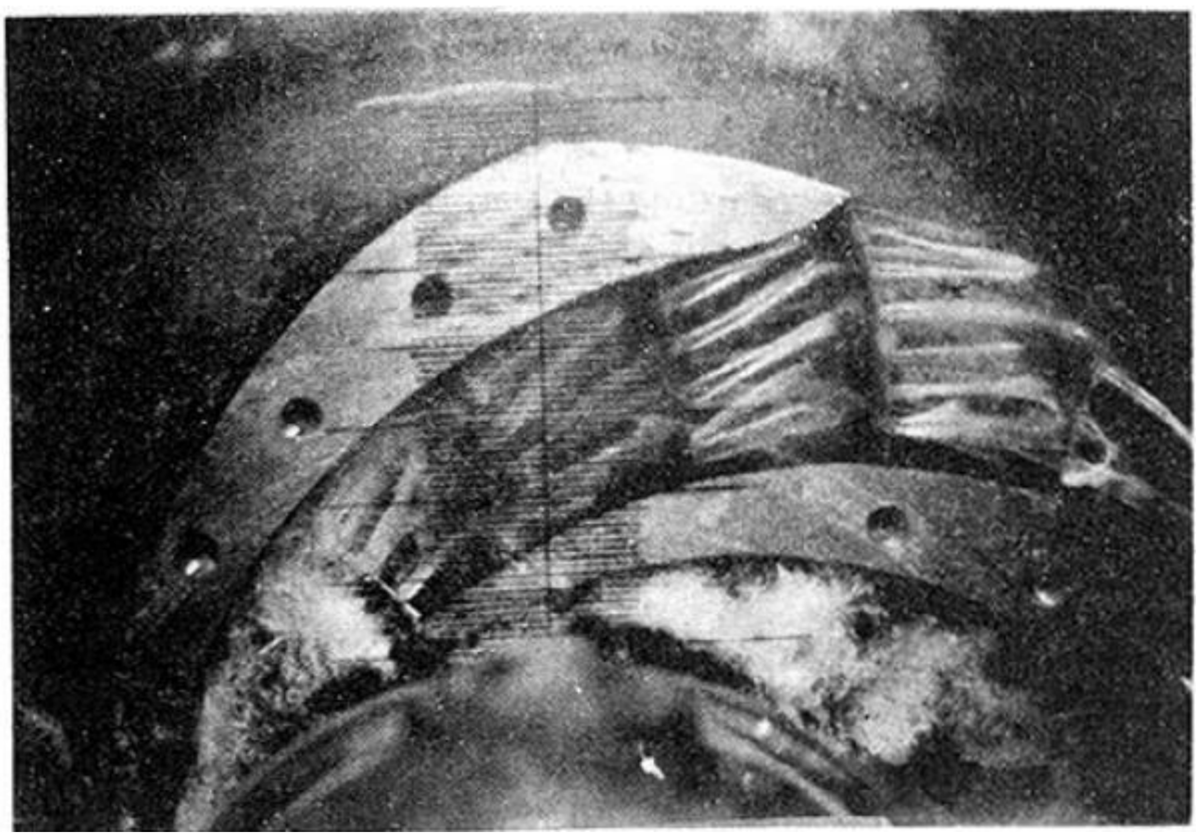

Figure 5 Centrifugal pump visualization at 1750 rpm and 0.017% GVF air with silk threads, Minemura [3]

The investigators calculated the behavior of bubble flow in the pump by numerically solving the equations of motion for the bubbles. They found that on the inlet to the pump, three phenomena occurred. The bubbles would travel on streamlines indiscernible from those of the water for small diameters ($d < 0.1$ mm). As the seed bubbles increased in size, so would the deviation from the liquid streamlines. They also found a correlation for the local Reynolds number of the bubble to the bubble shape. The local Reynolds number was defined by the diameter of the bubble and the relative velocity of the bubble with respect to the water. For low Reynolds numbers, the bubble was spherical; as it increased, the bubbles would become elliptical in shape. At even higher Reynolds numbers, the bubble would regain a spherical shape. Finally, it was found that most of the bubbles would travel toward the area where the inlet pipe met the volute of the pump. On a shrouded impeller, it would be toward the entrance of the shroud. At this point there is an increased chance of bubble stagnation and coalescence. Within the impeller itself, bubble tracking was only possible near the impeller blades. Both the analytical analysis and the results show the bubbles diverging from the liquid streamlines and moving toward the pressure side of the impeller blades as shown in Figure 6. According to the analytical analysis, the effect would be enhances with larger diameter bubbles.

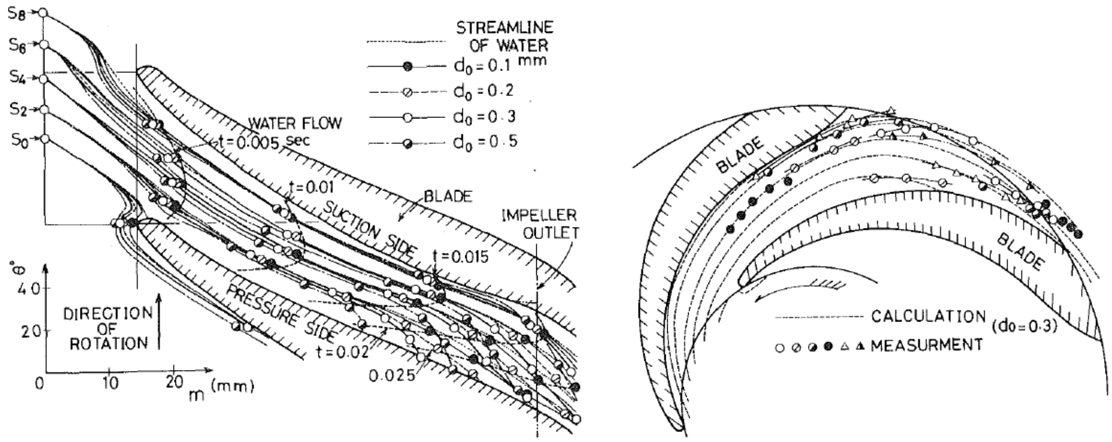

Figure 6 Analytical (left) and experimental (right, 1300 rpm) bubble trajectories for centrifugal pump, Minemura [3]

2.2 ESP Two Phase Visualization

An extensive study completed on both pump construction and visualization of an ESP pump directly related to the petroleum production industry was performed by Barrios [4]. She built a one stage pump using a GC1000 impeller and diffuser from Baker Hughes Centrilift, which was a single blade conventional mixed flow ESP, as shown in Figure 7.

Figure 7 One-stage prototype of GC1000 conventional ESP for visualization and performance testing, Barrios [4]

For this prototype, the flow is conditioned by the diffuser before being accelerated in the impeller. After acceleration through the impeller, the flow is drained by 8 plastic taps mounted radially on the casing directly surrounding the impeller in a modified diffuser section. To allow visualization, the hub or the upper shroud was machined away from the vanes on the impeller and replaced with a clear polymer plate acting as a viewport through the back of the impeller. This window rotated with the shaft and was cased circumferentially by a stainless steel ring and bearing. Although testing one full stage instead of only the impeller greatly enhanced the flow preconditioning, several geometric variations from a true ESP configuration would affect the flow fields and results of the visualization. These are:

1. The inlet flow to the diffuser stage is not axial along the pipe/shaft and enters from direction possibly causing poorly mixed flow,
2. The outlet flow through the modified diffuser and outlet ports do not force the flow to turn and travel axially and inward radially as a true mixed flow ESP,
3. And finally the removal of the hub to mate to the clear viewing window changed the hub to a flat plate which essentially changed the mixed flow impeller into a radial flow impeller.

Since a full scale stage was tested, the expected performance of the pump is the same as those given by the manufacturer. The maximum flow rate of liquid (water) through the pump was 10,500 BPD and the BEP was 6,100 BPD at a 3600 rpm shaft speed. The testing regimen for this work ranged from 100 BPD to 700 BPD and 0 to 2 scf/h. This came to a maximum of 4.28 % GVF and a minimum of 0.06 % GVF. These conditions were about 10% of the BEP of the pump. The validity of the results was established through a similarity analysis correlating three non-dimensional numbers; the specific speed, specific head, and specific capacity, which in centrifugal pumps are called the affinity laws. When one of the numbers was kept constant over several operating speeds (rpm), the other two would also remain constant over the operating speeds. After testing the pump at speeds ranging from 300 rpm to 1500 rpm, it was determined that similarity was attained for all speeds 600 rpm and above. This analysis only established macroscopic similarity in the pump. Thus microscopic fluctuations and structures are not guaranteed to be similar even though macroscopic parameters such as bulk head and flow rate for the pump remain similar and may be scaled through the use of the non-dimensional numbers (also known as the affinity laws for pumps).

Through the viewport on the back of the pump and the use of high speed photography, two phase flow behavior was observed at varying GVFs at rotational speeds of 600 rpm, 900 rpm, 1200 rpm, and 1500 rpm. Because, the field operating speed is 3600 rpm, data from 1500 rpm tests are nearest the true operating conditions of the pump. The conditions tested the effect of GVF on the pressure rise across the impeller and the shortened and modified diffuser is shown in Figure 8. It shows a sudden drop at 0.51 % GVF, which was attributed to the onset of the surging condition.

The resulting still photographs of the flow visualization shows the FS (Flow Structure) at various locations in Figure 9 through Figure 11. The figures show the distribution and size of the bubbles as well as the relative paths of bubble motion. These paths were generated by observing and tracking the bubble locations in a sequential series of frames from the high speed videos. The data shows the density of bubbles increasing between the blades before the surging condition occurs (FS1-FS4). Before surging, recirculation occurs from the pressure side to the suction side at the outlet of the impeller. This recirculation causes bubbles originating at the inlet of the impeller to undergo a change in the normal streamline and travel to the pressure side of the blade. Also, recirculation occurs across the width of the channel at the outlet of the pump.

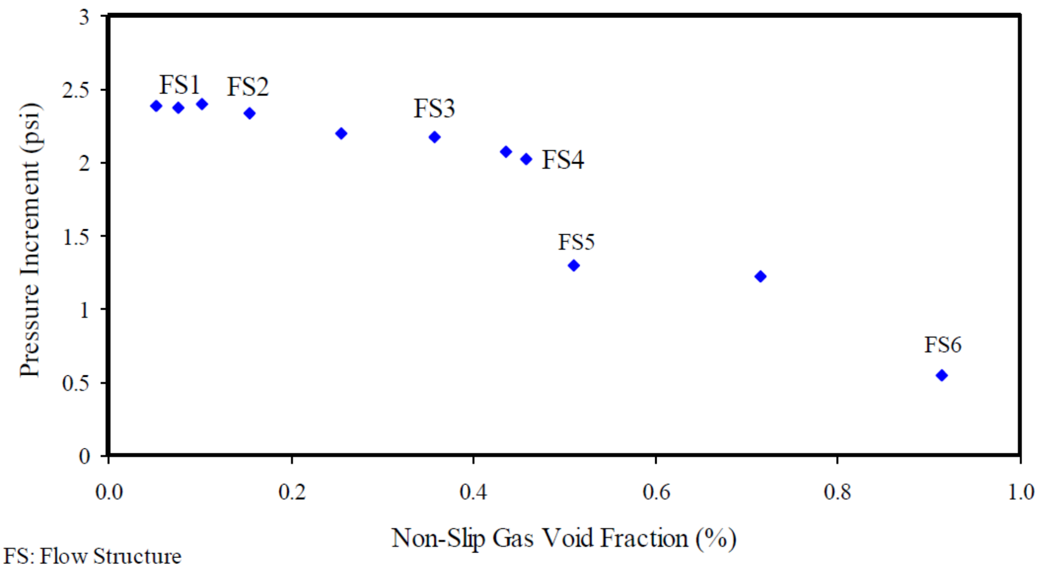

Figure 8 Effect of GVF on pressure generated by modified stage at 1500 rpm and 435 BPD with visualization conditions (FS locations), Barrios [4]

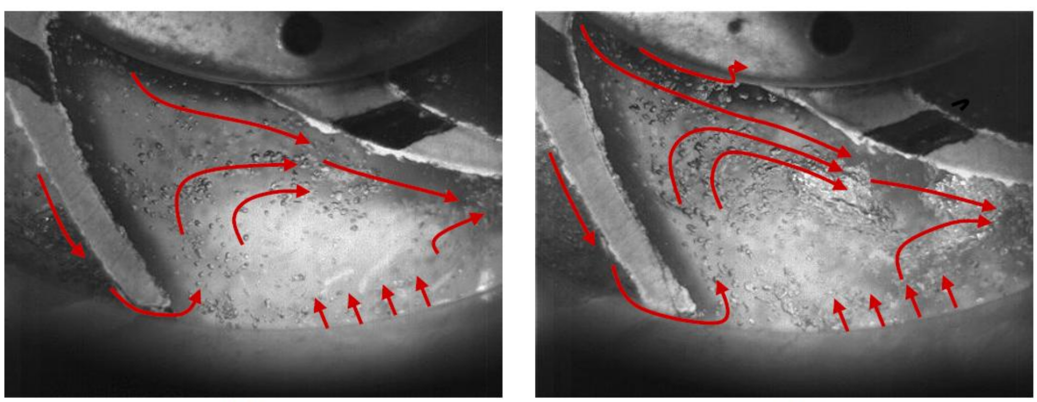

FS1 FS2

Figure 9 Two phase still photographs with bubble streamlines for FS1 and FS2 at 1500 rpm and 435 BPD, Barrios [4]

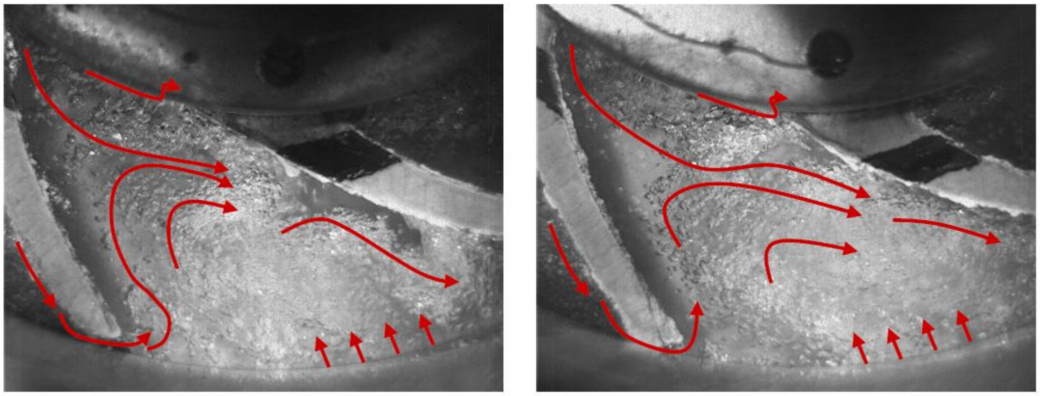

FS3 FS4

Figure 10 Two phase still photographs with bubble streamlines for FS3 and FS4 at 1500 rpm and 435 BPD, Barrios [4]

At the onset of surging at 0.51% GVF (FS5), a stagnant bubble forms at the inlet of the channel. This was attributed to the blockage of inlet gas by the recirculation from the preceding blade. Although this bubble forms on the upper shroud of the impeller, there is still liquid flow through the impeller channel nearer to the lower shroud. Also, after the onset of surging, large head degradation was observed. It was approximately 40% at FS5 and 80% at FS6.

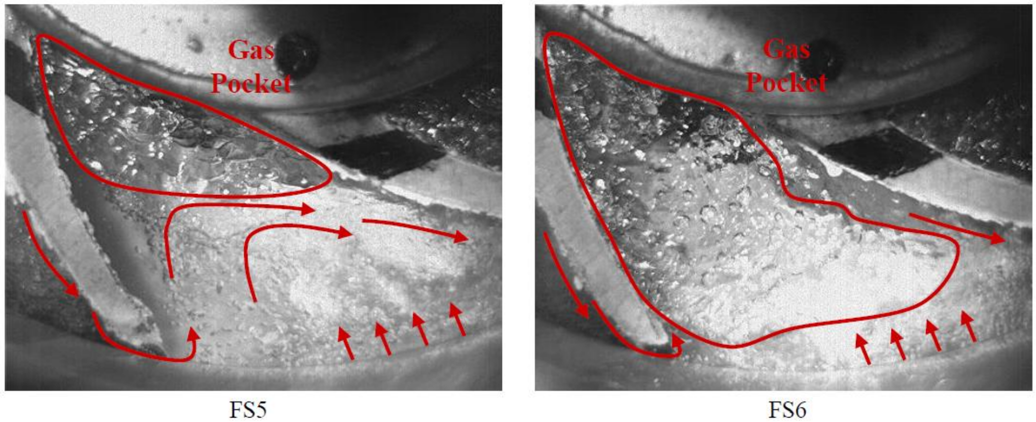

Figure 11 Two phase still photographs with bubble streamlines for FS5 and FS6 at 1500 rpm and 435 BPD, Barrios [4]

2.3 Full Scale MVP Testing and Visualization

A subsequent ESP test facility was designed, constructed, and tested on the pump presented in this work: the Baker Hughes Centrilift G470 MVP. This test loop was also completed at the Turbomachinery Laboratory at Texas A&M University. To complete the current study, a branch off of the original pump flow loop was designed and constructed. Thus many of the components are shared between the two studies. The primary goal of the study was to complete performance testing on the MVP pump, which had not been previously extensively studied. Performance data at varying GVFs, shaft rotational speeds, inlet pressures, and inlet liquid flow rates was desired. Besides performance characterization of the G470 MVP pump, pressure taps along one diffuser stage, at the pressure side, the meridian plane, and the suction side of the diffuser channel, were drilled to allow observation of the spatial pressure contour along the diffuser. Also, the casing of one diffuser channel was machined away from the pump and a clear polymer viewport was installed to allow two phase flow visualization and tomography measurements along the diffuser. Further, tomography measurements and calibration were completed at the inlet of the pump. The construction and initial test results were reported by Kirkland [5] on Kirkland and Pirouzpanah"s work.

Kirkland designed the pump test loop to operate at flow rates, rotational speeds, GVFs, and inlet pressures similar to those seen in actual downhole applications. Thus, no similarity analysis is needed to validate the results and justify comparison and relevance to industrial applications. The test parameters for Kirkland"s test loop are shown in Table 2. As shown, the rotational speeds, flow rates, and GVFs tested are exactly in the ranges seen in field applications of ESPs.

Table 2 Designed testing ranges for G470 MVP test loop, Kirkland [5]

Parameter	Unit	Minimum Test Value	Maximum Test Value
Inlet Pressure	psig	100	400
Inlet GVF	%	0	35
Rotational Speed	RPM	1800	3600
Liquid Flow Rate	BPD	10000	35000

Since the testing conditions were similar to those seen in field ESP applications, large amounts of water and air were necessary to obtain these proper testing conditions. To reasonably pump these large amounts of fluids without wasting the domestic water supply, and the compressor capacity at the Turbomachinery Laboratory, a closed loop system was developed. A P&ID diagram of the facility is shown in Figure 12. This system hinges around a 1760 gallon cyclone separator tank that is designed to take 450 psig working pressure at ambient temperature (typically less than 200 ^{0}F). The system in operation draws water from the pressurized tank through a metering section composed of pressure, temperature, and flow rate measurement and a PI controlled globe valve. It also draws air off of the top of the tank and again passes the air through a similar metering section and control valve. Flow rate, pressure, and temperature are metered for the air as well. The two inlet streams then enter the inlet mixing piping then the pump inlet. After passing through three stages full stages of the G470 MVP, the exiting flow passes through a final control valve which in single phase flow regulates flow rate and in two phase flow regulates GVF. The two phase flow then passes into the separator tank tangential to the tank wall. This causes a vortex or cyclone to form causing centrifugal separation; the more dense water is accelerated to the outside and downward in the tank and the less dense air forms a column in the center of the tank. Since large amounts of energy are introduced into the system by the MVP, the temperature of the fluid in the closed loop will rise. To mitigate problems with steam generation and weakening of the polymer parts in contact with the process fluid, heat removal was a necessity. Thus, a second cooling loop was designed and implemented. This system drew heated water from the lower portion of the tank, passed it through a filter and through an ambient air fan cooled heat exchanger. Then a centrifugal pump supplied the necessary energy to maintain flow through the heat dissipation system moving the cooled water back to the separator tank. The filter removes particles on the order of 10 μm (25 μin) from the fluid, which maintains a very low turbidity and allows the best visualization.

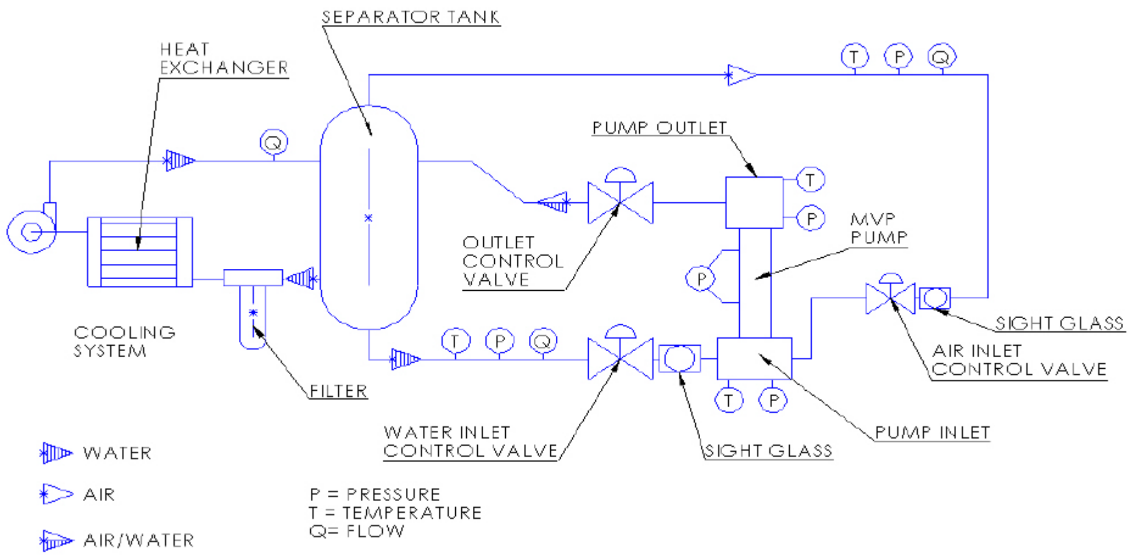

Figure 12 P&ID diagram of the G470 MVP performance test facility, Kirkland [5]

A 3D Solidworks view of the system is shown in Figure 13. All of the components described above are easily observed in this figure.

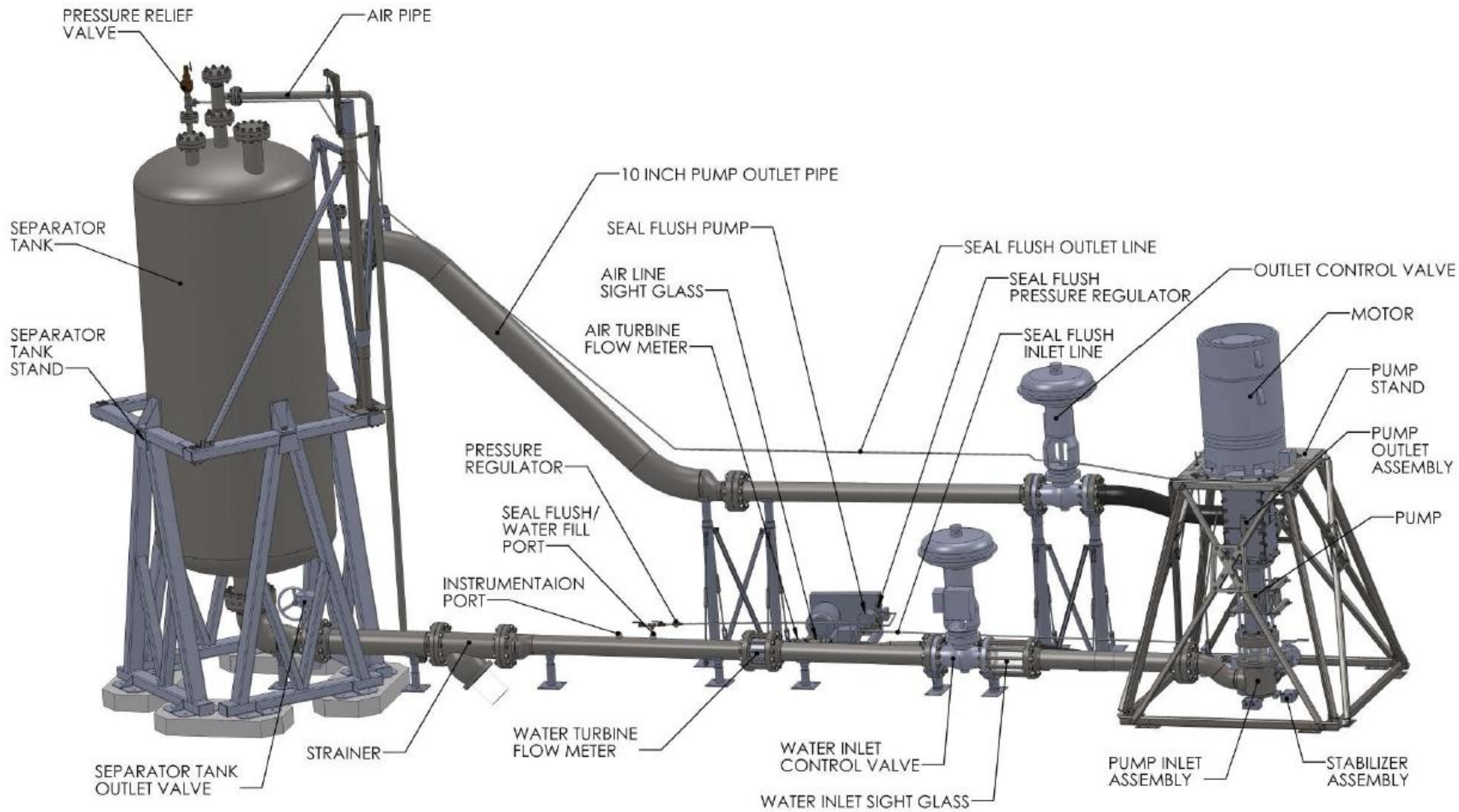

Figure 13 Virtual (Solidworks) view of the G470 MVP test facility, Kirkland [5]

The initial performance head-flow rate curves at 3000, 3300, and 3600 operating speeds show normal behavior for pure water. As the inlet GVF was varied from 0 to 35%, obvious maximum extrema occurred on the curves. From the work done by Barrios, the maxima could be interpreted as the point near which surging occurs. Since the G470 MVP is the pump examined in this work, it gives an initial point to observe with high speed visualization with the expectations of finding bubble coalescence and stagnation on the impeller blades.

3 EXPERIMENTAL FACILITY

An important and significant portion of this work was the design and construction of the test facility. To date, no full scale completely transparent mixed flow centrifugal pump (impeller, diffuser, and casing) has been designed and constructed for testing especially two phase testing at moderate pressures, full speeds and flow rates, to the author‟s best knowledge. At least in recent history, some manufacturing processes used for the fabrication of the components of the rig were not prevalent or available. Furthermore, some of the materials used in these processes were also not available. An overview of the facility is presented followed with an in-depth analysis of the component design.

3.1 Facility Overview

Before considering the construction of the clear pump components, it was necessary to design, procure, and construct a facility to handle moderate pressures, high flow rates, as well as supply the necessary inlet fluids to test.

For the inlet fluids, the industrial conditions to be mimicked were crude oil and the slurry common to production with some amount of free natural gas involved. For practicality and safety, to be used at the Texas A&M University Turbomachinery Laboratory by graduate researchers, domestic potable water and atmospheric air were chosen as the two phases. Domestic water differs some with crude oil in density and viscosity, but approximates the large range of crude production from actual wells acceptably. The properties of air also vary from those of production natural gas, which is composed mostly of methane, but approximates the behavior of natural gas acceptably as well. Also, using natural gas and crude oil at the facility would pose an unacceptable danger to the staff at the Turbomachinery Laboratory as well as a fire and explosion hazard to the entire laboratory facility. One final issue of using crude oil and natural gas is the problem of separation. Separation of oil and natural gas would require an involved and expensive system, whereas the separation of water and air may be accomplished through a simple cyclone separator.

Next a system to handle the fluids was necessary. The maximum capacity of the pump was expected to be approximately 1600 gpm (55,000 BPD) of pure water and approximately 400 scfm of air at 100 psig inlet pressure. Since drawing and draining that volume of fluid from the domestic water source and from the industrial compressors and air supplied by the Turbomachinery Laboratory would be absurd, a closed loop facility was designed. Since the original MVP test loop designed by Kirkland [5] is also housed at the Turbomachinery Laboratory, the new MVP visualization test rig was constructed beside the original loop with modifications to the piping and flow control system. A P&ID of the old system with the new modified system is shown in Figure 14 and Figure 15. The flow originates in the cyclone separator tank. The water falls to the bottom and is drawn off through the water inlet pipe. From there, the temperature and pressure are measured before the flow enters a turbine flowmeter. Then, a flow control valve regulates the liquid flow into the pump. With the new rig added, the flow goes through a sight glass, which gives the operators a visual metric by which to observe the flow and ensure that no air is entrained in the water feed line. The water then passes through a tee with butterfly valves on each outlet. This allows the operator to either operate the original MVP test rig, or the MVP visualization rig. The same general layout was constructed on the air inlet line, except the line was smaller and originated at the top of the separator tank. The two inlet lines then run to mixing sections of the piping and to the inlet of the pump. The pumps both have pressure and temperature taps at their inlets and outlets. The outlet piping then runs to another tee with butterfly valves to direct the flow. Finally, the one or two phase outlet flow will be throttled by a final control valve and piped tangentially into the separator tank where the cyclone forms with the denser water flowing to the wall of the tank and the less dense air separating out and flowing upward in a column in the center. Table 3 is a listing of the existing equipment in the previously constructed test loop used in the MVP visualization test facility with important parameters.

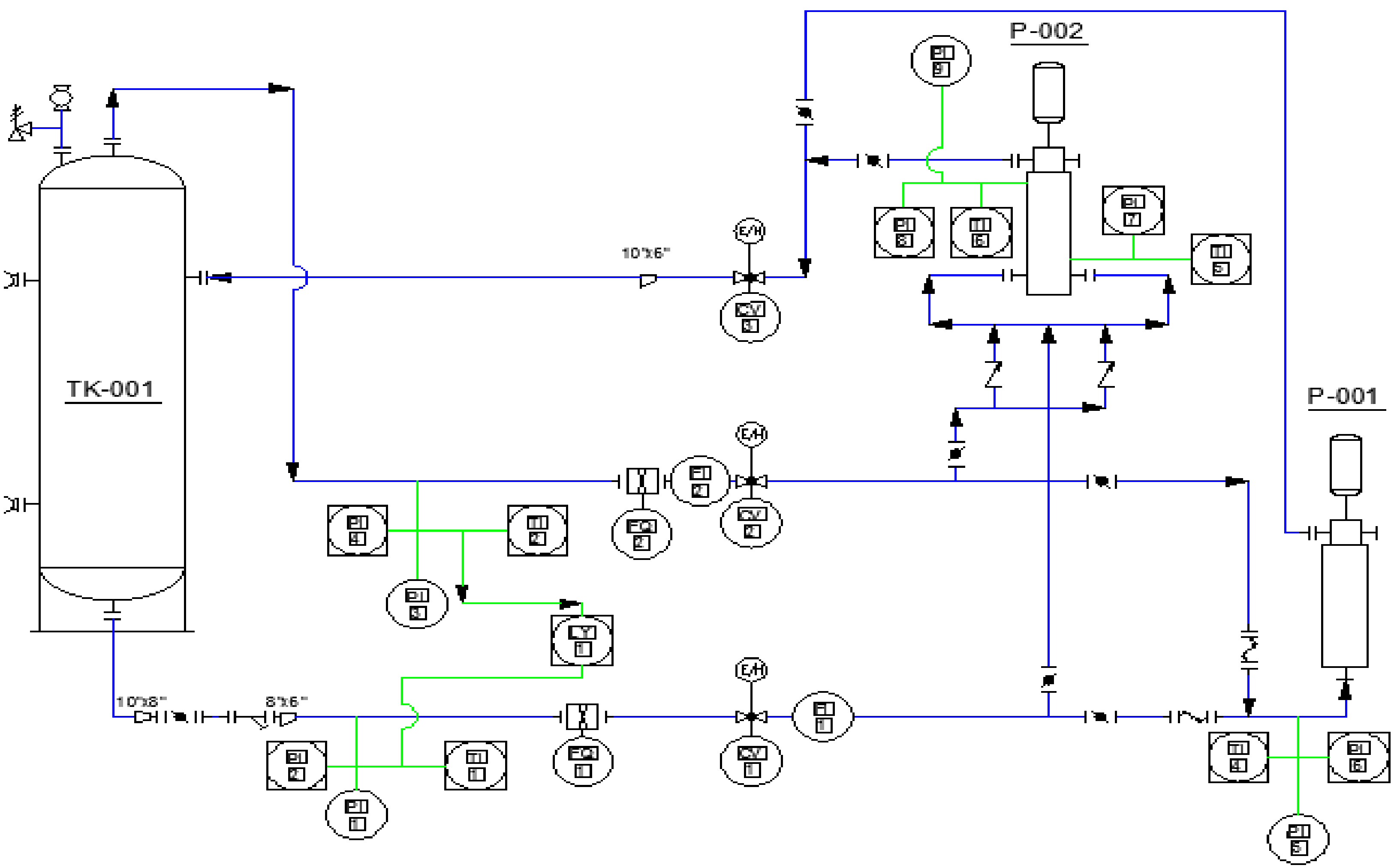

Figure 14 P&ID of primary flow loop for existing MVP and MVP visualization test facility

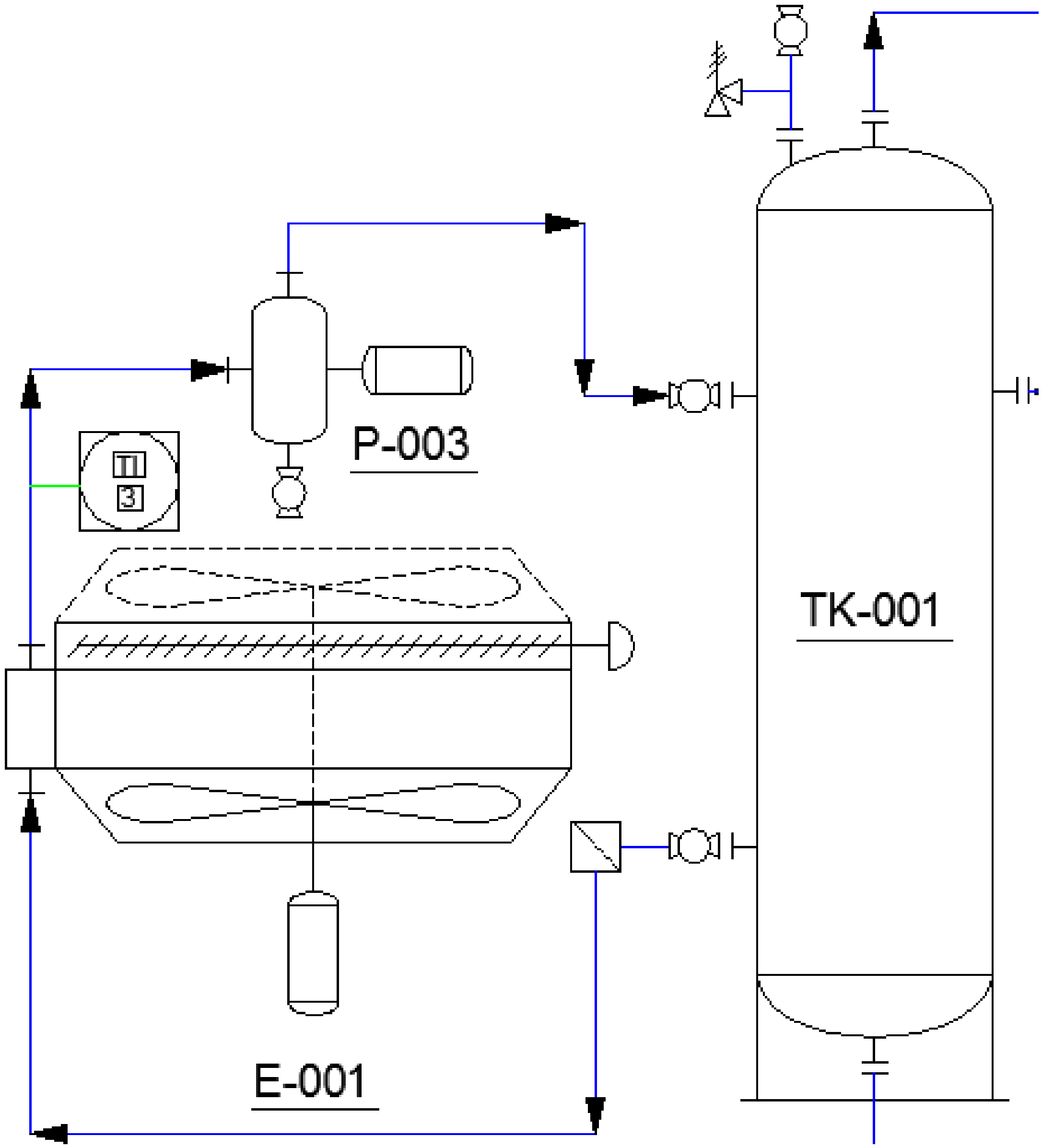

Figure 15 P&ID of secondary cooling loop for MVP and MVP visualization test facility

Table 3 Existing equipment in primary test loop

Equipment	Manufacturer	Material	Size	Pressure Rating (MAWP @ Ambient Temp.)
Pressure Vessel	Wyatt M. & B. Wks. Inc.	304L Stainless Steel	1760 gal	400psig @ 212 ^{0}F
Control Valve (Water Inlet)	Fisher Controls	Body – Carbon Steel Plug, Stem, and Seat – Stainless Steel	6”	600# Flanges, 1500psig
Control Valve (Outlet)	Fisher Controls	Body – Carbon Steel Plug, Stem, and Seat – Stainless Steel	6”	600# Flanges, 1500psig
Control Valve (Air Inlet)	Fisher Controls	Body – Carbon Steel Plug, Stem, and Seat – Stainless Steel	3”	600# Flanges, 1500psig

Table 4 is a listing of the existing instrumentation in the previously constructed test loop used in the MVP visualization test facility with important parameters.

Table 4 Existing instrumentation in primary test loop

Instrument Description	Manufacturer	Part No.	Units	Range	Uncertainty	Output
Type T Thermocouple	Omega	TQSS-18U-6	^{0}F	-325 to 662	1.8 ^{0}F or 0.75%	-6 to 21 mV
Air Turbine Flowmeter	Omega	FTB-938	ACFM	8 to 130	1 %	Sine Wave (Hz) – 30mV P-P
Liquid Turbine Flowmeter	Turbines Inc.	WM0600X6	GPM	250 to 2500	1.0 %	Sine Wave (Hz) – 0 to 10V P-P
Pressure Transducer	Omega	PS481A-500G5V	psig	0 to 500	0.3 %	1 to 5 V
Pressure gauge	Ashcroft	Type 1009	psig	0 to 600	1 %	Analog Visual Dial

A secondary recycle cooling loop is also attached to the cyclone separator to maintain the temperature of the test fluids at an acceptable level. Since there are various polymer pressure containing components which contact the process stream, it is necessary to maintain the temperature of the fluid by dumping the excess energy (in the form of heat added to the system by the test pump) to the atmosphere. This is done by recirculating the warmed water in the system through a particulate filter, and an air cooled heat exchanger with a secondary centrifugal pump. A listing of the recirculation equipment is shown in Table 5.

Table 5 Existing equipment in cooling recirculation loop

Equipment	Manufacturer	Model Number	Size	Pressure Rating (MAWP @ Ambient Temp.)
Particulate Filter	Pentair Industrial	C1616304FAD40	30" Filters – 16" Diameter	400psig @ 300 ^{0}F
Recirculation Pump	Ingersoll-Rand Cameron Div.	400 gpm Ser: 1287026	3X4X7AL (Outlet X Inlet X Impeller Dia.)	920psig
Heat Exchanger	SnyderGeneral	ALR115C	10-1HP Fans	450psig

3.2 Clear MVP G470 Pump Design

In designing the test facility, the casing, impeller, and diffuser were critical components for ensuring quality visualization and performance. At the start of the project, the only information known about the Baker Hughes Centrilift MVP G470 pump was the internal flow paths used for CFD analysis. Figure 16 shows the flow paths of the G470, where the flow moves from right to left. The split vane area is seen on the right portion of the figure. This split vane is designed to deflect a high velocity stream of fluid across the suction side of the vane to minimize gas stagnation, recirculation, and coalescence in two phase flow conditions. These phenomena cause head and efficiency degradation in the pump, and are flow structures to be analyzed in the testing of the pump.

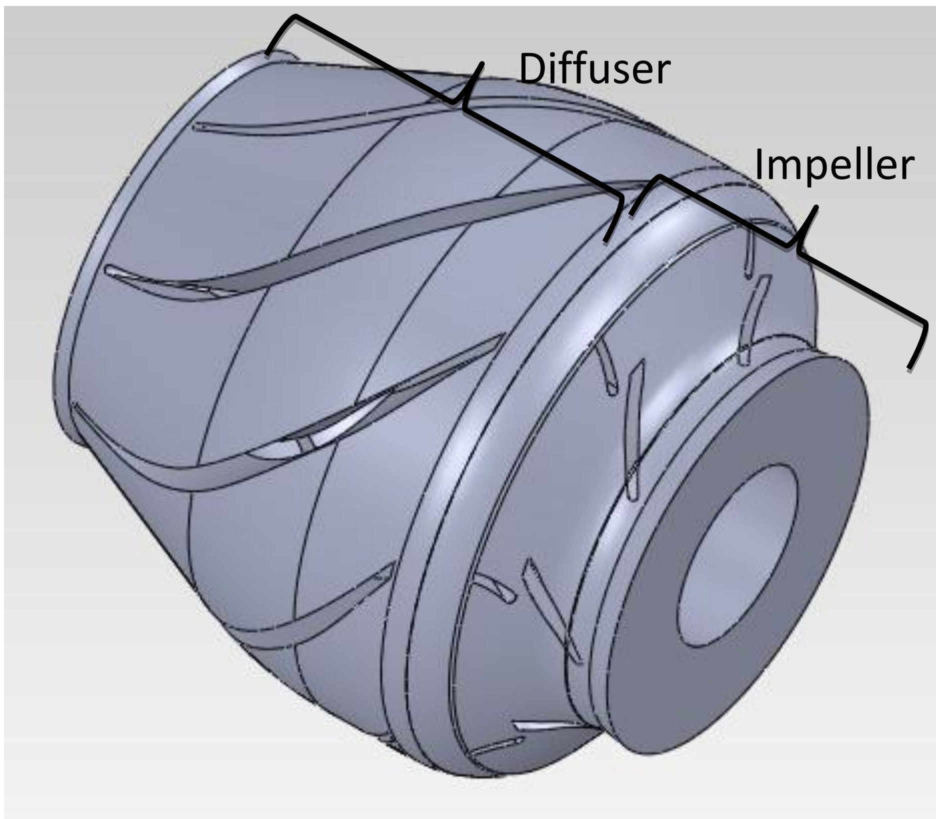

Figure 16 Internal flow paths of the impeller (right) and diffuser (left) of the G470 pump

The pump was designed and constructed in a horizontal pump skid layout and operates with the skid in a vertical direction to simulate downhole orientation. The exterior and layout is shown in Figure 17. Major components and the general flow directions are labeled in the figure.

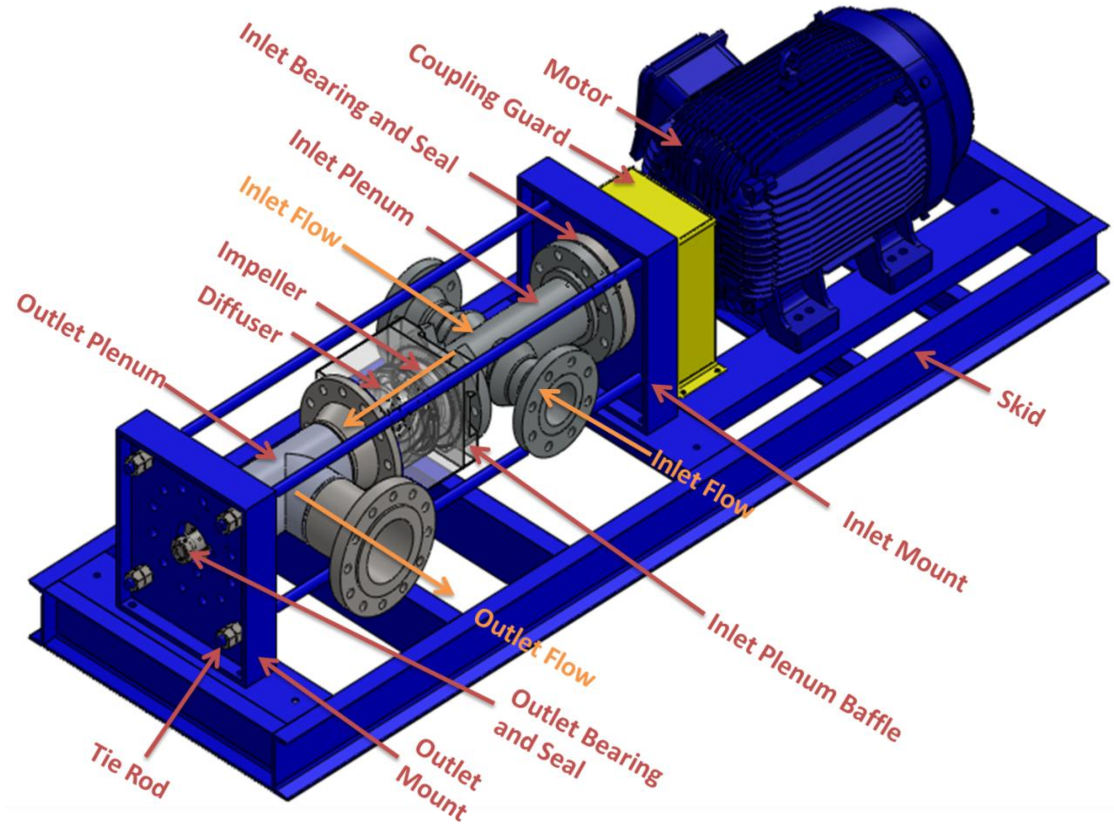

Figure 17 External layout of pump skid in the horizontal orientation

To gain a general understanding of the layout of the internal components of the pump, Figure 18 shows a cutaway view of the pump. Major components are labeled in the figure.

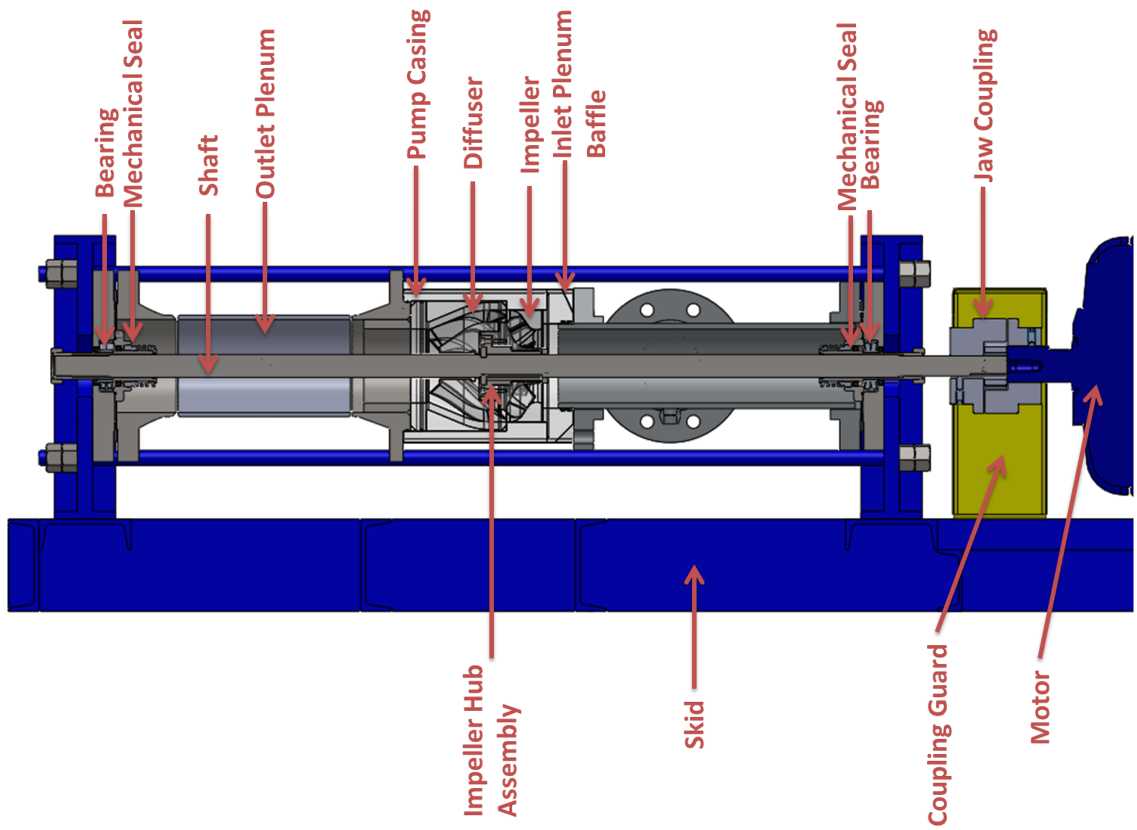

Figure 18 Internal layout of the pump skid in the horizontal orientation

3.2.1 Diffuser Design

The clear pump casing, impeller, and diffuser have design dependencies with each other, but the diffuser was the first component fully designed. For the diffuser design, a systematic process was developed and completed to ensure that safety, performance, visualization quality, and reliability were maximized. This was as follows:

1. Obtain primary flow paths for Baker Hughes Centrilift G-470 MVP pump.

2. Use 3D parametric modeling (Solidworks software) to reverse engineer critical pump geometries.
3. Investigate manufacturing processes and materials suitable for construction. This allowed accurate data on required lead time, mechanical properties, and optical properties on potential materials of construction.
4. Develop mounting and attachment method.
5. Determine expected loads from CFD predictions.
6. Complete FEA and stress analysis to determine required material thicknesses.
7. Determine required manufacturing tolerances.
8. Draw proper engineering manufacturing drawings with applicable geometrical tolerances.
9. Submit RFQs to prototyping and manufacturing companies.
10. Collect bids and finalize design and drawings.
11. Procure part.

This general design system was used for most components, but typically for common or pre-engineered components in a simplified format.

For the diffuser design, the solid model of the primary flow paths was imported into Solidworks. Then a cylinder was superimposed on the flow paths, which were subtracted from the cylinder to obtain the vane shapes. Further modifications were required to accommodate the shaft and the mounting method for the diffuser. The first design had the diffuser and the casing combined in one large part, but due to manufacturing and materials limitations, that design was modified. The final completed pump assembly uses the principle of a pressure containing transparent casing with a thin walled diffuser which transfers the pressure to the casing primarily through incompressible stationary water drawn from the process stream. Thus, a thin walled diffuser canister with thickened mounting faces on the inlet and outlet was developed. This design also required the addition of O-ring seals between the casing and the exit mount on the diffuser and between the casing and the outlet piping of the pump. Dimensioning was done to match the design of the Baker Hughes design for the flow paths and to common sizes and sizes recommended by the Parker ORD-5700 O-Ring Handbook.

Various materials and manufacturing methods were considered for the construction of the diffuser. For manufacturing, 5-axis CNC milling, rapid prototyping in the form of SLA, and casting were considered. 5-axis CNC milling was not capable of producing such a complex part and casting was only feasible in production type quantities. Thus the only method feasible for manufacturing the diffuser was SLA rapid prototyping. Several photo-curing polymers are available, so one with properties similar to PC was desired. The critical properties were mechanical strength, elastic modulus, clarity, and toughness. Two common clear SLA materials are manufactured by DSM and marketed as Somos WaterShed XC11122 and Somos WaterClear Ultra 10122. Based off of manufacturer recommendation and previous experience with Somos WaterShed XC11122, it was decided to use Somos WaterClear Ultra 10122 for improved clarity and mechanical strength; a listing of the critical properties is shown in Table 6. The index of refraction was desired to be as near as possible to water (1.33) to minimize light distortion during visualization.

Table 6 Critical properties of DSM Somos WaterClear Ultra 10122, Royal DSM [6]

Property	Unit	Value
Tensile Strength at Break	ksi [MPa]	7.9 – 8.1 [55-56]
Tensile Modulus	ksi [MPa]	414-421 [2,860 – 2,900]
Elongation at Break	%	6 – 9
Elongation at Yield	%	4
Poisson's Ratio	-	0.40 – 0.42
Izod Impact (Notched)	ft-lb/in [J/m]	0.44 – 0.48 [0.24 – 0.26]
Index of Refraction	-	1.52

Then several FEA analyses using Solidworks Simulation were completed to determine whether any design modifications were needed in the vanes and pressure containing portion of the diffuser. To determine the expected loads, the differential pressure across the vanes was determined from the CFD work completed by Marsis [7]. The maximum pressure differential was 50 psig, and was applied across the entire vane as a worst case scenario. The other major load considered was the pressure across the diffuser shroud. Since the pump produces a maximum of 50 psig head, the worst case scenario for the pressure differential across the diffuser shroud was approximately 50 psig. A 10 psig safety factor was added to the worst case scenario and applied to the model. A 3/8" x 45^0 chamfer was used as a fixed constraint, since split rings fit between the diffuser canister and the casing and constrain the diffuser and prevent rotation and axial motion. To account for any eccentricity between the shaft and the diffuser, an allowance for a 0.002” deflection was considered in the ID of the diffuser hub. Gravity was applied with the diffuser in the vertical position as in downhole and testing conditions. The geometry was automatically meshed with Solidworks Simulation with user entered mesh controls for critical areas where sudden geometrical gradients could cause error in the FEA analysis. A mesh composed of 130,956 nodes was generated with 93% of the nodes with an aspect ratio less than 3. After running the FEA solver, the von Mises stress was determined, as well as the strain, and an FOS based on the tensile strength at break. The resulting minimum FOS was greater than 3.5 on the diffuser. Thus, the original Baker Hughes Centrilift G470 design was deemed acceptable. Figure 19 shows the FOS plot generated by the Solidworks Simulation FEA; the full report on the FEA including assumptions, material properties, loading, fixtures, and stress and strain results are found in Appendix A. The minimum FOS for the diffuser was 3.7 and thus deemed safe for operation with the Somos WaterClear Ultra 10122. Another consideration was the total deflection of the polymer components in the pump, since the elastic modulus is two orders of magnitude less than more common pump materials such as steel. To achieve adequate operational behavior the maximum deflection was determined with the FEA. As shown in Appendix A, the maximum deflection of the pump blade was 0.004” and would not present any issues during operation and testing.

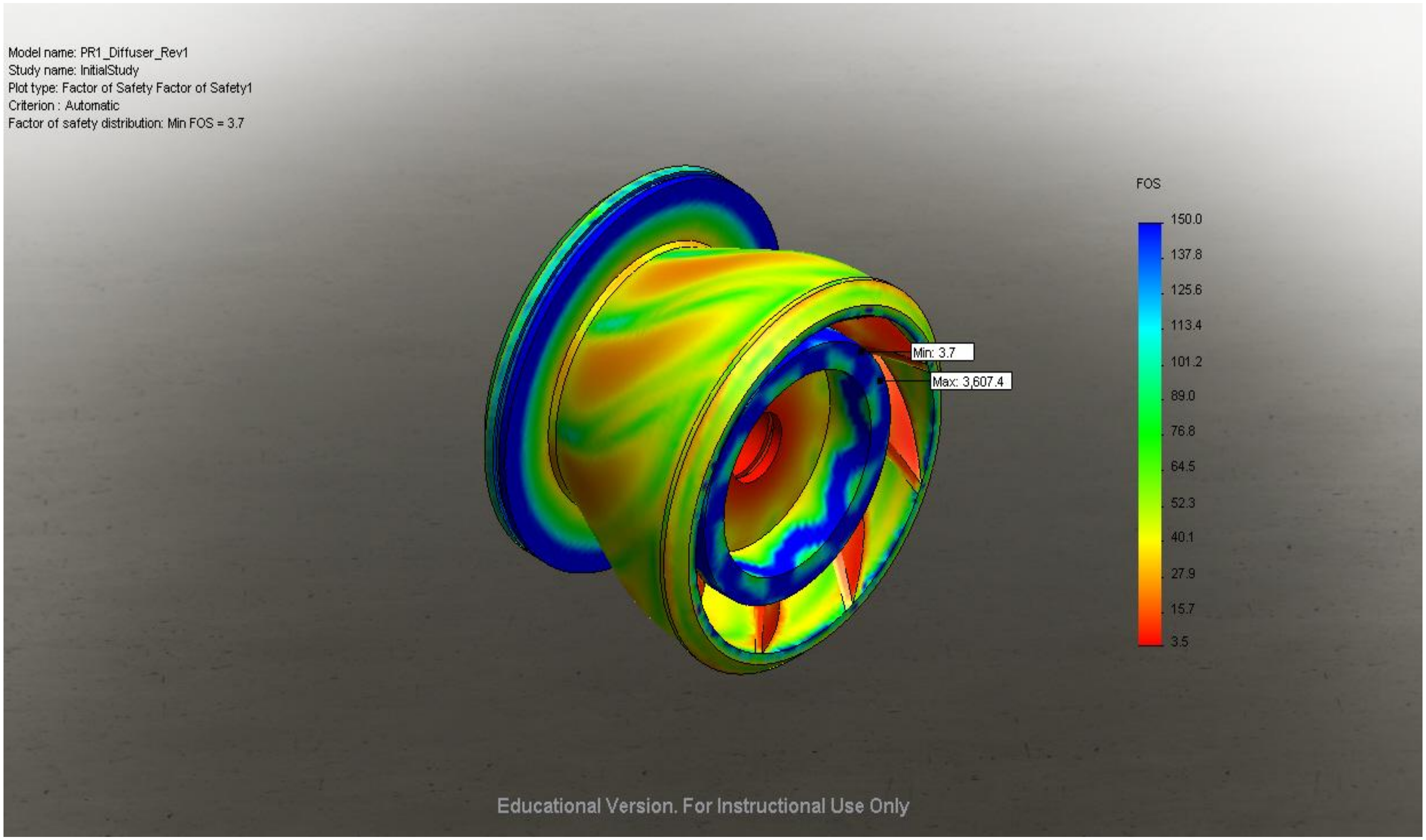

Figure 19 Factor of safety plot of diffuser FEA results

After the FEA was completed on the diffuser, determination of proper tolerances for manufacturing was necessary. Although much tighter tolerances were necessary, the SLA process used with the Somos WaterClear could only guarantee ±0.005” per inch on any given dimension. To overcome this problem for critical tolerances which had tighter requirements, the 3D Solidworks model used for manufacture was modified to account for the maximum amount of deviation in the SLA manufacturing from the drawn dimensions. Then finish machining was specified for the critical and tight tolerance locations. Finally, a polish and clear coat were specified to maximize the clarity of the part.

Tolerances were determined by design calculations, common ESP clearances, and O-Ring requirements. The split ring chamfer and length requirements for the diffuser canister and casing were designed for a FN 2 or light interference fit, Jones [8]. Thus when the outlet was pulled against the split rings and diffuser canister, the canister would be locked in place. The tolerance between the casing and the leading mount edge of the diffuser canister, the inner and outer diameters at the close clearance seal between the diffuser and impeller, and the concentricity at these locations were matched to those of a similar ESP from Baker Hughes Centrilift. Also, all dimensions dealing with O-Ring grooves and gland dimensions were determined from the Parker ORD-5700 O-Ring Handbook. Upon completion of dimensioning with tolerances, the part was sent for manufacture. The completed diffuser is shown in Figure 20; dimensioned drawings are also included in Appendix C.

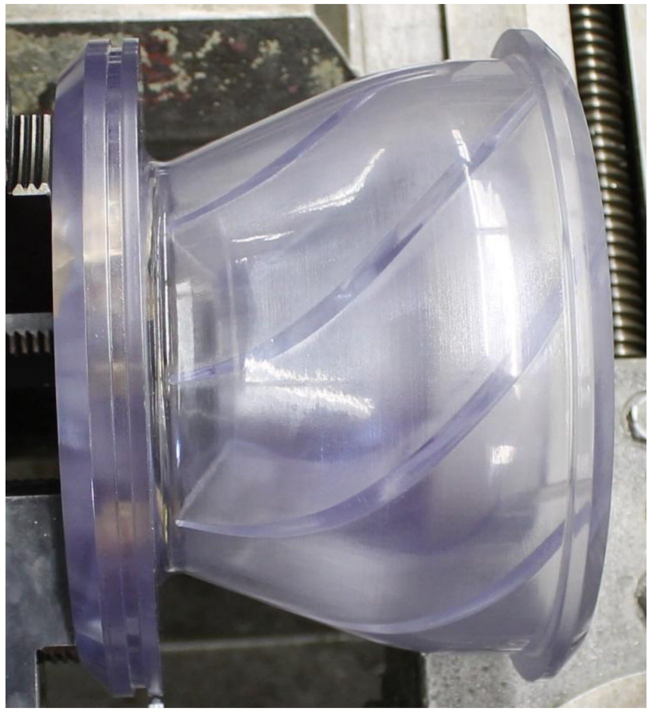

Figure 20 Completed clear functional diffuser

3.2.2 Impeller, Impeller Hub, and Shaft Design

The impeller design methodology was similar to that of the diffuser. Four main areas were considered in the design. These were: 1) the geometry, material, and manufacturing for visualization, 2) the loading and stress on the vanes, and 3) the attachment of the impeller to a hub and the shaft, and 4) the required manufacturing tolerances.

The impeller internal geometry was obtained from the flow paths just as the diffuser. The shroud of the impeller typically is a uniform thickness and contours to the blade. This would cause issues with diffraction of the light and subsequently the images when looking down the eye of the impeller through the shroud. To mitigate this problem, the shroud was thickened and made into a cylindrical shape. The impeller is flat across the eye and the same diameter down the entire shroud length as shown in Figure 21.

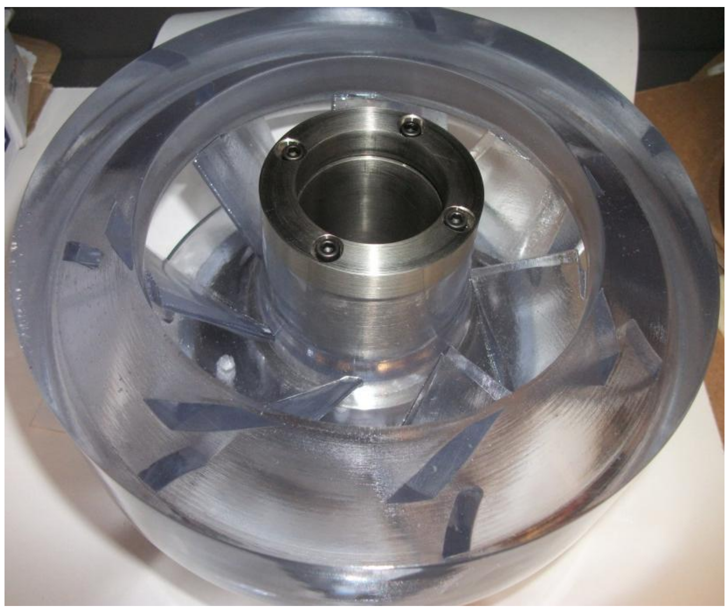

Figure 21 Impeller with flat shroud at eye and constant shroud diameter

With the mechanical property, transparent, and geometry requirements similar to the diffuser, manufacturing and material selection was the same. Although Somos WaterClear Ultra 10122 was used with the SLA rapid prototyping, other options were considered. Since the WaterClear Ultra 10122 develops a haze with increased thickness, polycarbonate was considered for manufacture due to its superior transparency. This was initially considered due to the 4” length of the impeller, which can be procured, as compared to the 6 ¼” length of the diffuser. Unfortunately, 5-axis CNC machining was not capable of milling the channels under the shroud. Some consideration was then given to vibration or sonic welding the shroud to the hub and vanes. Several concerns related to manufacturing tolerances and mechanical strength prevented the use of that manufacturing method. With the SLA manufacturing method, there was still some concern with the mechanical strength and large deflections in the impeller.

To mitigate weakness in the impeller vanes, several FEA analyses were completed to ensure adequate mechanical strength and limit deflection of the vanes. To adequately simulate the stress condition of the impeller in operation, the loading on the impeller must be determined as accurately as possible. Three main loads were considered:

1. Centrifugal forces,
2. Axial forces developed due to the pressure rise across the pump, and
3. Pressure forces on the blades.

The centrifugal force generated on the impeller was applied with Solidworks Simulation as a predefined option where only the rotational speed of 3600 rpm was required. The axial force on the impeller due to the pressure gradient throughout the pump was estimated by previous data taken on the G470 pump in Kirkland‟s [5] test facility. To estimate the worst case scenario, the maximum head generated by one stage of the G470 MVP pump of 70 psig was applied to the outlet area of the shroud axially opposite the flow in the pump. With a factor of safety of 1.3, a resultant force of 1500

lb_f was applied to the shroud of the impeller. From CFD results local pressure distributions were known across both the impeller and diffuser. These results matched the overall pump performance within 6.5% at 20% GVF from the testing done on Kirkland"s [5] facility. Multiple iterations were required to obtain accurate pressure distributions across the blade. Initially, the highest local pressure on the pressure side of the vane was compared to the lowest local pressure on the suction side of the vane. This gave a worst case scenario pressure differential for each blade. FEA results using this large pressure differential across the entire blade showed excessive stress and deflection in the impeller blades. Thus, a refinement was developed where each blade was broken into 7 regions allowing more precise pressures to be applied to the FEA model. CFD data for both 10% GVF and 25% GVF were available, but 10% GVF data was the more extreme case and was selected as the one analyzed by the FEA. The pressure distribution for 10% GVF is shown in Figure 22. A factor of safety of 1.3 was applied to the pressure distribution before simulation. This factor was applied to increase the highest pressures and decrease the lowest pressures; which effectively increased the pressure differential on the vanes. Thus, harsher conditions than given in the CFD were analyzed with FEA.

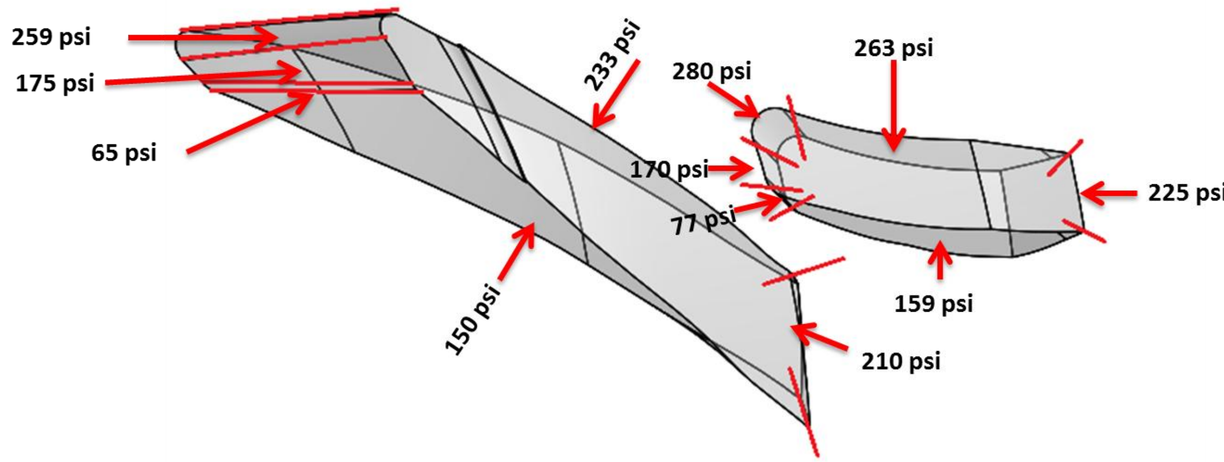

Figure 22 Pressure distribution at 10% GVF from CFD used for FEA structural analysis

A series of designs and analyses were completed to determine the optimum impeller design. First, the impeller with original blade thickness was simulated using cast carbon steel in an attempt to approximate the stresses and deflection in an actual impeller. This gave a baseline by which to compare subsequent impeller designs with the Somos WaterClear Ultra 10122 material. The baseline analysis actually showed stresses above the yield stress of the steel at a knife edge formed near the attachment point of the leading edge of the main vane and the shroud. Since, these impellers operate acceptably in the field, subsequent designs where stresses above the yield stresses are found in this region will be deemed acceptable. Then analyses were done with Somos WaterClear Ultra 10122 with multiple blade thicknesses to determine the final design blade thickness. The test matrix and results is shown in Table 7. Reports on the FEA analyses for all of the tests in Table 7 are in Appendix B. A primary blade thickness of 0.171" was the original Baker Hughes design; thicknesses of 0.336" and 0.419" were approximately 2 and 2.5 times the thickness of the blade respectively. To thicken the blade uniformly, the blade volume was rotated about the axis of the impeller and merged together. Smoothing was applied to the leading edge to remove irregular geometries. Since the gap between the primary and secondary blade is critical to the flow properties of the G470 MVP especially in eliminating the gas pocket on the suction side of the blade, the blades were thickened away from each other. The primary blade was thickened toward the suction side and the secondary blade was thickened toward the pressure side. Also, the knife edge where the leading edge of the primary vane attaches to the shroud is caused by a small channel that directs a high speed stream of flow toward the suction side of the vane. This is the reason why this geometry was left on the impeller even though it was overstressed. By leaving these two critical geometries intact per the Baker Hughes design, the flow characteristics of the transparent impeller should mimic the original design. The 0.336" thick impeller was chosen for construction because the thickness of the blades was as not excessive as in the 0.419" impeller and the only locations where the stress was greater than the yield stress was in the knife edge. Also, the stress ratio was on the order of the original steel design.

Table 7 Impeller testing and design matrix and results

Primary Blade Thickness [in]	Secondary Blade Thickness [in]	GVF [%]	Material	Maximum Deflection [mil]	Maximum von Mises Stress [ksi]	Yield Stress [ksi]	Stress Ratio [-]
0.171	0.129	10	Cast Steel	0.61	50.5	36.0	1.40
0.171	0.129	10	Ultra 10122	51.69	55.6	8.0	6.95
0.336	0.251	10	Ultra 10122	24.37	14.5	8.0	1.81
0.419	0.312	10	Ultra 10122	19.21	8.9	8.0	1.11

The FOS results of the final 0.336" blade thickness impeller FEA are shown in Figure 23. The FOS is greater than 5 over the majority of the impeller, and is greater than 2 over the majority of the blade. In some small localized regions on the impeller, the FOS is as low as 1.25; but only in the knife edges are the FOSs lower than 1. The impeller with the blades thickened by about 2 times with trailing edges of the primary and secondary blades of 0.336" and 0.251" respectively was chosen for manufacture.

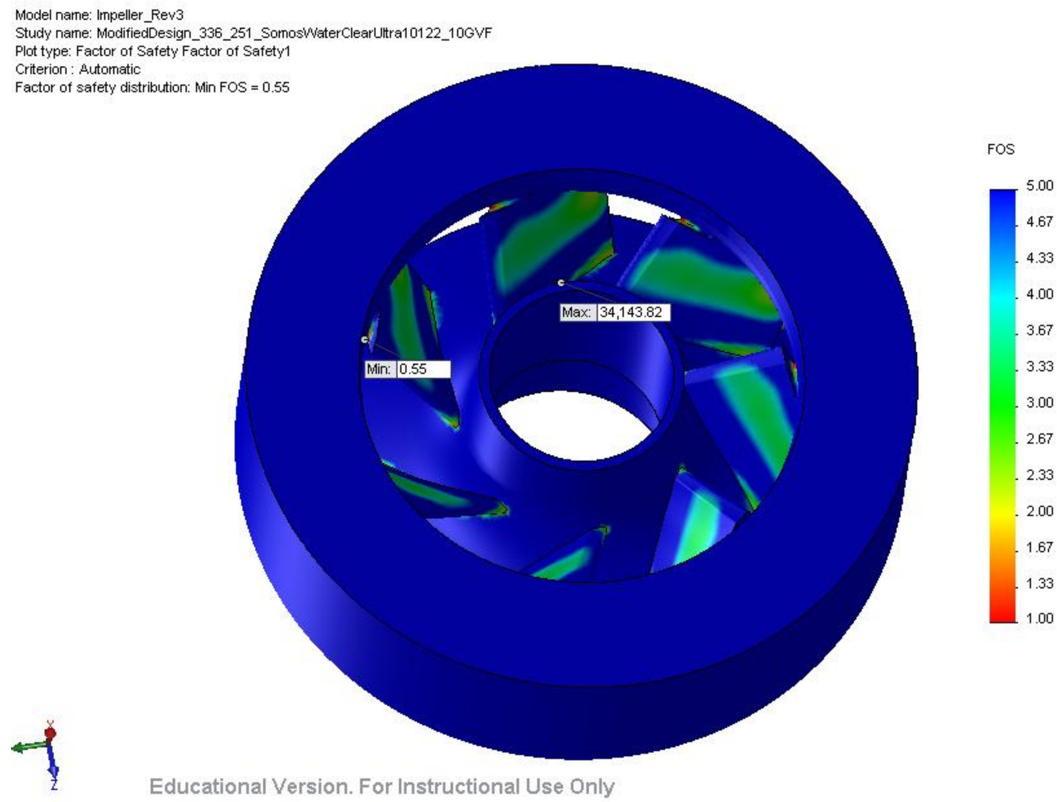

Figure 23 FOS plot for impeller with blades thickened by a factor of approximately 2

Upon completion of the vane design, a method of attachment to the shaft was necessary. Since the impeller was constructed of a polymer, using the standard bore taper and taper-lock bushing, would introduce excessive stress on the impeller hub and crack or deform the impeller. Thus, a collar was developed with a keyway and split ring to locate the impeller-collar assembly on the shaft. Socket head machine screws fix the plastic impeller to the close diametrical tolerance collar. A lock ring applies compressive force to the eye of the impeller to reduce the tensile force on the screws in the hub of the impeller due to back pressure from the head generated by the pump. This lock ring transfers force by cap screws threaded into the inlet side of the collar. This collar assembly was constructed of type 304 stainless steel and is shown in Figure 24.

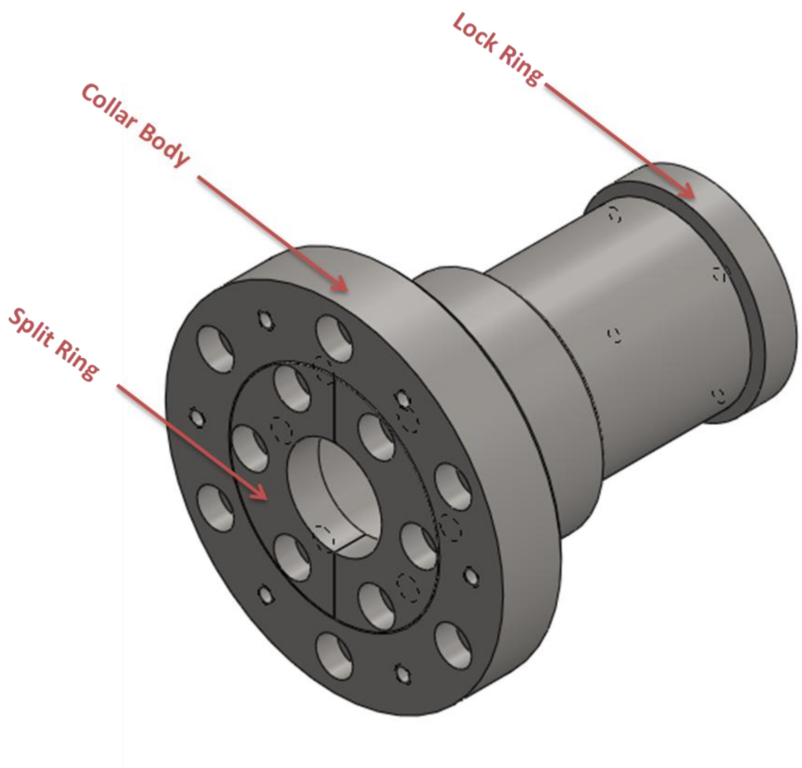

Figure 24 Impeller collar assembly

Stress analysis was completed by hand. The collar fits over a 1 ½” shaft and the split ring fits in a 1 3/8” groove in the shaft. This allows the location of the impeller to be accurately held. The shear stress in the split rings, shaft, and screw holes were calculated for a 1500 lb_f force from back pressure and was well below the yield strength of the stainless steel. Also, screw thread pull-out calculations from the *AISI Supplement 2 to the North American Specification for the Design of Cold-Formed Steel Structural Members* were completed to verify that the socket head screws securing the plastic impeller and other components would not fail. The shaft dimension of 1 ½" diameter was chosen to be the same as the actual G470 pump. A 3D modeled view of the entire shaft, collar, and impeller assembly is shown in Figure 25.

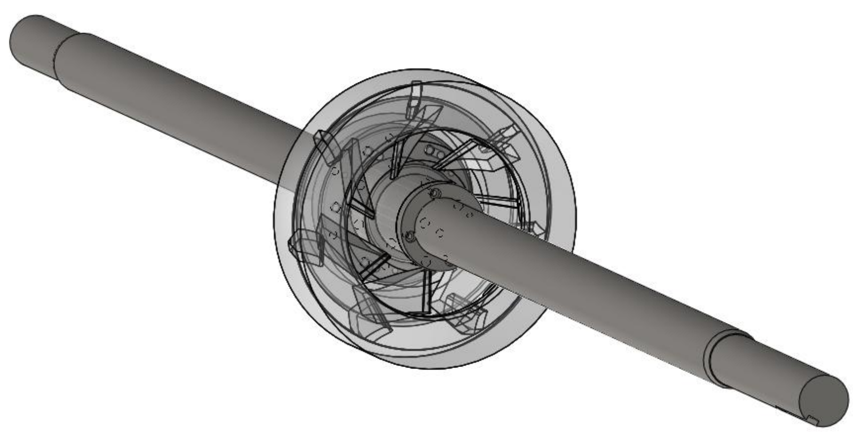

Figure 25 Model of shaft, collar, and impeller assembly

The final requirement for design and manufacture of the impeller, collar, and shaft is tolerancing and dimensioning. The diametrical linear, concentric, and runout tolerance for the outlet seal and shroud outer diameter were matched to those of a typical ESP. The collar to impeller fits were determined using *Machinery's Handbook 23rd*

Edition. A close LC 3 fit was used in the critical 2 ½” diameter portion of the collar between the collar and impeller. This gave a clearance of 0.000” to 0.003”. The other diametrical fits between the collar and the impeller were loosened to LC 5 fits to prevent over constraining the design and causing interference between the parts. The hole patterns were dimensioned on the manufacturing tolerances of standard socket head screws and tapped holes. A precision ground shaft with a diametrical change along the length of 0.0005” was obtained to allow a close tight fit for the collar to the shaft of 0.000” to 0.0015”. The tolerances on the lock ring ID were the same as those of the collar. The precise and tight tolerances required in the impeller, shaft, and collar ensure no rubbing or interference in the pump and minimal imbalance. The final assembly is shown in Figure 26 and manufacturing drawings are found in Appendix C.

3.2.3 Casing, Split Rings, and Inlet Baffle Design

To understand the casing and fluid visualization and containment components Figure 27 shows a general layout complete with the diffuser and impeller in the vertical operating position.

Figure 26 Impeller, collar, and shaft completed assembly

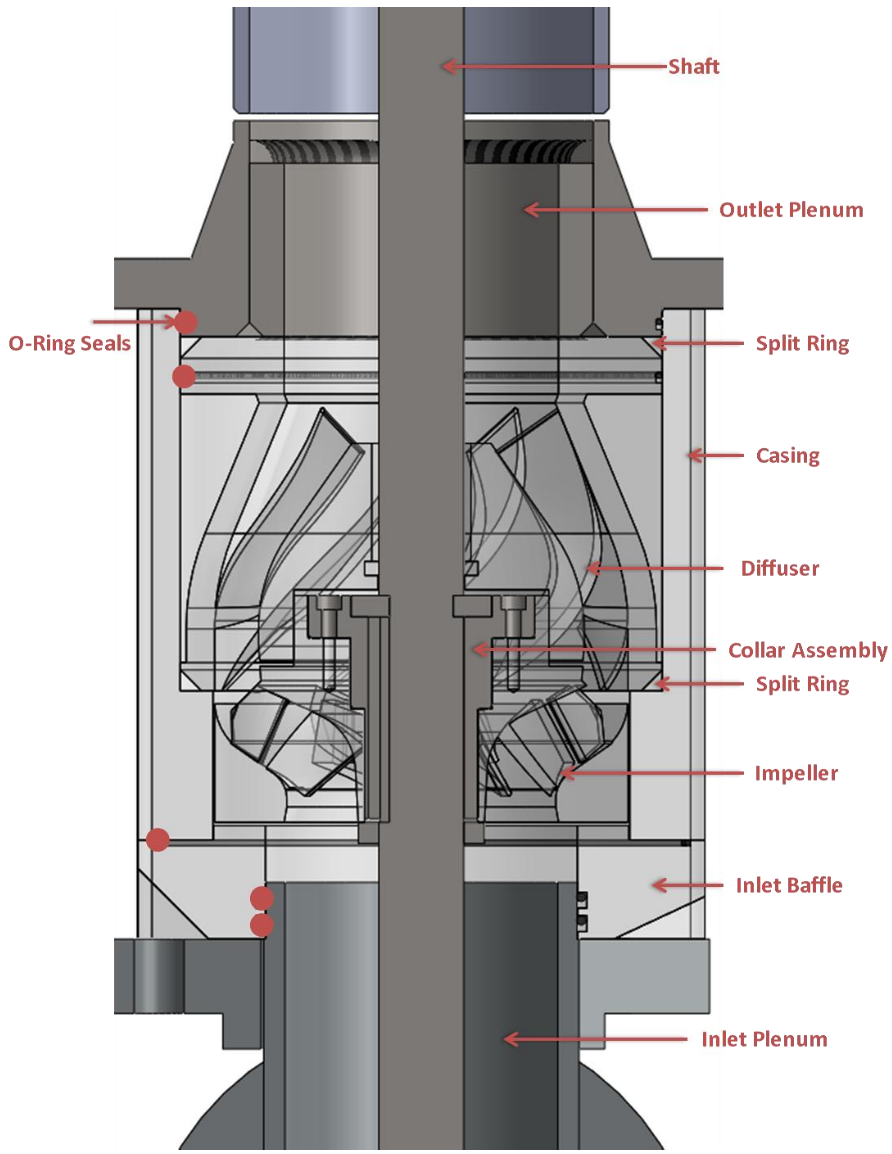

Figure 27 Flow and visualization containment with internals

The casing and flow containment is designed to allow safe high quality visualization of the impeller and diffuser of the pump with two phase flow. As previously discussed, the diffuser was designed as a canister. For the longevity of the testing facility, this enables researchers to remove the internals of the pump and insert other pump models for testing and visualization. The tolerances determined in the diffuser tolerance calculations allow the diffuser to properly fit into the casing. It rests on a set of split rings that center the diffuser and give an interference fit between the diffuser and the casing. Then a second set of split rings on the top of the diffuser act in the same manner. Finally, the outlet plenum exerts a seating force against the split rings and the diffuser. This allows the diffuser to maintain its location and not to slip or rotate during operation. Then the force is transferred through the lower set of split rings to the casing. The casing is then seated against a face O-Ring seal to the inlet baffle. The transparent portion of the pump is sealed via O-Ring seals between each plenum and the mating plastic component. The inlet plenum contains three angled faces designed to allow visualization into the eye of the impeller with little interference.

The dimensioning and tolerances for the split rings were calculated simultaneously with those of the diffuser. An engineering drawing is in Appendix C. The split rings were constructed of PMMA (poly-methyl methacrylate).

Two factors were critical for the design of the casing, shown in Figure 28; clarity, and safety or mechanical integrity. The original inlet design pressure of the facility was 400 psig. Fluids contained at that pressure are dangerous and proper engineering consideration is required. To determine a minimum wall thickness both stress calculations and ASME Boiler and Pressure Vessel code calculation were considered. When calculating hoop and longitudinal stress calculations in the casing, standard calculations for thin walled pressure vessels are not applicable because the ratio of the wall thickness to the radius is too large and the stresses are not uniform within the wall. ASME Boiler and Pressure Vessel (B&PV) Code Section VIII Division 1 has calculations for the strength and wall thickness requirements that account for both circumferential and longitudinal stresses, ASME [9]. The calculations require a design pressure, radius, joint efficiency (for welded vessels), and the allowable stress for the design material. There is one equation for the circumferential and longitudinal stresses, and the one that gives the larger required wall thickness controls the design. The maximum design pressure at the inlet of the pump was 400 psig. With a 70 psig maximum head, there was a safety factor of 30 psig added so the calculation design pressure was 500 psig. Also, polycarbonate does not appear in the B&PV materials property table, but the general trend in yield stress versus allowable stress is a 2:1 ratio. Thus, the 8500 psig yield strength for Makrolon polycarbonate, Omnexus [10], was reduced to 4250 psig allowable stress for design. The circumferential stress controlled the design with a minimum required thickness of 0.54”. The minimum wall thickness for the casing was ¾” allowing a generous safety factor in pressure containment. A small chamfer was added to the ID of the outlet of the casing to facility assembly with an O-Ring seal. Polycarbonate is commercially available up to 4” thick, and the casing was nearly 10” thick, so the manufacturer split the component into three parts and glued along the seam. A dimensioned engineering drawing of the casing is shown in Appendix C.

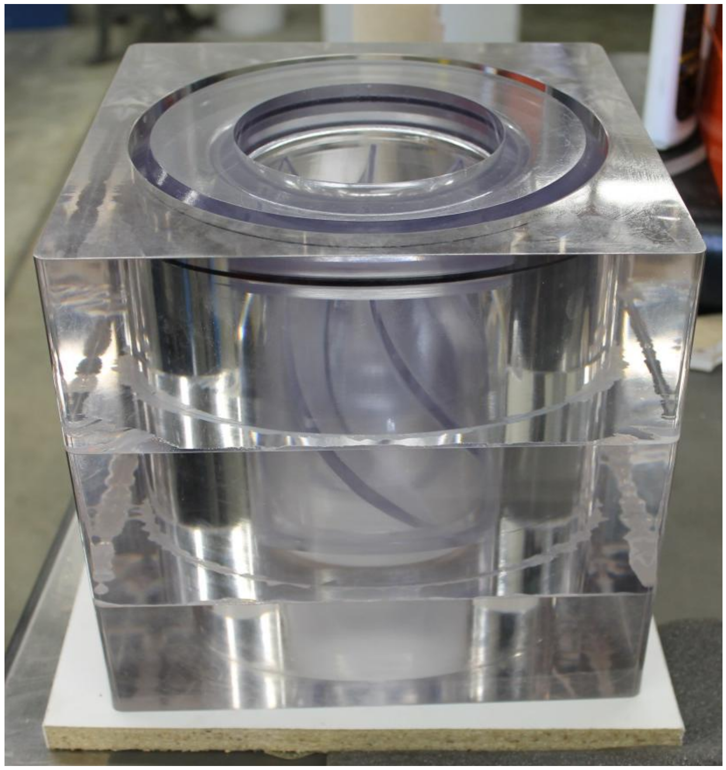

Figure 28 Pump casing with diffuser installed

The inlet baffle was added later in the design process to allow visualization at the eye of the impeller and is shown in Figure 29. To allow a view of the eye of the impeller, the slip on flange that pressed against the plastic pump parts was milled with a 45^0 notch removed. Then three angled viewports were added to the plenum design as shown in the figure. This was to allow different viewing angles of the impeller. One viewport was made with a 25^0 angle from the front horizontal face. That was to make parallel faces of the impeller hub and the viewport to minimize distortion of the visualization. Besides the viewport, O-Ring seals sealed against the inlet piping and a face O-Ring seal sealed against the casing. To give the required sealing force on the O-

Rings, end plates and tie rods attach to the end of the plenums to generate the required compressive force. A dimensioned engineering drawing of the inlet plenum baffle is in Appendix C.

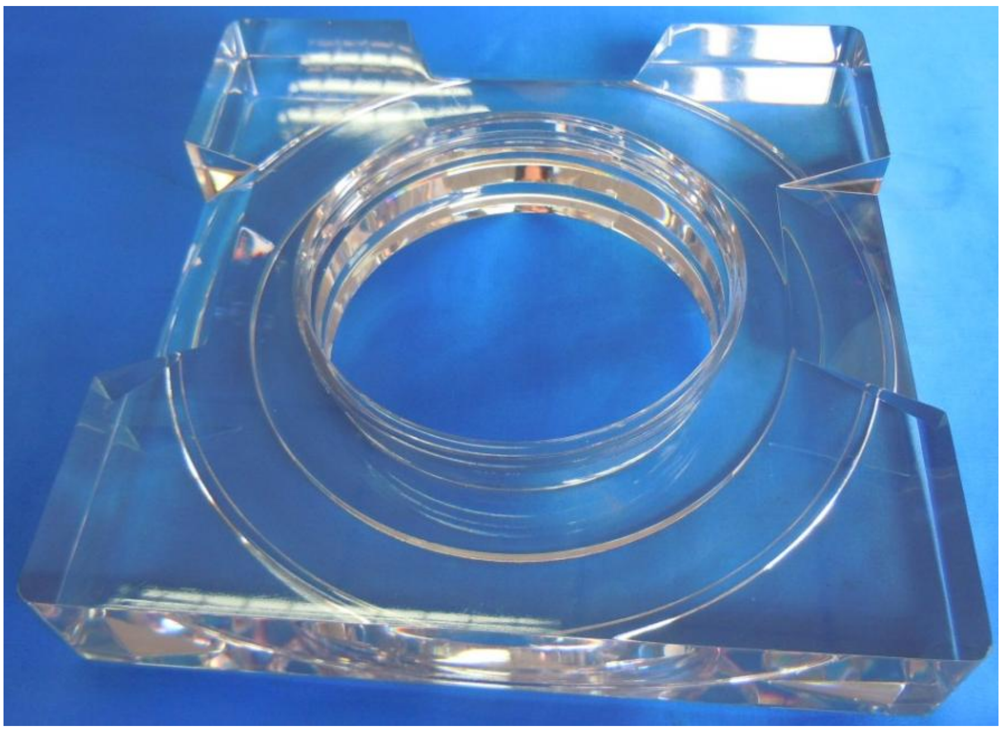

Figure 29 Inlet plenum baffle

3.2.4 Inlet and Outlet Plenums, Mechanical Seals, and Mounting Plates

The inlet and outlet plenums and the mechanical seals finish out the design of the wetted areas of the pump. All components are shown in Figure 30.

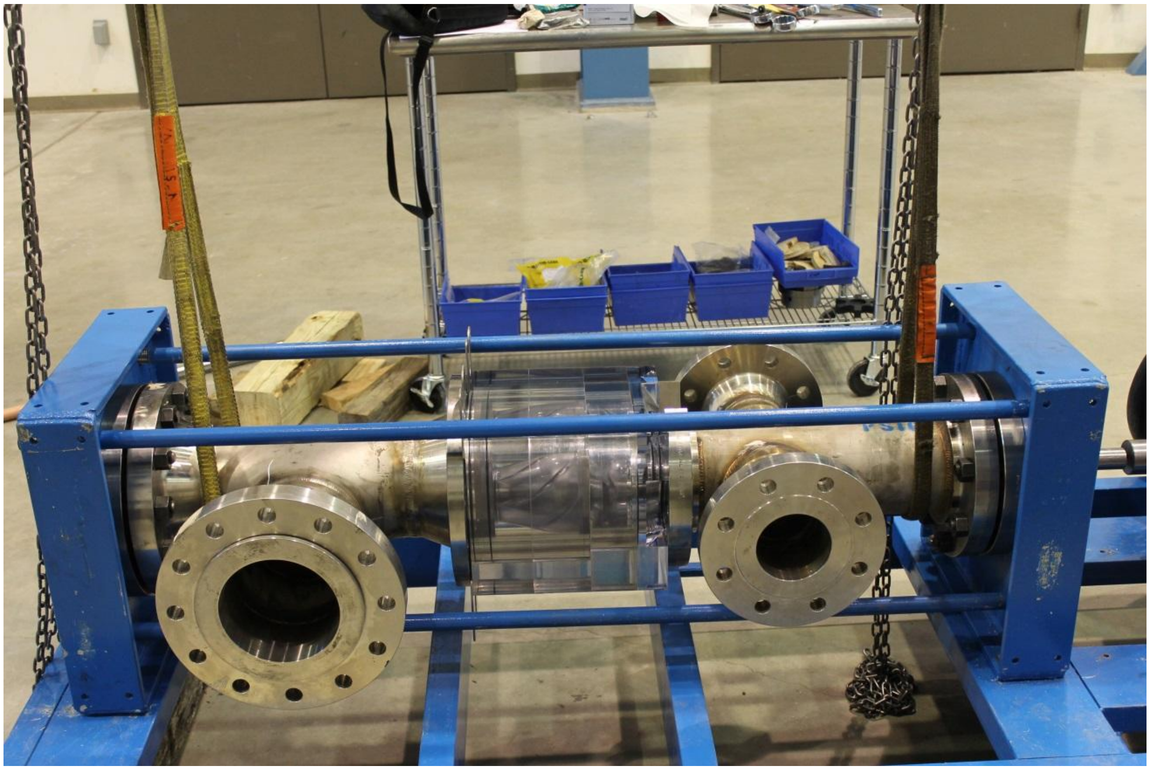

Figure 30 Entire pump assembly

The inlet plenum has dual opposing inlets with perforated plates for two phase flow mixing. The dual inlets also were designed to give balanced pressure forces and flow on the pump inlet and the shaft. There is a flanged connection where the shaft enters the pump. This is followed by a length of pipe long enough to ergonomically place the high speed camera in front of the viewport cut from the flange on the other end of the pipe. The inlet pipe is a 5” pipe chosen to match the inlet diameter of the G470 impeller eye. The milled out flange was welded on the inlet pipe with 1” of the pipe sticking out. The portion of the pipe that was sticking out was precisely machined to seal against the O-Rings in the inlet plenum baffle. Finally, a ½ NPT instrument and seal flush port was welded on the back side of the plenum. The piping was constructed and tested to ASME B31.3 Process Piping code by an independent supplier with certified personnel. Details of these requirements can be found in the 3.4 Piping Design section. Dimensioned engineering drawings of the inlet plenum are in Appendix C.

The outlet plenum has only one outlet with a lap joint flange (rotating flange) to account for any angular misalignment. To match the outlet diameter of the diffuser to mitigate any sudden geometrical changes in the flow and seal the pump, a custom fitting was designed. A 6”-300# weld neck flange was machined with an O-Ring seal that inserts into the pump casing. To maintain a uniform diameter of the outlet flow of the pump, an insert was machined and welded into the flange. The shaft exits the pump through a flanged connection. A ½ NPT instrumentation port was welded on the back side of the plenum as on the inlet plenum. The piping was constructed and tested to ASME B31.3 Process Piping code by an independent supplier with certified personnel. Details of these requirements can be found in the 3.4 Piping Design section. Dimensioned engineering drawings of the outlet plenum are in Appendix C.

At the shaft entrance and exit for both plenums is a flanged connection. Bolted to these flanges are mechanical seal glands that are modified from 300# blind flanges. The face mechanical seals are designed by my colleague Klayton Kirkland to handle 200 psig pressures, which limits the operating range of the pump design. The cut away view of the seal assembly is shown in Figure 31. There is a shaft collar with an O-Ring seal that the rotating face is mounted on. A set collar at the end of the shaft collar sets the axial position of the shaft and impeller in the pump. On the modified blind flange is set a spherical bearing protected by lip seals. The stationary face adapter bolts to the blind flange and supports the stationary face of the mechanical seal. Also, a seal flush port allows the removal of gas pockets which can coalesce around the faces and overheat the faces. Dimensioned engineering drawings of the mechanical seals are in Appendix C.

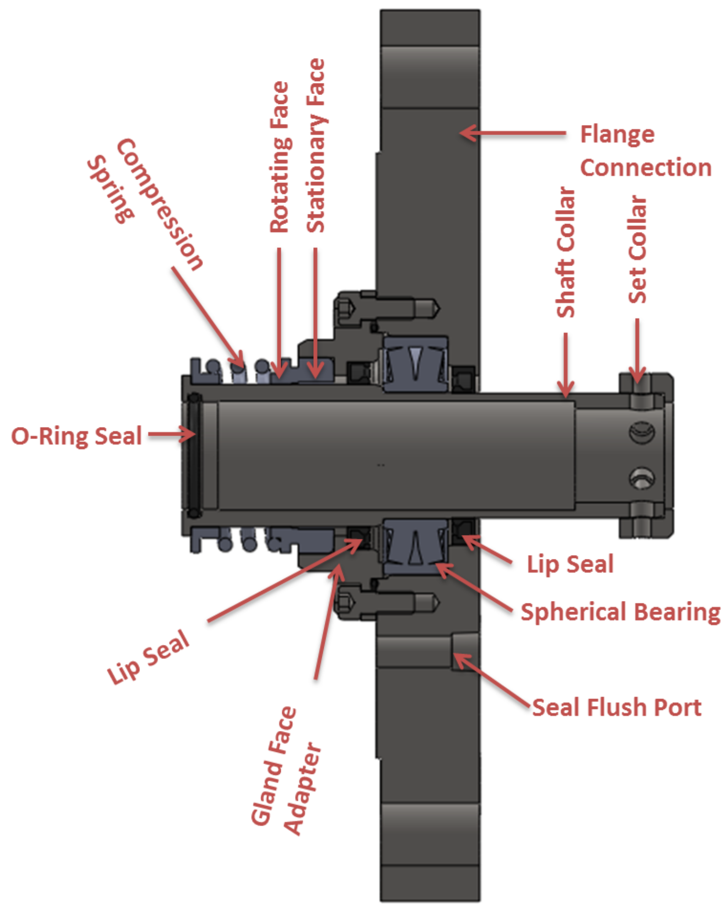

Figure 31 Mechanical seal diagram

3.2.5 Pump Mounts, Tie Rods, and Skid Design

Since the pump design includes a face sealed O-Ring, the necessary compression force to obtain a proper seal under operating conditions is necessary. Mounting plates and tie rods generate this necessary force. To first determine the required force, gasket sealing and operating stresses and subsequent compressive forces were calculated for elastomeric (O-Ring) gaskets. These calculations are from the ASME B&PV Section VIII Division 1 Appendix 2 code, ASME [9]. For elastomeric gaskets, the seating force is zero, so the required compressive force for the operating condition dominates. The required compressive force to contain 500 psig fluids (with safety factor and maximum pump head as discussed in 3.2.3) on a 2-271 size O-Ring was 34,500 lb_f. For four tie rods at 1" diameter with 8UNC threaded ends, the stress required is 14 ksi with a torque of 145 ft-lb on the nuts, ASME [11]. From ASME Section II-D, for general carbon steels, this leads to a safety factor of approximately 1.7, ASME [12].

With this known required loading, the mounting plates were designed. Several thicknesses of steel and arrangement of rib patterns were tested using Solidworks FEA analysis. The final design which gave a minimum FOS on the outlet and inlet of 1.5 and 1.4 respectively featured a 1" thick carbon steel plate with ½" thick and 4" wide ribs welded around the entire plate. The FOS diagram from the FEA of the inlet (right) and outlet (left) mount is shown in Figure 32.

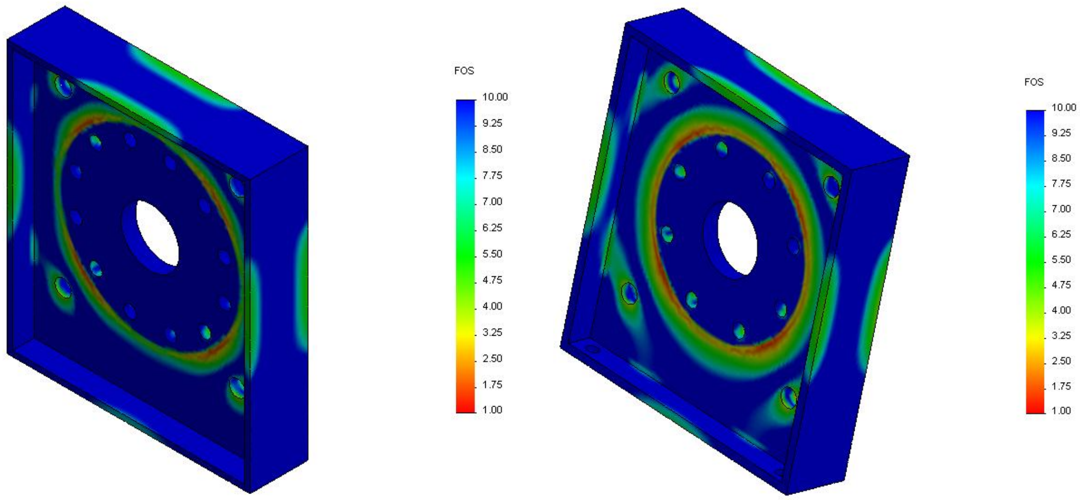

Figure 32 Inlet (right) and outlet (left) FOS diagram with tie rod loading.

The inlet and outlet mounts attach to the pump skid where both the entire pump and motor are aligned. This skid was modeled after API horizontal mount pump skids. This allowed the motor to be mounted to the skid in the horizontal position and hoisted to the vertical operating position. Once in the vertical operating position, it is bolted into place on a support structure and the pipes and pump are attached to the skid for testing and operation. The skid with the mounting plates, tie rods, and motor are shown in Figure 33. Dimensioned engineering drawings of the pump mounts and skid are in Appendix C.

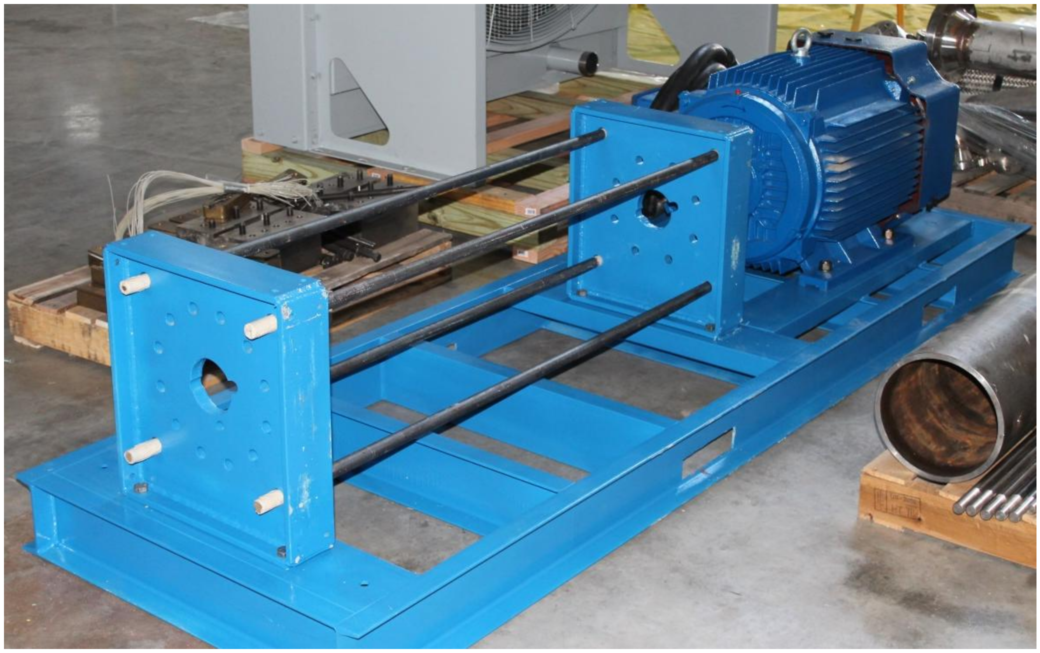

Figure 33 Skid, motor, mounting plates, and tie rods

3.2.6 Power and Electrical Design

An electric motor was necessary to power the shaft of the clear G470 MVP ESP that was constructed. By sizing the motor, the electrical system to power the system was also sized. The work done by Kirkland [5] required the use of a 250 hp motor. Since that G470 MVP was three stages, by linear scaling 83 hp is required for one stage. The nearest common motor size is 100 hp requiring 109 fully loaded amps (FLA), 480 volt, and 3 phase power. For powering the pump, a horizontal mount TEFC motor was used for safety and ease of mounting and alignment. To power that motor, a 100 hp VFD was required. With the 20% required safety factor, a 130 amp minimum system requirement was set. From there, a 200 amp busway switch and a 150 amp shut off switch within the testing facility were procured. To facilitate pump maintenance and modifications, a 150 amp receptacle assembly and flexible cord for the motor were procured.

The final component required to power the pump was a coupling from the motor to the pump. Since the pump has spherical roller bearings and set collars between the seal assembly and the shaft, all axial force generated in the pump was transferred to the seal glands and the main body of the pump. Knowing this, no thrust considerations are required. For effectiveness, ease of alignment, loose alignment requirements, and simplicity of procurement and assembly, a three jaw coupling with a nitrile rubber spider was used, as shown in Figure 34. The specifications with the coupling allowed for a 0.015" parallel misalignment and a 2^0 angular misalignment between the shafts. A coupling guard was also manufactured and attached as a safety precaution.

3.3 Structural Design

For effective operation of the test facility two major structural systems were designed and constructed. The principle system designed and built was the rig support system. It included piping support, pump skid support, and a monorail trolley lift system to facilitate construction and assembly. The other system was a piping support structure for securing the piping modification from the existing MVP rig from Kirkland"s [5] work. Both were built in a modular style that required only assembly in the cell. This was done to limit field welding necessary in the testing facilities.

Figure 34 Three jaw coupling for shaft power transfer

3.3.1 Rig Support Structure Design

The rig support was designed with the objectives to adequately fix and lift the pump skid assembly safely, mitigate any vibration issues, and support the piping and pipe supports. The general layout of the rig support was a rectangular frame constructed of W4X13 „I-beam" structural steel. The frame was anchored to the concrete foundation of the Turbomachinery Laboratory and extended to near the cell roof to accommodate a suspended I-beam (W5X18) with a monorail overhead chain hoist crane. This design was implemented to lift the horizontal pump skid into the vertical operating position. Also, several cross beams gave lateral support to the structure and attachment points for pipe supports. A support frame for securing the pump skid assembly attached to the rear to columns. This frame contains two L2X2X1/4 steel runner guides for alignment of the pump skid assembly during lifting. The frame also includes 8 bolting holes for securing the pump skid assembly in the vertical operating position. Grade 8 bolts were used for all construction on the rig support structure. The completed structure is shown in Figure 35.

University and OSHA regulations require that the structure be built and tested to ANSI B30.2 code. To satisfy these requirements, the structure was analyzed with FEA completed by Solidworks Simulation. The entire pump skid, pump, and motor assembly weighed 2350 lb_f per a measurement by an inspector from Advanced Overhead Cranes. The general analysis assumptions used in the FEA are as follows:

1. The load tested was 2500lb_f acting in a vertically down direction.
2. For the analysis of the track, the force was acting on the extreme end of the beam (at the end of the overhung region).
3. For the analyses of the headers, the force was acting solely on one of the headers; it was positioned directly below the bolt connection between the headers and the track.
4. For bolted connections in tension, the force was assumed to act on the washer surface only when acting on the beam.
5. The piping load was shared uniformly by the lower headers and the piping support beam. All were connected to the columns through a force acting downward on the bolt holes.

Figure 35 Pump rig support structure with monorail crane

Each component was independently analyzed and the minimum FOS was 2.28. After assembly of the structure, a 2 ton hoist and trolley were added to the monorail. The entire crane was then certified to the ANSI B30.2 code by an independent inspector from Advanced Overhead Cranes. Engineering drawings of the rig support structure are found in Appendix C.

3.3.2 Piping Support Structure Design

The piping support structure was principally designed to support the 600 lb_f outlet control valve and the tee where the two flows from the test facilities converge which weighs another 270 lb_f. The structure also supports all piping mating to these components. To determine structural feasibility analytical beam stress and deflection calculations were used. The columns were constructed of S4X7.7 structural steel beam, and the cross members were constructed of S3X5.7 beam. L3X5X1/4 and ¼" plate were used for brackets allowing the structure to be assembled without any field welding. For rigidity, the structure was anchored to the concrete foundation. Grade 8 bolts were used for all construction of the piping support assembly. Figure 36 shows the piping support design. Engineering drawings of the piping support structure are found in Appendix C.

3.4 Piping Design

A fairly complex piping system was necessary for connecting the existing inlets and outlet to both the original MVP test facility and the MVP Visualization facility and directing the flow to the appropriate facility. The inlet water and air piping first pass through control valves. Then tees were designed with manually actuated butterfly valves attached to control the flow direction. On the existing test rig, a double braided flexible hose connects the inlets to the pump directly from the butterfly valves. On the MVP Visualization rig, the butterfly valves connect to braided hoses and then hard piping to pass through the wall in the laboratory facility.

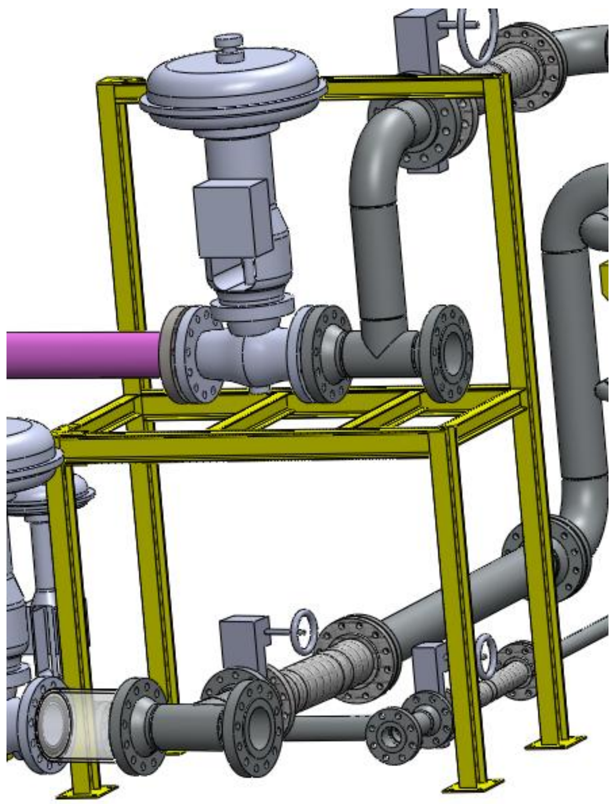

Figure 36 Piping support design

After passing through the wall, the inlets split for symmetric flow into the inlet of the pump. The air inlet meets the water inlet at two mixing tees and has two swing check valves to prevent water back flow in to the air line. At the outlet of the pumps, both pass through a combination of hard piping and braided hoses through butterfly valves and another flow directing tee. Then from the tee, the flow passes through the control valve and into the separator tank. A labeled diagram of the piping system is shown in Figure 37. Engineering drawings of the piping support structure are found in Appendix C.

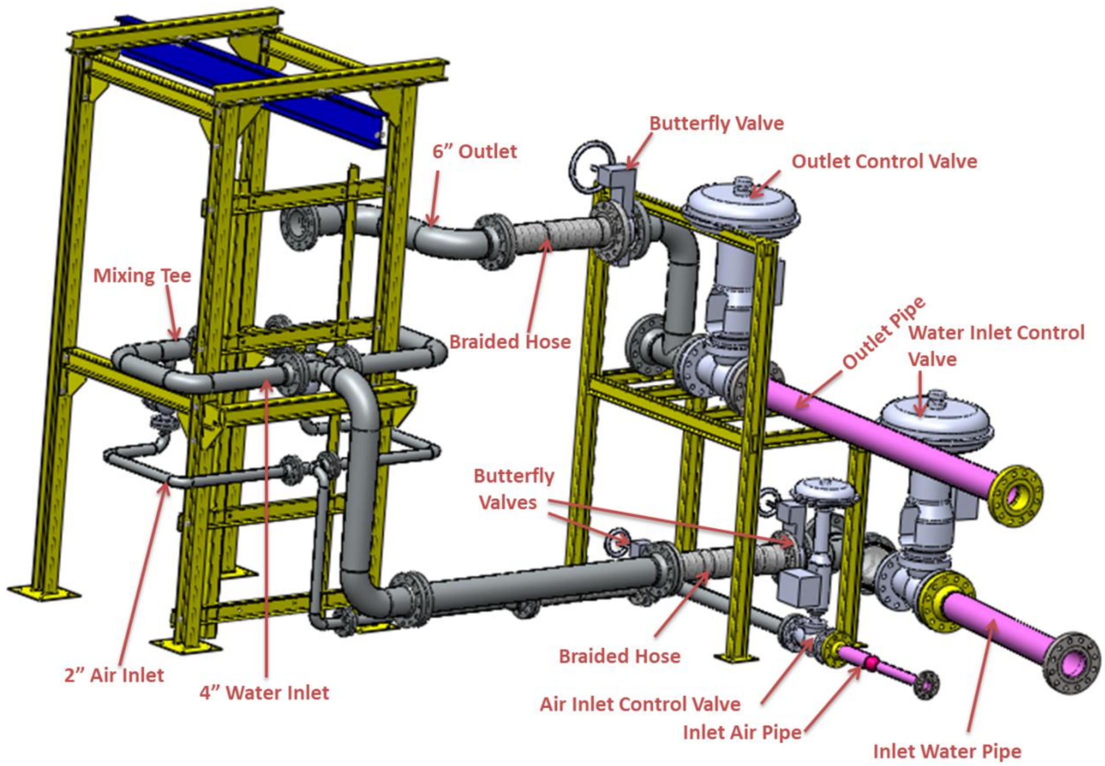

Figure 37 Piping design diagram

The piping was designed to the ASME B31.3 Process Piping code to ensure safety and reliability. To minimize corrosion and rust in the system and the turbidity of the water, 304L stainless steel was used for all piping components. This allows the best clarity of the test fluid in the system for flow visualization in the clear pump. The maximum allowable working pressure (MAWP) of the tank is 400psig, but earlier design of the piping by Kirkland [5], anticipated testing pressures up to 1000psig. Thus, class 600 flanges and schedule 40 piping were used for the existing piping. Maximum testing pressures are now 400 psig with possible 650 psig pressures occurring between the outlet of the MVP test rig and the control valve. Flanges in the existing loop were maintained at class 600, but flanges in the Visualization loop were class 300. All piping was maintained at schedule 40 thickness. 6” piping was rated to 575 psig, but with 300# flanges may be re-rated to 600 psig below 200 ^{0}F. 6” piping rated to 575 psig with 600# flanges may be re-rated to 1050 psig below 200 ^{0}F (well above the maximum outlet pressure generated in both test facilities). 2” and 4” piping was rated to 600 psig and was limited by the flanges.

For construction, all mill test reports (MTRs) were included and all welders and welding practices were certified to the applicable codes. Also, NDE was specified in accordance with the ASME code. 100% visual and dye penetrant testing were done on the welds. On 10% of the welds radiographic testing was completed. Finally, a hydrostatic test of 1.3 times the MAWP for each pipe was completed. These stringent fabrication and testing requirements were also applied to the inlet and outlet plenum discussed in 3.2.4 Inlet and Outlet Plenums, Mechanical Seals, and Mounting Plates, except that no hydrostatic test was required since no method for sealing the open pipe ends was available.

3.5 Instrumentation and Data Acquisition

Two major control and instrumentation systems were incorporated into the visualization facility. They were: system controls and visualization equipment.

3.5.1 System Controls

The system controls described in 3.1 Facility Overview were used in conjunction with this test facility. Only pressure and temperature probes were added at the inlet and outlet of the pump. During testing, it was found that the air control system inherited from the original MVP test facility did not have the required low range. A small turbine flowmeter, and manually operated control valve was temporarily added in the air inlet line. Also, the cracking pressure of the ASME code check valves was large enough to cause non-uniform air flow rates in the line and a surging type of performance from the pump. To mitigate this problem, manual operated ball valves were used to isolate the air line from the water line when not in operation. A listing of the instrumentation added to the test loop is shown in Table 8. One pressure transducer and thermocouple was added to the taps in the inlet and outlet plenums and a pressure gauge was added at the outlet of the pump. The calibration curve for the pressure transducers is shown in Appendix D.

Table 8 Instrumentation on MVP visualization rig

Instrument Description	Manufacturer	Part No.	Units	Range	Uncertainty	Output
Type T Thermocouple	Omega	TQSS-116U-12	^{0}F	-325 to 662	1.8 ^{0}F or 0.75%	-6 to 21 mV
Air Turbine Flowmeter	Omega	FTB-933	ACFM	1 to 10	1 %	Sine Wave (Hz) – 30mV P-P
Pressure Transducer	Omega	PX429-250GI	psig	0 to 250	0.08 %	4 to 20 mA
Pressure gauge	Omega	PGT-45B-150	psig	0 to 150	0.25 %	0.5 psig subd. dial

National Instruments LabVIEW was used with NI cRIO – 9074 chassis and various modules for voltage input, thermocouple input, and control outputs. This data was acquired by a LabVIEW Virtual Instrument, which is shown in Figure 38.

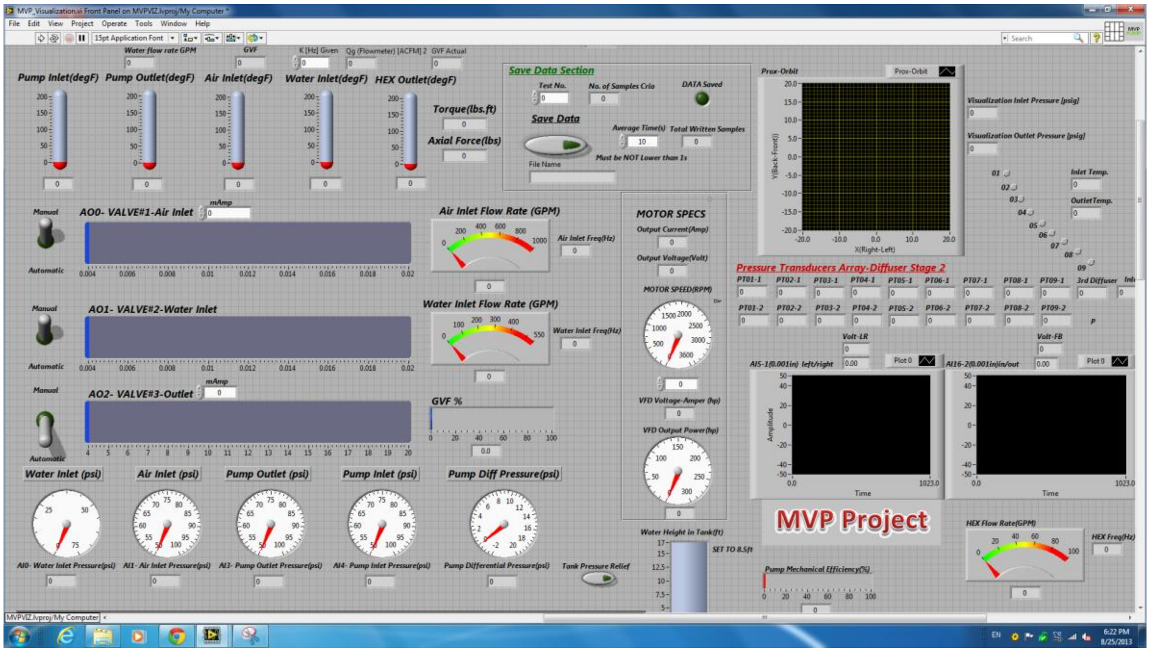

Figure 38 LabVIEW virtual instrument modified for visualization

For accurate measurement and control of the air inlet flow, a code was added to the LabVIEW VI to convert a desired GVF to the required air flow in ACFM and the output of the flowmeter in Hz. The interface is shown in Figure 39. The code converted the desired GVF into required air flow by using the water flow rate, the inlet and outlet air pressures and temperatures to determine the required flow through the meter. Then using the calibration curve in Appendix D, the desired output frequency in Hz was calculated.

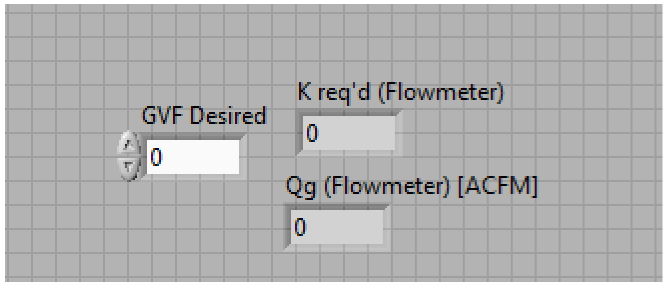

Figure 39 Air flow control calculator

3.5.2 Visualization Equipment

To ensure quality visualization results, an advanced camera and lighting system was used. With expected test speeds ranging from 1800 to 3600 rpm, and desired frame rates from 5,400 fps to 21,600 fps to enable a photograph taken every 1^0 to 2^0 of rotation, a suitable form of high speed photography was necessary. The camera used was the Phantom V711 manufactured by Vision Research. It contains a (complementary metal oxide semiconductor) CMOS sensor and has a maximum resolution of 1280x800 and with a reduced resolution has a maximum shutter speed of 680,000 fps. With high speed photography, due to low exposure times, much higher light intensity is required. To provide adequate light, two halogen light sources were used to illuminate the region of interest during photography. These were the OSL1 lights manufactured by ThorLabs which produced 40,000 foot candles of light. The lights and V711 camera are shown in Figure 40 during testing of the MVP Visualization rig.

Figure 40 V711 Phantom camera and ThorLabs OSL1 light sources during testing

4 PROCEDURES

General procedures for pump assembly, start-up, and shut-down operations, and draining were necessary to operate the complex test loop.

4.1 Start-Up Procedure

1. Ensure all personnel employed on this project are fully trained on this SOP and all of the required safety and emergency measures, and are wearing the appropriate personal protective equipment (PPE) while working.
2. Ensure all guards and safety protection devices are securely in place and in proper working condition.
3. Ensure all gate valves to the MVP Visualization and MVP rigs are in the closed position. These are the air and water inlet valves and the two-phase outlet valves. A position gauge clearly shows whether the valve is closed or open and must read closed.
4. Ensure that instrument air which controls pneumatically operated control valves is pressurized and working properly.
5. Initialize the Data Acquisition software (LabVIEW) and ensure that instrumentation is working properly.
6. Troubleshoot any instrumentation as necessary. Consider restarting power on all powered instruments and/or the NI cRIO chasses.

7. Fill tank with water to desired level using domestic water source and data acquisition information (LabVIEW VI). Use valve at instrumentation tap on 6” water inlet line connected to domestic water source.
8. Pressurize tank with air compressor to desired level. Maximum allowable pressure for the pump (limited by the mechanical seals) is 200 psig. To pressurize, turn compressor in laboratory test cell to on and close the bleeder valve. Then open the ball valve that runs to the 2” air inlet line. Once proper pressure has been reached, close ball valve on the 2” air inlet line, turn the compressor off and open the bleeder valve on the compressor.
9. Initialize the filter, pump, and heat exchanger unit and ensure that line valves are open and all components in proper working order. Close the ball valve on the recirculation pump drain. If the outside ambient temperature is near or above 100 ^{0}F, do not initialize the filter and heat exchanger due to lack of heat removal ability. To initialize the heat exchanger, turn on electrical switch on exterior of building near door. Then pull red emergency stop switch on heat exchanger unit labeled „MVP." The heat exchanger fans should be activated. Next, check that ball valves on the filter and pump recirculation loop are open. Turn switch adjacent to VFD near door on interior of building to on. If the pressure on the tank is between 25 and 80 psig run the pump at 30 Hz on the VFD. If above 80 psig, run the pump to 60 Hz.

10. Attach motor power cord to receptacle and lock mechanical latches into place. Turn on variable frequency drive (VFD) and ensure that the drive is functioning properly.
11. Crack open butterfly valve for water inlet to pressurize pump to tank pressure.
12. Bleed air from mechanical seals with ball valve located on top of outlet mount. Open up seal flush valve located beside the bleeder ball valve located on top of the outlet mount.
13. Fully open all butterfly valves (air and water inlet and outlet) to the MVP Visualization rig while leaving the valves on the piping going to the MVP rig closed.
14. Prepare for data acquisition; get all instrumentation and visualization equipment set correctly.
15. Set the VFD to the desired speed and while giving an audible countdown and informing all personnel and visitors that the motor will commence running the pump.
16. VFD operator must stay near the VFD stop switch or the emergency power shut down switch in the cell until the motor and pump successfully attain steady operating conditions.
17. Perform all tests and necessary research work. Limit temperature of the fluid to less than 105 ^{0}F to ensure the strength and rigidity of the polymer components of the rig.

18. If operating with the 1-10 ACFM flowmeter (Omega model FTB-933), to introduce air for two phase flow, first ensure that the 3” control valve and 3” butterfly valve are open. Attach a hose from the air bleeder line near the flowmeter and control valve to the facility drain. Open the bleeder line and drain all liquids. Then open the control valve approximately 1-2 turns and simultaneously open the ball valve inline between the manual control valve and the bleeder valve. Have the bleeder valve only cracked and crack the ball valves near the air and water mixing tee (near the pump inlet). Simultaneously close the bleeder valve and check to verify that air is entrained in the pump.

4.2 Shut-Down Procedure

1. Ensure all personnel employed on this project are fully trained on this SOP and all of the required safety and emergency measures, and are wearing the appropriate personal protective equipment (PPE) while working.
2. Ensure all guards and safety protection devices are securely in place and in proper working condition.
3. If two phase flow testing is occurring with the 1-10 ACFM flowmeter, close the ball valves at air and water mixing tee near the pump simultaneously with the ball valve directly after the manual needle control valve. This prevents water from back flowing into the turbine flowmeter, which could ruin the turbine flowmeter.

4. With the hose attached to the bleeder, open the bleeder valve to remove any liquids from the air line.
5. Shut down the motor by pressing the stop button on the VFD. Wait for the motor to come to a stop.
6. Close all butterfly valves to the MVP Visualization rig: 6” inlet valve, 3” inlet valve, 6” outlet valve.
7. Shut down heat exchanger pump by pressing the stop button on the VFD. Also press the emergency stop button on the heat exchanger to stop the fans and close the line valves in the subsystem as needed (typically not necessary).
8. Turn off the interior and exterior switches to the recirculation pump and heat exchanger fans.
9. Stop LabVIEW VI.
10. Turn off electrical switch to the right of the VFD.

4.3 Draining Procedure

Multiple draining procedures may be completed on the MVP Visualization test facility. They are described below.

4.3.1 Entire System Drain

1. Discharge pressurized air from system. Open the vent valve on the top of the tank with the chain handle. This step is the most critical, because opening any other drain valves under pressure could potentially injure an

operator or equipment due to large amounts of high velocity air or water being depressurized.

2. Leave butterfly valve on bottom of tank open.
3. Attach hose to drain connection on water inlet line.
4. Open valve and drain water to outside storm drain.
5. Wait for at least 1 minute and carefully open the vent on the outlet mount of the pump to release any air and prevent vacuum formation.
6. Open plug in bottom of Y-strainer to drain low lying water.
7. Close all opened plugs and drains to maintain clean system.

4.3.2 Pump Drain with Modified Air Flow Line

1. Discharge pressurized air from system. Open the vent valve on the top of the tank with the chain handle. This step is the most critical, because opening any other drain valves under pressure could potentially injure an operator or equipment due to large amounts of high velocity air or water being depressurized.
2. Check that inlet and outlet butterfly valves to Visualization test facility are closed.
3. Open ball valve at air and water mixing tee.
4. Attach hose to drain near flow control valve.
5. Check that the ball valve downstream from the needle control valve is closed. This ensures that no water will flow into the turbine flowmeter.
6. Carefully open the drain valve.

7. Wait for at least 1 minute and carefully open the vent on the outlet mount of the pump to release any air and prevent vacuum formation.
8. Close all opened plugs and drains to maintain clean system.

4.3.3 Pump Drain with No Air Flow Line Modifications

1. Discharge pressurized air from system. Open the vent valve on the top of the tank with the chain handle. This step is the most critical, because opening any other drain valves under pressure could potentially injure an operator or equipment due to large amounts of high velocity air or water being depressurized.
2. Check that inlet and outlet butterfly valves to Visualization test facility are open.
3. Close butterfly valve on bottom of tank.
4. Attach hose to drain connection on water inlet line.
5. Open valve and drain water to outside storm drain.
6. Wait for at least 1 minute and carefully open the vent on the outlet mount of the pump to release any air and prevent vacuum formation.
7. Open plug in bottom of Y-strainer to drain low lying water.
8. Close all opened plugs and drains to maintain clean system.

5 RESULTS

Although visualization was the primary goal of the study, other analyses pertinent to standard pump testing were completed. During the design and testing, a vibration analysis for determining natural frequency was completed. Also, as with any pump testing, some performance curves were generated primarily the head-flow rate curve for pure water and some limited GVFs.

5.1 Natural Frequency Analysis

One concern with designing any rotating machine is the natural frequency of the rotor. This natural frequency sets the critical speed of the machine, which the condition when the rotational speed of the machine is on or near the natural frequency. At this condition, it is possible for vibrations to grow exponentially. This can lead to catastrophic failure of the machine component. To mitigate catastrophic failure, during the design and fabrication of the G470 MVP visualization pump, a numerical and physical natural frequency analysis was completed. The XLTRC2 software was used to break the shaft into 35 elements. The locations of the bearings were input and the mass, location, and moments of inertia of the impeller were input to the analysis. The software returned an expected natural frequency of 2080 rpm. An analysis of the simplified bearing, mass, and shaft system was also completed using the basic principles. The equivalent stiffness of a simply supported beam and equivalent mass of a shaft for the rotor were calculated. From there, the root of equivalent stiffness divided by mass gave a natural frequency of 2160 rpm. The results of the two analyses agreed within 4%, but final verification was completed using the modal impact test procedure. First the inlet and outlet mounts were attached to the mechanical seal assemblies. The shaft with the impeller hub and impeller was mounted between the mounts and seals for testing. Accelerometers were attached to the shaft near the impeller and the outlet mechanical seal. This allowed a comparison of the magnitudes of the vibration signal at each location. The accelerometers were attached to a two channel spectrum analyzer. A rubber dead blow hammer was used to excite the rotor. The test set up is shown in Figure 41.

By observing the frequency composition of the acceleration signal and comparing the magnitudes, the natural frequency and effect of running at the critical speed were predicted. As shown in Figure 42, the natural frequency peak occurred at 39.2 Hz or 2352 rpm. The measured natural frequency was less than 9% different than that calculated with basic principles, but is the actual natural frequency. The difference between the analytically determined natural frequencies and the experimental natural frequency is due to inaccuracies in the modeling. Figure 42 also shows the relative difference in magnitude of the two acceleration signals. The acceleration at the impeller assembly is approximately four times larger than that at the outlet seal. The outlet seal signal is below the impeller signal in Figure 42. The 4:1 ratio should not be large enough to lead to catastrophic failure in operation at the critical speed. Also, in pumps, the water and especially the two phase flow will dampen the vibrations of the rotor.

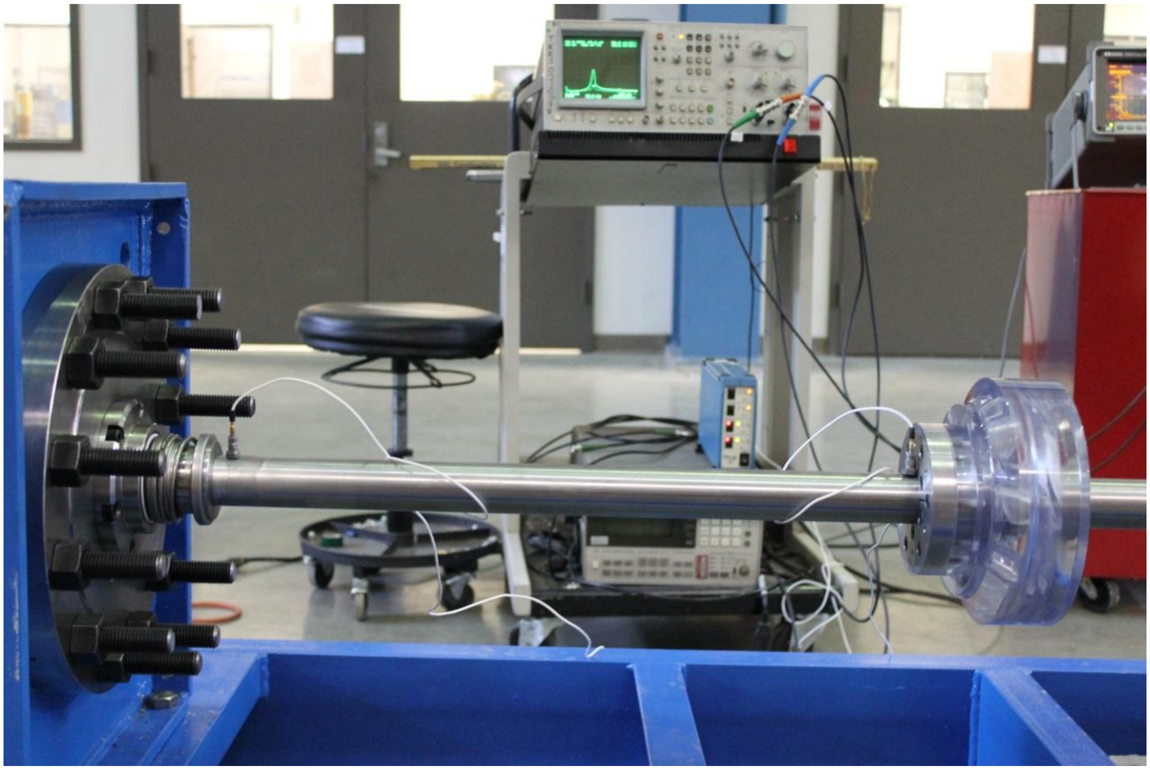

Figure 41 Rotor modal impact test set up

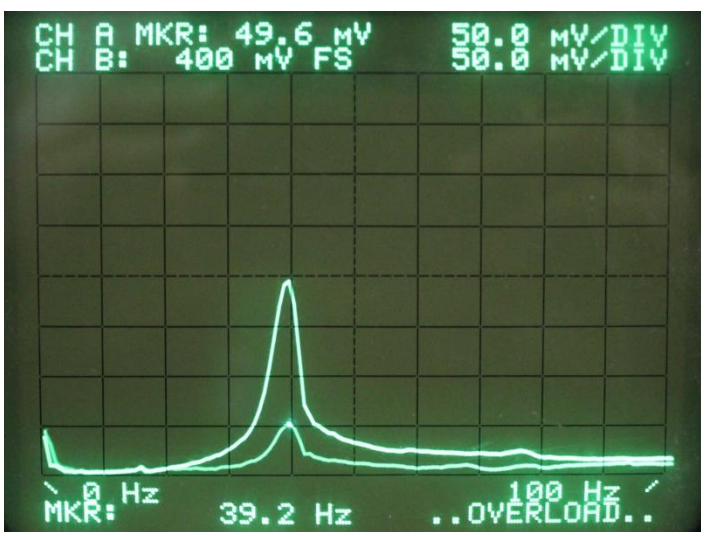

Figure 42 Acceleration signals from modal impact test on pump rotor

5.2 Performance Curves

To characterize the MVP visualization facility and head losses intrinsic to the test loop, data was collected to construct a system curve with pure water. This curve, Figure 43, shows the variation of head losses with flow rate of the entire visualization flow loop from the feed line from the tank to the return line to the tank. All tests in this work were completed at 1800 rpm. For the system curve, inlet pressures varied between 55 and 60 psig with pure water (0% GVF).

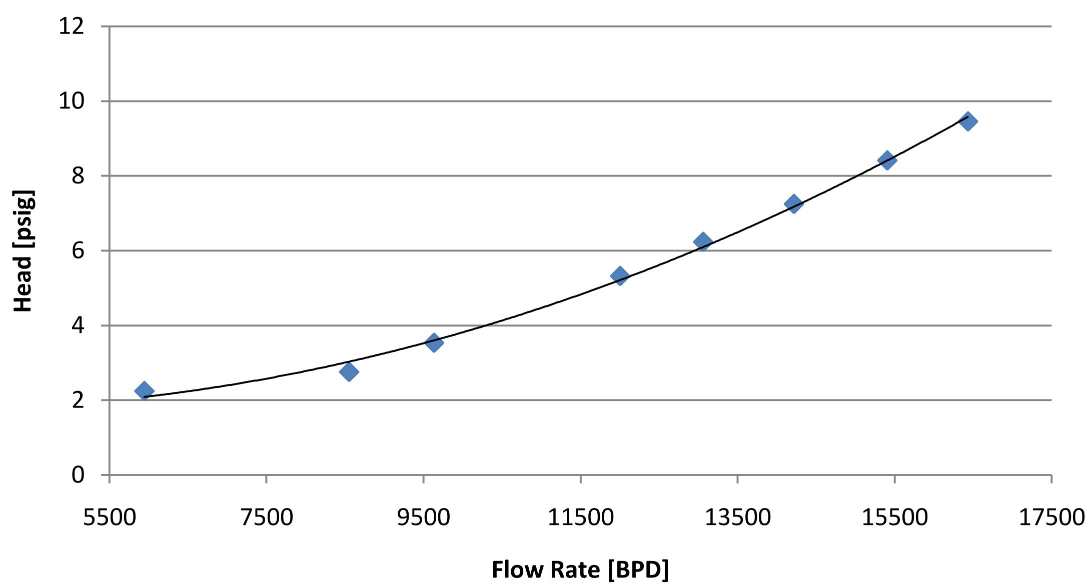

Figure 43 MVP Visualization system head loss curve

After the system curve had been determined, performance curves of the pump with pure water (or at 0% GVF) and at the testing condition of 2% GVF were constructed. Due to flowmeter restrictions and pump head limitations, the testing envelop was limited to a minimum of approximately 230 gpm and a maximum of approximately 510 gpm of water. The inlet pressure for the pure water performance curve varied between 54 and 61 psig. For the 2% GVF performance curve, the inlet pressure was maintained at pressures between 66 and 70 psig. The two performance curves are shown in Figure 44. The 2% GVF curve was determined to illustrate the performance curve where the diffuser visualization was completed.

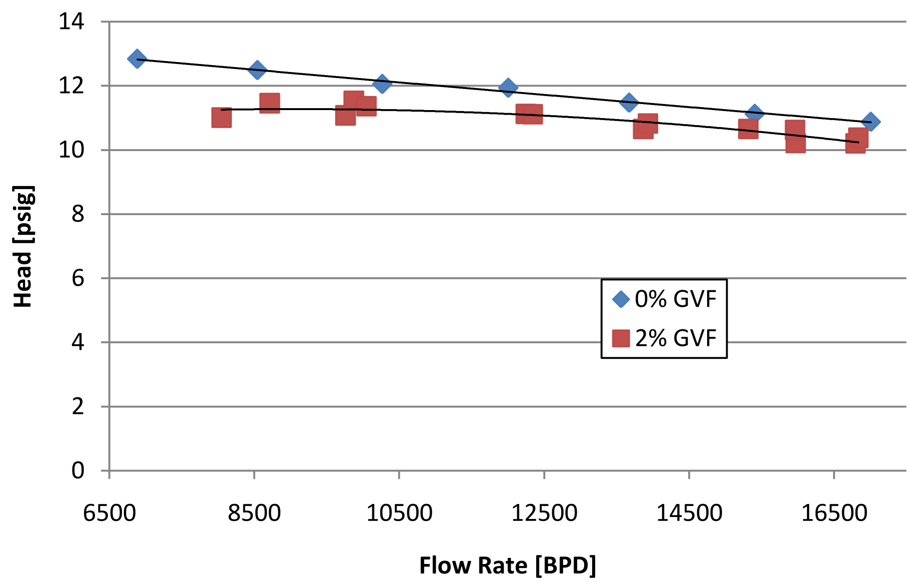

Figure 44 Pump performance curves

5.3 Impeller Visualization

To complete impeller visualization, the viewport located in the inlet plenum baffle was employed. The high speed camera was placed parallel to the viewport with an 18-55mm lens. Several lighting schemes were attempted with the final arrangement being two OSL1 lights pointed at the front of the impeller directly above the lens with one pointing at a slight downward angle toward the viewport. A still photograph from the high speed video is shown in Figure 45. The blades and blade rotation direction are labeled. A recirculation zone around the secondary blade was observed as labeled in the figure. No recirculation around the secondary blade was predicted by the Marsis“ [7] CFD simulations. The photography was taken looking upwards at the eye of the impeller at the blades, with an emphasis on the flow through the gap between the split vanes. The visualization was completed with a trace of air seeded into the flow from 110 psig shop air passed through a regulator at the inlet plenum tap. The pump was operating at 1800 rpm with a 60 psig pump inlet pressure. The liquid flow rate is 13,700 bpd and there is a trace GVF present.

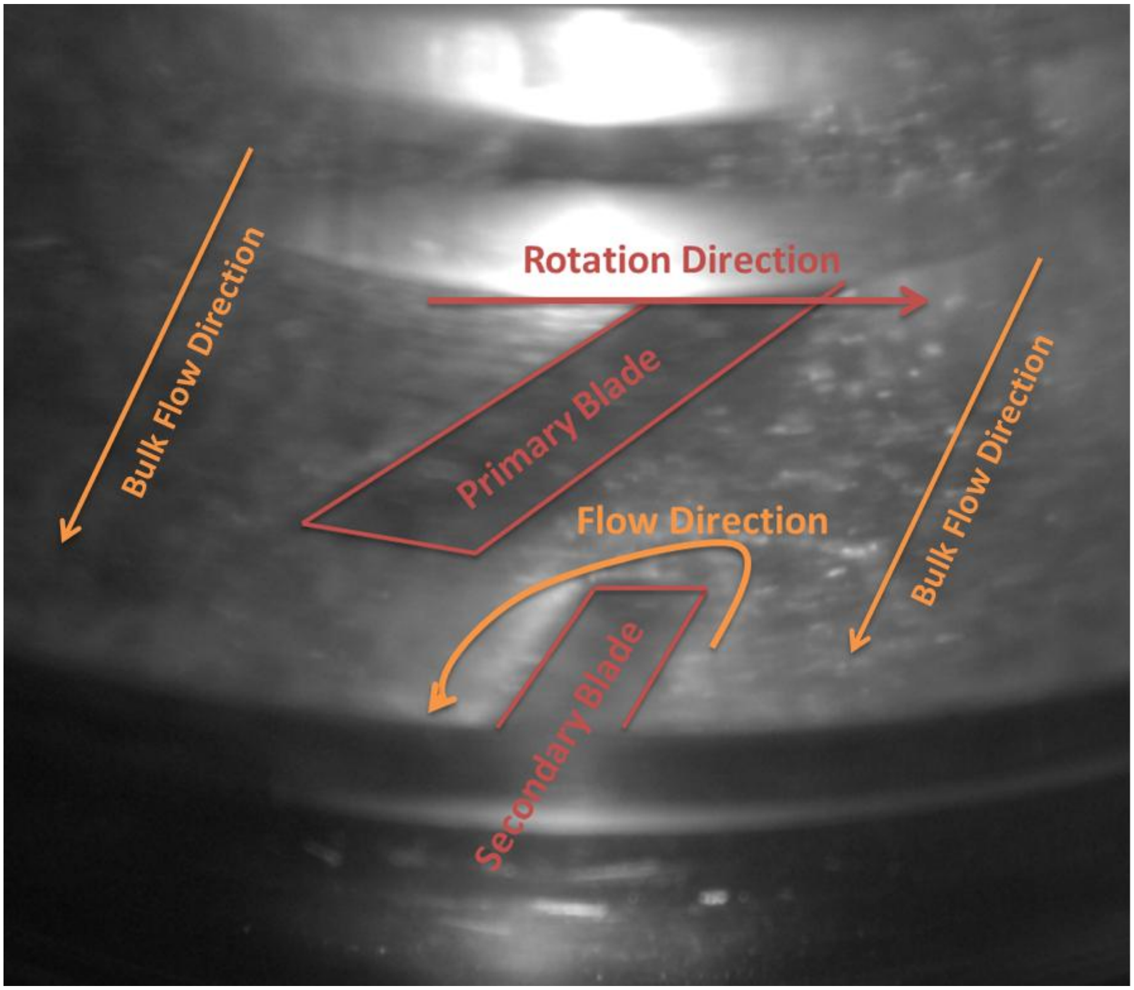

Figure 45 Impeller eye split vane recirculation visualization at 1800 rpm, 13700bpd, trace GVF, 60 psig inlet

A video of the impeller eye is shown below in Figure 46. The video was taken at 10,800 fps or one frame per 1^0 of impeller rotation. The exposure time for each frame was 91.5 μs and the resolution was 800X600 pixels with a 12 bit grayscale pixel resolution.

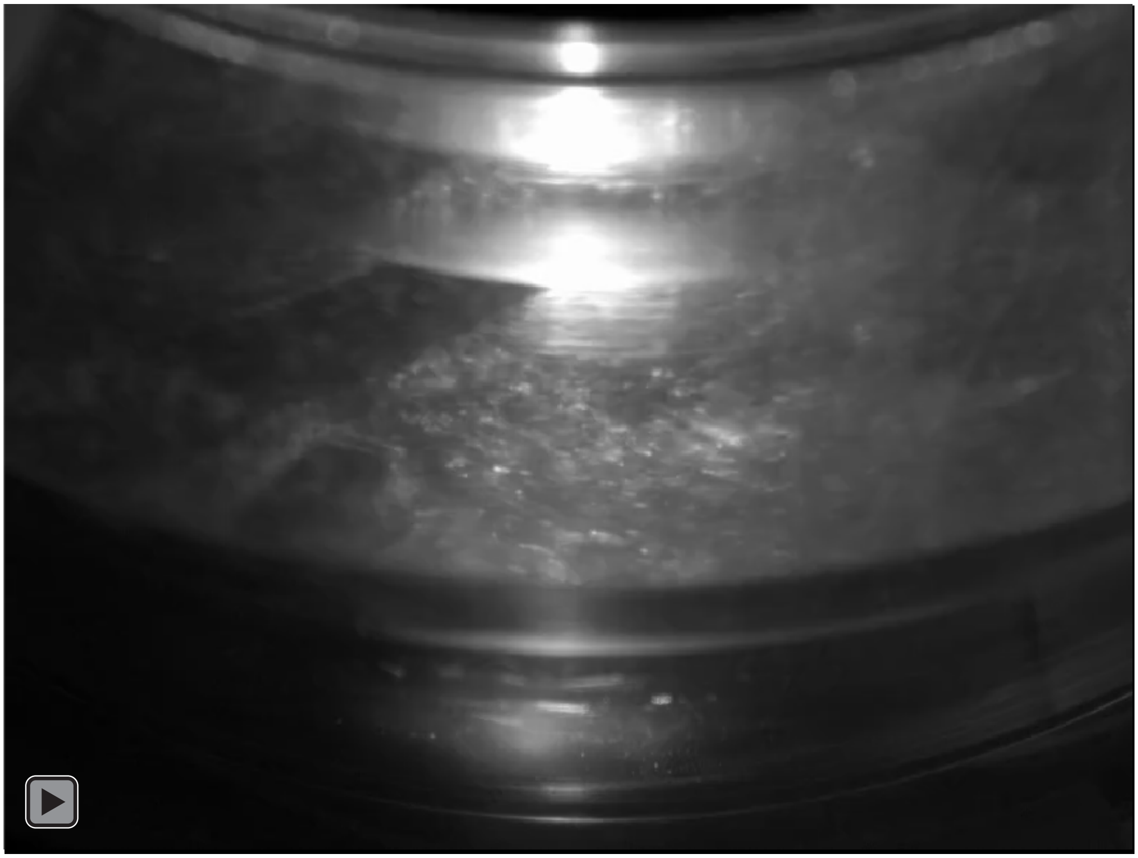

Figure 46 10,800 fps clip of impeller eye at 13,700 bpd flow rate and a trace GVF

5.4 Diffuser Visualization

Diffuser visualization was completed at several liquid flow rates at 2% GVF and 1800 rpm at inlet pressures varying from 66 to 70 psig. For the tests, the inlet water flow rate was varied between 8,000 and 17,000 bpd, while maintaining the inlet pressure and GVF. This was done to examine the effect of flow rate on recirculation zones and separation locations in the diffuser. By observing these phenomena and trends, a comparison with previous work completed by Marsis [7] was possible.

For all diffuser visualization, the V711 high speed camera was used with an 18-55 mm lens. The frame speed was 10,800 fps and the exposure time was 30 μs. The picture resolution was 800X600 pixels and each pixel had 12 bit grayscale resolution. Two OSL1 lighting modules were used to supply adequate lighting for the high speed photography.

As discussed above, the testing conditions remain constant on all critical parameters except the inlet water flow rate. The flow rates tested were 8,000, 10,000, 12,000, 14,000, 16,000, and 17,000 bpd. Videos were captured of the inlet and outlet region of the diffuser separately. In the inlet region of the diffuser, steady recirculation and stagnation zones occurred at 8,000, 10,000, and 12,000 bpd flow rates. Above that level, turbulent recirculation occurred, but not in a steady region and not with stagnation. In the outlet of the diffuser on the other hand, steady recirculation and stagnation zones were observed at all testing conditions. Above 14,000 bpd, the separation point from the suction side of the blade remains in a nearly constant location. Both sets of data show that the recirculation zones in the diffuser decrease in size with decreased head and increased flow rate. Also, for the diffuser, when a steady stagnant recirculation zone forms, a high velocity stream of two phase flow forms on the pressure side of the diffuser blade.

In the following images and video clips, the inlet of the diffuser is always below the bottom of the image and the outlet is at the top. The rotation of the impeller is to the left in all of the images as well. Shown in Figure 47 is the inlet of the diffuser with 8,000 bpd of water flowing through the pump. This flow rate shows the largest and worst stagnation and recirculation zones. The stagnation shown in the exit of this frame is also shown in the entrance of Figure 48. The other clips of the inlet of the diffuser with higher flow regimes are found in Appendix E.

Shown in Figure 48 is the outlet of the diffuser with 8,000 bpd of water flowing through the pump. This flow rate shows the largest and worst stagnation and recirculation zones. The flow even appears to separate from the blade before entering the frame of the image. The lower portion of the image is shared with the inlet clip of the diffuser. The other clips of the outlet of the diffuser with higher flow regimes are found in Appendix E.

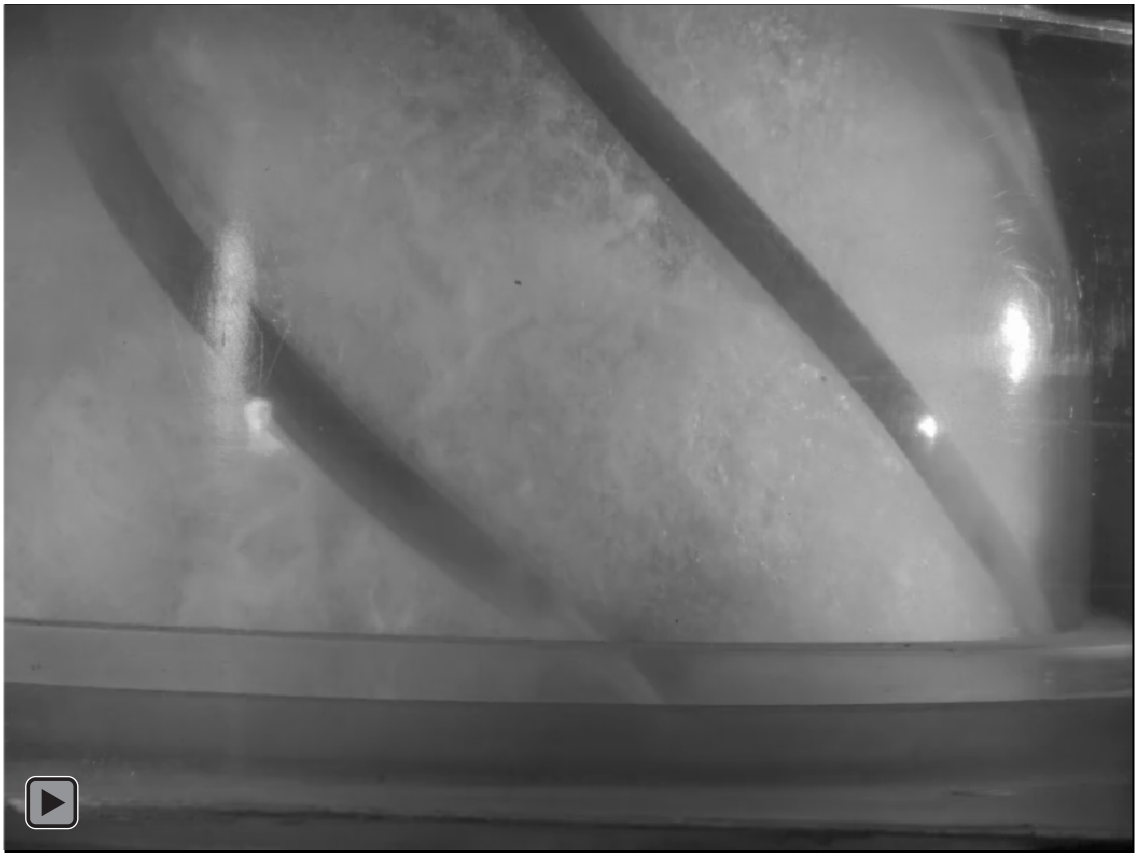

Figure 47 10,800 fps clip of diffuser inlet at 8,000 bpd flow rate and 2% GVF

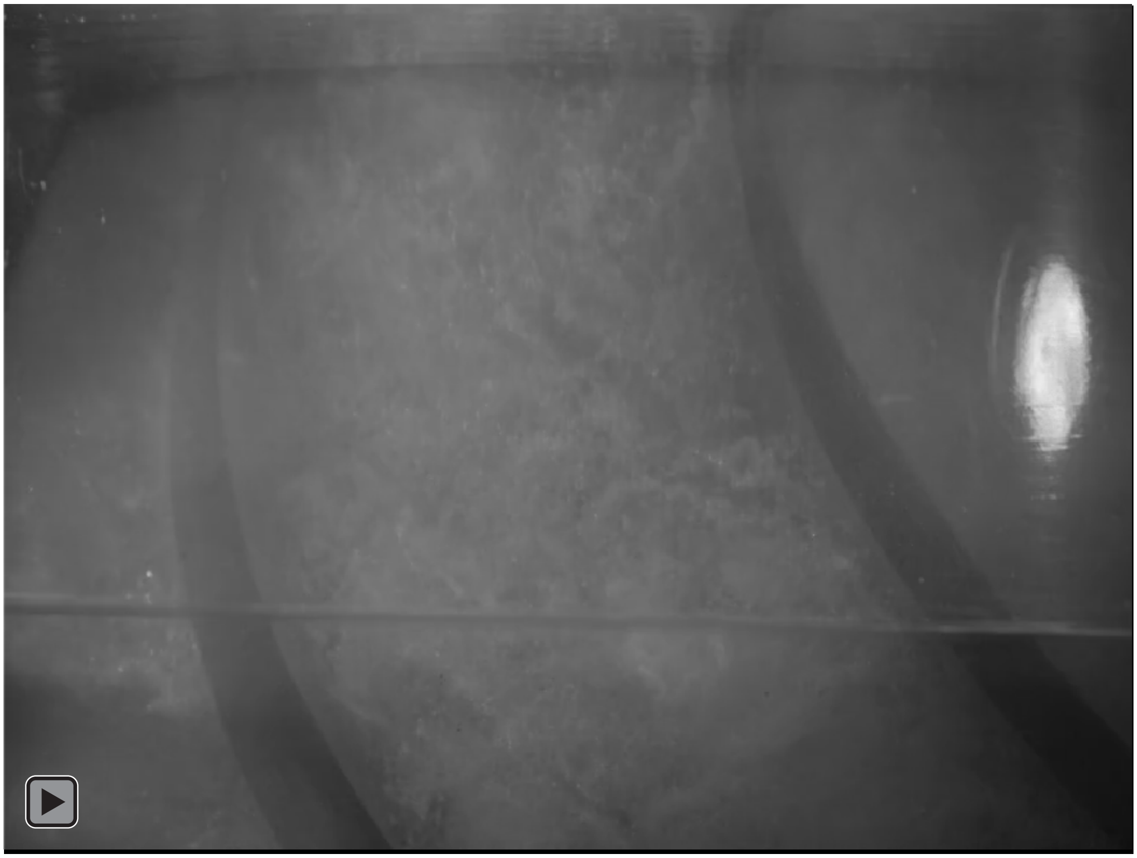

Figure 48 10,800 fps clip of diffuser outlet at 8,000 bpd flow rate and 2% GVF

Still images were removed from the high speed videos and the approximate shear boundary layer between the stagnant and high velocity was sketched. The stills of the inlet and outlet of the diffuser are shown in Figure 49 through Figure 54. For 8,000 bpd, the recirculation zone fills approximately 75% of the outlet of the diffuser. Also, the separation point is in the first quarter of the diffuser.

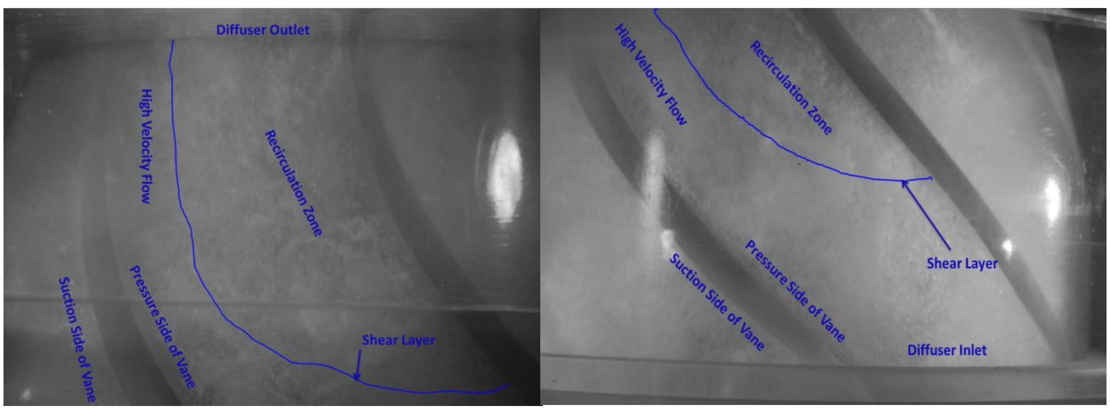

Figure 49 Outlet (left) and inlet (right) of diffuser with 8,000 bpd inlet water and 2% GVF air

As seen in Figure 50, for the 10,000 bpd flow, the recirculation zone fills only 67% of the area at the outlet of the diffuser. The separation point is in the first third of the diffuser.

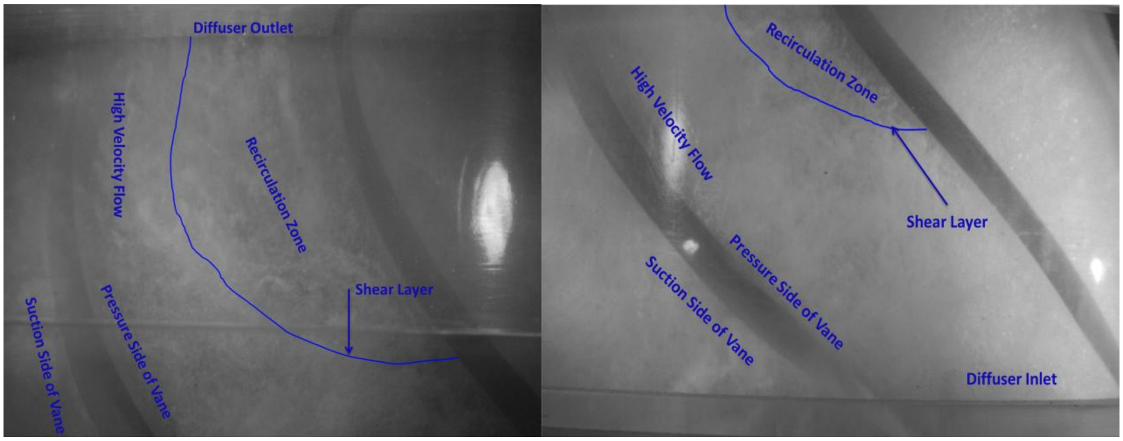

Figure 50 Outlet (left) and inlet (right) of diffuser with 10,000 bpd inlet water and 2% GVF air

As seen in Figure 51, for the 12,000 bpd flow, the recirculation zone fills only approximately 50% of the area at the outlet of the diffuser. The separation point is slightly less than half of the diffuser from the inlet.

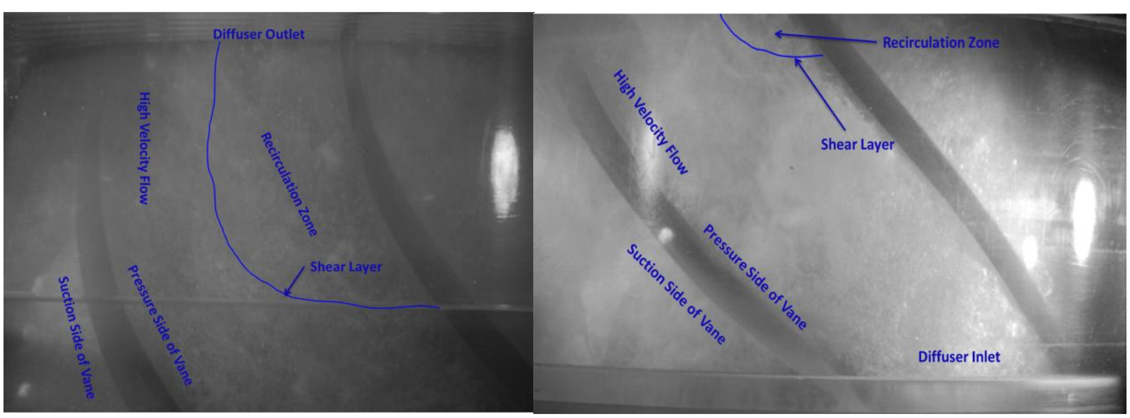

Figure 51 Outlet (left) and inlet (right) of diffuser with 12,000 bpd inlet water and 2% GVF air

As seen in Figure 52, for the 14,000 bpd flow, the recirculation zone continues to fill approximately 50% of the area at the outlet of the diffuser. The separation point is slightly past the halfway point from the inlet.

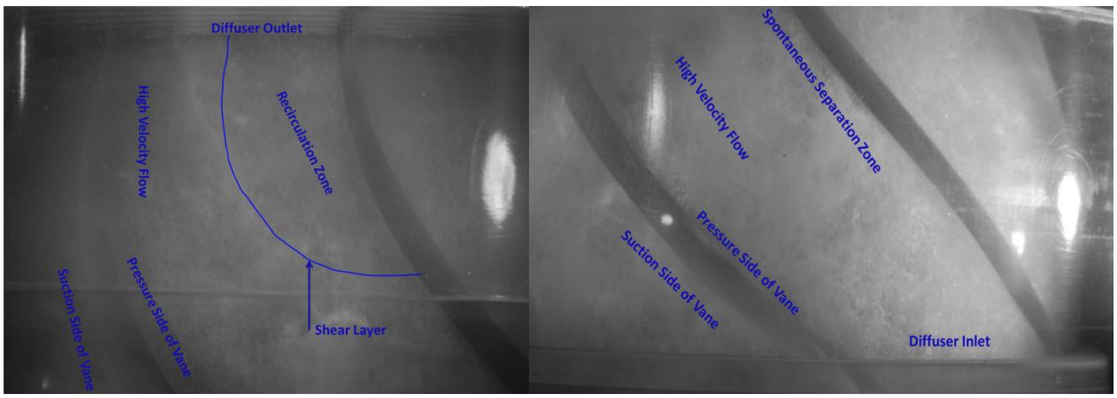

Figure 52 Outlet (left) and inlet (right) of diffuser with 14,000 bpd inlet water and 2% GVF air

As seen in Figure 53, for the 16,000 bpd flow, the recirculation zone fills only approximately 30% of the area at the outlet of the diffuser. The separation point is still slightly past the halfway point from the inlet.

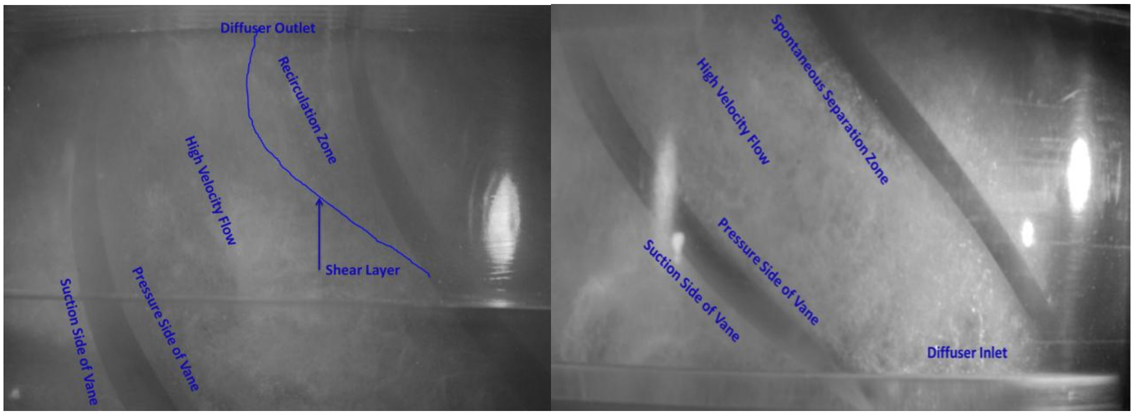

Figure 53 Outlet (left) and inlet (right) of diffuser with 16,000 bpd inlet water and 2% GVF air

As seen in Figure 54, for the 17,000 bpd flow, the recirculation zone fills only approximately 25% of the area at the outlet of the diffuser. The separation point still remains slightly past the halfway point from the inlet.

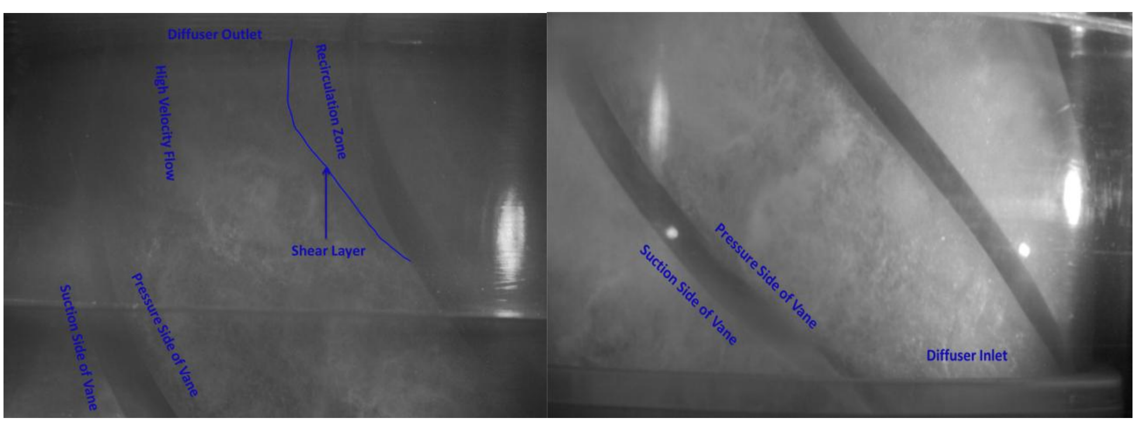

Figure 54 Outlet (left) and inlet (right) of diffuser with 17,000 bpd inlet water and 2% GVF air

6 RECOMMENDATIONS AND CONCLUSIONS

The scope of this work was design, construction, and preliminary visualization of the G470 MVP pump. To the author‟s knowledge, no transparent full size, flow rate, and rotational speed MVP ESP test facility has been developed. Thus, a major portion of the work was designing and constructing this cutting edge test facility. The remainder of the work was instrumentation and preliminary analysis primarily through visualization. To completely analyze the two phase flow characteristics of the pump further extensive testing must be completed.

Recommendations:

- For further testing with small air flow rates and low GVFs as completed in previous work, the 1 to 10 ACFM flowmeter should be recalibrated and wired to the NI DAQ and programmed into LabVIEW.
- To adequately compare the numerical CFD results to the pump, a velocimetry study in the impeller and diffuser is required.
- A larger range of GVFs should be tested.
- The pump should be tested at the full speed of 3600 rpm.
- The gap between the impeller face and the inlet plenum baffle should be reduced from approximately 1/16” to 0.02”.

- The ASME swing check valves have a cracking pressure of 4 psig, which was too large to obtain a steady low air flow rate. They should be permanently replaced with a valve which does not obstruct the air flow.
- To test up to 400 psig inlet pressures, the mechanical seals which are rated to 200 psig must be replaced for high pressure testing. Also the brass fittings and components must be checked to ensure a design pressure of 500 psig.

Conclusions:

- Although the SLA material loses optical transparency with thickness, when it is wetted it performs adequately for visualization in the G470 MVP.
- Visualization into the impeller was obscured by bubbles in the annulus between the casing and the impeller. It is also impeded by the bubbles in the channel between the impeller shroud and the inlet plenum baffle.
- Recirculation backwards around the leading edge of the secondary blade was observed in the impeller. This helps explain erosion on the secondary blade in operation when solid fines are in the flow. This flow recirculation was not predicted by Marsis‟ [7] CFD work.
- Stagnant recirculation zones occurred on the suction side of the diffuser blade at all flow conditions, which points to a design deficiency in the G470.

- Stagnant recirculation zones decrease in size as liquid flow rate is increased for constant GVF. The area of the outlet where flow is impeded by the stagnant zone also decreases to approximately 25 to 35% of the outlet area. It then remains relatively steady after approximately 16,000 bpd liquid flow rate.
- The point of separation from the suction side of the diffuser blade stays at a relatively constant location in the diffuser above 14,000 bpd liquid flow rate. This agrees with the CFD completed by Marsis [7].

7 REFERENCES

[1] Economides, M., Hill, A., Ehlig-Economides, C., 2013, "Petroleum Production Systems," Prentice Hall, Westford, Massachusetts, pp. 752.

[2] Takacs, G., 2009, "Electrical Submersible Pumps Manual: Design, Operations, and Maintenance," Gulf Professional Publishing, Burlington, Massachusetts, pp. 440.

[3] Minemura, K., and Murakami, M., 1980, "A Theoretical Study on Air Bubble Motion in a Centrifugal Pump Impeller," Journal of Fluids Engineering, Transactions of the ASME, **102**(December) pp. 446-53.

[4] Barrios, L., 2007, "Visualization and Modeling of Multiphase Performance Inside an Electrical Submersible Pump," The University of Tulsa, Tulsa, Oklahoma, pp. 1-169.

[5] Kirkland, K., 2012, "Design and Fabrication of a Vertical Pump Multiphase Flow Loop," Texas A&M University, College Station, Texas, pp. 1-63.

[6] Royal DSM N. V. Somos, 2012, "Product Data Somos WaterClear Ultra 10122," DSM IP Assets B. V., Elgin, Illinois.

[7] Marsis, E., 2012, "CFD Simulation and Experimental Testing of Multiphase Flow Inside the MVP Electrical Submersible Pump," Texas A&M University, College Station, Texas, pp. 1-96.

[8] Jones, F., Horton, H., and Oberg, E., 1990, "Machinery's Handbook 23rd Revised Edition," Industrial Press Inc., New York, New York, pp. 2511.

[9] ASME, 2010, "Rules for Construction of Pressure Vessels," American Society of Mechanical Engineers, Fairfield, New Jersey, pp. 850.

[10] Omnexus, 2012, "Properties Profiles of PC - Polycarbonate," SpecialChem S. A., Paris, France.

[11] ASME, 2010, "Guidelines for Pressure Boundary Bolted Flange Joint Assembly," American Society of Mechanical Engineers, Fairfield, New Jersey, pp. 88.

[12] ASME, 2010, "Boiler and Pressure Vessel Code - Materials - Properties (Customary)," American Society of Mechanical Engineers, Fairfield, New Jersey, pp. 912.

APPENDIX A

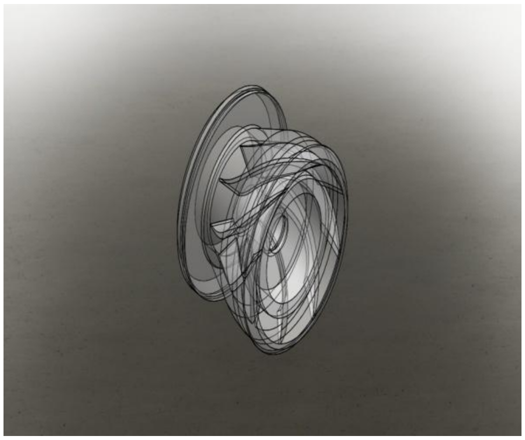

Simulation of PR1_Diffuser_Rev1

Date: Monday, August 19, 2013
Designer: Joseph Marchetti
Study name: InitialStudy
Analysis type: Static

Description

This is the baseline simulation of the ability of the diffuser per Baker Hughes Centrilift MVP (Multi-vane pump) ESP (electric submersible pump). This is to determine whether the original pump diffuser design as the canister design will be acceptable.

Assumptions

Comments:
This analysis has been run under several assumptions:
1) The friction rings on the diffuser canister will give a fixed and static mount to the canister.
2) The shaft running through the shroud will allow up to 0.002" interference with the diffuser (worst case scenario).
3) The maximum pressure differential across a vane is 50 psig (per CFD results).
4) The maximum pressure differential across the casing is 60 psig. (Max head generated = 50 psig + 10 psig safety factor).
5) Gravity acts on the diffuser downward along the shaft toward the inlet.

Model Information

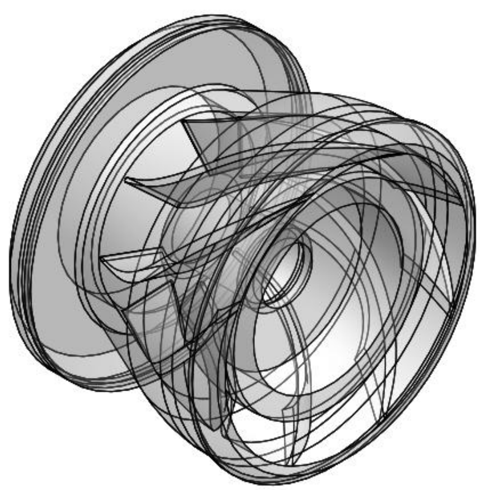

Model name: PR1_Diffuser_Rev1

Solid Bodies			
Document Name and Reference	**Treated As**	**Volumetric Properties**	**Document Path/Date Modified**

Cut-Revolve6 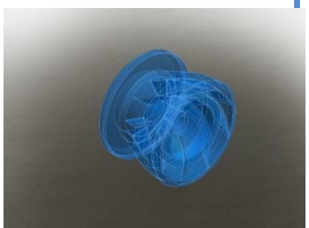	Solid Body	Mass:2.52463 kg Volume:0.002 35947 m^3 Density:1070 kg/m^3 Weight:24.74 14 N	C:\Users\JoeyM\Desktop\MVP Visualization\Design and Procurement\PR1_Diffuser\PR1_Diffuser_Rev1.SLDPRT Aug 19 14:19:47 2013

Study Properties

Study name	InitialStudy
Analysis type	Static
Mesh type	Solid Mesh
Thermal Effect:	On
Thermal option	Include temperature loads
Zero strain temperature	298 Kelvin
Include fluid pressure effects from SolidWorks Flow Simulation	Off
Solver type	FFEPlus
Inplane Effect:	Off
Soft Spring:	Off
Inertial Relief:	Off
Incompatible bonding options	Automatic
Large displacement	Off
Compute free body forces	On
Friction	Off
Use Adaptive Method:	Off
Result folder	SolidWorks document (C:\Users\JoeyM\Desktop\MVP Visualization\Design and Procurement\PR1_Diffuser)

Units

Unit system:	SI (MKS)
Length/Displacement	mm
Temperature	Kelvin
Angular velocity	Rad/sec
Pressure/Stress	N/m^2

Material Properties

Model Reference	Properties		Components
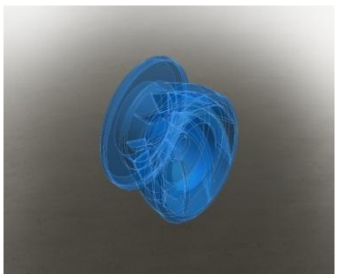	**Name:**	Somos WaterClear XC 10122	SolidBody 1(Cut-Revolve6)(PR1_Diffuser _Rev1)
	Model type:	Linear Elastic Isotropic	
	Default failure criterion:	Unknown	
	Yield strength:	5.5e+007 N/m^2	
	Tensile strength:	5.5e+007 N/m^2	
	Elastic modulus:	2.86e+009 N/m^2	
	Poisson's ratio:	0.4	
	Mass density:	1070 kg/m^3	
	Shear modulus:	8.622e+008 N/m^2	
Curve Data:N/A			

Comments:
The materials properties supplied about the Somos WaterClear Ultra 10122 were used per the data sheet. Polycarbonate was modified to develop the Somos WaterClear Ultra 10122.

Loads and Fixtures

Fixture name	Fixture Image	Fixture Details
Fixed-1	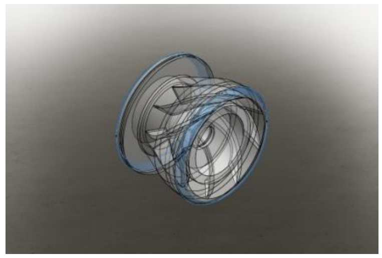	**Entities:** 2 face(s) **Type:** Fixed Geometry

Resultant Forces

Components	X	Y	Z
Reaction force(N)	279.24	1.70734	-3.95143
Reaction Moment(N-m)	0	0	0

Fixture name	Fixture Image	Fixture Details
On Cylindrical Faces-1	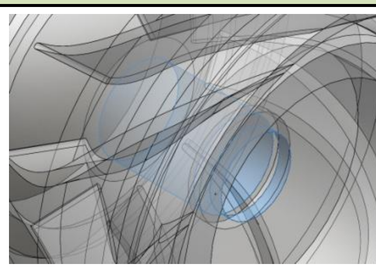	**Entities:** 2 face(s) **Type:** On Cylindrical Faces **Translation:** 0.002, ---, --- **Units:** in

Resultant Forces

Components	X	Y	Z
Reaction force(N)	-0.000755065	-1.59601	3.95863
Reaction Moment(N-m)	0	0	0

Load name	Load Image	Load Details
Gravity-1	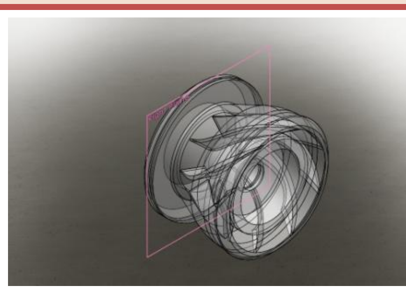	**Reference:** Right Plane **Values:** 0 0 9.81 **Units:** SI

Pressure-1	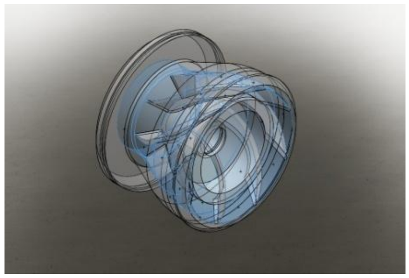	**Entities:** 19 face(s) **Type:** Normal to selected face **Value:** 60 **Units:** psi
Pressure-2	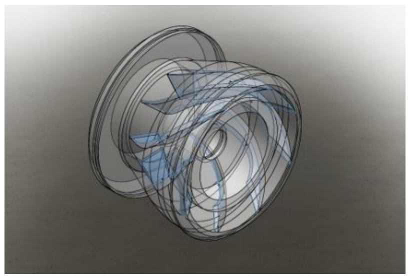	**Entities:** 8 face(s) **Type:** Normal to selected face **Value:** 50 **Units:** psi

Mesh Information

Mesh type	Solid Mesh
Mesher Used:	Standard mesh
Automatic Transition:	Off
Include Mesh Auto Loops:	Off
Jacobian points	At Nodes
Element Size	0.262185 in
Tolerance	0.0131092 in
Mesh Quality	High

Mesh Information - Details

Total Nodes	130956
Total Elements	79963
Maximum Aspect Ratio	15.01
% of elements with Aspect Ratio < 3	93
% of elements with Aspect Ratio > 10	0.0263
% of distorted elements(Jacobian)	0
Time to complete mesh(hh;mm;ss):	00:00:22
Computer name:	MORRISONLAB24

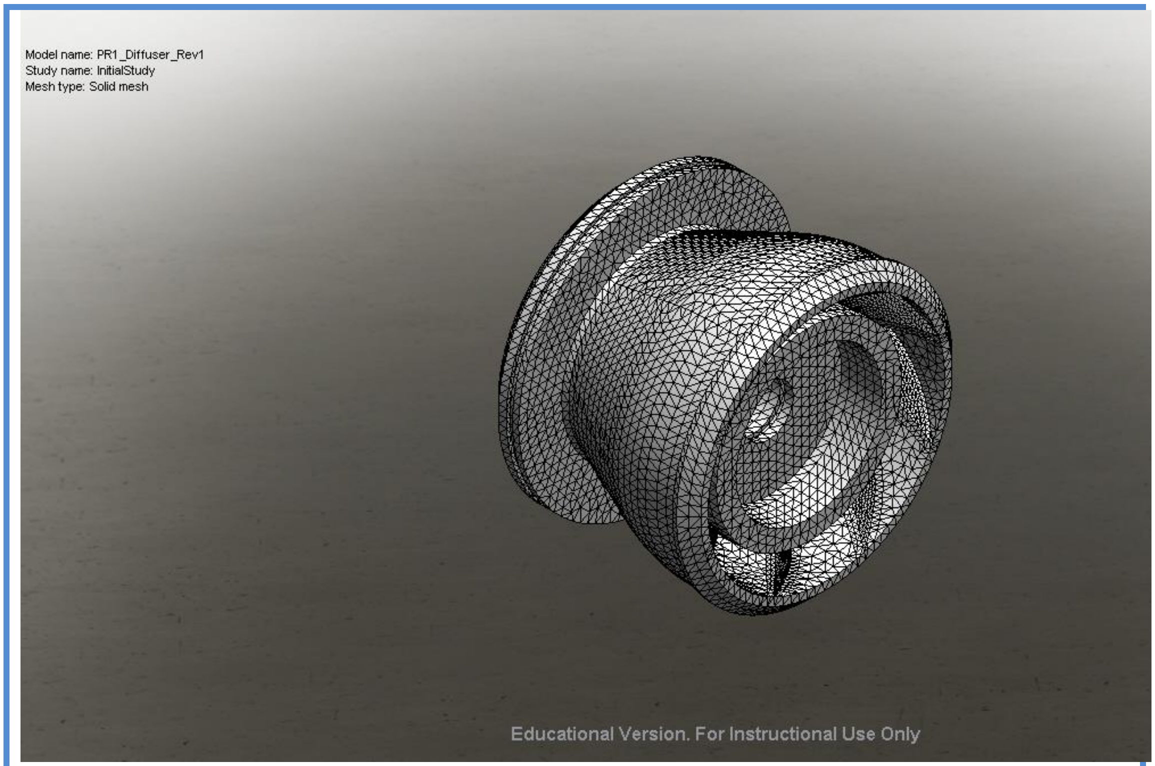

Mesh Control Information:

Mesh Control Name	Mesh Control Image	Mesh Control Details
Control -1	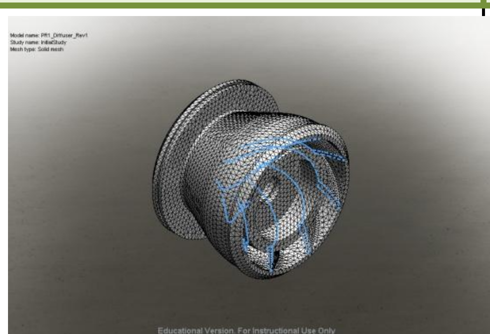	**Entities:** 40 edge(s) **Units:** in **Size:** 0.131059 **Ratio:** 1.5

Control -2	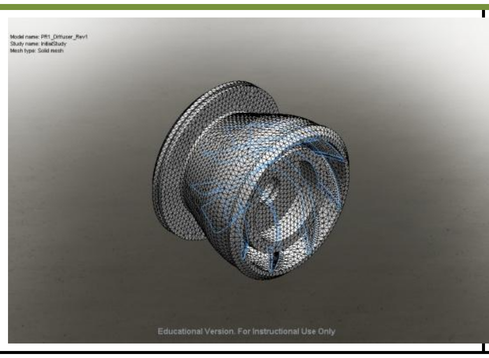	**Entities:** 16 face(s) **Units:** in **Size:** 0.131059 **Ratio:** 1.5

Resultant Forces

Reaction Forces

Selection set	Units	Sum X	Sum Y	Sum Z	Resultant
Entire Model	N	279.239	0.100277	0.0068512	279.239

Reaction Moments

Selection set	Units	Sum X	Sum Y	Sum Z	Resultant
Entire Model	N-m	0	0	0	0

Study Results

Name	Type	Min	Max
Stress1	VON: von Mises Stress	2.2113 psi Node: 3576	2170.81 psi Node: 130297

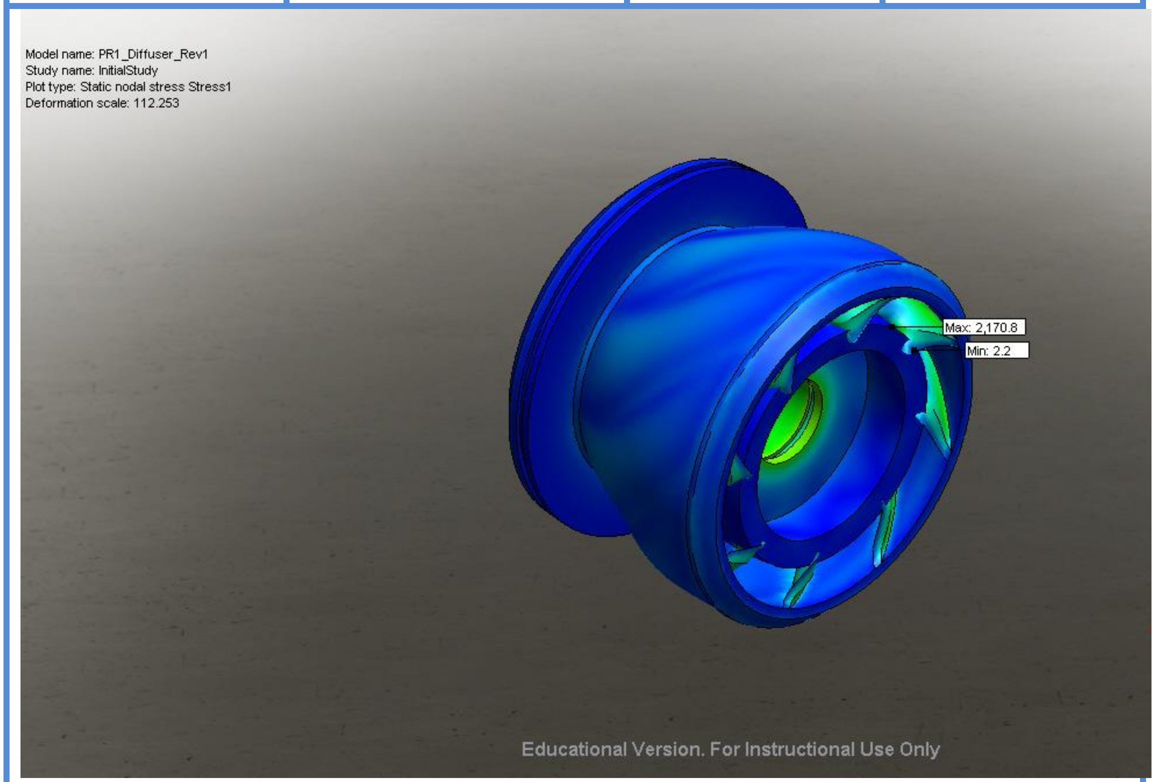

PR1_Diffuser_Rev1-InitialStudy-Stress-Stress1

Name	Type	Min	Max
Displacement1	URES: Resultant Displacement	0 in Node: 1264	0.0083464 in Node: 96251

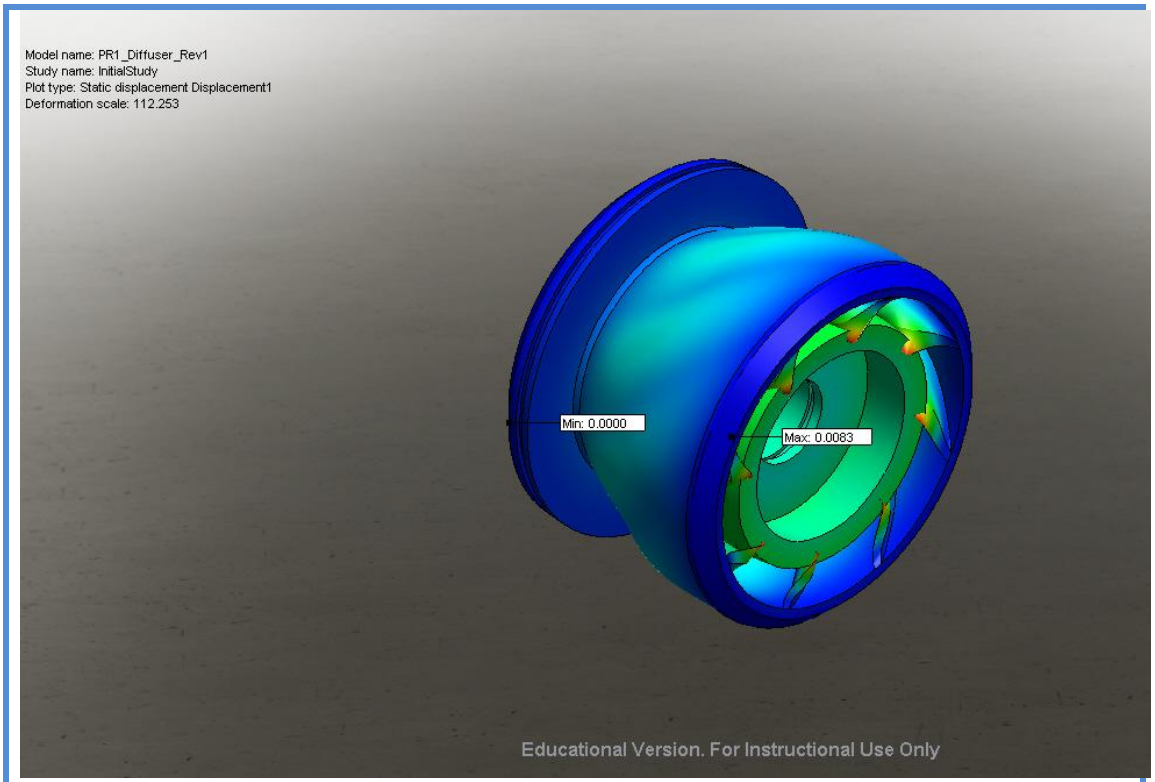

PR1_Diffuser_Rev1-InitialStudy-Displacement-Displacement1

Name	Type	Min	Max
Strain1	ESTRN: Equivalent Strain	1.19136e-005 Element: 62914	0.00433733 Element: 21862

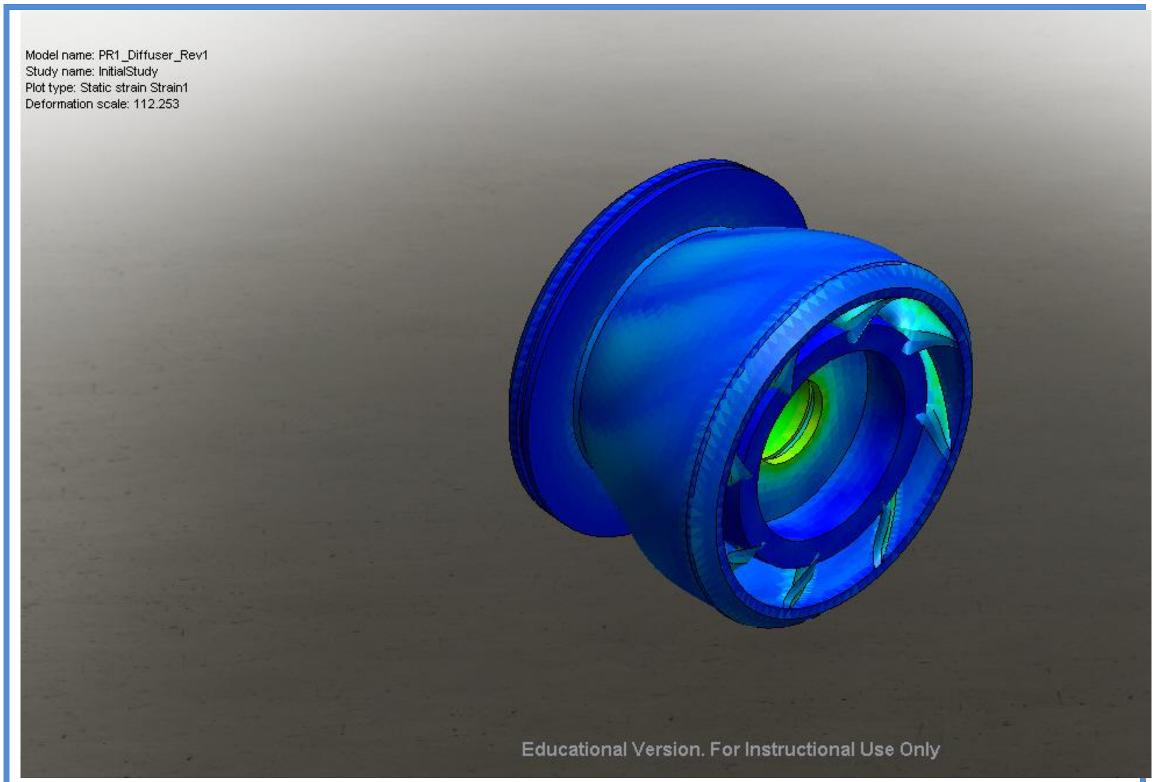

PR1_Diffuser_Rev1-InitialStudy-Strain-Strain1

Name	Type
Displacement1{1}	Deformed Shape

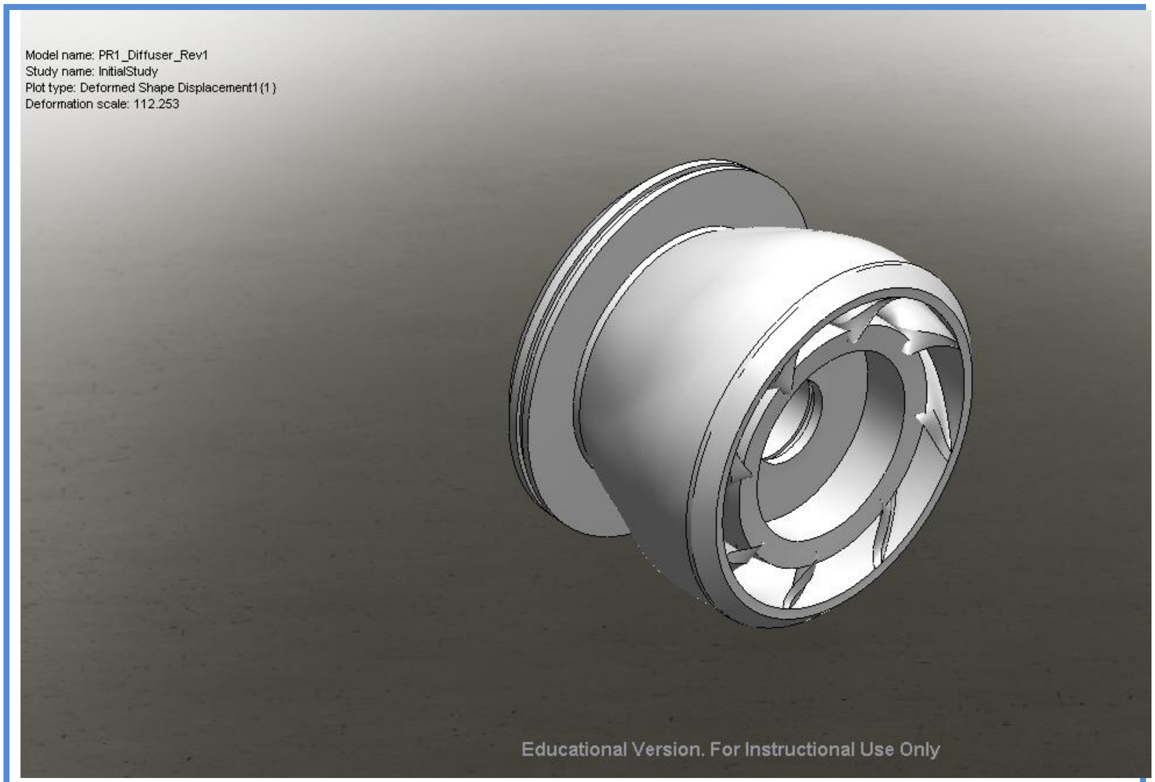

PR1_Diffuser_Rev1-InitialStudy-Displacement-Displacement1{1}

Name	Type	Min	Max
Factor of Safety1	Automatic	3.6747 Node: 130297	3607.42 Node: 3576

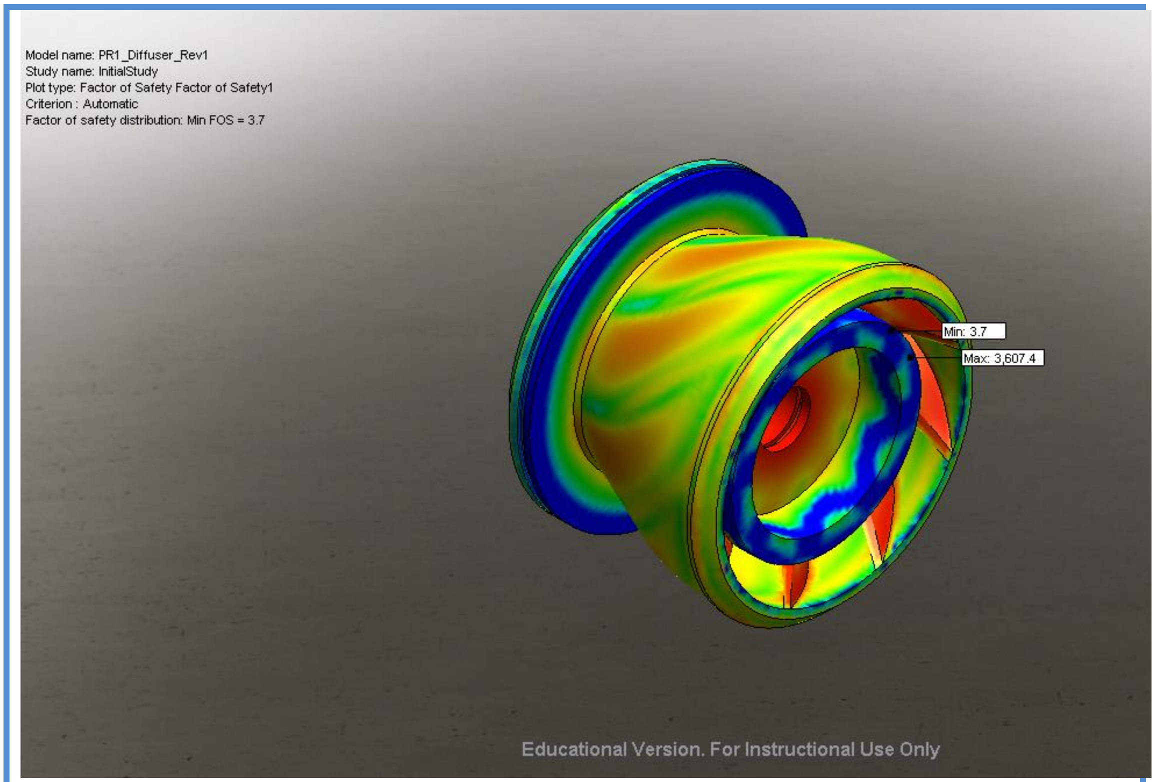

PR1_Diffuser_Rev1-InitialStudy-Factor of Safety-Factor of Safety1

Conclusion

Comments:

The initial design by Centrilift by this analysis appears to be acceptable constructed of Somos WaterClear Ultra XC10122. It has a minimum safety factor greater than 3.5.

B.1 Impeller FEA Report: Primary Blade Thickness: 0.171”, Material: Cast Carbon Steel

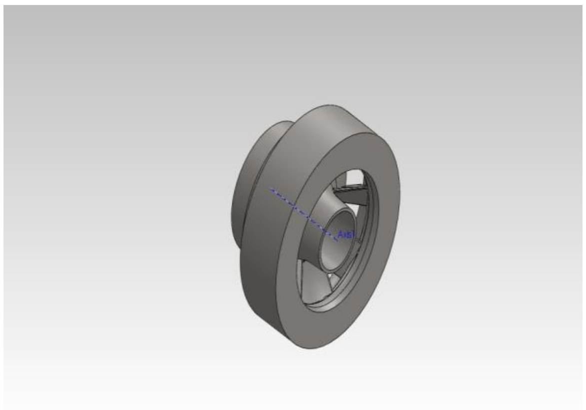

Simulation of Impeller_Original Geometry

Date: Thursday, August 22, 2013
Designer: Joseph Marchetti
Study name: RefinedPreliminaryAnalysis_CarbonSteel_10GVF
Analysis type: Static

Description

This analysis was used to validate and determine required design parameters in the G470 MVP impeller. It gives a baseline study completed on the original blade geometry and thickness with cast carbon steel. The thickness of the trailing edge of the main vane is 0.171” and the trailing edge of the secondary vane is 0.129”. The analysis was completed at 10% GVF (harsher than 25% GVF) with Solidworks defined Cast Carbon Steel.

Assumptions

Comments:
The assumptions are as follows:
1) The hub gives a fixed constraint.
2) The pump is operated under steady state stress conditions. Rotational speed, back pressure axial force, and pressure distribution around the blade is constant.
3) A 1.3 safety factor was applied to the back pressure axial force and pressure differential across the vanes.

Model Information

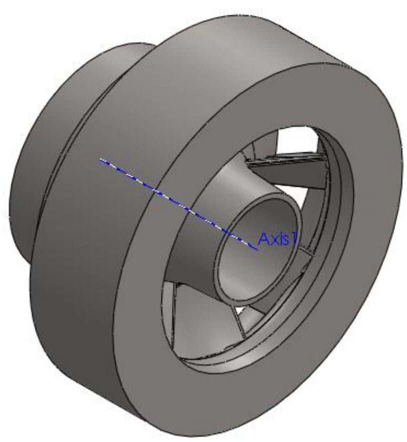

Model name: Impeller_OriginalGeometry
Current Configuration: Default

Solid Bodies			
Document Name and Reference	**Treated As**	**Volumetric Properties**	**Document Path/Date Modified**

Revolve3 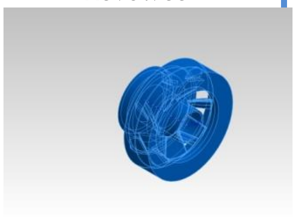	Solid Body	**Mass:7.56193 kg Volume:0.000969479 m^3 Density:7800 kg/m^3 Weight:74.1069 N**	**C:\Users\JoeyM\Desktop\MVP Visualization\Design and Procurement\PR10_Impeller\Impeller_OriginalGeometry.SLDPRT** Jan 14 11:42:22 2013

Study Properties

Study name	RefinedPreliminaryAnalysis_CarbonSteel_10GVF
Analysis type	Static
Mesh type	Solid Mesh
Thermal Effect:	On
Thermal option	Include temperature loads
Zero strain temperature	298 Kelvin
Include fluid pressure effects from SolidWorks Flow Simulation	Off
Solver type	FFEPlus
Inplane Effect:	Off
Soft Spring:	Off
Inertial Relief:	Off
Incompatible bonding options	Automatic
Large displacement	Off
Compute free body forces	On
Friction	Off
Use Adaptive Method:	Off
Result folder	SolidWorks document (C:\Users\JoeyM\Desktop\MVP Visualization\Design and Procurement\PR10_Impeller)

Units

Unit system:	SI (MKS)
Length/Displacement	mm
Temperature	Kelvin
Angular velocity	Rad/sec
Pressure/Stress	N/m^2

Material Properties

Model Reference	Properties		Components
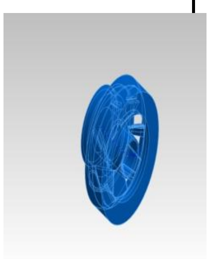	**Name:** **Model type:** **Default failure criterion:** **Yield strength:** **Tensile strength:** **Elastic modulus:** **Poisson's ratio:** **Mass density:** **Shear modulus:** **Thermal expansion coefficient:**	Cast Carbon Steel Linear Elastic Isotropic Max von Mises Stress 2.48168e+008 N/m^2 4.82549e+008 N/m^2 2e+011 N/m^2 0.32 7800 kg/m^3 7.6e+010 N/m^2 1.2e-005 /Kelvin	SolidBody 8(Revolve3)(Impeller_OriginalGeometry)
Curve Data:N/A			

Comments:
A Solidworks defined material named Cast Carbon Steel was used for the analysis.

Loads and Fixtures

Fixture name	Fixture Image	Fixture Details
Fixed-1	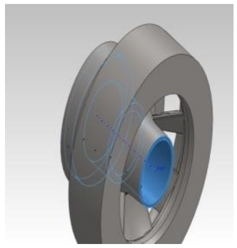	**Entities:** 6 face(s) **Type:** Fixed Geometry

Resultant Forces

Components	X	Y	Z	Resultant
Reaction force(N)	-13618	0.00235619	0.120091	13618
Reaction Moment(N-m)	0	0	0	0

Load name	Load Image	Load Details
Centrifugal-1	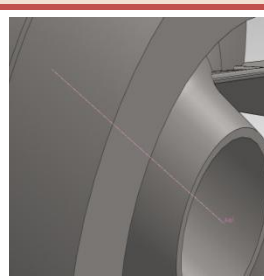	**Centrifugal, Ref:** Axis1 **Angular Velocity:** -60 Hz **Angular Acceleration:** 0 Hz/s
Force-1	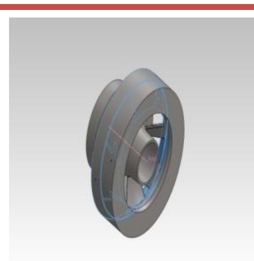	**Entities:** 3 face(s) **Reference:** Axis1 **Type:** Apply force **Values:** ---, ---, -1500 lbf
Pressure-2	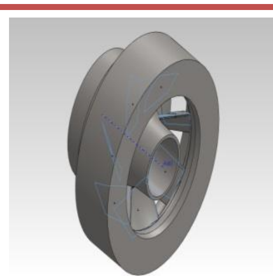	**Entities:** 7 face(s) **Type:** Normal to selected face **Value:** 108 **Units:** psi

Pressure-3	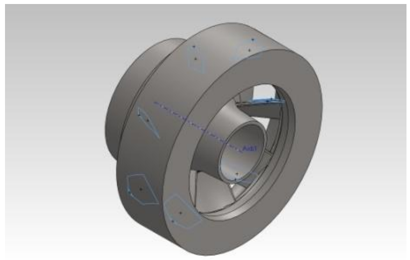	**Entities:** 14 face(s) **Type:** Normal to selected face **Value:** 135.2 **Units:** psi
Pressure-4	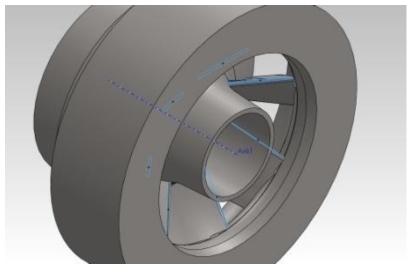	**Entities:** 7 face(s) **Type:** Normal to selected face **Value:** 337 **Units:** psi
Pressure-5	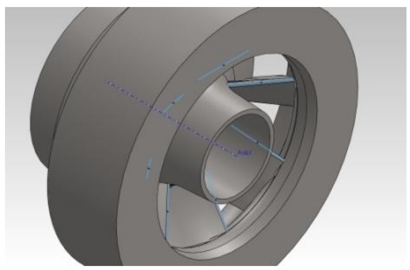	**Entities:** 7 face(s) **Type:** Normal to selected face **Value:** 175 **Units:** psi
Pressure-6	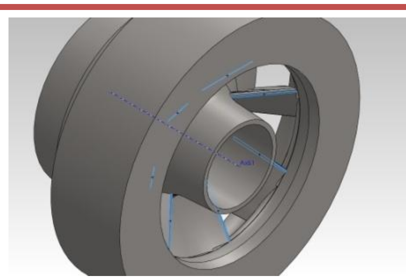	**Entities:** 7 face(s) **Type:** Normal to selected face **Value:** 45 **Units:** psi
Pressure-7	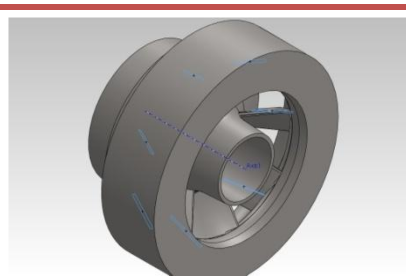	**Entities:** 7 face(s) **Type:** Normal to selected face **Value:** 342 **Units:** psi

Pressure-8	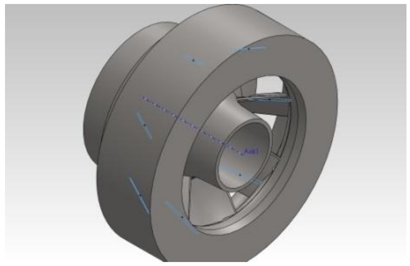	**Entities:** 7 face(s) **Type:** Normal to selected face **Value:** 54 **Units:** psi
Pressure-9	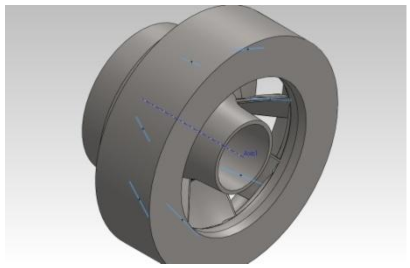	**Entities:** 7 face(s) **Type:** Normal to selected face **Value:** 170 **Units:** psi
Pressure-10	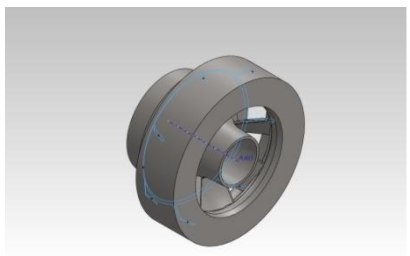	**Entities:** 8 face(s) **Type:** Normal to selected face **Value:** 225 **Units:** psi
Pressure-11	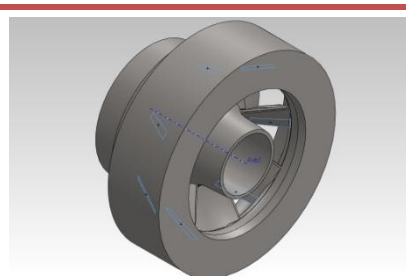	**Entities:** 7 face(s) **Type:** Normal to selected face **Value:** 210 **Units:** psi

Comments:
Three major loadings were considered:
1) Centrifugal forces generated by a 60Hz rotational speed,
2) Pressure distributions on the vanes from CFD at 10% GVF, and
3) Back pressure from 70 psig maximum head in the pump on the outlet area of the impeller.
A safety factor of 1.3 was applied to Items 2 and 3.

Mesh Information

Mesh type	Solid Mesh
Mesher Used:	Curvature based mesh
Jacobian points	4 Points
Maximum element size	0 in
Minimum element size	0 in
Mesh Quality	High

Mesh Information - Details

Total Nodes	191167
Total Elements	120055
Maximum Aspect Ratio	54.87
% of elements with Aspect Ratio < 3	95.9
% of elements with Aspect Ratio > 10	0.2
% of distorted elements(Jacobian)	0
Time to complete mesh(hh;mm;ss):	00:00:27
Computer name:	MORRISONLAB24

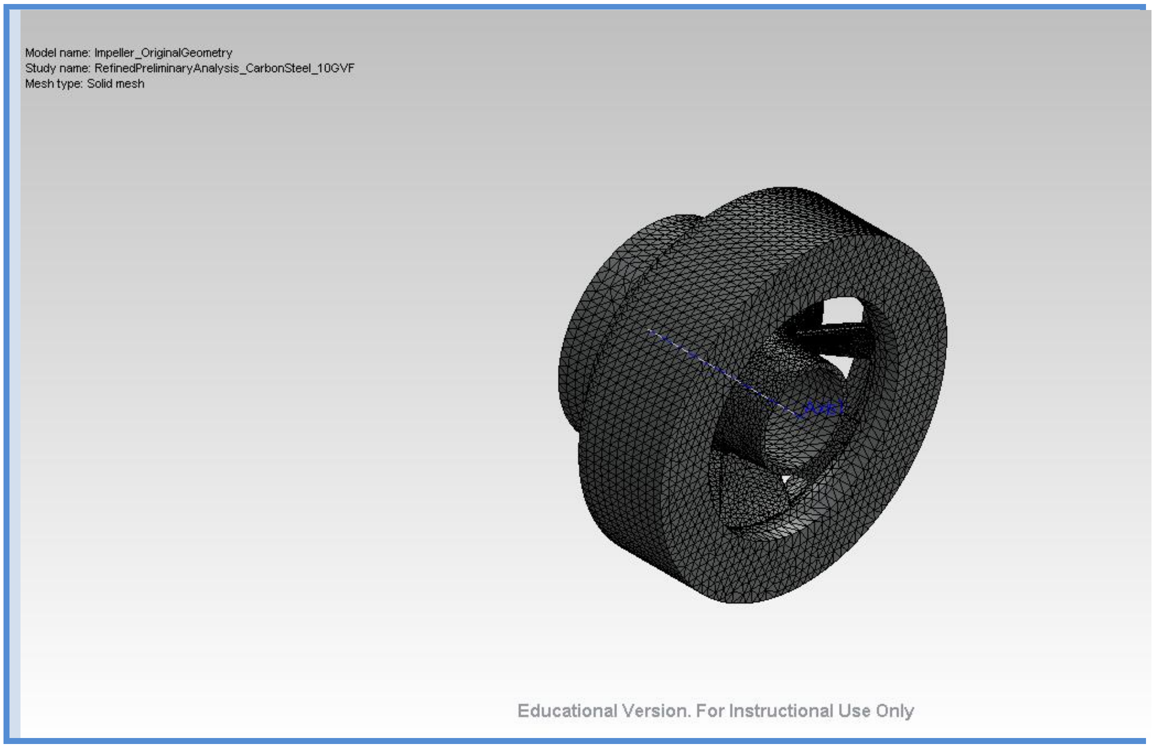

Mesh Control Information:

Mesh Control Name	Mesh Control Image	Mesh Control Details
Control -1	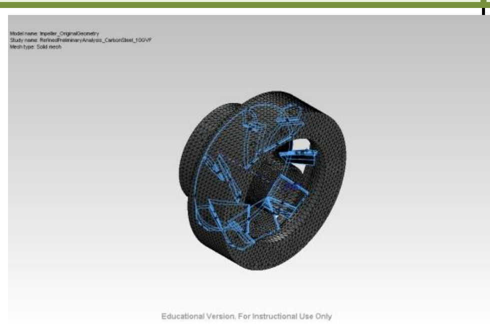	**Entities:** 113 face(s) **Units:** in **Size:** 0.097436 **Ratio:** 1.5
Control -2	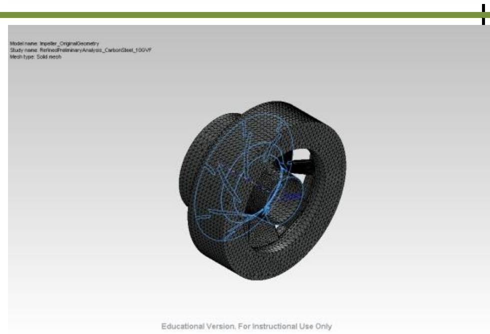	**Entities:** 9 face(s) **Units:** in **Size:** 0.097436 **Ratio:** 1.5

Resultant Forces

Reaction Forces

Selection set	Units	Sum X	Sum Y	Sum Z	Resultant
Entire Model	N	-13618	0.00235619	0.120091	13618

Reaction Moments

Selection set	Units	Sum X	Sum Y	Sum Z	Resultant
Entire Model	N-m	0	0	0	0

Study Results

Name	Type	Min	Max
Stress1	VON: von Mises Stress	0.413091 psi Node: 167992	50553.5 psi Node: 184744

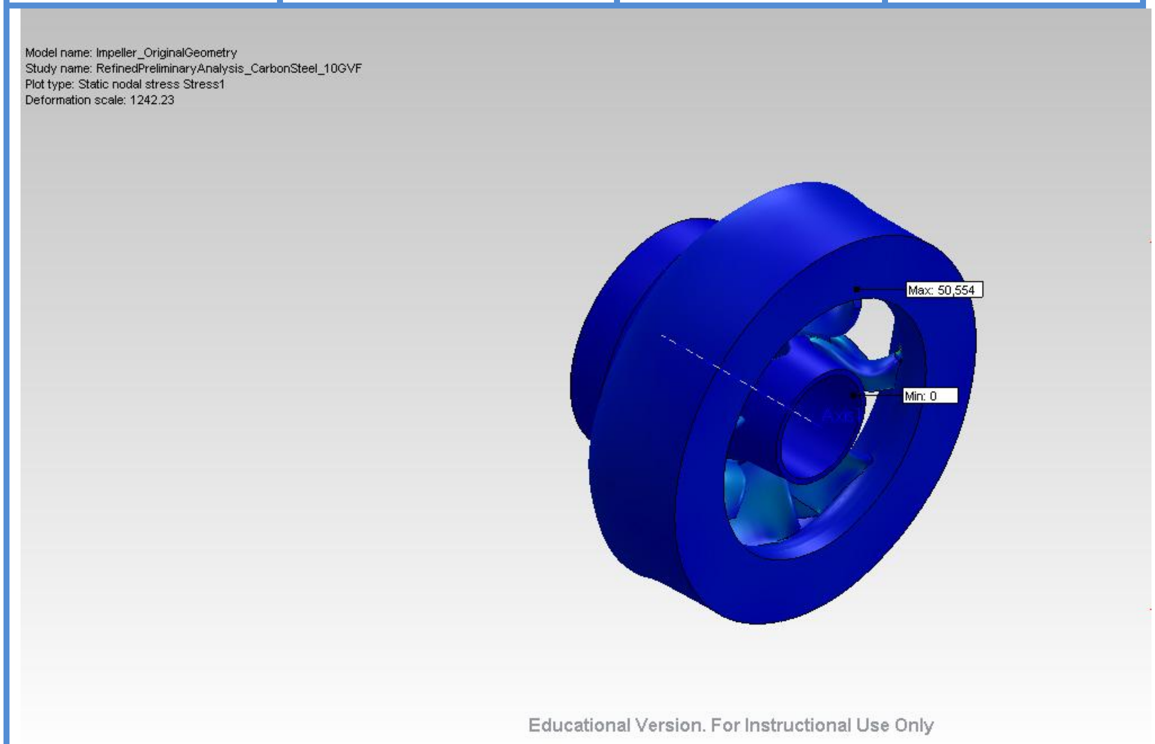

Impeller_OriginalGeometry-RefinedPreliminaryAnalysis_CarbonSteel_10GVF-Stress-Stress1

Name	Type	Min	Max
Displacement1	URES: Resultant Displacement	0 mil Node: 2403	0.606686 mil Node: 11535

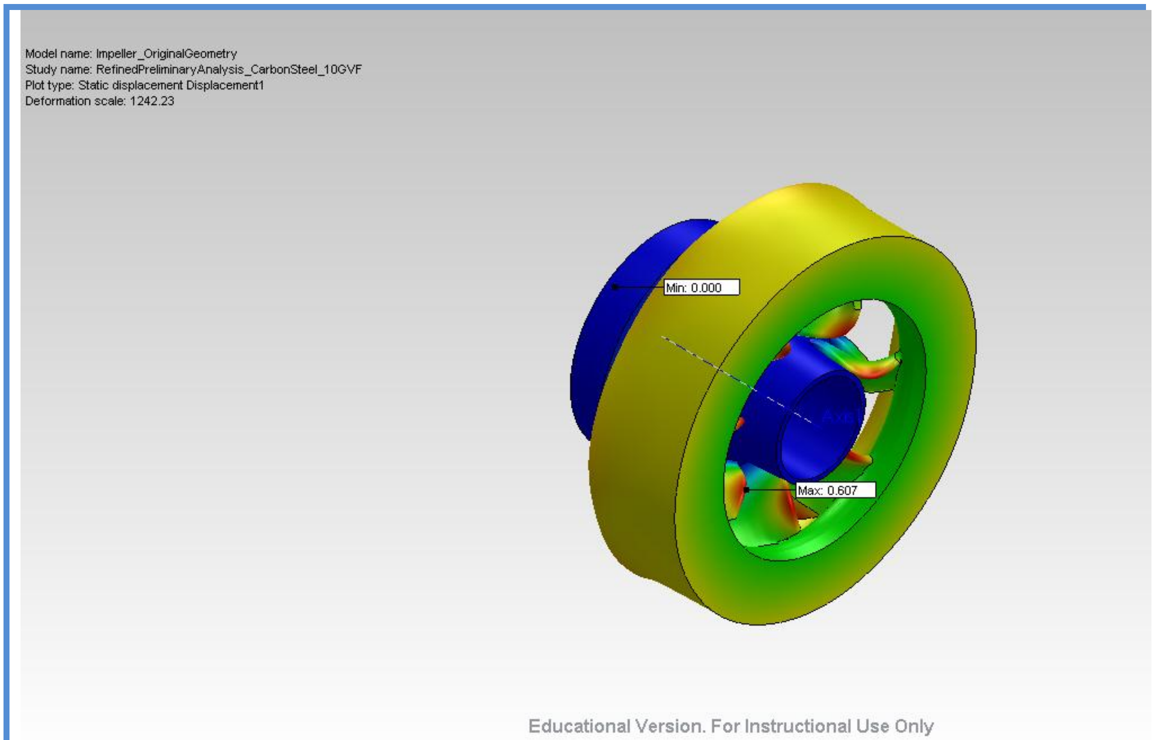

Impeller_OriginalGeometry-RefinedPreliminaryAnalysis_CarbonSteel_10GVF-Displacement-Displacement1

Name	Type	Min	Max
Strain1	ESTRN: Equivalent Strain	3.57046e-008 Element: 96036	0.000735417 Element: 37710

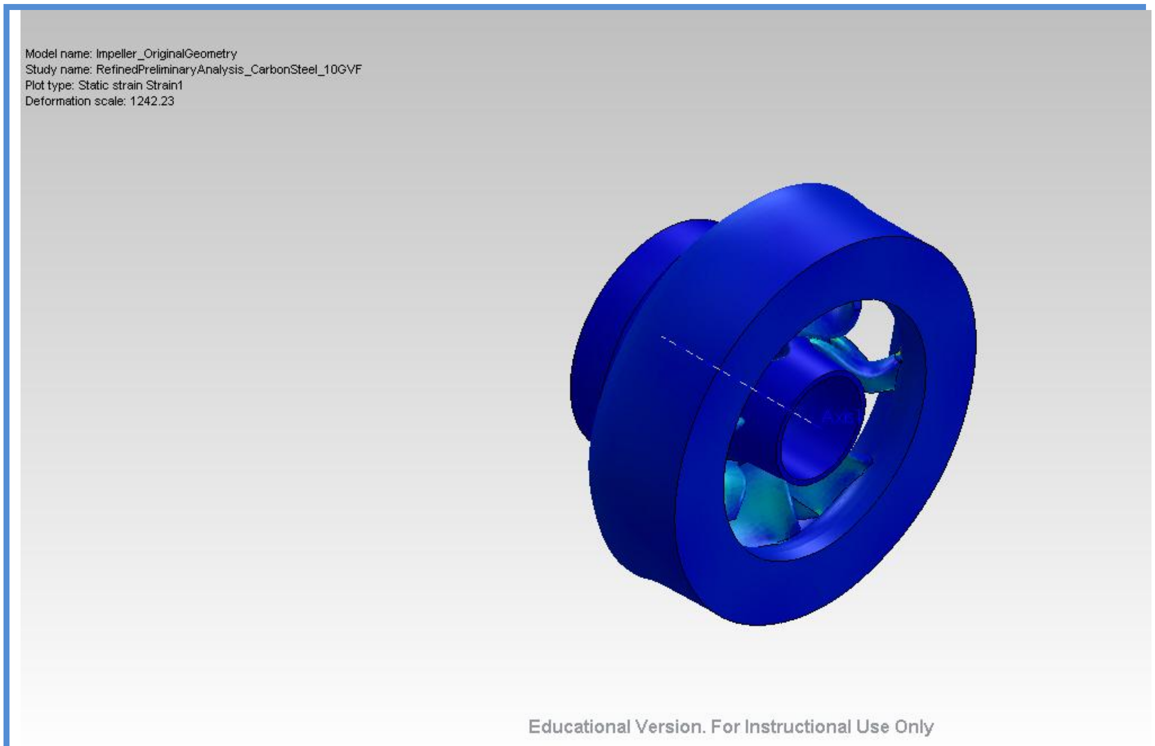

Impeller_OriginalGeometry-RefinedPreliminaryAnalysis_CarbonSteel_10GVF-Strain-Strain1

Name	Type	Min	Max
Factor of Safety1	Automatic	0.711993 Node: 184744	87132.7 Node: 167992

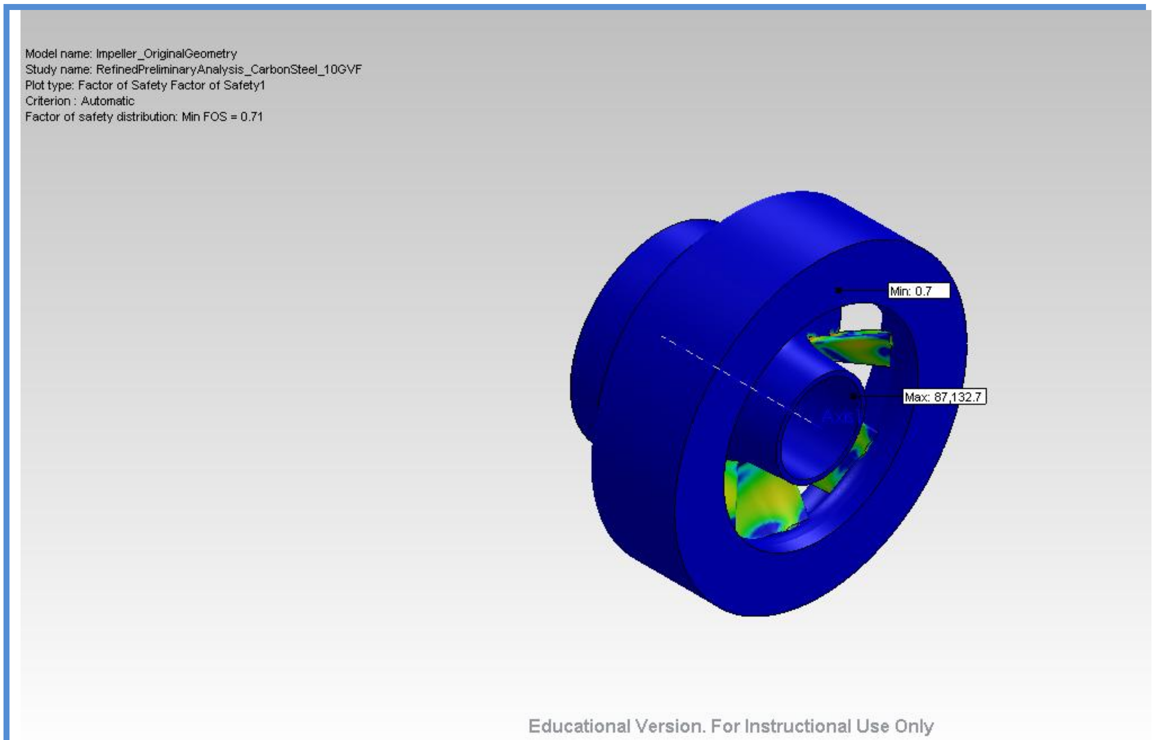

Impeller_OriginalGeometry-RefinedPreliminaryAnalysis_CarbonSteel_10GVF-Factor of Safety-Factor of Safety1

Conclusion

Comments:

The maximum displacement in the analysis is about 0.0006" at the tail of the secondary vane and near the center of the leading edge of the large blade. Even with carbon steel, there is a region which is stressed above the yield strength of the steel. This is at the knife edge in the leading edge of the main blade at the attachment point to the shroud. Thus this concern is mitigated because as it is, the impeller currently operates acceptably near the design condition. Thus, design problems with the polymer version of the impeller should also perform acceptably and safely as long as the material is only stressed past its yield stress at the knife edge.

B.2 Impeller FEA Report: Primary Blade Thickness: 0.171", Material: Somos WaterClear Ultra 10122

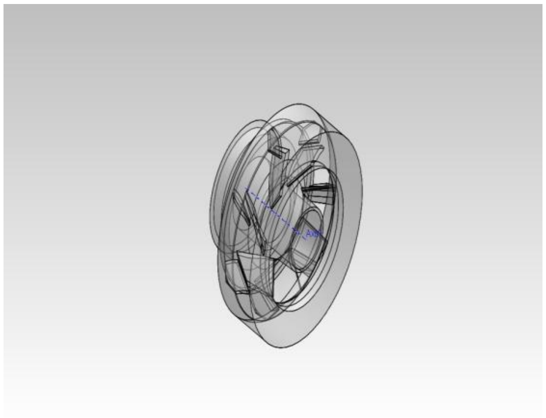

Simulation of Impeller_Original Geometry

Date: Thursday, August 22, 2013
Designer: Joseph Marchetti
Study name: RefinedPreliminaryAnalysis_SOMOSXC10122_10 GVF
Analysis type: Static

Description

This analysis was used to validate and determine required design parameters in the G470 MVP impeller. It analyzes the required blade thickness by determining the feasibility of the blades with base trailing edge thicknesses of 0.171" on the main vane and 0.129" on the secondary vane. This is the original thickness of the blades per the Baker Hughes design. The analysis was completed at 10% GVF (harsher than 25% GVF) with Somos WaterClear Ultra 10122.

Assumptions

Comments:
The assumptions are as follows:
1) The hub gives a fixed constraint.
2) The pump is operated under steady state stress conditions. Rotational speed, back pressure axial force, and pressure distribution around the blade is constant.
3) A 1.3 safety factor was applied to the back pressure axial force and pressure differential across the vanes.

Model Information

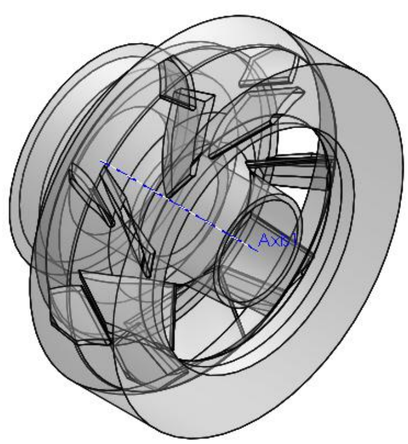

Model name: Impeller_OriginalGeometry
Current Configuration: Default

Solid Bodies

Document Name and Reference	Treated As	Volumetric Properties	Document Path/Date Modified

Revolve3 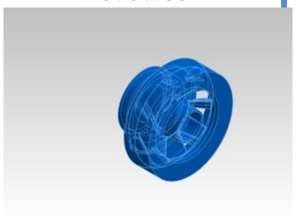	Solid Body	Mass:1.03734 kg Volume:0.000969479 m^3 Density:1070 kg/m^3 Weight:10.166 N	C:\Users\JoeyM\Desktop\MVP Visualization\Design and Procurement\PR10_Impeller\Impeller_OriginalGeometry.SLDPRT Jan 14 11:42:22 2013

Study Properties

Study name	RefinedPreliminaryAnalysis_SOMOSXC10122_10GVF
Analysis type	Static
Mesh type	Solid Mesh
Thermal Effect:	On
Thermal option	Include temperature loads
Zero strain temperature	298 Kelvin
Include fluid pressure effects from SolidWorks Flow Simulation	Off
Solver type	FFEPlus
Inplane Effect:	Off
Soft Spring:	Off
Inertial Relief:	Off
Incompatible bonding options	Automatic
Large displacement	Off
Compute free body forces	On
Friction	Off
Use Adaptive Method:	Off
Result folder	SolidWorks document (C:\Users\JoeyM\Desktop\MVP Visualization\Design and Procurement\PR10_Impeller)

Units

Unit system:	SI (MKS)
Length/Displacement	mm
Temperature	Kelvin
Angular velocity	Rad/sec
Pressure/Stress	N/m^2

Material Properties

Model Reference	Properties		Components
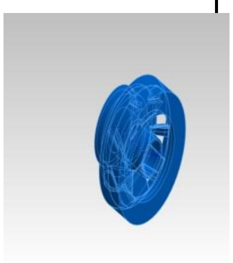	**Name:**	Somos WaterClear XC 10122	SolidBody 8(Revolve3)(Impeller _OriginalGeometry)
	Model type:	Linear Elastic Isotropic	
	Default failure criterion:	Max von Mises Stress	
	Yield strength:	5.5e+007 N/m^2	
	Tensile strength:	5.5e+007 N/m^2	
	Elastic modulus:	2.86e+009 N/m^2	
	Poisson's ratio:	0.4	
	Mass density:	1070 kg/m^3	
	Shear modulus:	8.622e+008 N/m^2	
Curve Data:N/A			

Comments:
Material properties were taken from the specification sheet from the manufacturer of the SLA resin: DSM. It was modified from Solidworks predefined polycarbonate.

Loads and Fixtures

Fixture name	Fixture Image	Fixture Details
Fixed-1	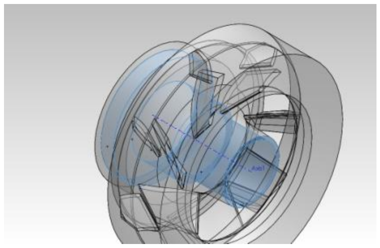	**Entities:** 6 face(s) **Type:** Fixed Geometry

Resultant Forces

Components	X	Y	Z	Resultant
Reaction force(N)	-13617.9	-0.0858392	-0.098007	13617.9
Reaction Moment(N-m)	0	0	0	0

Load name	Load Image	Load Details
Centrifugal-1	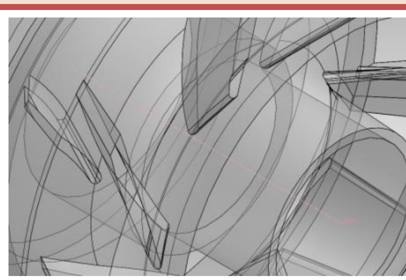	**Centrifugal, Ref:** Axis1 **Angular Velocity:** -60 Hz **Angular Acceleration:** 0 Hz/s
Force-1	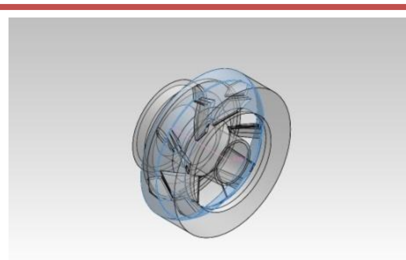	**Entities:** 3 face(s) **Reference:** Axis1 **Type:** Apply force **Values:** ---, ---, -1500 lbf
Pressure-2	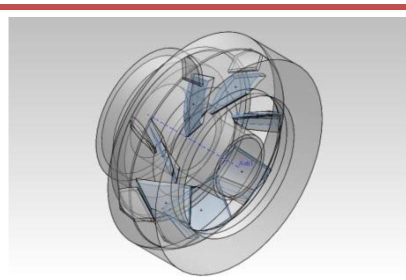	**Entities:** 7 face(s) **Type:** Normal to selected face **Value:** 108 **Units:** psi

Pressure-3	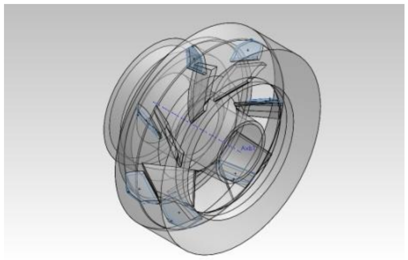	**Entities:** 14 face(s) **Type:** Normal to selected face **Value:** 135.2 **Units:** psi
Pressure-4	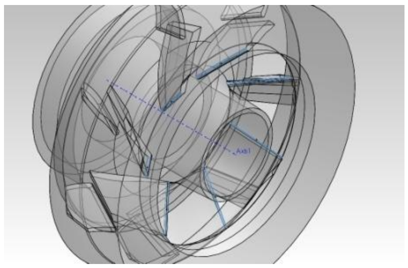	**Entities:** 7 face(s) **Type:** Normal to selected face **Value:** 337 **Units:** psi
Pressure-5	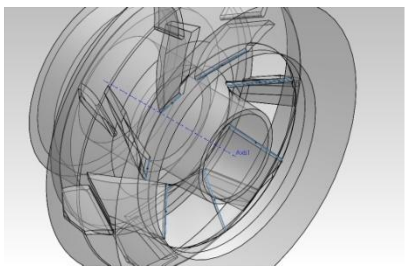	**Entities:** 7 face(s) **Type:** Normal to selected face **Value:** 175 **Units:** psi
Pressure-6	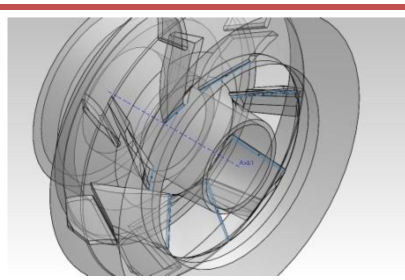	**Entities:** 7 face(s) **Type:** Normal to selected face **Value:** 45 **Units:** psi
Pressure-7	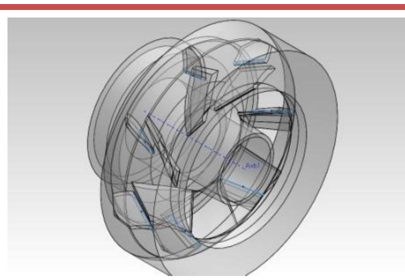	**Entities:** 7 face(s) **Type:** Normal to selected face **Value:** 342 **Units:** psi

Pressure-8	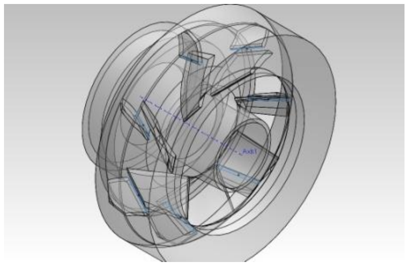	**Entities:** 7 face(s) **Type:** Normal to selected face **Value:** 54 **Units:** psi
Pressure-9	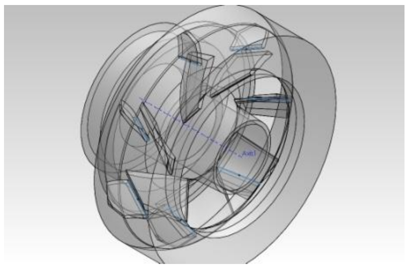	**Entities:** 7 face(s) **Type:** Normal to selected face **Value:** 170 **Units:** psi
Pressure-10	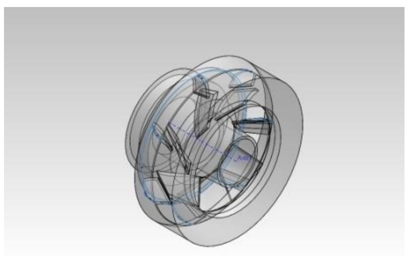	**Entities:** 8 face(s) **Type:** Normal to selected face **Value:** 225 **Units:** psi
Pressure-11	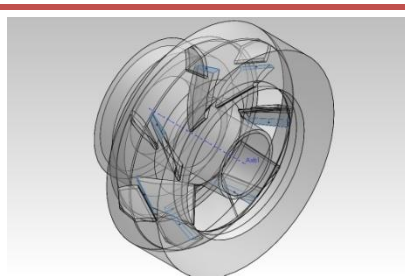	**Entities:** 7 face(s) **Type:** Normal to selected face **Value:** 210 **Units:** psi

Comments:
Three major loadings were considered:
1) Centrifugal forces generated by a 60Hz rotational speed,
2) Pressure distributions on the vanes from CFD at 10% GVF, and
3) Back pressure from 70 psig maximum head in the pump on the outlet area of the impeller.
A safety factor of 1.3 was applied to Items 2 and 3.

Mesh Information

Mesh type	Solid Mesh
Mesher Used:	Curvature based mesh
Jacobian points	4 Points
Maximum element size	0 in
Minimum element size	0 in
Mesh Quality	High

Mesh Information - Details

Total Nodes	191167
Total Elements	120055
Maximum Aspect Ratio	54.87
% of elements with Aspect Ratio < 3	95.9
% of elements with Aspect Ratio > 10	0.2
% of distorted elements(Jacobian)	0
Time to complete mesh(hh;mm;ss):	00:00:27
Computer name:	MORRISONLAB24

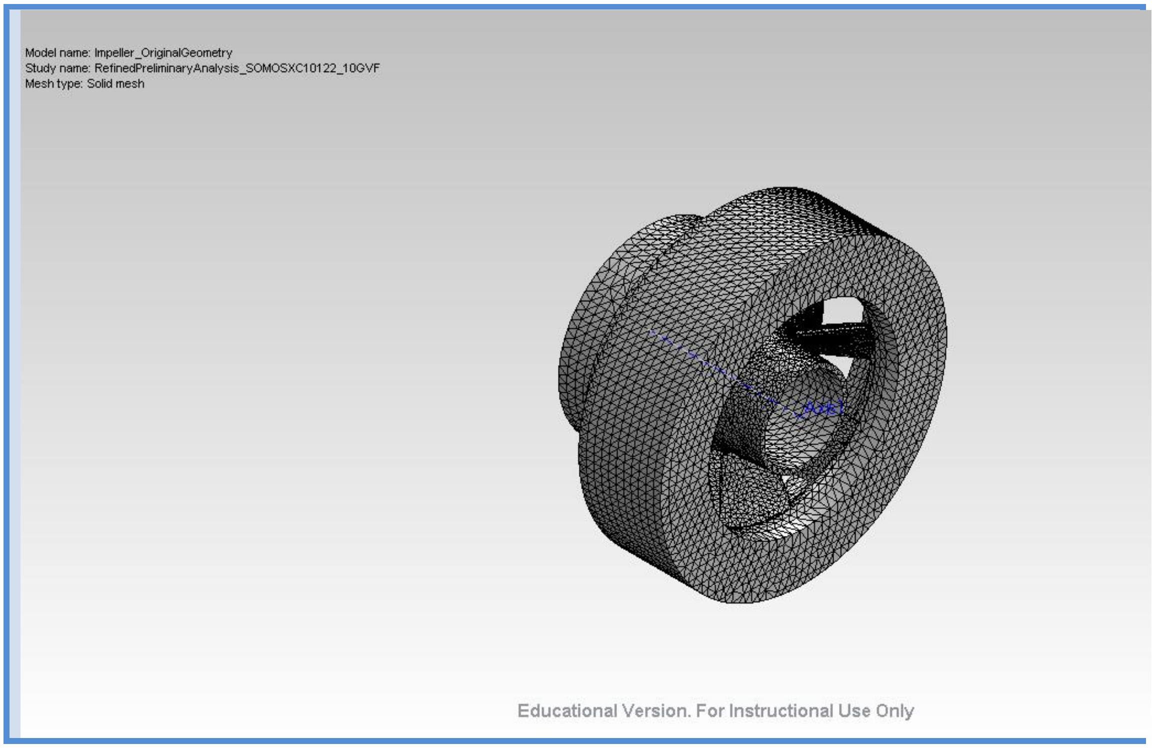

Mesh Control Information:

Mesh Control Name	Mesh Control Image	Mesh Control Details
Control -1	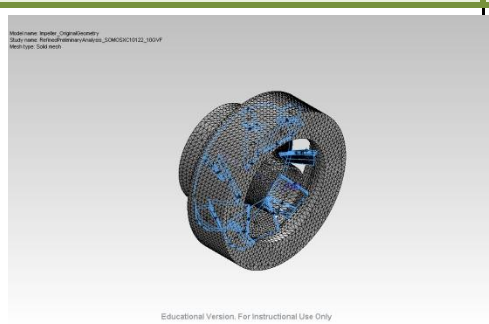	**Entities:** 113 face(s) **Units:** in **Size:** 0.097436 **Ratio:** 1.5
Control -2	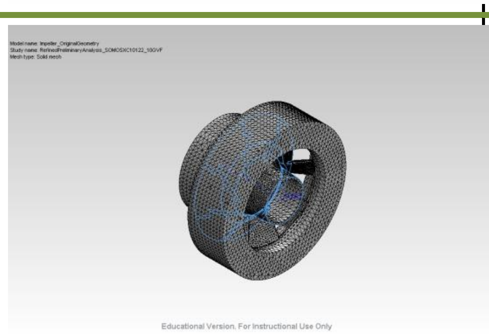	**Entities:** 9 face(s) **Units:** in **Size:** 0.097436 **Ratio:** 1.5

Resultant Forces

Reaction Forces

Selection set	Units	Sum X	Sum Y	Sum Z	Resultant
Entire Model	N	-13617.9	-0.0858392	-0.098007	13617.9

Reaction Moments

Selection set	Units	Sum X	Sum Y	Sum Z	Resultant
Entire Model	N-m	0	0	0	0

Study Results

Name	Type	Min	Max
Stress1	VON: von Mises Stress	0.112989 psi Node: 168453	55607.5 psi Node: 184744

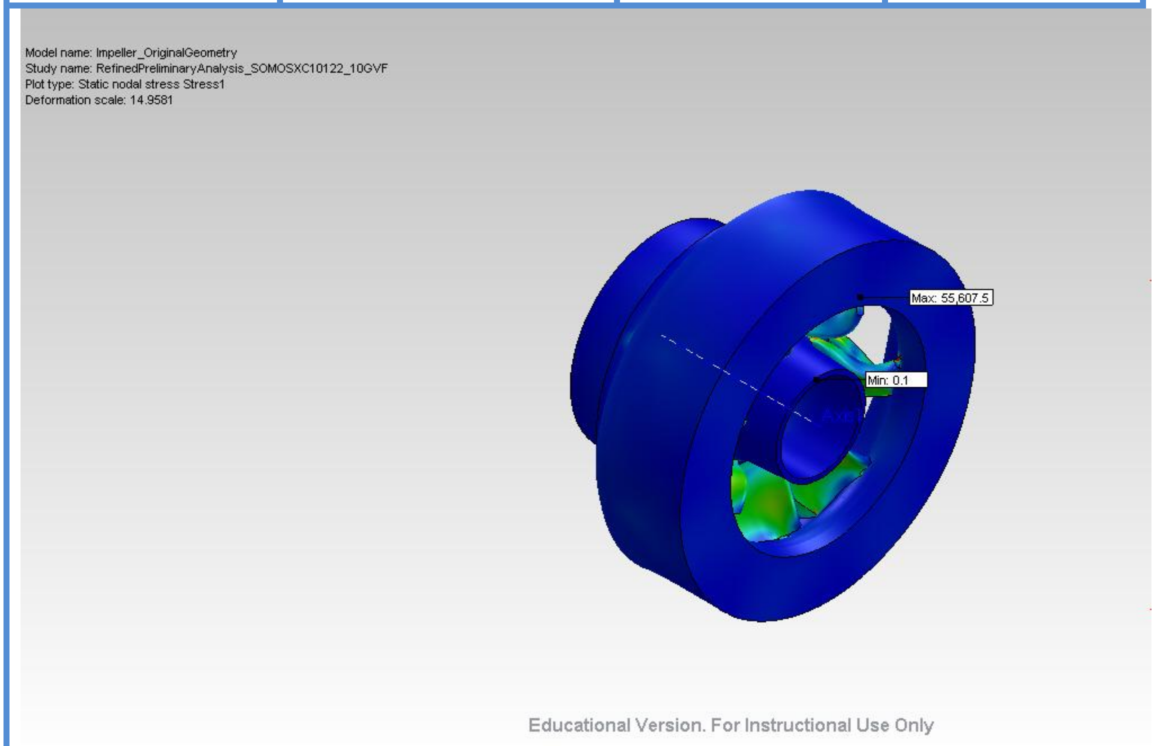

Impeller_OriginalGeometry-RefinedPreliminaryAnalysis_SOMOSXC10122_10GVF-Stress-Stress1

Name	Type	Min	Max
Displacement1	URES: Resultant Displacement	0 mil Node: 2403	51.687 mil Node: 114999

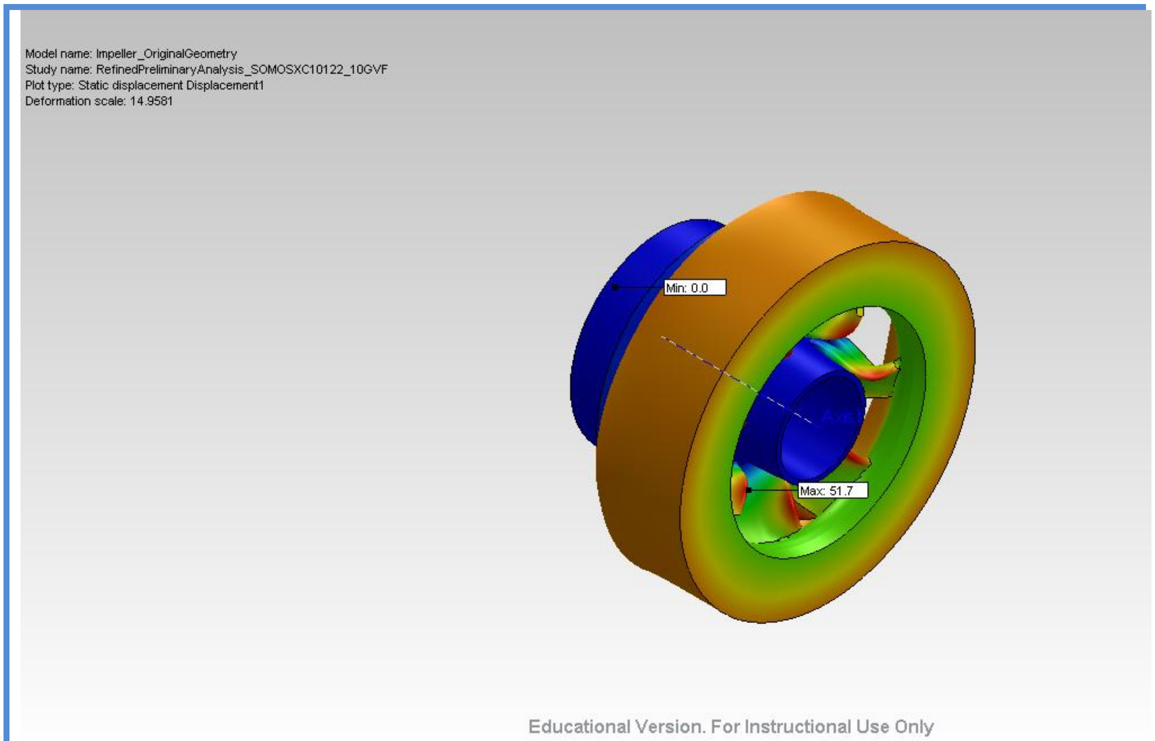

Impeller_OriginalGeometry-RefinedPreliminaryAnalysis_SOMOSXC10122_10GVF-Displacement-Displacement1

Name	Type	Min	Max
Strain1	ESTRN: Equivalent Strain	3.0783e-007 Element: 65780	0.0601504 Element: 10675

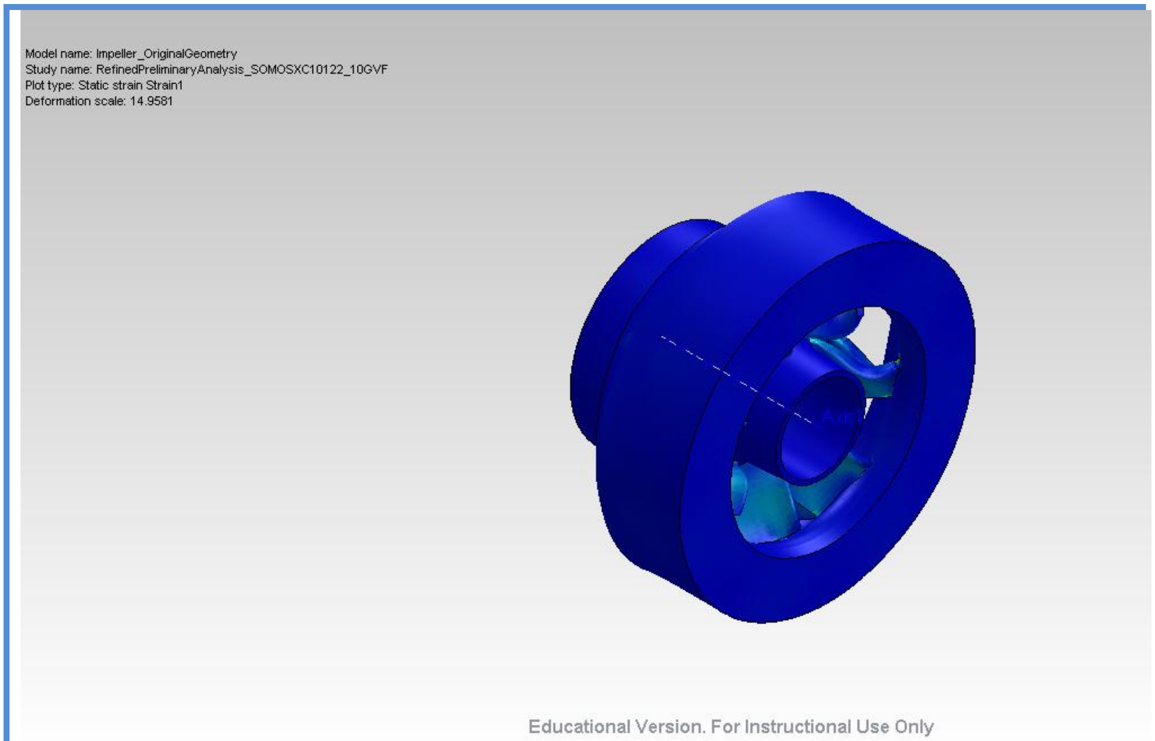

Impeller_OriginalGeometry-RefinedPreliminaryAnalysis_SOMOSXC10122_10GVF-Strain-Strain1

Name	Type	Min	Max
Factor of Safety1	Automatic	0.143453 Node: 184744	70600.2 Node: 168453

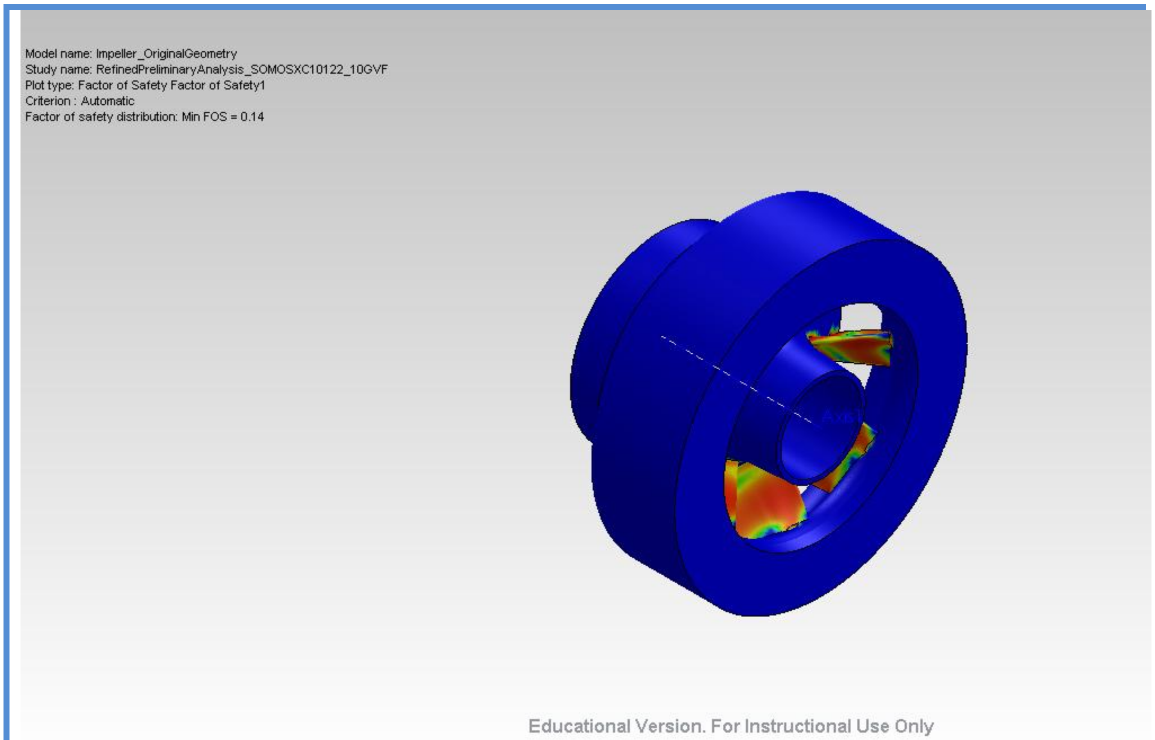

Impeller_OriginalGeometry-RefinedPreliminaryAnalysis_SOMOSXC10122_10GVF-Factor of Safety-Factor of Safety1

Conclusion

Comments:

The impeller design is NOT acceptable for manufacture and operation. There are multiple locations with yield stresses above the yield stress. Those are more than only the location of the knife edge in the leading edge of the main blade at the attachment point to the shroud. The maximum deflection in the impeller is approximately 52 mils, which is greater than that for a steel or cast iron impeller. It has an unacceptable deflection more than 25 mil. Redesign with blade thickening is required.

B.3 Impeller FEA Report: Primary Blade Thickness: 0.336", Material: Somos WaterClear Ultra 10122

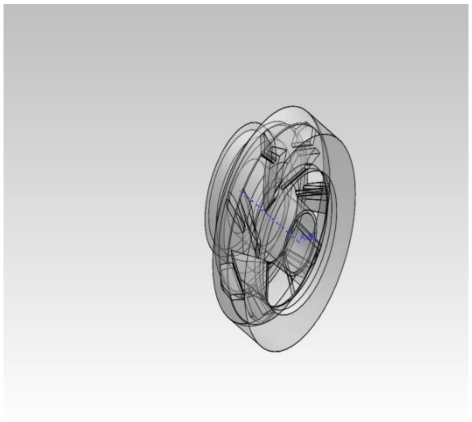

Simulation of Impeller_Rev3

Date: Thursday, August 22, 2013
Designer: Joseph Marchetti
Study name: ModifiedDesign_336_251_SomosWaterClearUltra10122_10GVF
Analysis type: Static

Description

This analysis was used to validate and determine required design parameters in the G470 MVP impeller. It analyzes the required blade thickness by determining the feasibility of the blades with base trailing edge thicknesses of 0.336" on the main vane and 0.251" on the secondary vane. The analysis was completed at 10% GVF (harsher than 25% GVF) with Somos WaterClear Ultra 10122.

Assumptions

Comments:
The assumptions are as follows:
1) The hub gives a fixed constraint.
2) The pump is operated under steady state stress conditions. Rotational speed, back pressure axial force, and pressure distribution around the blade is constant.
3) A 1.3 safety factor was applied to the back pressure axial force and pressure differential across the vanes.

Model Information

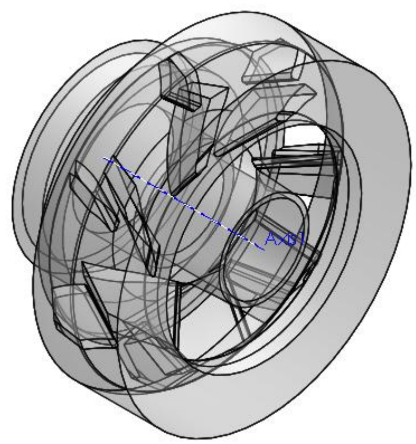

Model name: **Impeller_Rev3**

Current Configuration: **Default**

Solid Bodies			
Document Name and Reference	Treated As	Volumetric Properties	Document Path/Date Modified

Revolve2 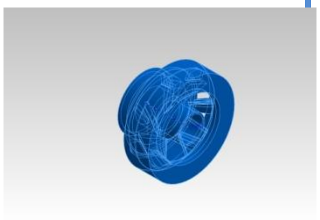	**Solid Body**	Mass:1.07641 kg Volume:0.00100599 m^3 Density:1070 kg/m^3 Weight:10.5488 N	C:\Users\JoeyM\Desktop\MVP Visualization\Design and Procurement\PR10_Impeller\Impeller_Rev3.SLDPRT **Jan 14 18:02:49 2013**

Study Properties

Study name	ModifiedDesign_336_251_SomosWaterClearUltra10122_10GVF
Analysis type	Static
Mesh type	Solid Mesh
Thermal Effect:	On
Thermal option	Include temperature loads
Zero strain temperature	298 Kelvin
Include fluid pressure effects from SolidWorks Flow Simulation	Off
Solver type	FFEPlus
Inplane Effect:	Off
Soft Spring:	Off
Inertial Relief:	Off
Incompatible bonding options	Automatic
Large displacement	Off
Compute free body forces	On
Friction	Off
Use Adaptive Method:	Off
Result folder	SolidWorks document (C:\Users\JoeyM\Desktop\MVP

	Visualization\Design and Procurement\PR10_Impeller)

Units

Unit system:	SI (MKS)
Length/Displacement	mm
Temperature	Kelvin
Angular velocity	Rad/sec
Pressure/Stress	N/m^2

Material Properties

Model Reference	Properties		Components
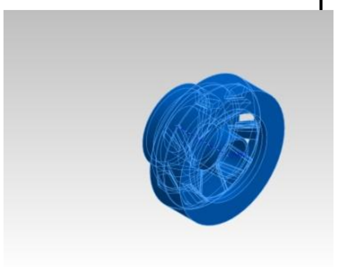	Name:	Somos WaterClear XC 10122	SolidBody 10(Revolve2)(Impeller_Rev3)
	Model type:	Linear Elastic Isotropic	
	Default failure criterion:	Max von Mises Stress	
	Yield strength:	5.5e+007 N/m^2	
	Tensile strength:	5.5e+007 N/m^2	
	Elastic modulus:	2.86e+009 N/m^2	
	Poisson's ratio:	0.4	
	Mass density:	1070 kg/m^3	
	Shear modulus:	8.622e+008 N/m^2	
Curve Data:N/A			

Comments:
Material properties were taken from the specification sheet from the manufacturer of the SLA resin: DSM. It was modified from Solidworks predefined polycarbonate.

Loads and Fixtures

Fixture name	Fixture Image	Fixture Details
Fixed-1	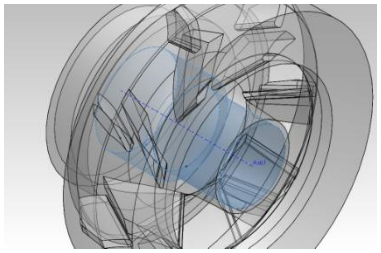	Entities: **2 face(s)** Type: **Fixed Geometry**

Resultant Forces

Components	X	Y	Z	Resultant
Reaction force(N)	-13167.1	-0.0777183	-0.295805	13167.1
Reaction Moment(N-m)	0	0	0	0

Load name	Load Image	Load Details
Centrifugal-1	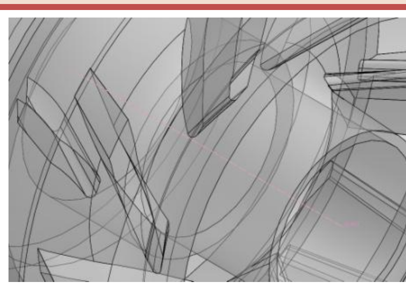	Centrifugal, Ref: **Axis1** Angular Velocity: **-60 Hz** Angular Acceleration: **0 Hz/s**
Force-1	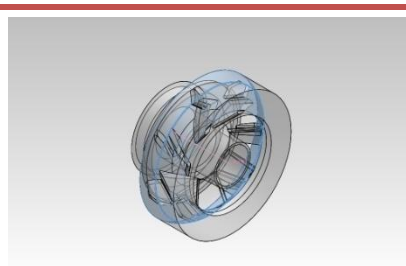	Entities: **3 face(s)** Reference: **Axis1** Type: **Apply force** Values: **---, ---, -1500 lbf**
Pressure-2	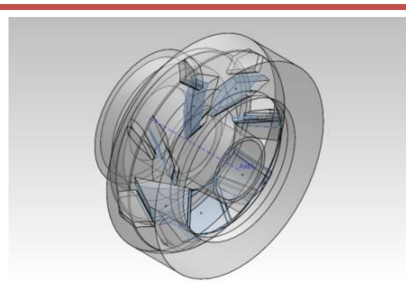	Entities: **7 face(s)** Type: **Normal to selected face** Value: **108** Units: **psi**

Pressure-3	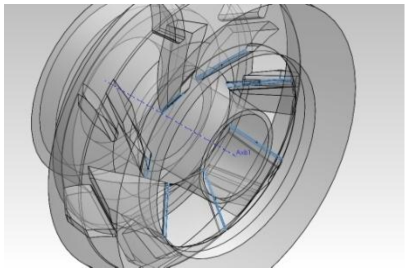	Entities: **7 face(s)** Type: **Normal to selected face** Value: **337** Units: **psi**
Pressure-4	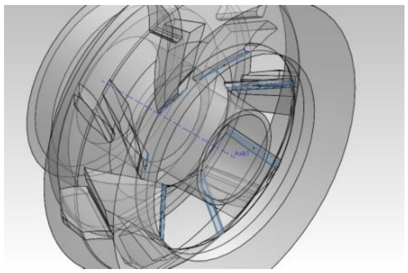	Entities: **7 face(s)** Type: **Normal to selected face** Value: **175** Units: **psi**
Pressure-5	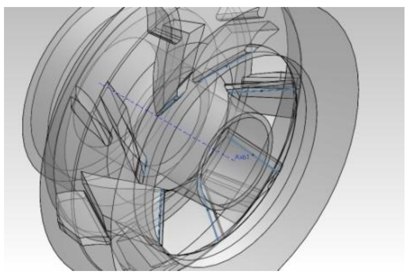	Entities: **7 face(s)** Type: **Normal to selected face** Value: **45** Units: **psi**
Pressure-6	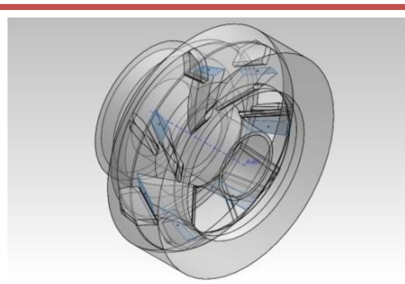	Entities: **7 face(s)** Type: **Normal to selected face** Value: **210** Units: **psi**
Pressure-7	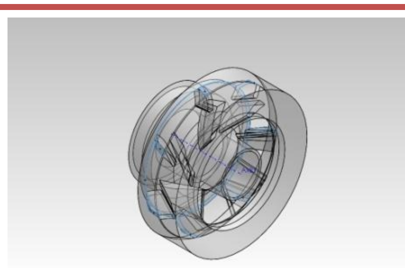	Entities: **8 face(s)** Type: **Normal to selected face** Value: **225** Units: **psi**

Pressure-8	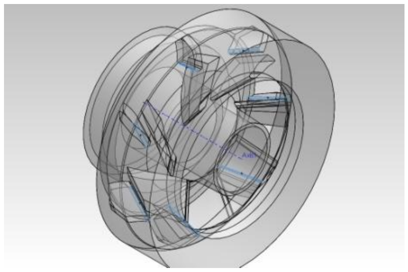	Entities: **7 face(s)** Type: **Normal to selected face** Value: **342** Units: **psi**
Pressure-9	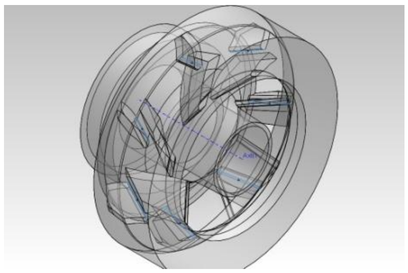	Entities: **7 face(s)** Type: **Normal to selected face** Value: **54** Units: **psi**
Pressure-10	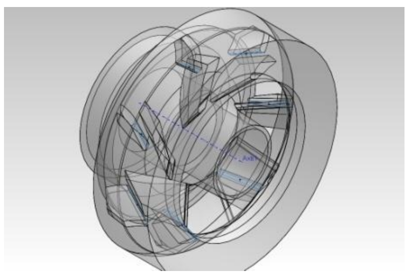	Entities: **7 face(s)** Type: **Normal to selected face** Value: **170** Units: **psi**
Pressure-11	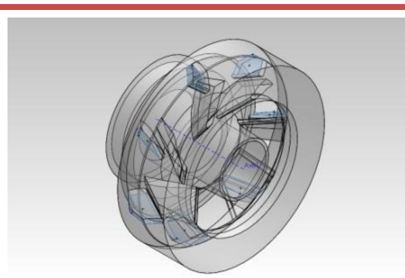	Entities: **14 face(s)** Type: **Normal to selected face** Value: **135.2** Units: **psi**

Comments:

Three major loadings were considered:
1) Centrifugal forces generated by a 60Hz rotational speed,
2) Pressure distributions on the vanes from CFD at 10% GVF, and
3) Back pressure from 70 psig maximum head in the pump on the outlet area of the impeller.
A safety factor of 1.3 was applied to Items 2 and 3.

Mesh Information

Mesh type	Solid Mesh
Mesher Used:	Standard mesh
Automatic Transition:	Off
Include Mesh Auto Loops:	Off
Jacobian points	At Nodes
Element Size	0.197309 in
Tolerance	0.00986545 in
Mesh Quality	High

Mesh Information - Details

Total Nodes	238886
Total Elements	153383
Maximum Aspect Ratio	55.402
% of elements with Aspect Ratio < 3	96.8
% of elements with Aspect Ratio > 10	0.0665
% of distorted elements(Jacobian)	0
Time to complete mesh(hh;mm;ss):	00:00:30
Computer name:	MORRISONLAB24

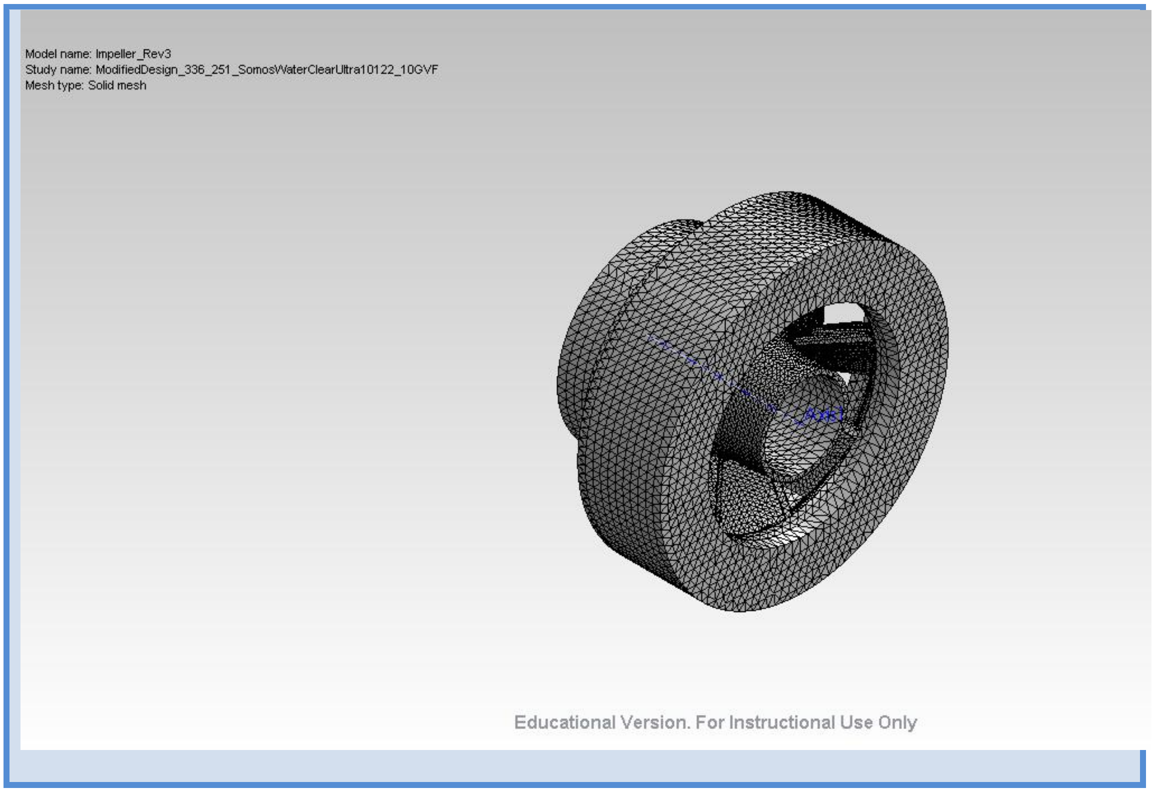

Mesh Control Information:

Mesh Control Name	Mesh Control Image	Mesh Control Details
Control -4	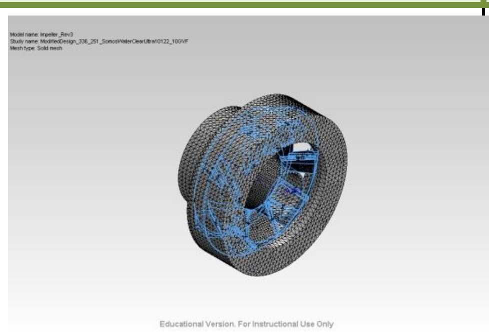	Entities: **110 face(s)** Units: **in** Size: **0.098644** Ratio: **1.5**

Control -6	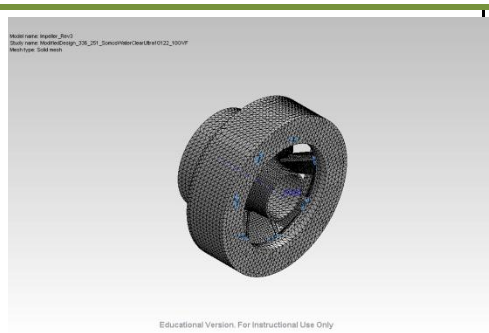	Entities: **14 face(s)** Units: **in** Size: **0.098644** Ratio: **1.5**

Resultant Forces

Reaction Forces

Selection set	Units	Sum X	Sum Y	Sum Z	Resultant
Entire Model	N	-13167.1	-0.0777183	-0.295805	13167.1

Reaction Moments

Selection set	Units	Sum X	Sum Y	Sum Z	Resultant
Entire Model	N-m	0	0	0	0

Study Results

Name	Type	Min	Max
Stress1	VON: von Mises Stress	0.233632 psi Node: 4204	14483 psi Node: 229065

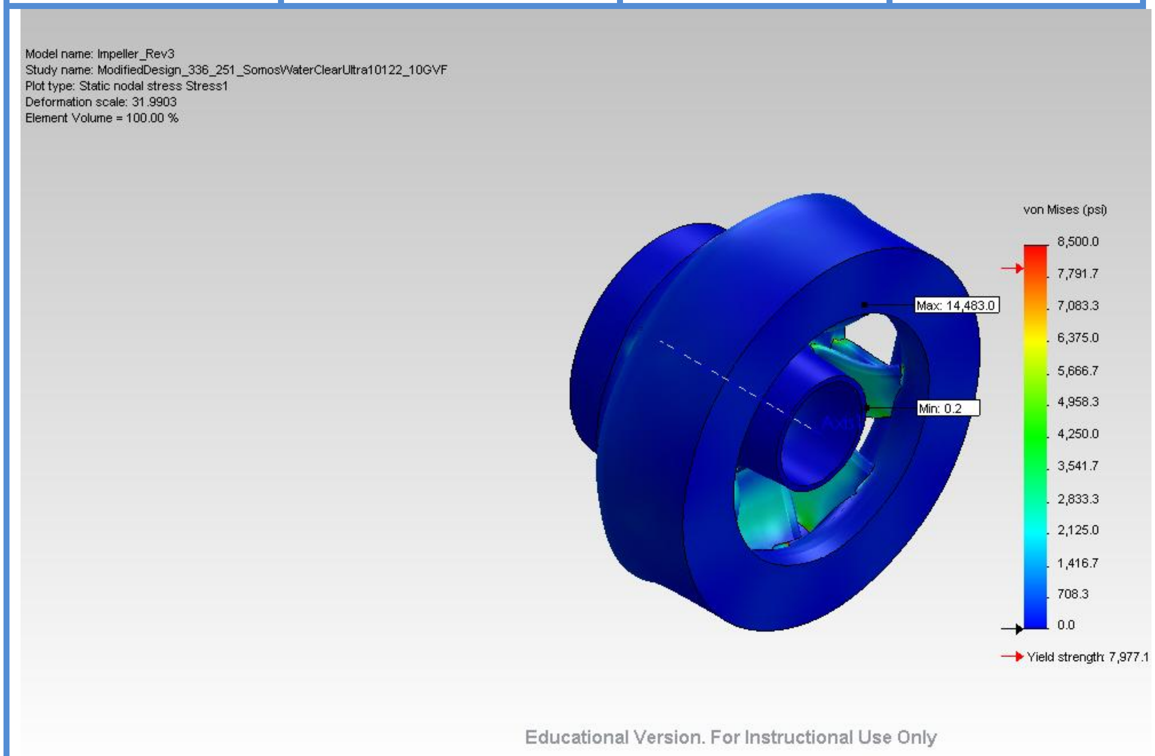

Impeller_Rev3-ModifiedDesign_336_251_SomosWaterClearUltra10122_10GVF-Stress-Stress1

Name	Type	Min	Max
Displacement1	URES: Resultant Displacement	0 mil Node: 7031	24.3682 mil Node: 5961

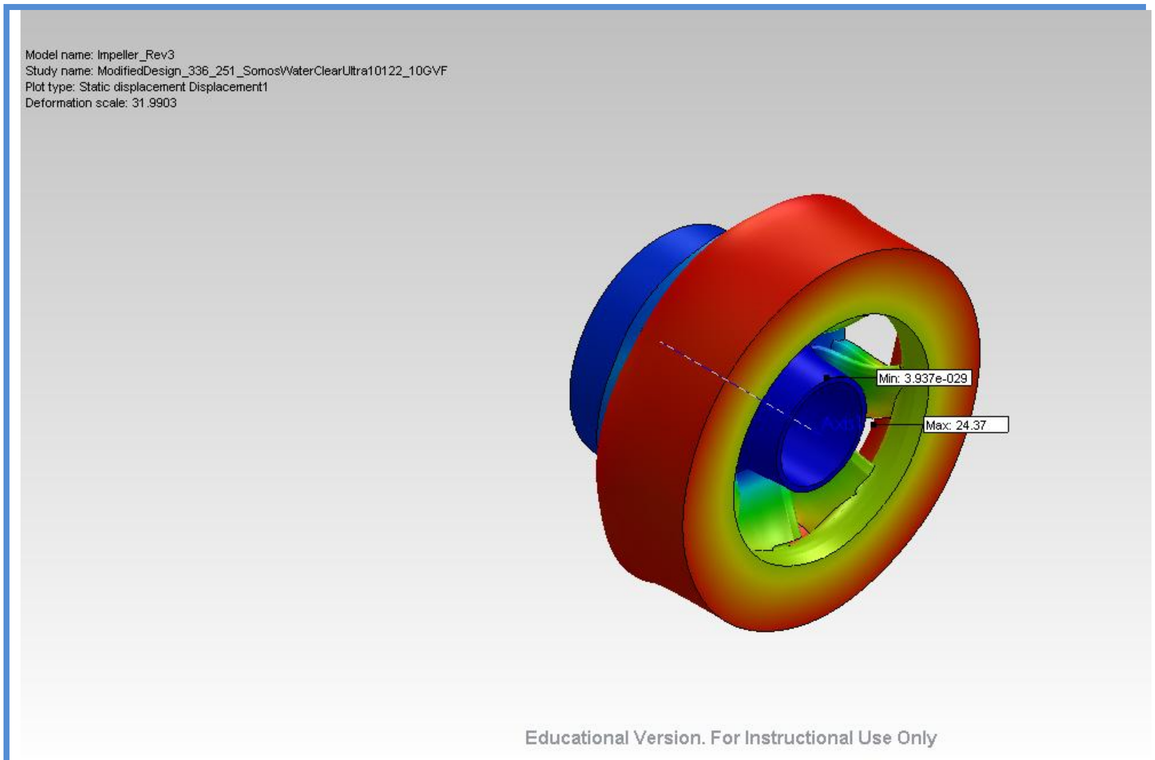

Impeller_Rev3-ModifiedDesign_336_251_SomosWaterClearUltra10122_10GVF-Displacement-Displacement1

Name	Type	Min	Max
Strain1	ESTRN: Equivalent Strain	8.11495e-007 Element: 78686	0.0184302 Element: 16296

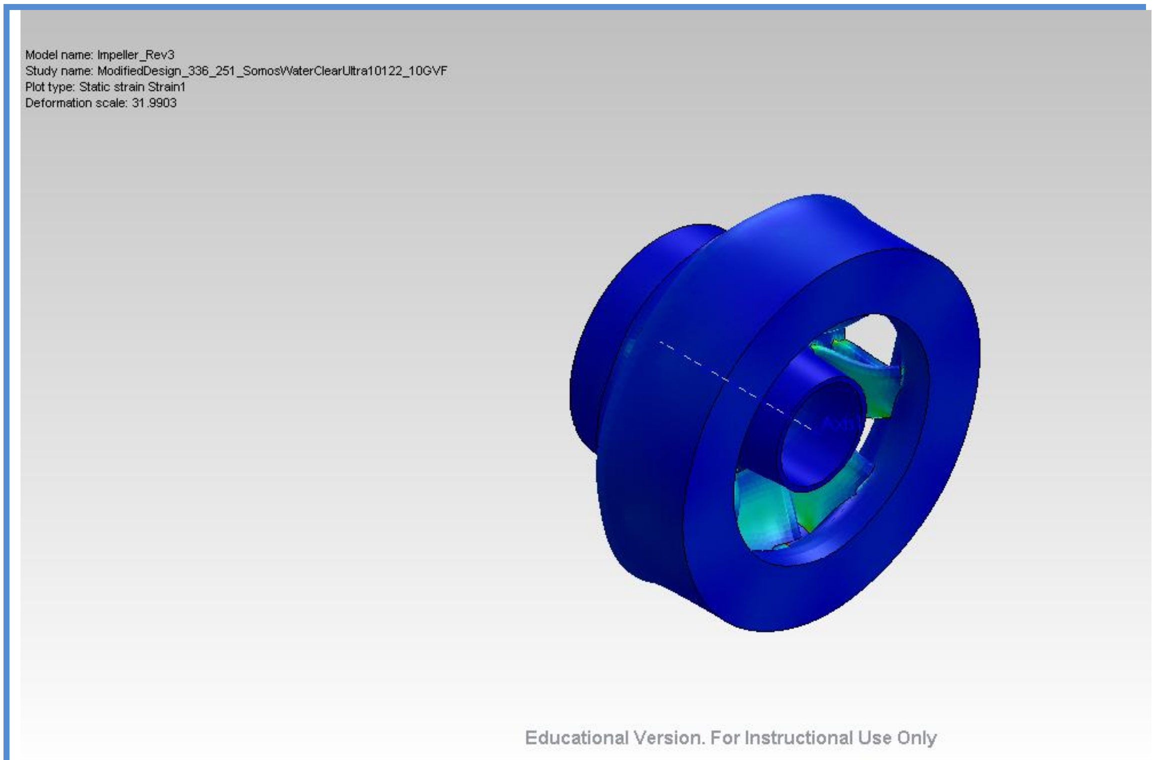

Impeller_Rev3-ModifiedDesign_336_251_SomosWaterClearUltra10122_10GVF-Strain-Strain1

Name	Type
Displacement1{1}	URES: Resultant Displacement

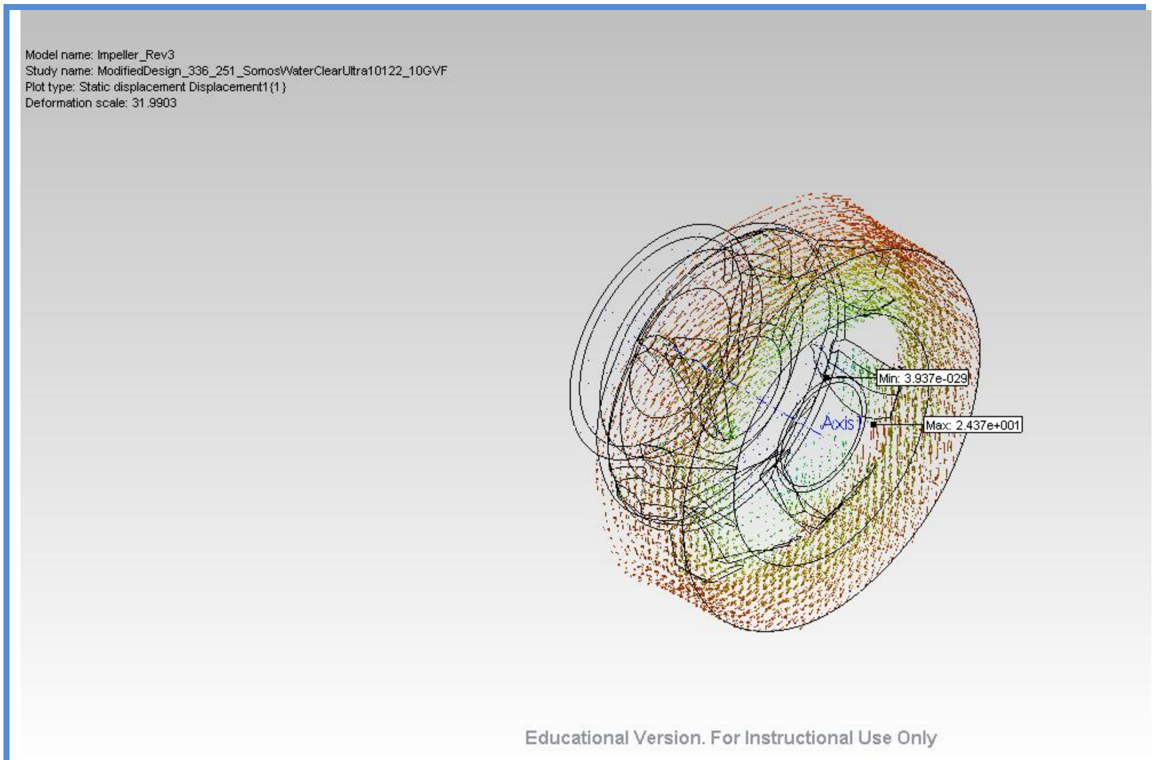

Impeller_Rev3-ModifiedDesign_336_251_SomosWaterClearUltra10122_10GVF-Displacement-Displacement1{1}

Name	Type	Min	Max
Factor of Safety1	Automatic	0.55079 Node: 229065	34143.8 Node: 4204

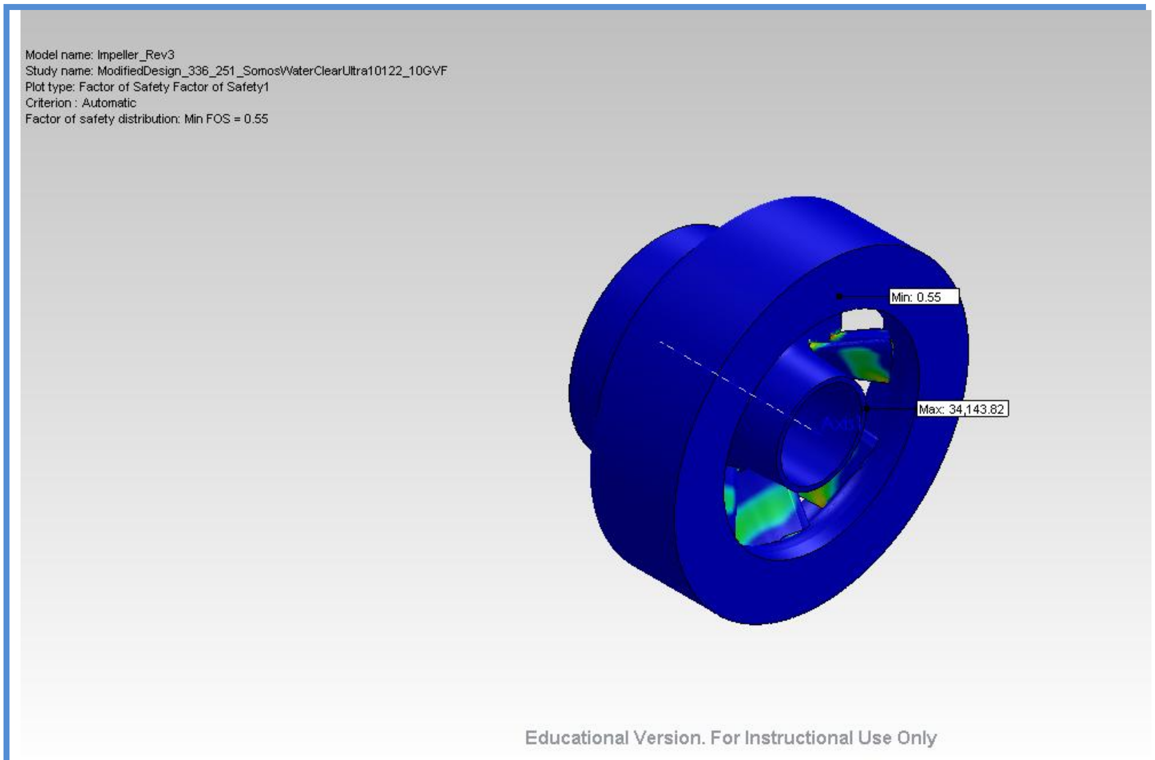

Impeller_Rev3-ModifiedDesign_336_251_SomosWaterClearUltra10122_10GVF-Factor of Safety-Factor of Safety1

Name	Type
Displacement2	Deformed Shape

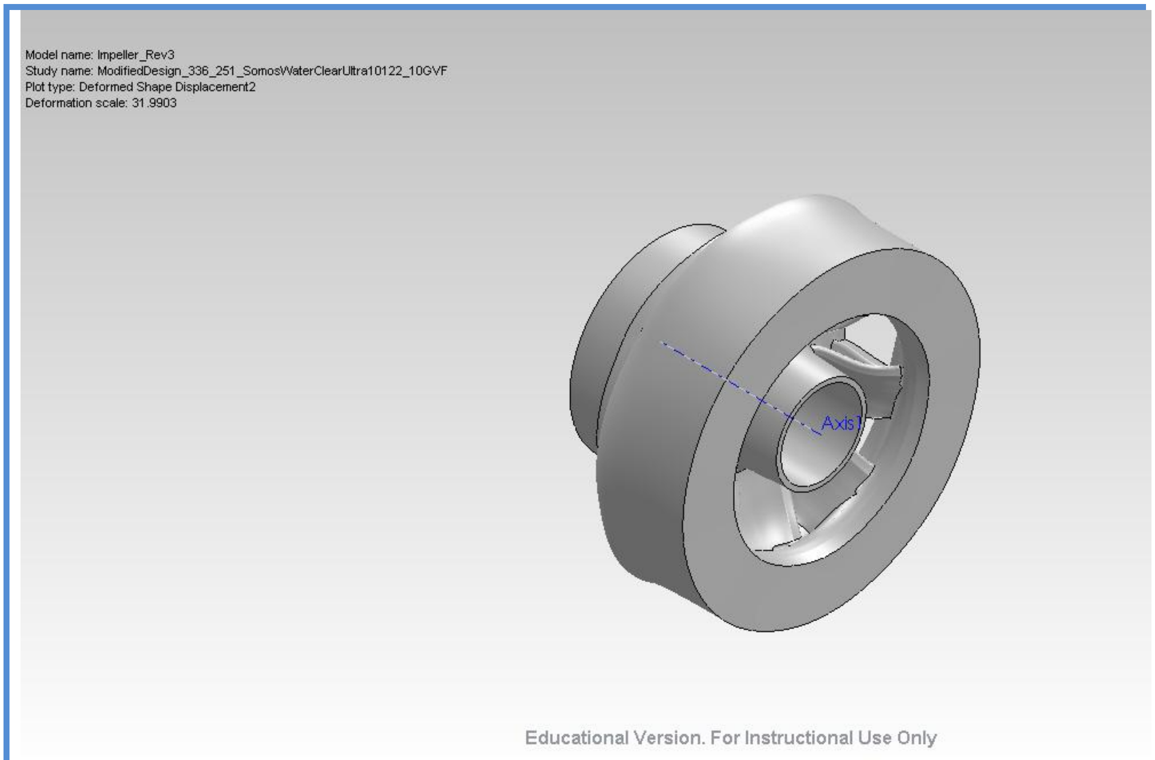

Impeller_Rev3-ModifiedDesign_336_251_SomosWaterClearUltra10122_10GVF-Displacement-Displacement2

Conclusion

Comments:

The impeller design is acceptable for manufacture and operation. The only location with stresses above the yield stress is the knife edge in the leading edge of the main blade at the attachment point to the shroud. The maximum deflection in the impeller is approximately 24 mils, which is greater than that for a steel or cast iron impeller. It has an acceptable deflection less than 25 mil.

B.4 Impeller FEA Report: Primary Blade Thickness: 0.419”, Material: Somos WaterClear Ultra 10122

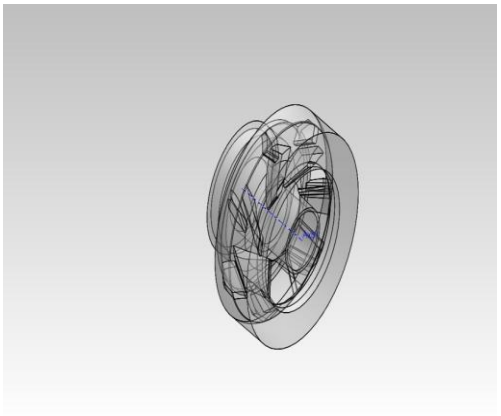

Simulation of Impeller_Rev4

Date: Thursday, August 22, 2013
Designer: Joseph Marchetti
Study name: ModifiedDesign_419_312_WaterClearUltra10122_10GVF
Analysis type: Static

Description

This analysis was used to validate and determine required design parameters in the G470 MVP impeller. It analyzes the required blade thickness by determining the feasibility of the blades with base trailing edge thicknesses of 0.419" on the main vane and 0.312" on the secondary vane. The analysis was completed at 10% GVF (harsher than 25% GVF) with Somos WaterClear Ultra 10122.

Assumptions

Comments:
The assumptions are as follows:
1) The hub gives a fixed constraint.
2) The pump is operated under steady state stress conditions. Rotational speed, back pressure axial force, and pressure distribution around the blade is constant.
3) A 1.3 safety factor was applied to the back pressure axial force and pressure differential across the vanes.

Model Information

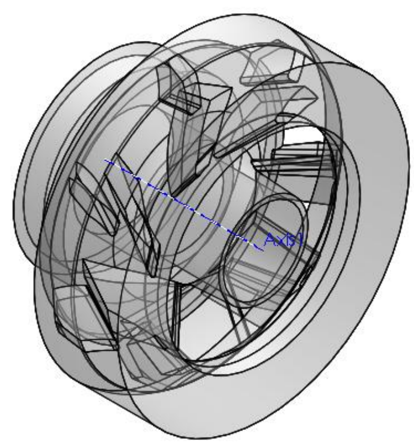

Model name: **Impeller_Rev4**

Current Configuration: **Default**

Solid Bodies			
Document Name and Reference	Treated As	Volumetric Properties	Document Path/Date Modified

Revolve2 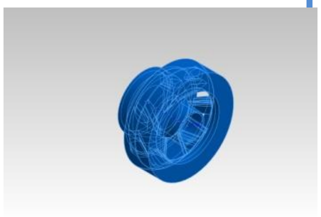	**Solid Body**	Mass:1.0959 kg Volume:0.001 0242 m^3 Density:1070 kg/m^3 Weight:10.739 8 N	C:\Users\JoeyM\Desktop\MVP Visualization\Design and Procurement\PR10_Impeller\Impeller_Rev4.SLDPRT **Jan 14 18:02:37 2013**

Study Properties

Study name	ModifiedDesign_419_312_WaterClearUltra10122_10GVF
Analysis type	Static
Mesh type	Solid Mesh
Thermal Effect:	On
Thermal option	Include temperature loads
Zero strain temperature	298 Kelvin
Include fluid pressure effects from SolidWorks Flow Simulation	Off
Solver type	FFEPlus
Inplane Effect:	Off
Soft Spring:	Off
Inertial Relief:	Off
Incompatible bonding options	Automatic
Large displacement	Off
Compute free body forces	On
Friction	Off
Use Adaptive Method:	Off
Result folder	SolidWorks document (C:\Users\JoeyM\Desktop\MVP Visualization\Design and Procurement\PR10_Impeller)

Units

Unit system:	SI (MKS)
Length/Displacement	mm
Temperature	Kelvin
Angular velocity	Rad/sec
Pressure/Stress	N/m^2

Material Properties

Model Reference	Properties		Components
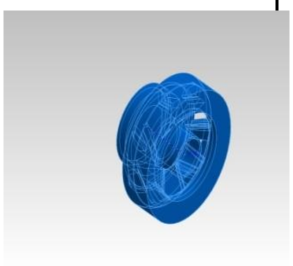	Name:	Somos WaterClear XC 10122	SolidBody 10(Revolve2)(Impeller_Rev4)
	Model type:	Linear Elastic Isotropic	
	Default failure criterion:	Max von Mises Stress	
	Yield strength:	5.5e+007 N/m^2	
	Tensile strength:	5.5e+007 N/m^2	
	Elastic modulus:	2.86e+009 N/m^2	
	Poisson's ratio:	0.4	
	Mass density:	1070 kg/m^3	
	Shear modulus:	8.622e+008 N/m^2	
Curve Data:N/A			

Comments:
Material properties were taken from the specification sheet from the manufacturer of the SLA resin: DSM. It was modified from Solidworks predefined polycarbonate.

Loads and Fixtures

Fixture name	Fixture Image	Fixture Details
Fixed-1	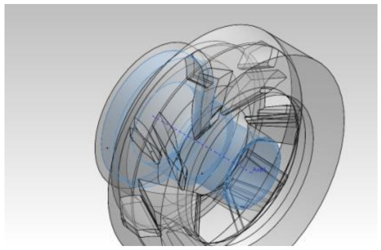	Entities: **6 face(s)** Type: **Fixed Geometry**

Resultant Forces

Components	X	Y	Z	Resultant
Reaction force(N)	-13180.8	-0.472809	-0.0666308	13180.8
Reaction Moment(N-m)	0	0	0	0

Load name	Load Image	Load Details
Centrifugal-1	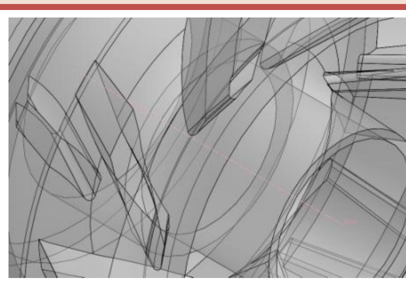	Centrifugal, Ref: **Axis1** Angular Velocity: **-60 Hz** Angular Acceleration: **0 Hz/s**
Force-1	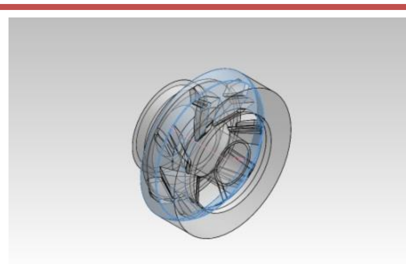	Entities: **3 face(s)** Reference: **Axis1** Type: **Apply force** Values: **---, ---, -1500 lbf**
Pressure-2	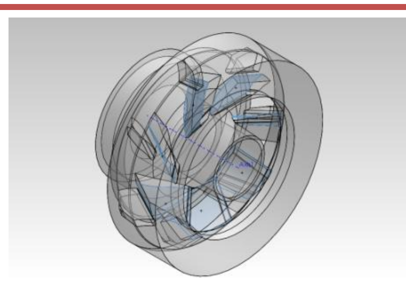	Entities: **7 face(s)** Type: **Normal to selected face** Value: **108** Units: **psi**

Pressure-3	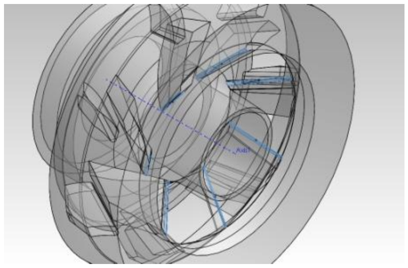	Entities: **7 face(s)** Type: **Normal to selected face** Value: **337** Units: **psi**
Pressure-4	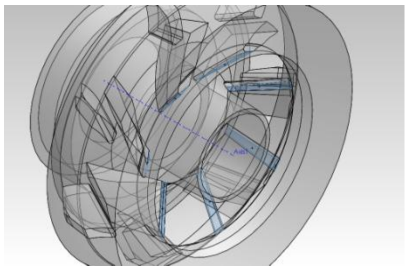	Entities: **7 face(s)** Type: **Normal to selected face** Value: **175** Units: **psi**
Pressure-5	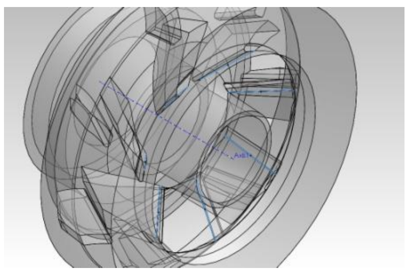	Entities: **7 face(s)** Type: **Normal to selected face** Value: **45** Units: **psi**
Pressure-6	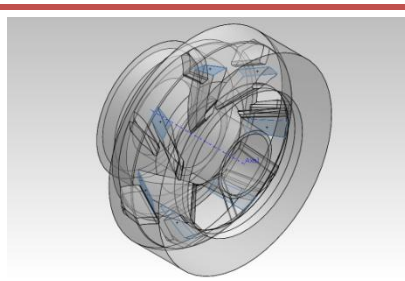	Entities: **7 face(s)** Type: **Normal to selected face** Value: **210** Units: **psi**
Pressure-7	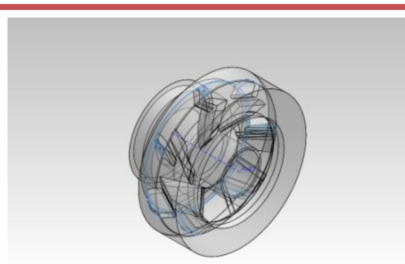	Entities: **8 face(s)** Type: **Normal to selected face** Value: **225** Units: **psi**

Pressure-8	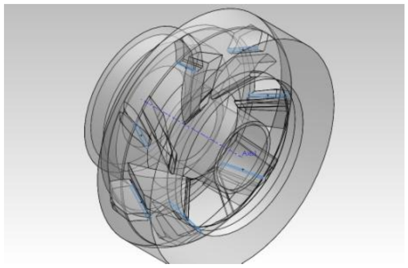	Entities: **7 face(s)** Type: **Normal to selected face** Value: **342** Units: **psi**
Pressure-9	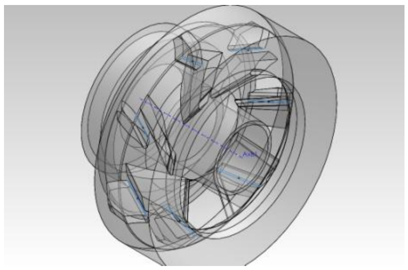	Entities: **7 face(s)** Type: **Normal to selected face** Value: **54** Units: **psi**
Pressure-10	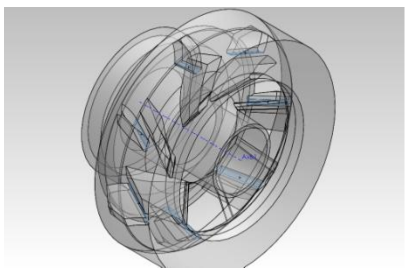	Entities: **7 face(s)** Type: **Normal to selected face** Value: **170** Units: **psi**
Pressure-11	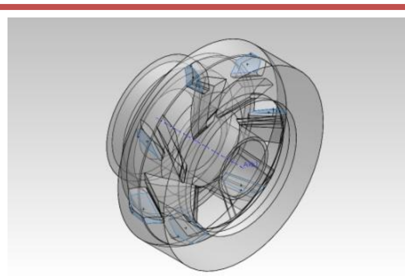	Entities: **14 face(s)** Type: **Normal to selected face** Value: **135.2** Units: **psi**

Comments:
Three major loadings were considered:
1) Centrifugal forces generated by a 60Hz rotational speed,
2) Pressure distributions on the vanes from CFD at 10% GVF, and
3) Back pressure from 70 psig maximum head in the pump on the outlet area of the impeller.
A safety factor of 1.3 was applied to Items 2 and 3.

Mesh Information

Mesh type	Solid Mesh
Mesher Used:	Standard mesh
Automatic Transition:	Off
Include Mesh Auto Loops:	Off
Jacobian points	At Nodes
Element Size	0.197309 in
Tolerance	0.00986545 in
Mesh Quality	High

Mesh Information - Details

Total Nodes	247456
Total Elements	159790
Maximum Aspect Ratio	55.63
% of elements with Aspect Ratio < 3	97.1
% of elements with Aspect Ratio > 10	0.0601
% of distorted elements(Jacobian)	0
Time to complete mesh(hh;mm;ss):	00:00:30
Computer name:	MORRISONLAB24

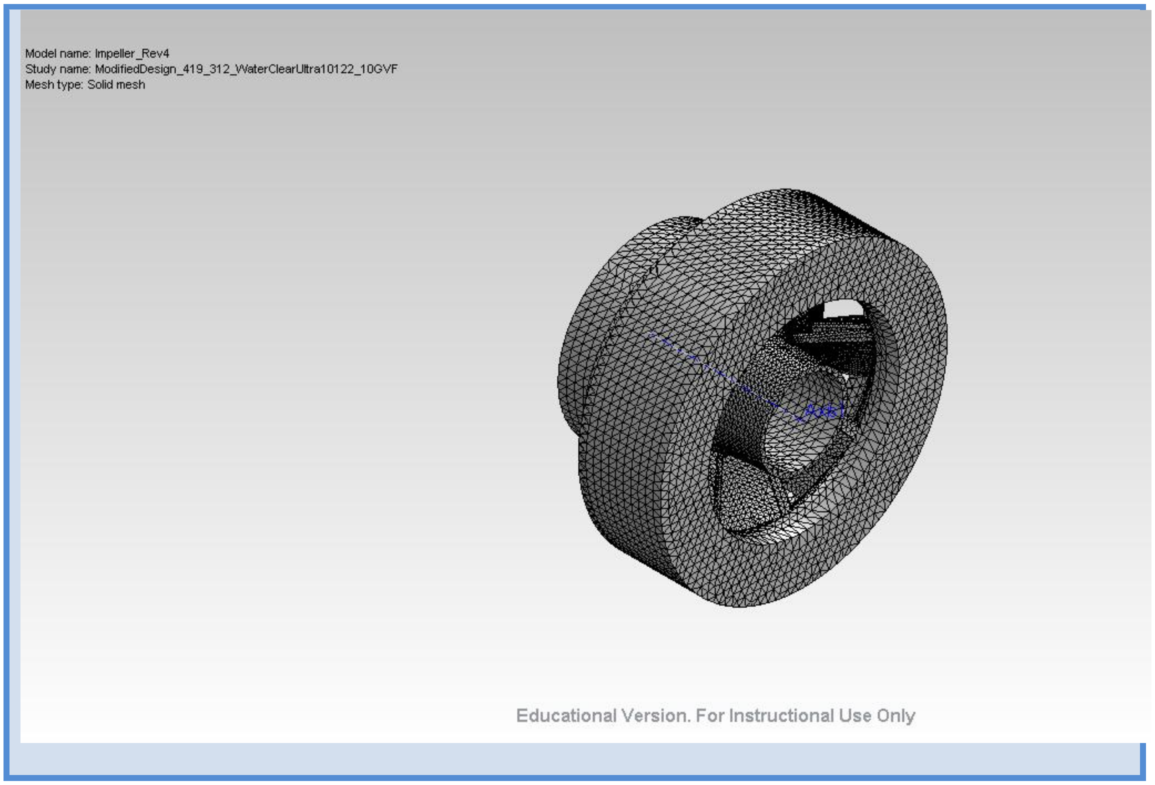

Mesh Control Information:

Mesh Control Name	Mesh Control Image	Mesh Control Details
Control -4	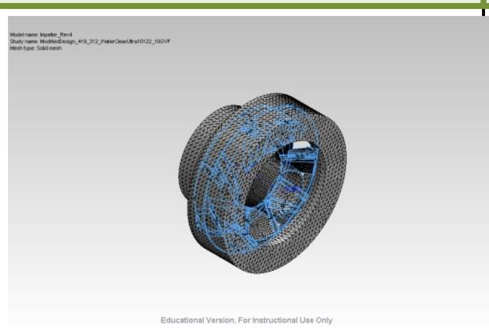	Entities: **110 face(s)** Units: **in** Size: **0.098644** Ratio: **1.5**

Control -6	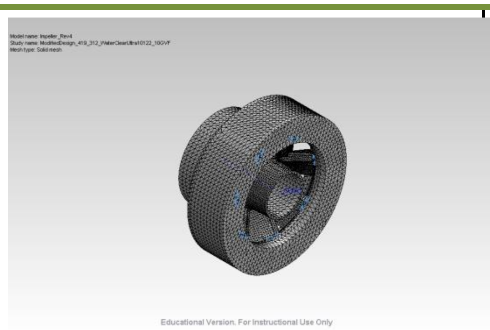	Entities: Units: Size: Ratio:	**14 face(s)** **in** **0.098644** **1.5**

Resultant Forces

Reaction Forces

Selection set	Units	Sum X	Sum Y	Sum Z	Resultant
Entire Model	N	-13180.8	-0.472809	-0.0666308	13180.8

Reaction Moments

Selection set	Units	Sum X	Sum Y	Sum Z	Resultant
Entire Model	N-m	0	0	0	0

Study Results

Name	Type	Min	Max
Stress1	VON: von Mises Stress	0.155149 psi Node: 216611	8923.95 psi Node: 237874

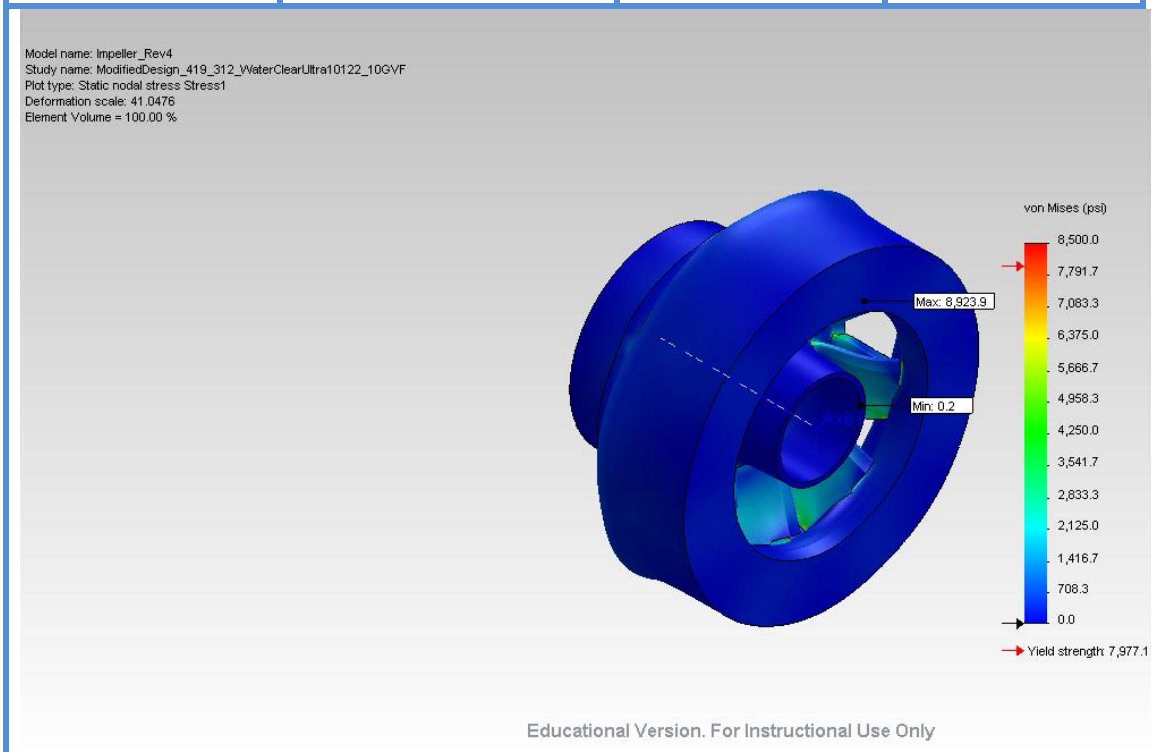

Impeller_Rev4-ModifiedDesign_419_312_WaterClearUltra10122_10GVF-Stress-Stress1

Name	Type	Min	Max
Displacement1	URES: Resultant Displacement	0 mil Node: 3563	19.2072 mil Node: 207123

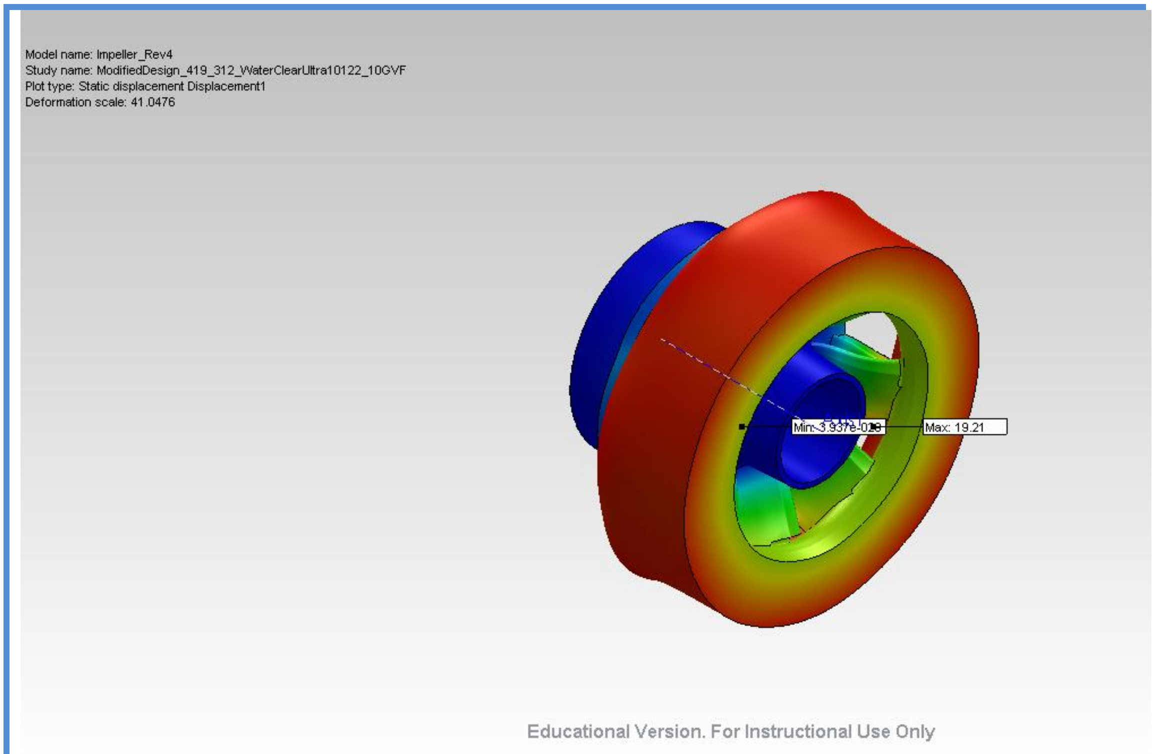

Impeller_Rev4-ModifiedDesign_419_312_WaterClearUltra10122_10GVF-Displacement-Displacement1

Name	Type	Min	Max
Strain1	ESTRN: Equivalent Strain	3.93151e-007 Element: 78638	0.0131975 Element: 96545

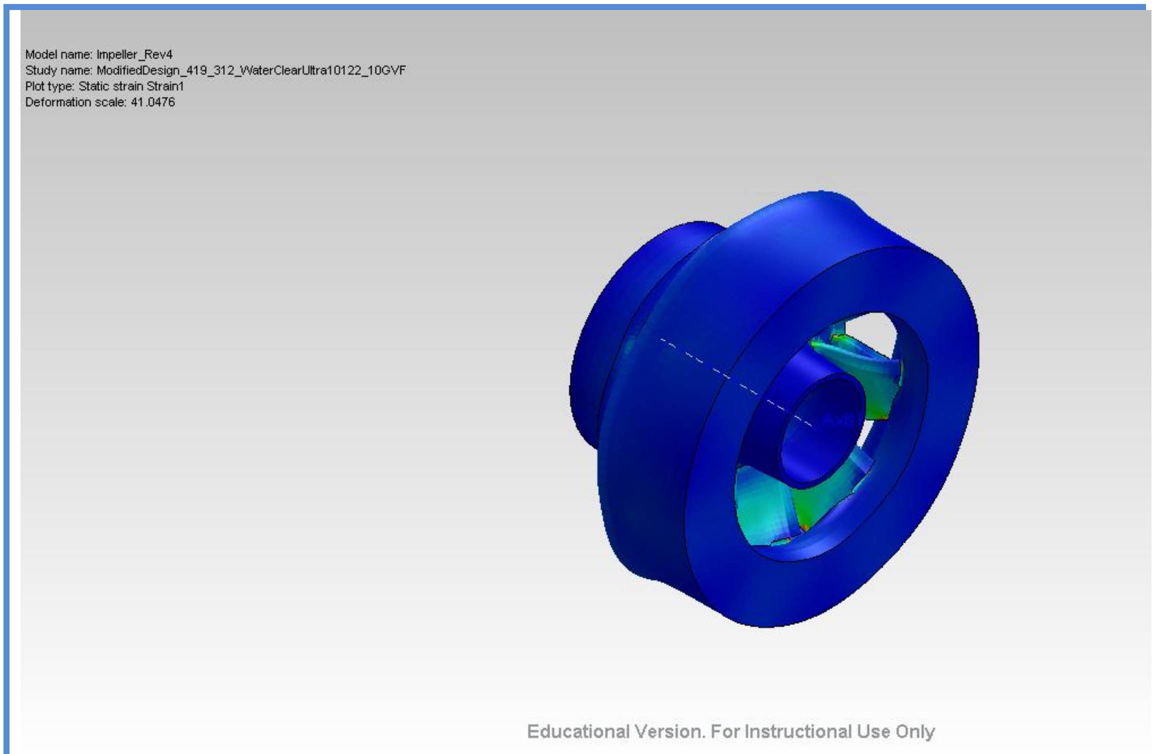

Impeller_Rev4-ModifiedDesign_419_312_WaterClearUltra10122_10GVF-Strain-Strain1

Name	Type
Displacement1{1}	URES: Resultant Displacement

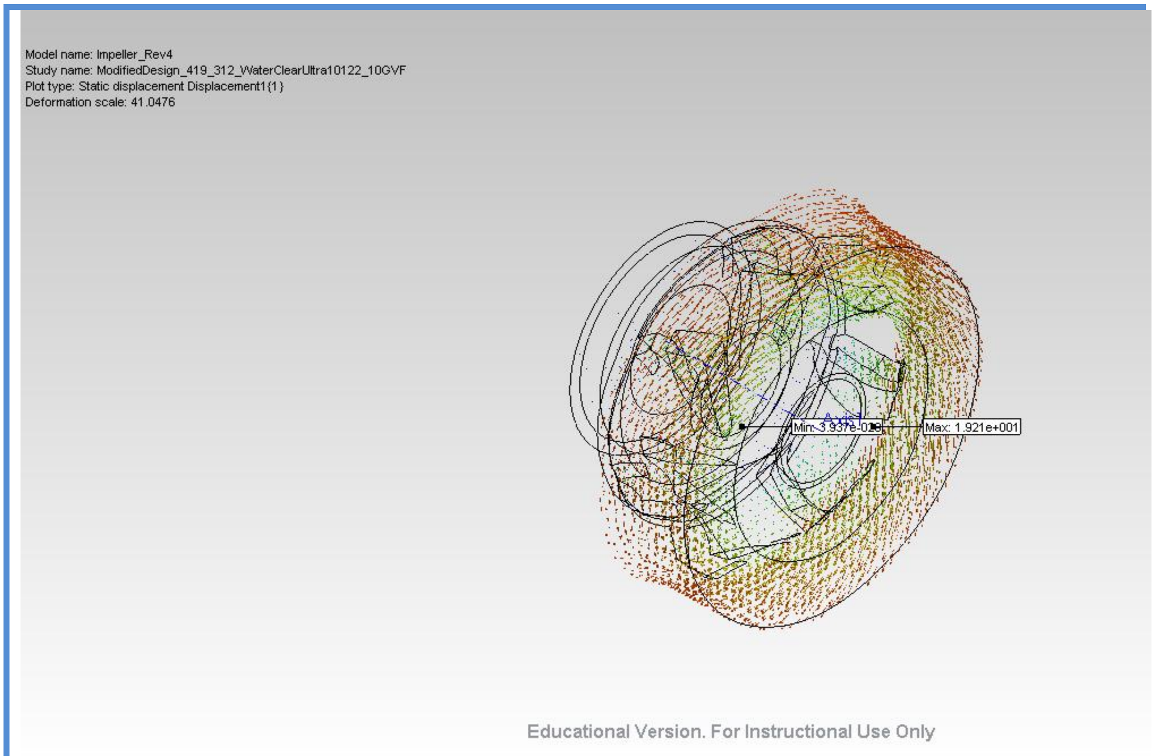

Impeller_Rev4-ModifiedDesign_419_312_WaterClearUltra10122_10GVF-Displacement-Displacement1{1}

Name	Type	Min	Max
Factor of Safety1	Automatic	0.893895 Node: 237874	51415.7 Node: 216611

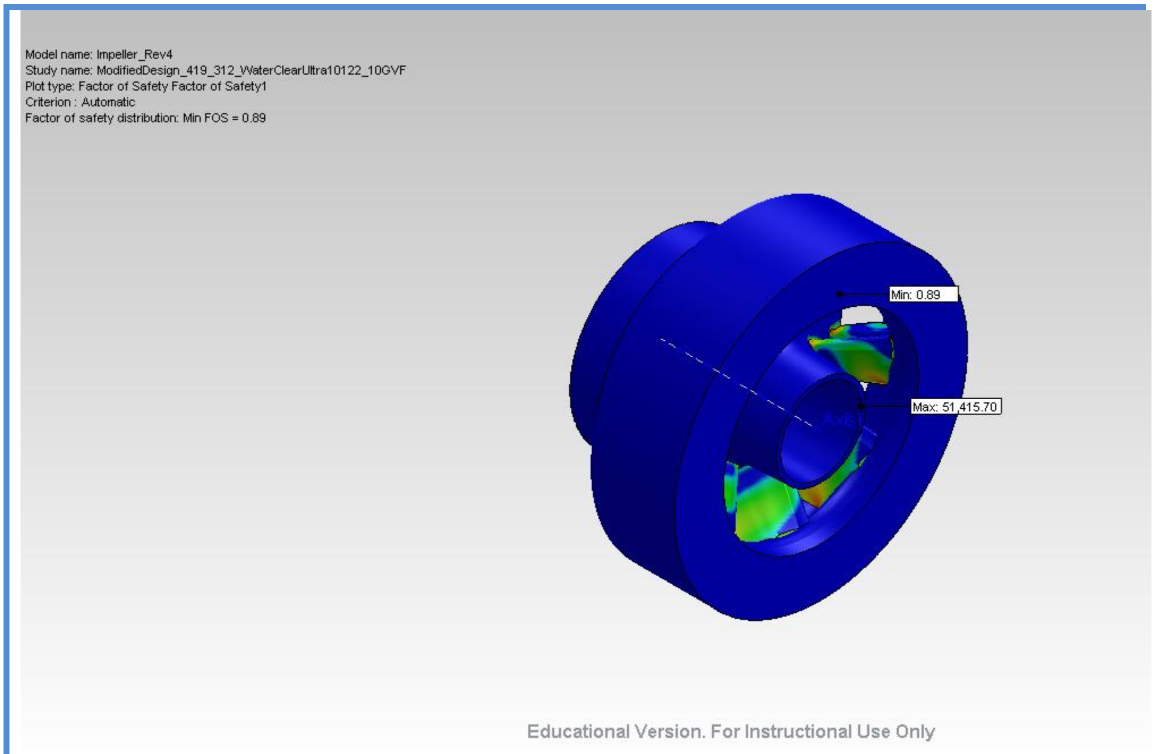

Impeller_Rev4-ModifiedDesign_419_312_WaterClearUltra10122_10GVF-Factor of Safety-Factor of Safety1

Conclusion

Comments:

The impeller design is acceptable for manufacture and operation. The only location with stresses above the yield stress is the knife edge in the leading edge of the main blade at the attachment point to the shroud. The maximum deflection in the impeller is approximately 19 mils, which is greater than that for a steel or cast iron impeller. It is an acceptable deflection less than 25 mils, but the blade thickness is large and could possibly affect the flow through the impeller and vary considerably from the actual G470 pump.

APPENDIX C

This appendix contains pertinent and necessary technical drawings critical to the design of this testing facility. The order of the drawings follows the order and organization of the Experimental Facility section.

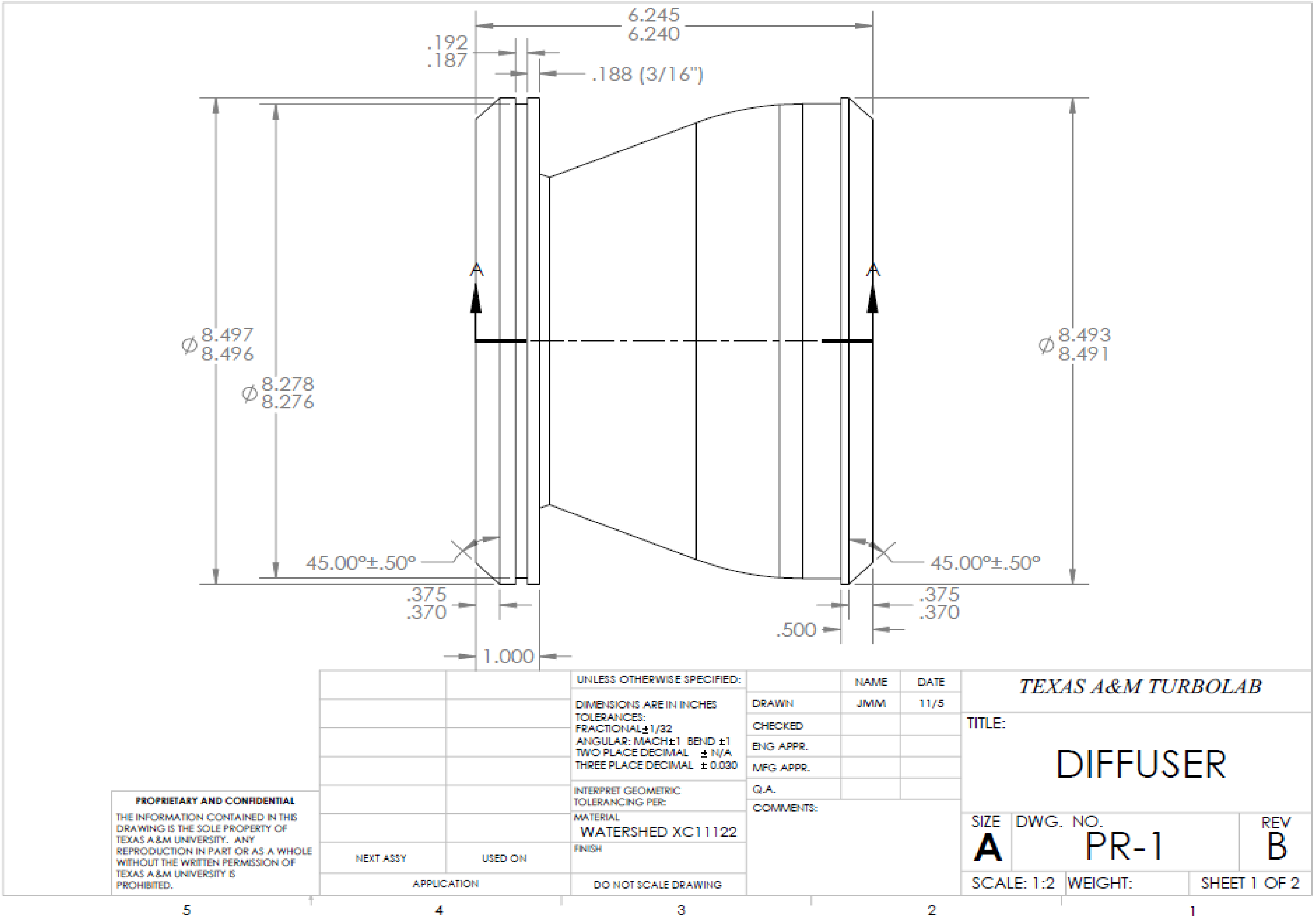
6.245
6.240
.192
.187
.188 (3/16")
A
A
Ø 8.497
8.496
Ø 8.278
8.276
Ø 8.493
8.491
45.00°±.50°
45.00°±.50°
.375
.370
.375
.370
.500
1.000
UNLESS OTHERWISE SPECIFIED:
DIMENSIONS ARE IN INCHES
TOLERANCES:
FRACTIONAL±1/32
ANGULAR: MACH±1 BEND ±1
TWO PLACE DECIMAL ± N/A
THREE PLACE DECIMAL ± 0.030
INTERPRET GEOMETRIC TOLERANCING PER:
MATERIAL
WATERSHED XC11122
FINISH
DO NOT SCALE DRAWING
NAME
DATE
DRAWN
JMM
11/5
CHECKED
ENG APPR.
MFG APPR.
Q.A.
COMMENTS:
TEXAS A&M TURBOLAB
TITLE:
DIFFUSER
SIZE
A
DWG. NO.
PR-1
REV
B
SCALE: 1:2
WEIGHT:
SHEET 1 OF 2
PROPRIETARY AND CONFIDENTIAL
THE INFORMATION CONTAINED IN THIS DRAWING IS THE SOLE PROPERTY OF TEXAS A&M UNIVERSITY. ANY REPRODUCTION IN PART OR AS A WHOLE WITHOUT THE WRITTEN PERMISSION OF TEXAS A&M UNIVERSITY IS PROHIBITED.
NEXT ASSY
USED ON
APPLICATION
5
4
3
2
1

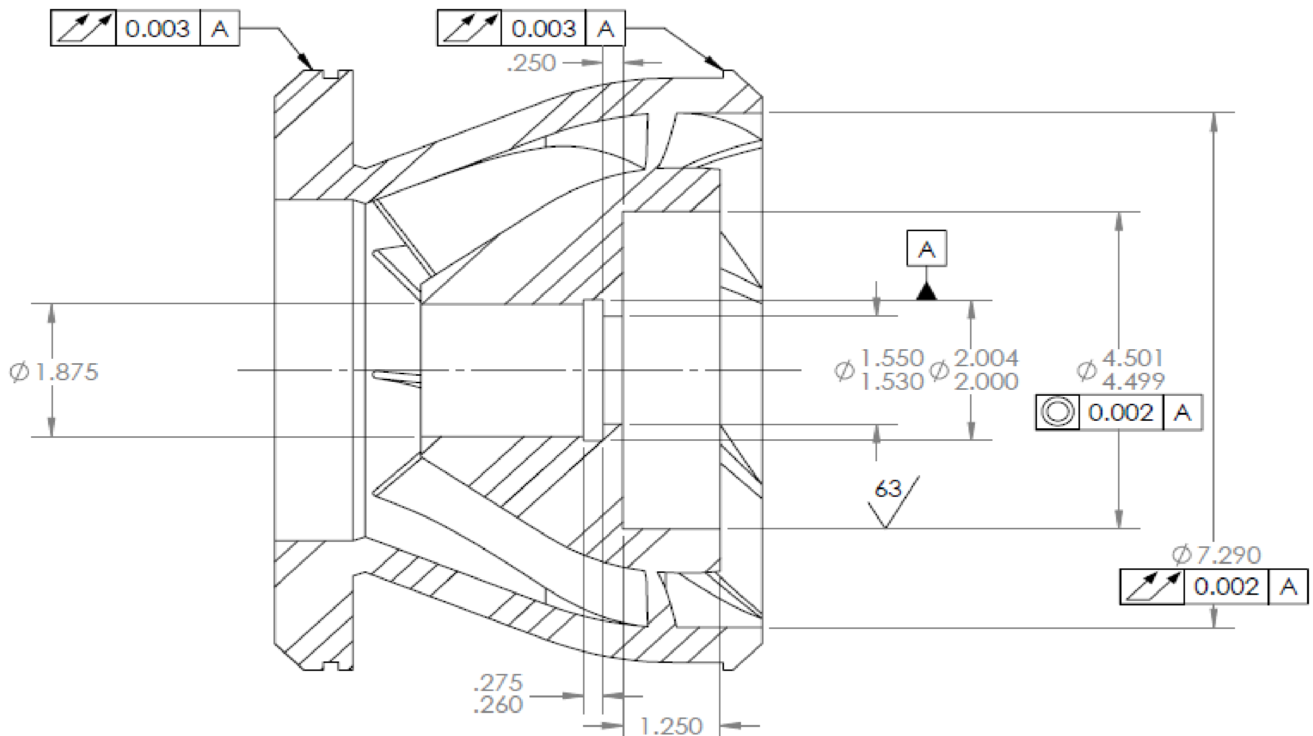

SECTION A-A

PROPRIETARY AND CONFIDENTIAL

THE INFORMATION CONTAINED IN THIS DRAWING IS THE SOLE PROPERTY OF TEXAS A&M UNIVERSITY. ANY REPRODUCTION IN PART OR AS A WHOLE WITHOUT THE WRITTEN PERMISSION OF TEXAS A&M UNIVERSITY IS PROHIBITED.

NEXT ASSY | USED ON

APPLICATION

UNLESS OTHERWISE SPECIFIED:

DIMENSIONS ARE IN INCHES
TOLERANCES:
FRACTIONAL±1/32
ANGULAR: MACH±1 BEND ±1
TWO PLACE DECIMAL ± N/A
THREE PLACE DECIMAL ± 0.030

INTERPRET GEOMETRIC TOLERANCING PER:

MATERIAL
WATERSHED XC11122

FINISH

DO NOT SCALE DRAWING

	NAME	DATE
DRAWN	JMM	11/5
CHECKED		
ENG APPR.		
MFG APPR.		
Q.A.		

COMMENTS:

TEXAS A&M TURBOLAB

TITLE:

DIFFUSER

SIZE A | DWG. NO. PR-1 | REV B

SCALE: 1:2 | WEIGHT: | SHEET 2 OF 2

5 4 3 2 1

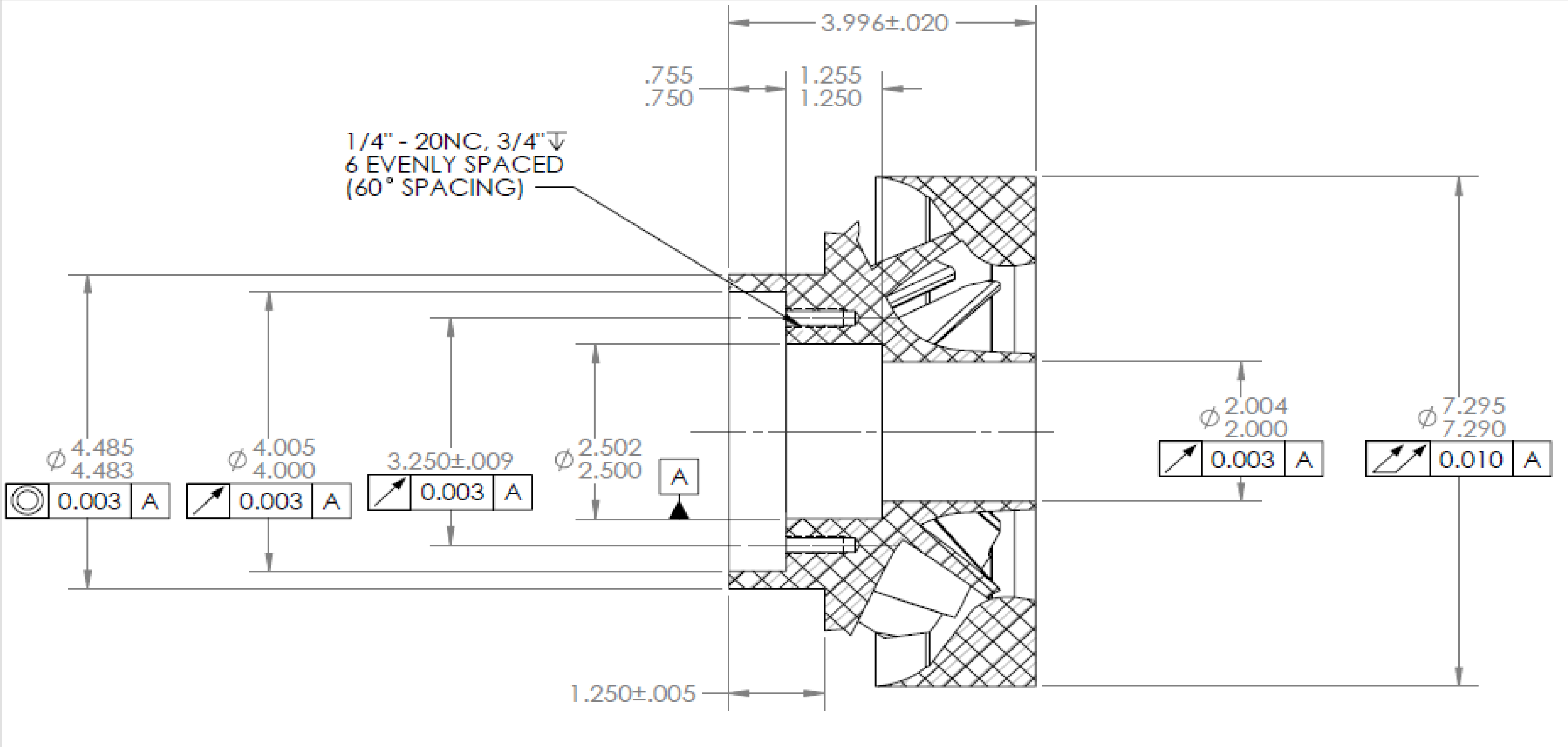

SECTION A-A

UNLESS OTHERWISE SPECIFIED:		NAME	DATE	TEXAS A&M TURBOLAB	
DIMENSIONS ARE IN INCHES TOLERANCES: FRACTIONAL ± 1/32 ANGULAR: MACH ± 1 BEND ± 1 TWO PLACE DECIMAL ± N/A THREE PLACE DECIMAL ± 0.030	DRAWN	JMM	2/6	TITLE:	
	CHECKED			IMPELLER	
	ENG APPR.				
	MFG APPR.				
INTERPRET GEOMETRIC TOLERANCING PER:	Q.A.				
MATERIAL SOMOS WATERCLEAR XC10122	COMMENTS:			SIZE A	DWG. NO. PR_10	REV C
FINISH					
DO NOT SCALE DRAWING				SCALE: 1:2 WEIGHT:	SHEET 1 OF 1

NEXT ASSY	USED ON
APPLICATION	

PROPRIETARY AND CONFIDENTIAL

THE INFORMATION CONTAINED IN THIS DRAWING IS THE SOLE PROPERTY OF TEXAS A&M UNIVERSITY. ANY REPRODUCTION IN PART OR AS A WHOLE WITHOUT THE WRITTEN PERMISSION OF TEXAS A&M UNIVERSITY IS PROHIBITED.

5 4 3 2 1

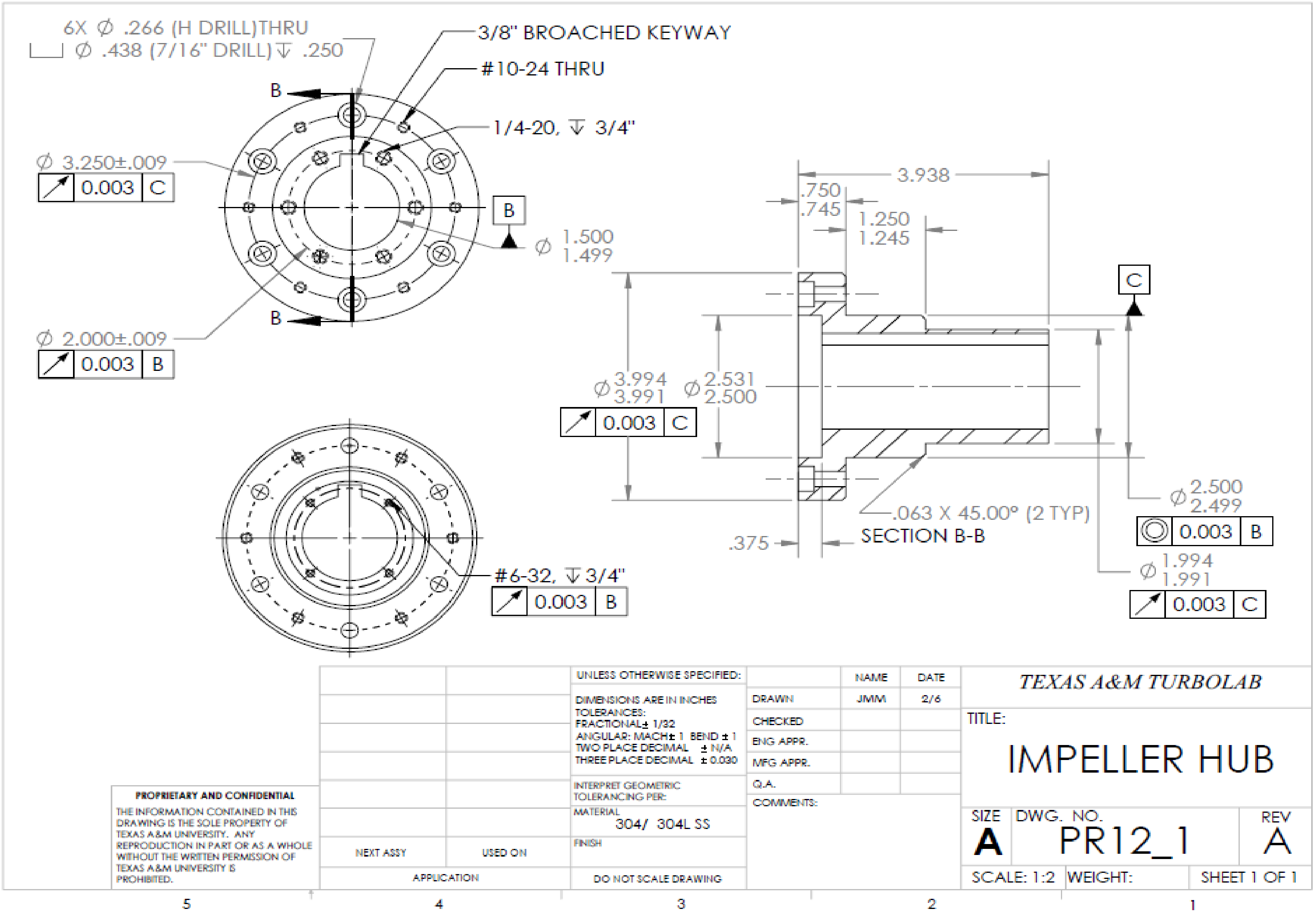

6X Ø .266 (H DRILL)THRU
⌴ Ø .438 (7/16" DRILL) ↧ .250
3/8" BROACHED KEYWAY
#10-24 THRU
1/4-20, ↧ 3/4"
B
Ø 3.250±.009
0.003 C
B
Ø 1.500
1.499
Ø 2.000±.009
0.003 B
3.938
.750
.745
1.250
1.245
C
Ø 3.994
3.991
Ø 2.531
2.500
0.003 C
.063 X 45.00° (2 TYP)
.375
SECTION B-B
Ø 2.500
2.499
0.003 B
Ø 1.994
1.991
0.003 C
#6-32, ↧ 3/4"
0.003 B
UNLESS OTHERWISE SPECIFIED:
DIMENSIONS ARE IN INCHES
TOLERANCES:
FRACTIONAL± 1/32
ANGULAR: MACH± 1 BEND ± 1
TWO PLACE DECIMAL ± N/A
THREE PLACE DECIMAL ± 0.030
INTERPRET GEOMETRIC TOLERANCING PER:
MATERIAL
304/ 304L SS
FINISH
DO NOT SCALE DRAWING
NEXT ASSY
USED ON
APPLICATION
NAME
DATE
DRAWN
JMM
2/6
CHECKED
ENG APPR.
MFG APPR.
Q.A.
COMMENTS:
TEXAS A&M TURBOLAB
TITLE:
IMPELLER HUB
SIZE
A
DWG. NO.
PR12_1
REV
A
SCALE: 1:2
WEIGHT:
SHEET 1 OF 1
PROPRIETARY AND CONFIDENTIAL
THE INFORMATION CONTAINED IN THIS DRAWING IS THE SOLE PROPERTY OF TEXAS A&M UNIVERSITY. ANY REPRODUCTION IN PART OR AS A WHOLE WITHOUT THE WRITTEN PERMISSION OF TEXAS A&M UNIVERSITY IS PROHIBITED.
5
4
3
2
1

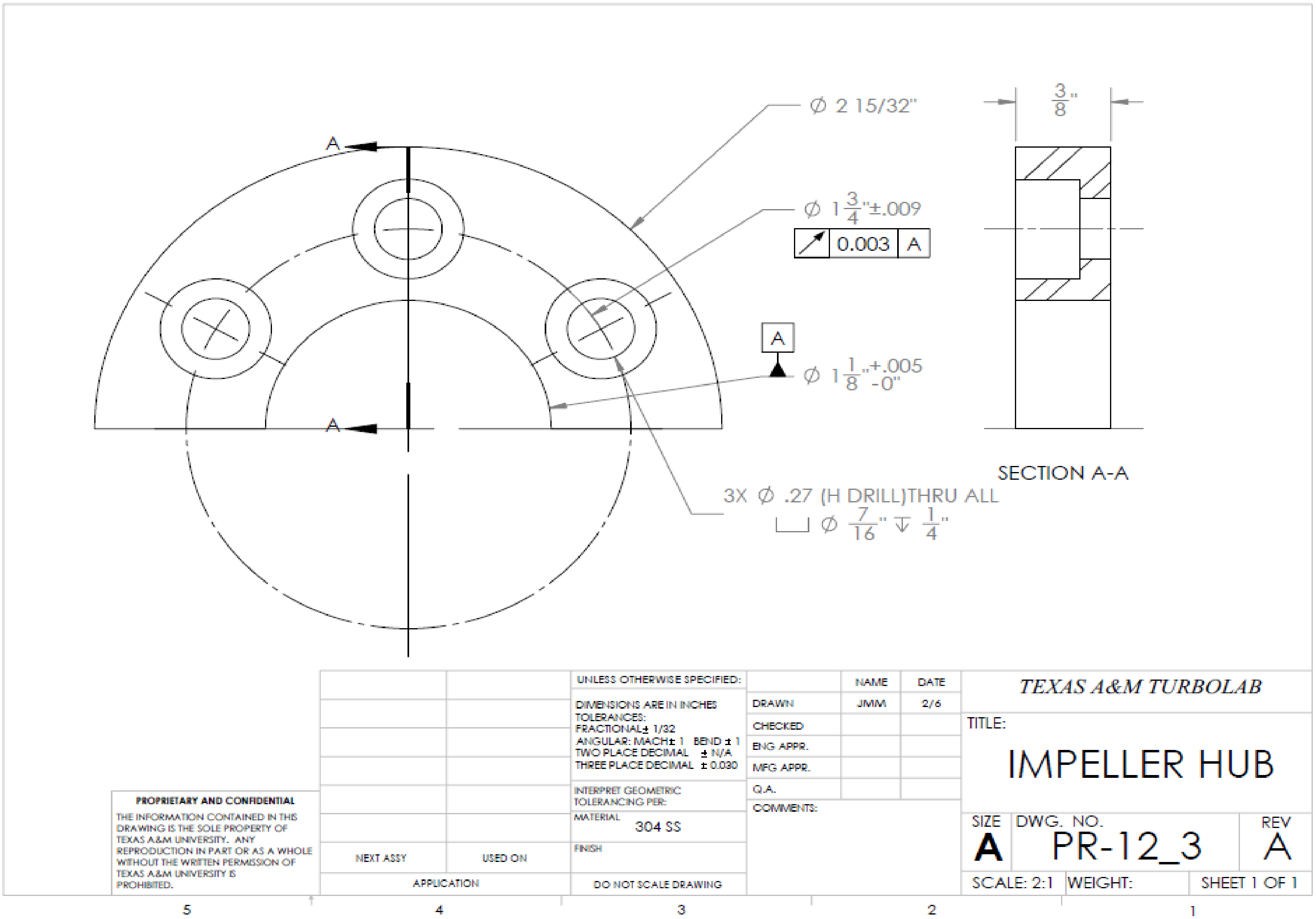

A
A
Ø 2 15/32"
Ø 1 3/4"±.009
0.003 A
A
Ø 1 1/8" +.005 -0"
3X Ø .27 (H DRILL)THRU ALL
⌴ Ø 7/16" ↧ 1/4"
3/8"
SECTION A-A
UNLESS OTHERWISE SPECIFIED:
DIMENSIONS ARE IN INCHES
TOLERANCES:
FRACTIONAL± 1/32
ANGULAR: MACH± 1 BEND ± 1
TWO PLACE DECIMAL ± N/A
THREE PLACE DECIMAL ± 0.030
INTERPRET GEOMETRIC TOLERANCING PER:
MATERIAL 304 SS
FINISH
DO NOT SCALE DRAWING
NAME DATE
DRAWN JMM 2/6
CHECKED
ENG APPR.
MFG APPR.
Q.A.
COMMENTS:
TEXAS A&M TURBOLAB
TITLE:
IMPELLER HUB
SIZE A
DWG. NO. PR-12_3
REV A
SCALE: 2:1 WEIGHT: SHEET 1 OF 1
NEXT ASSY USED ON
APPLICATION
PROPRIETARY AND CONFIDENTIAL
THE INFORMATION CONTAINED IN THIS DRAWING IS THE SOLE PROPERTY OF TEXAS A&M UNIVERSITY. ANY REPRODUCTION IN PART OR AS A WHOLE WITHOUT THE WRITTEN PERMISSION OF TEXAS A&M UNIVERSITY IS PROHIBITED.
5 4 3 2 1

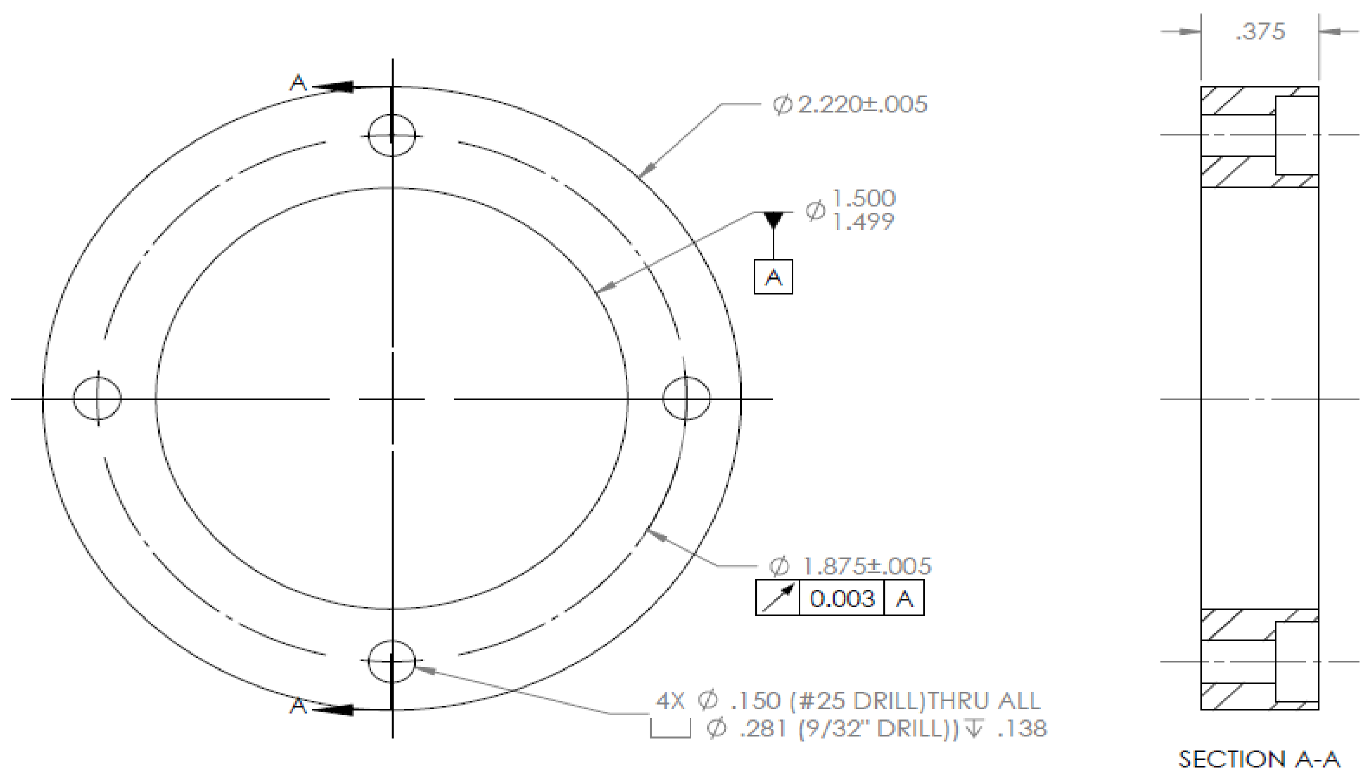

UNLESS OTHERWISE SPECIFIED:		NAME	DATE	TEXAS A&M TURBOLAB
DIMENSIONS ARE IN INCHES TOLERANCES: FRACTIONAL± 1/32 ANGULAR: MACH± 1 BEND ± 1 TWO PLACE DECIMAL ± N/A THREE PLACE DECIMAL ± 0.030	DRAWN	JMM	2/5	TITLE:
	CHECKED			IMPELLER HUB
	ENG APPR.			
	MFG APPR.			
INTERPRET GEOMETRIC TOLERANCING PER:	Q.A.			
MATERIAL 304L SS	COMMENTS:			SIZE A DWG. NO. PR-12_2 REV B
FINISH				
DO NOT SCALE DRAWING				SCALE: 2:1 WEIGHT: SHEET 1 OF 1

NEXT ASSY	USED ON
APPLICATION	

PROPRIETARY AND CONFIDENTIAL

THE INFORMATION CONTAINED IN THIS DRAWING IS THE SOLE PROPERTY OF TEXAS A&M UNIVERSITY. ANY REPRODUCTION IN PART OR AS A WHOLE WITHOUT THE WRITTEN PERMISSION OF TEXAS A&M UNIVERSITY IS PROHIBITED.

5 4 3 2 1

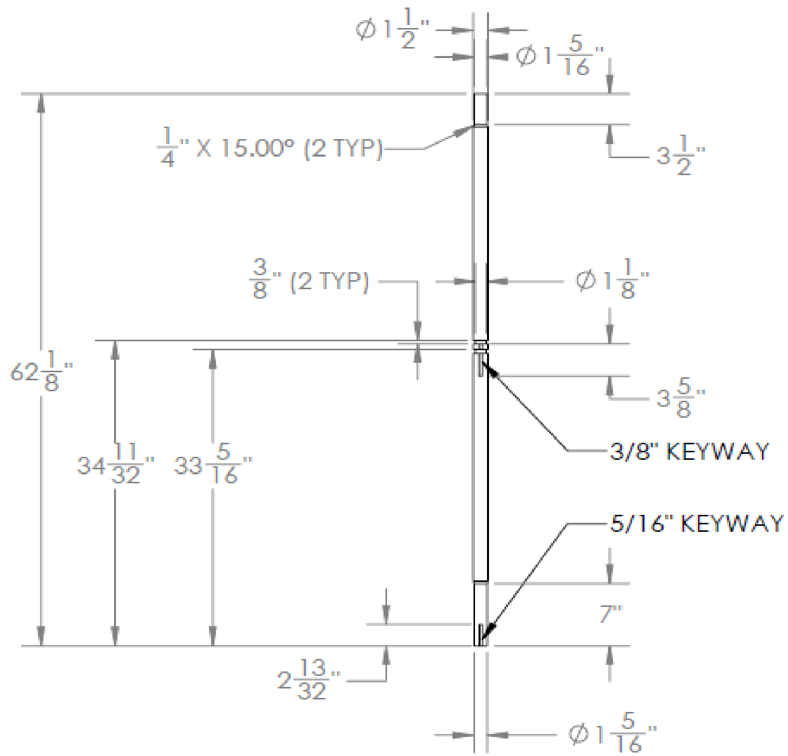

NEXT ASSY	USED ON	
APPLICATION		

PROPRIETARY AND CONFIDENTIAL

THE INFORMATION CONTAINED IN THIS DRAWING IS THE SOLE PROPERTY OF TEXAS A&M UNIVERSITY. ANY REPRODUCTION IN PART OR AS A WHOLE WITHOUT THE WRITTEN PERMISSION OF TEXAS A&M UNIVERSITY IS PROHIBITED.

UNLESS OTHERWISE SPECIFIED:
DIMENSIONS ARE IN INCHES
TOLERANCES:
FRACTIONAL± 1/32
ANGULAR: MACH± 1 BEND ± 1
TWO PLACE DECIMAL ± 0.06
THREE PLACE DECIMAL ± 0.015

INTERPRET GEOMETRIC TOLERANCING PER:

MATERIAL
304 SS

FINISH

DO NOT SCALE DRAWING

	NAME	DATE
DRAWN	JMM	5/29
CHECKED		
ENG APPR.		
MFG APPR.		
Q.A.		

COMMENTS:

TEXAS A&M TURBOLAB

TITLE:

PUMP SHAFT

SIZE	DWG. NO.	REV
A	PR-3	C

SCALE: 1:16 WEIGHT: SHEET 1 OF 1

5 4 3 2 1

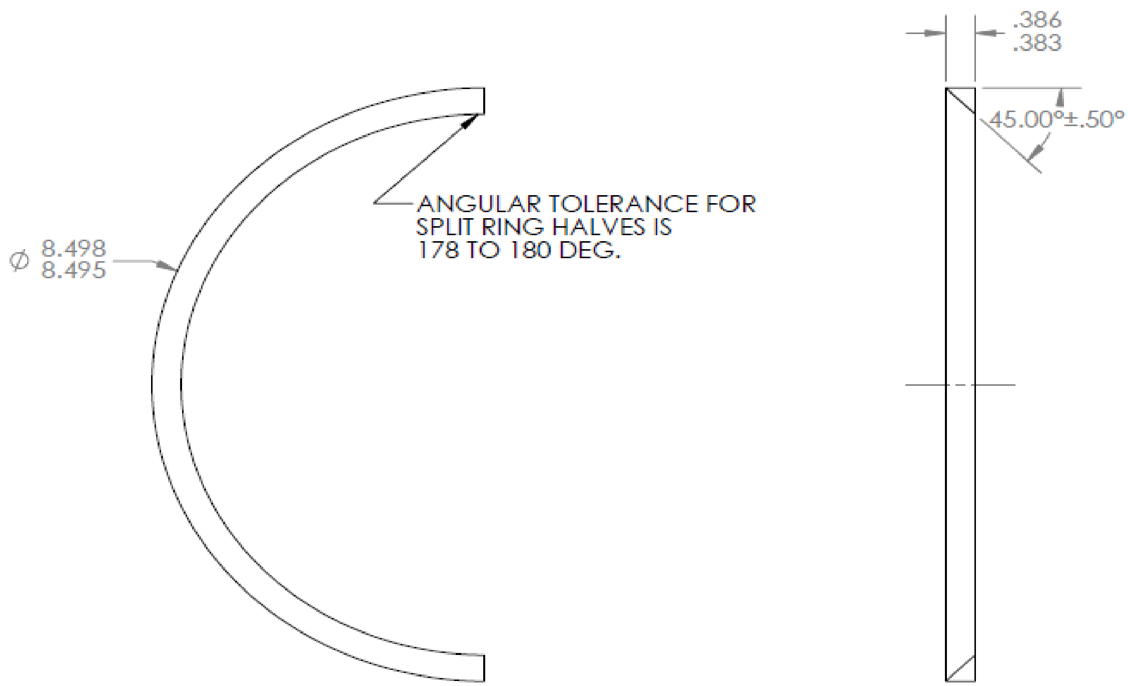

PROPRIETARY AND CONFIDENTIAL THE INFORMATION CONTAINED IN THIS DRAWING IS THE SOLE PROPERTY OF TEXAS A&M UNIVERSITY. ANY REPRODUCTION IN PART OR AS A WHOLE WITHOUT THE WRITTEN PERMISSION OF TEXAS A&M UNIVERSITY IS PROHIBITED.	NEXT ASSY	USED ON	
	APPLICATION		

UNLESS OTHERWISE SPECIFIED:
DIMENSIONS ARE IN INCHES
TOLERANCES:
FRACTIONAL 1/32
ANGULAR: MACH ±1 BEND ± 1
TWO PLACE DECIMAL ± N/A
THREE PLACE DECIMAL ± 0.030

INTERPRET GEOMETRIC TOLERANCING PER:

MATERIAL
POLYCARBONATE

FINISH

DO NOT SCALE DRAWING

	NAME	DATE
DRAWN	JMM	11/5
CHECKED		
ENG APPR.		
MFG APPR.		
Q.A.		

COMMENTS:

TEXAS A&M TURBOLAB

TITLE:
SPLIT RING

SIZE	DWG. NO.	REV
A	PR-8	B

SCALE: 1:2 WEIGHT: SHEET 1 OF 1

5 4 3 2 1

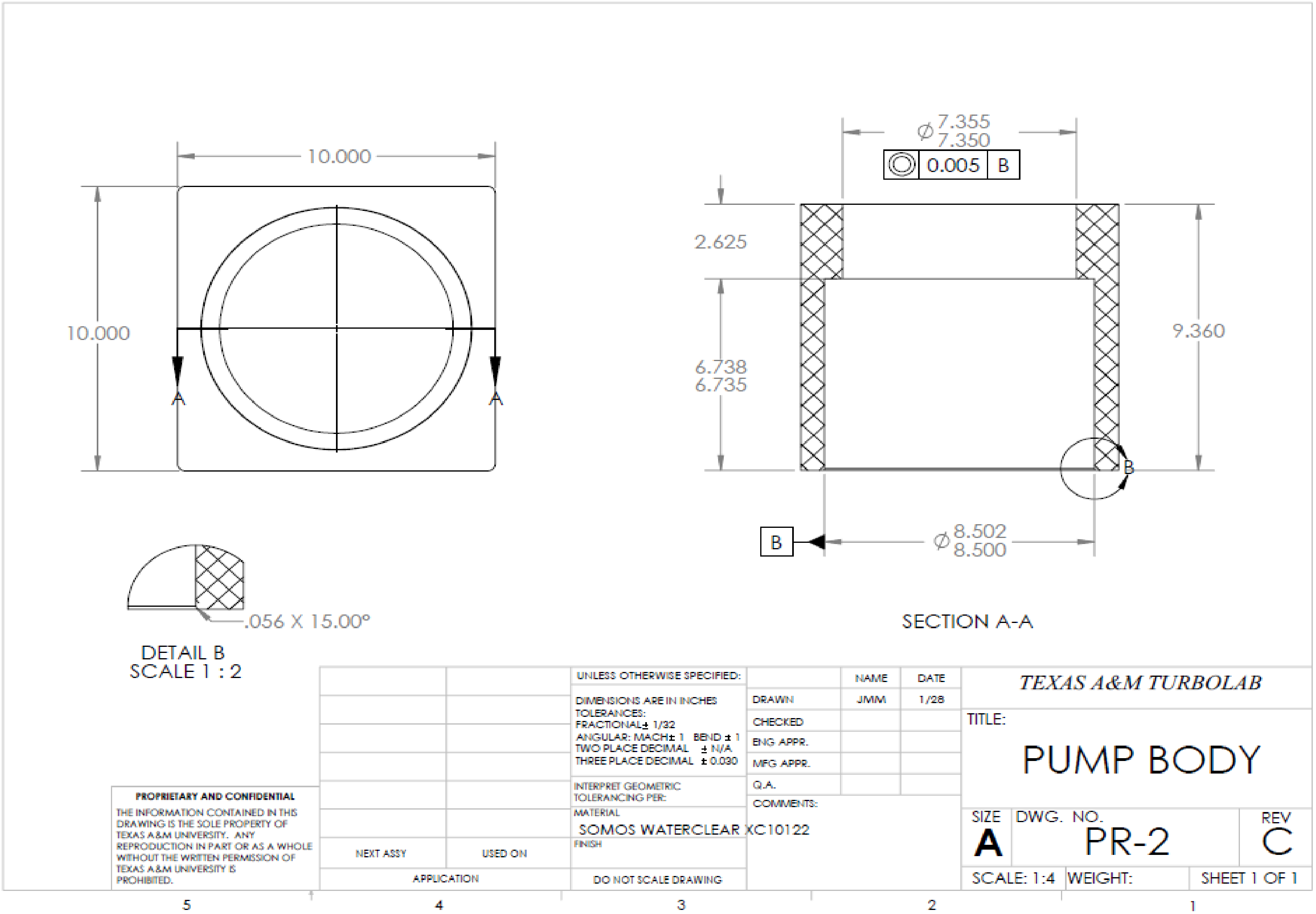
10.000
10.000
A
A
ϕ 7.355 7.350
0.005 B
2.625
6.738 6.735
9.360
B
B
ϕ 8.502 8.500
.056 X 15.00°
DETAIL B
SCALE 1 : 2
SECTION A-A
UNLESS OTHERWISE SPECIFIED:
DIMENSIONS ARE IN INCHES
TOLERANCES:
FRACTIONAL ± 1/32
ANGULAR: MACH ± 1 BEND ± 1
TWO PLACE DECIMAL ± N/A
THREE PLACE DECIMAL ± 0.030
INTERPRET GEOMETRIC TOLERANCING PER:
MATERIAL
SOMOS WATERCLEAR XC10122
FINISH
DO NOT SCALE DRAWING
NEXT ASSY
USED ON
APPLICATION
PROPRIETARY AND CONFIDENTIAL
THE INFORMATION CONTAINED IN THIS DRAWING IS THE SOLE PROPERTY OF TEXAS A&M UNIVERSITY. ANY REPRODUCTION IN PART OR AS A WHOLE WITHOUT THE WRITTEN PERMISSION OF TEXAS A&M UNIVERSITY IS PROHIBITED.
NAME
DATE
DRAWN
JMM
1/28
CHECKED
ENG APPR.
MFG APPR.
Q.A.
COMMENTS:
TEXAS A&M TURBOLAB
TITLE:
PUMP BODY
SIZE
A
DWG. NO.
PR-2
REV
C
SCALE: 1:4
WEIGHT:
SHEET 1 OF 1
5
4
3
2
1

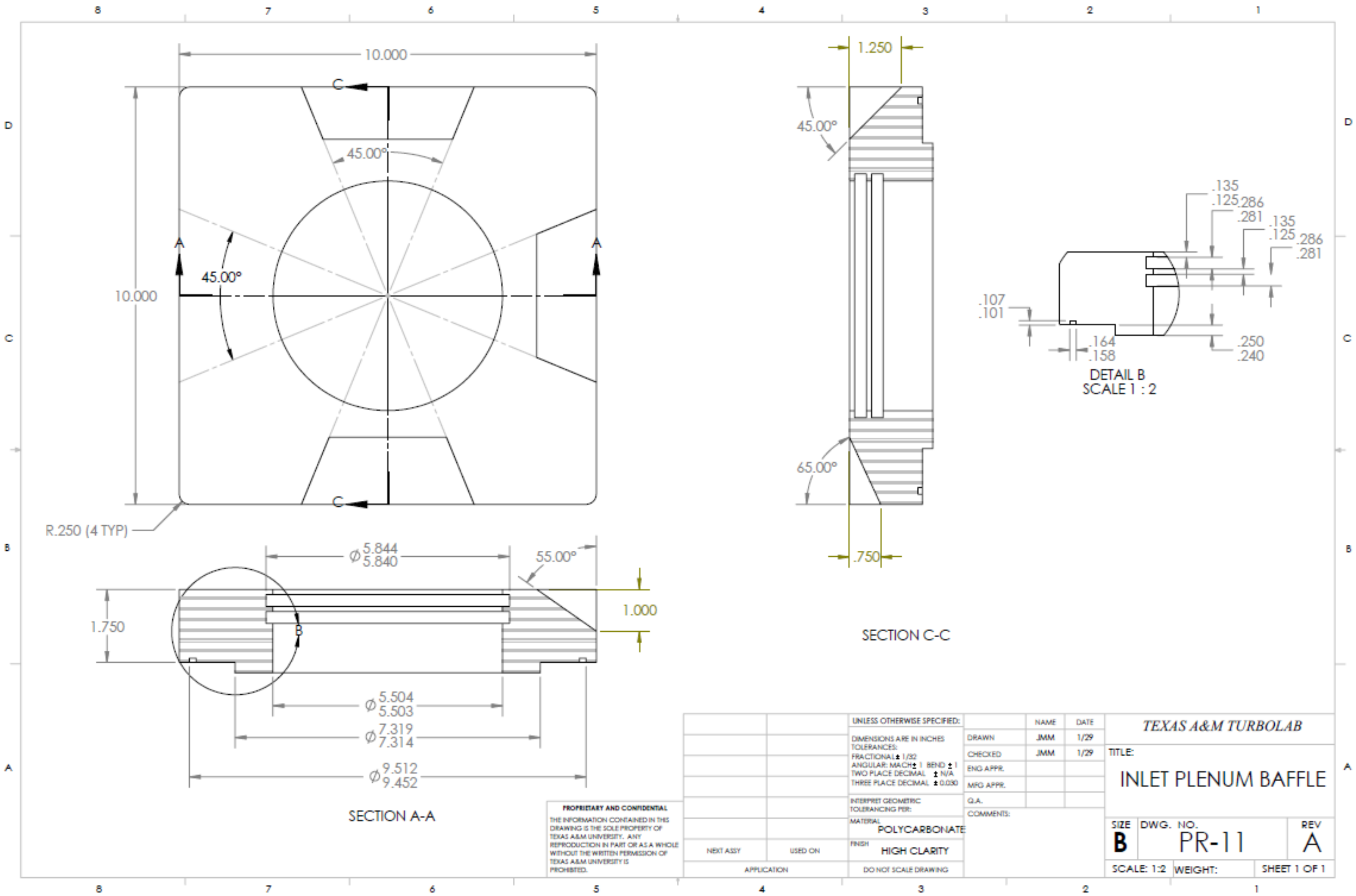
10.000
10.000
45.00°
45.00°
R.250 (4 TYP)
1.250
45.00°
65.00°
.750
SECTION C-C
.135
.125
.286
.281
.135
.125
.286
.281
.107
.101
.164
.158
.250
.240
DETAIL B
SCALE 1 : 2
Ø 5.844 5.840
55.00°
1.000
1.750
Ø 5.504 5.503
Ø 7.319 7.314
Ø 9.512 9.452
SECTION A-A
PROPRIETARY AND CONFIDENTIAL
THE INFORMATION CONTAINED IN THIS DRAWING IS THE SOLE PROPERTY OF TEXAS A&M UNIVERSITY. ANY REPRODUCTION IN PART OR AS A WHOLE WITHOUT THE WRITTEN PERMISSION OF TEXAS A&M UNIVERSITY IS PROHIBITED.
NEXT ASSY
USED ON
APPLICATION
UNLESS OTHERWISE SPECIFIED:
DIMENSIONS ARE IN INCHES
MATERIAL
POLYCARBONATE
FINISH
HIGH CLARITY
DO NOT SCALE DRAWING
NAME
DATE
DRAWN
JMM
1/29
CHECKED
JMM
1/29
ENG APPR.
MFG APPR.
Q.A.
COMMENTS:
TEXAS A&M TURBOLAB
TITLE:
INLET PLENUM BAFFLE
SIZE
B
DWG. NO.
PR-11
REV
A
SCALE: 1:2
WEIGHT:
SHEET 1 OF 1

NOTES:
1) DIMENSIONS ARE TO FLANGE FACES NOT RAISED GASKET FACE
2) STANDARD 1/8" WELD GAP FOR ROOT PASS FO WELD
3) STANDARD 2 HOLE FLANGE ALIGNMENT ON ALL FLANGES - CRITICAL FOR THIS APPLICATION
4) TO BE MARKED: MAWP 600 PSIG
5) HYDROTEST TO 780 PSIG PER ASME B31.3 PROCESS PIPING CODE

ITEM NO.	PART NUMBER	STANDARD	MATERIAL	QTY.
1	Weldolet, 5 X 4.0	ASTM A182 F304	UNS S30400	2
2	WNeck Flange 300-NPS4	ASTM A182 F304	UNS S30400	2
3	4 in, Schedule 40	ASTM A312 TP304	UNS S30400	1
4	Slip On Flange 300-NPS5	ASTM A182 F304	UNS S30400	1
5	*MODIFIED* 5 in, Schedule 80/XS - SEE ATTACHED DRAWING	ASTM A312 TP304	UNS S30400	1
6	4 in, Schedule 40	ASTM A312 TP304	UNS S30400	1
7	*MODIFIED* Slip On Flange 300-NPS5-FlatFace - SEE ATTACHED DWG	ASTM A182 F304	UNS S30400	1
8	Threadolet 5 X 0.5 NPT	ASTM A182 F304	UNS S30400	1

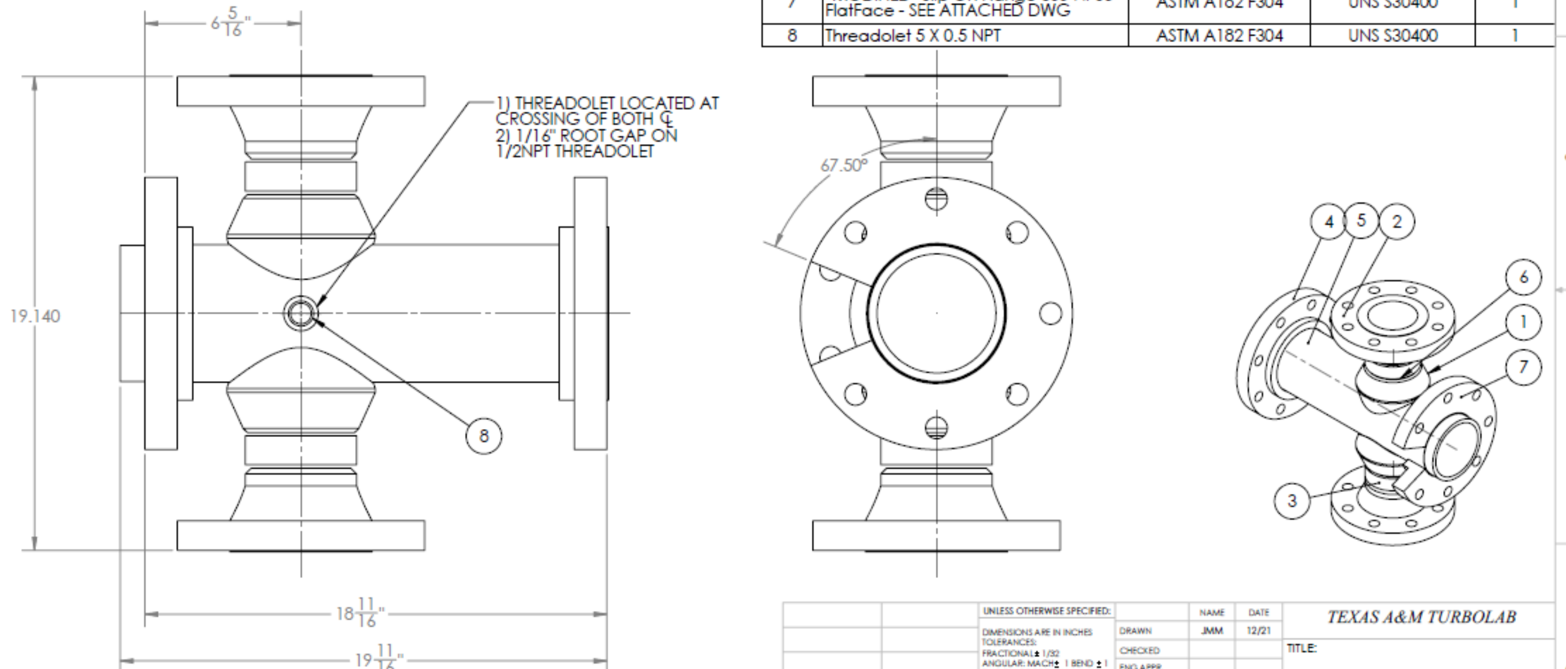

		UNLESS OTHERWISE SPECIFIED:		NAME	DATE
		DIMENSIONS ARE IN INCHES TOLERANCES: FRACTIONAL ± 1/32 ANGULAR: MACH ± 1 BEND ± 1 TWO PLACE DECIMAL ± N/A THREE PLACE DECIMAL ± 0.030	DRAWN	JMM	12/21
			CHECKED		
			ENG APPR.		
			MFG APPR.		
		INTERPRET GEOMETRIC TOLERANCING PER:	Q.A.		
		MATERIAL 304 SS	COMMENTS:		
NEXT ASSY	USED ON	FINISH			
APPLICATION		DO NOT SCALE DRAWING			

PROPRIETARY AND CONFIDENTIAL

THE INFORMATION CONTAINED IN THIS DRAWING IS THE SOLE PROPERTY OF TEXAS A&M UNIVERSITY. ANY REPRODUCTION IN PART OR AS A WHOLE WITHOUT THE WRITTEN PERMISSION OF TEXAS A&M UNIVERSITY IS PROHIBITED.

TEXAS A&M TURBOLAB

TITLE:

INLET PLENUM

SIZE	DWG. NO.	REV
B	P-8	C
SCALE: 1:8	WEIGHT:	SHEET 1 OF 1

ITEM NO.	PART NUMBER	STANDARD	MATERIAL	QTY.
1	*MODIFIED* RFWN Flange 300-NPS6 - SEE ATTACHED DWG	ASTM A182 F304	UNS S30400	1
2	Tee Inch 6 Sch40	ASTM A403 WP304	UNS S30400	1
3	WNeck Flange 300-NPS6	ASTM A182 F304	UNS S30400	1
4	StubEnd_6_300	ASTM A403 WP304	UNS S30400	1
5	Flange_6_300_LapJoint	ASTM A182 F304	UNS S30400	1
6	Threadolet_6_12NPT_3000	ASTM A403 WP304	UNS S30400	1

NOTES:
1) DIMENSIONS ARE TO FLANGE FACES NOT RAISED GASKET FACE
2) STANDARD 1/8" WELD GAP FOR ROOT PASS OF WELD
3) STANDARD 2 HOLE FLANGE ALIGNMENT ON ALL FLANGES
4) TO BE MARKED: MAWP 600 PSIG
5) HYDROTEST TO 780 PSIG PER ASME B31.3 PROCESS PIPING CODE

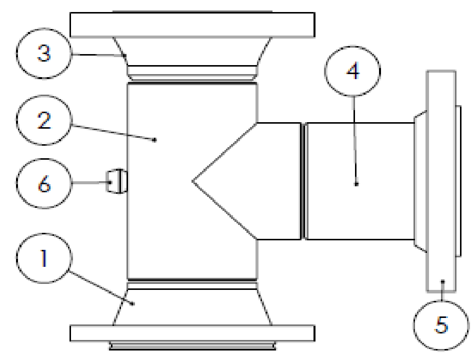

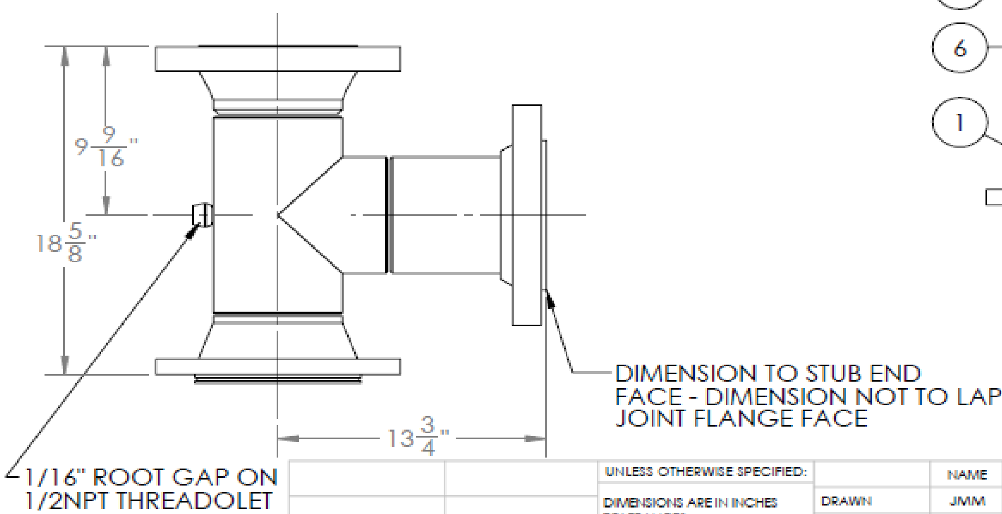

PROPRIETARY AND CONFIDENTIAL

THE INFORMATION CONTAINED IN THIS DRAWING IS THE SOLE PROPERTY OF TEXAS A&M UNIVERSITY. ANY REPRODUCTION IN PART OR AS A WHOLE WITHOUT THE WRITTEN PERMISSION OF TEXAS A&M UNIVERSITY IS PROHIBITED.

NEXT ASSY | USED ON

APPLICATION

UNLESS OTHERWISE SPECIFIED:

DIMENSIONS ARE IN INCHES
TOLERANCES:
FRACTIONAL ± 1/32
ANGULAR: MACH ± 1 BEND ± 1
TWO PLACE DECIMAL ± N/A
THREE PLACE DECIMAL ± N/A

INTERPRET GEOMETRIC TOLERANCING PER:

MATERIAL
304 SS

FINISH

DO NOT SCALE DRAWING

	NAME	DATE
DRAWN	JMM	11/28
CHECKED		
ENG APPR.		
MFG APPR.		
Q.A.		

COMMENTS:

TEXAS A&M TURBOLAB

TITLE:

OUTLET PLENUM

SIZE A | DWG. NO. P-22 | REV A

SCALE: 1:12 | WEIGHT: | SHEET 1 OF 1

5 4 3 2 1

ITEM NO.	PART NUMBER	MATERIAL	STANDARD	QTY.
1	ModFlange_6_300_RFWN_Rev3 *SEE P-22 ATTACHMENT 4*	UNS S30400	ASTM A182 F304	1
2	INSERT, 6" 300# FLG *SEE P-22 ATTACHMENT 3*	UNS S30400	N/A	1

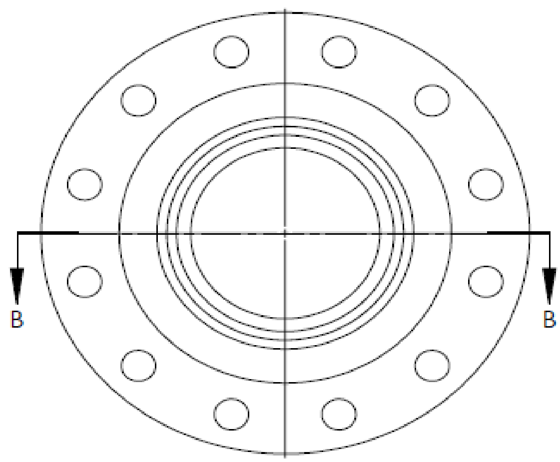

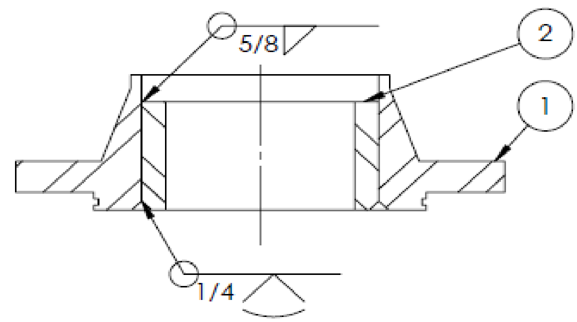

SECTION B-B

PROPRIETARY AND CONFIDENTIAL

THE INFORMATION CONTAINED IN THIS DRAWING IS THE SOLE PROPERTY OF TEXAS A&M UNIVERSITY. ANY REPRODUCTION IN PART OR AS A WHOLE WITHOUT THE WRITTEN PERMISSION OF TEXAS A&M UNIVERSITY IS PROHIBITED.

NEXT ASSY | USED ON

APPLICATION

UNLESS OTHERWISE SPECIFIED:

DIMENSIONS ARE IN INCHES
TOLERANCES:
FRACTIONAL±1/32
ANGULAR: MACH± 1 BEND ± 1
TWO PLACE DECIMAL ± N/A
THREE PLACE DECIMAL ± N/A

INTERPRET GEOMETRIC TOLERANCING PER:

MATERIAL
304 SS

FINISH

DO NOT SCALE DRAWING

	NAME	DATE
DRAWN	JMM	12/7
CHECKED		
ENG APPR.		
MFG APPR.		
Q.A.		

COMMENTS:

TEXAS A&M TURBOLAB

TITLE:

FLG, 6" 300# STD BORE, RFWN

SIZE A | DWG. NO. P-22 ATTACHMENT | REV

SCALE: 1:4 | WEIGHT: | SHEET 1 OF 1

5 4 3 2 1

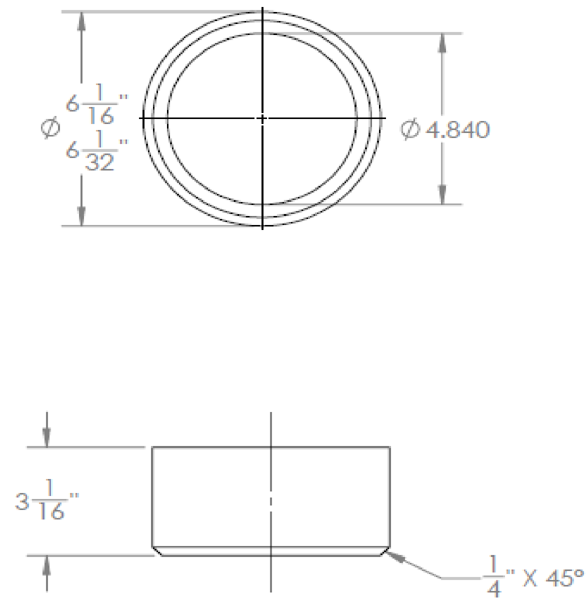

PROPRIETARY AND CONFIDENTIAL

THE INFORMATION CONTAINED IN THIS DRAWING IS THE SOLE PROPERTY OF TEXAS A&M UNIVERSITY. ANY REPRODUCTION IN PART OR AS A WHOLE WITHOUT THE WRITTEN PERMISSION OF TEXAS A&M UNIVERSITY IS PROHIBITED.

NEXT ASSY	USED ON
APPLICATION	

UNLESS OTHERWISE SPECIFIED:

DIMENSIONS ARE IN INCHES
TOLERANCES:
FRACTIONAL ± 1/32
ANGULAR: MACH ± 1 BEND ± 1
TWO PLACE DECIMAL ± N/A
THREE PLACE DECIMAL ± 0.030

INTERPRET GEOMETRIC TOLERANCING PER:

MATERIAL
304 SS

FINISH

DO NOT SCALE DRAWING

	NAME	DATE
DRAWN	JMM	12/7
CHECKED		
ENG APPR.		
MFG APPR.		
Q.A.		

COMMENTS:

TEXAS A&M TURBOLAB

TITLE:

INSERT, 6" 300# FLG

SIZE	DWG. NO.	REV
A	P-22 ATTACHMENT 3	

SCALE: 1:2 WEIGHT: SHEET 1 OF 1

5 4 3 2 1

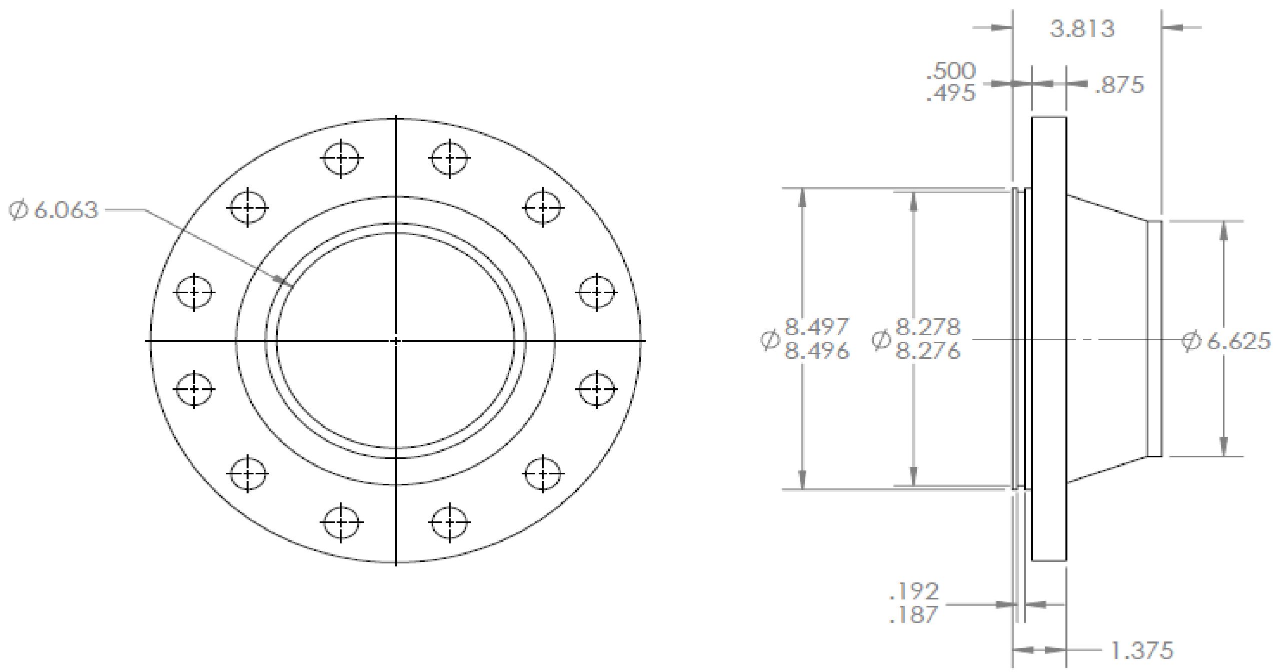

UNLESS OTHERWISE SPECIFIED:		NAME	DATE	TEXAS A&M TURBOLAB	
DIMENSIONS ARE IN INCHES TOLERANCES: FRACTIONAL ± 1/32 ANGULAR: MACH ± 1 BEND ± 1 TWO PLACE DECIMAL ± N/A THREE PLACE DECIMAL ± 0.030	DRAWN	JMM	12/7	TITLE:	
	CHECKED			FLG, 6" 300# STD WALL, RFWN	
	ENG APPR.				
	MFG APPR.				
INTERPRET GEOMETRIC TOLERANCING PER:	Q.A.				
MATERIAL 304 SS	COMMENTS:			SIZE A	DWG. NO. P-22 ATTACHMENT — REV B
FINISH					
DO NOT SCALE DRAWING				SCALE: 1:4 WEIGHT:	SHEET 1 OF 1

NEXT ASSY	USED ON
APPLICATION	

PROPRIETARY AND CONFIDENTIAL

THE INFORMATION CONTAINED IN THIS DRAWING IS THE SOLE PROPERTY OF TEXAS A&M UNIVERSITY. ANY REPRODUCTION IN PART OR AS A WHOLE WITHOUT THE WRITTEN PERMISSION OF TEXAS A&M UNIVERSITY IS PROHIBITED.

5 4 3 2 1

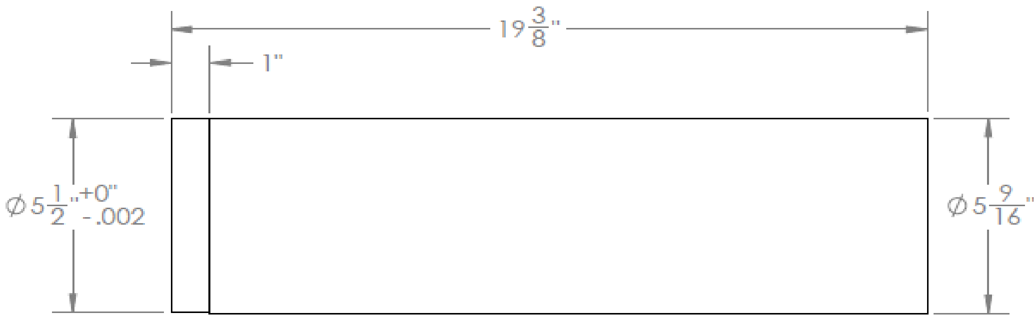

		UNLESS OTHERWISE SPECIFIED:		NAME	DATE
		DIMENSIONS ARE IN INCHES TOLERANCES: FRACTIONAL± 1/32 ANGULAR: MACH± 1 BEND ± 1 TWO PLACE DECIMAL ± N/A THREE PLACE DECIMAL ± 0.030	DRAWN	JMM	12/21
			CHECKED		
			ENG APPR.		
			MFG APPR.		
		INTERPRET GEOMETRIC TOLERANCING PER:	Q.A.		
		MATERIAL 304 SS	COMMENTS:		
NEXT ASSY	USED ON	FINISH			
APPLICATION		DO NOT SCALE DRAWING			

TEXAS A&M TURBOLAB

TITLE:

PART 5: PIPE, 5"
SCH 80/XS MODIFIED

SIZE	DWG. NO.	REV
A	P8_ATTACHMENT_MODPIPE	A

SCALE: 1:4 WEIGHT: SHEET 1 OF 1

PROPRIETARY AND CONFIDENTIAL
THE INFORMATION CONTAINED IN THIS DRAWING IS THE SOLE PROPERTY OF TEXAS A&M UNIVERSITY. ANY REPRODUCTION IN PART OR AS A WHOLE WITHOUT THE WRITTEN PERMISSION OF TEXAS A&M UNIVERSITY IS PROHIBITED.

5 4 3 2 1

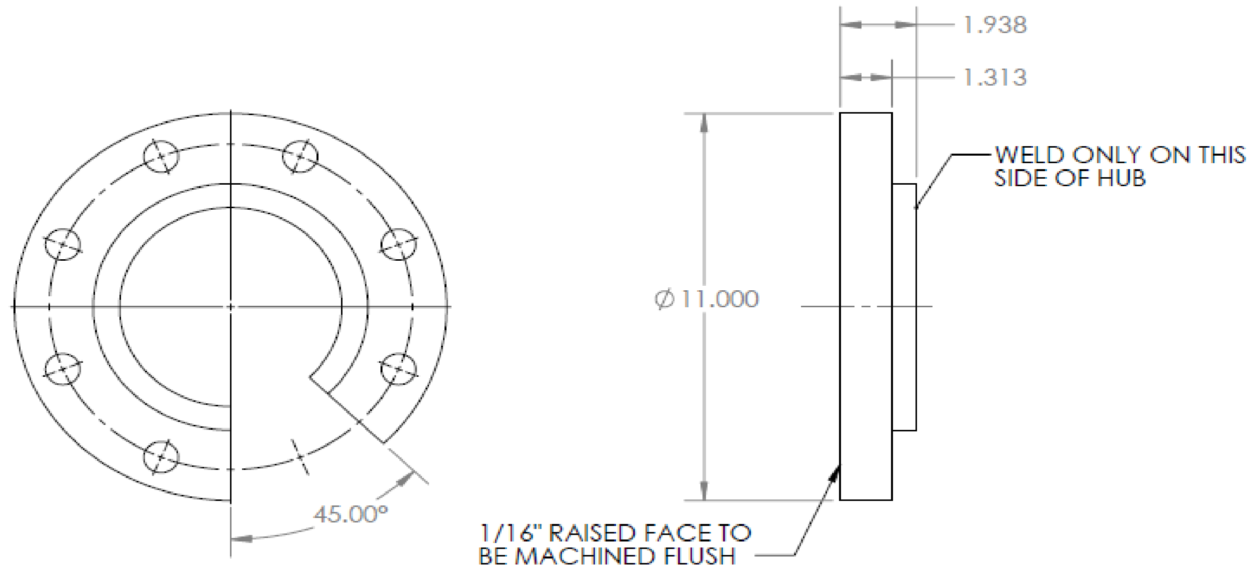

NEXT ASSY	USED ON
APPLICATION	

PROPRIETARY AND CONFIDENTIAL

THE INFORMATION CONTAINED IN THIS DRAWING IS THE SOLE PROPERTY OF TEXAS A&M UNIVERSITY. ANY REPRODUCTION IN PART OR AS A WHOLE WITHOUT THE WRITTEN PERMISSION OF TEXAS A&M UNIVERSITY IS PROHIBITED.

UNLESS OTHERWISE SPECIFIED:
DIMENSIONS ARE IN INCHES
TOLERANCES:
FRACTIONAL± 1/32
ANGULAR: MACH± 1 BEND ± 1
TWO PLACE DECIMAL ± N/A
THREE PLACE DECIMAL ± N/A

INTERPRET GEOMETRIC TOLERANCING PER:

MATERIAL
304 SS

FINISH

DO NOT SCALE DRAWING

	NAME	DATE
DRAWN	JMM	12/21
CHECKED		
ENG APPR.		
MFG APPR.		
Q.A.		

COMMENTS:

TEXAS A&M TURBOLAB

TITLE:

PART 7: FLANGE, SLIP ON
5" 300# MODVIEW

SIZE	DWG. NO.	REV
A	P8_ATTACHMENT _MODFLG	

SCALE: 1:4 WEIGHT: SHEET 1 OF 1

5 4 3 2 1

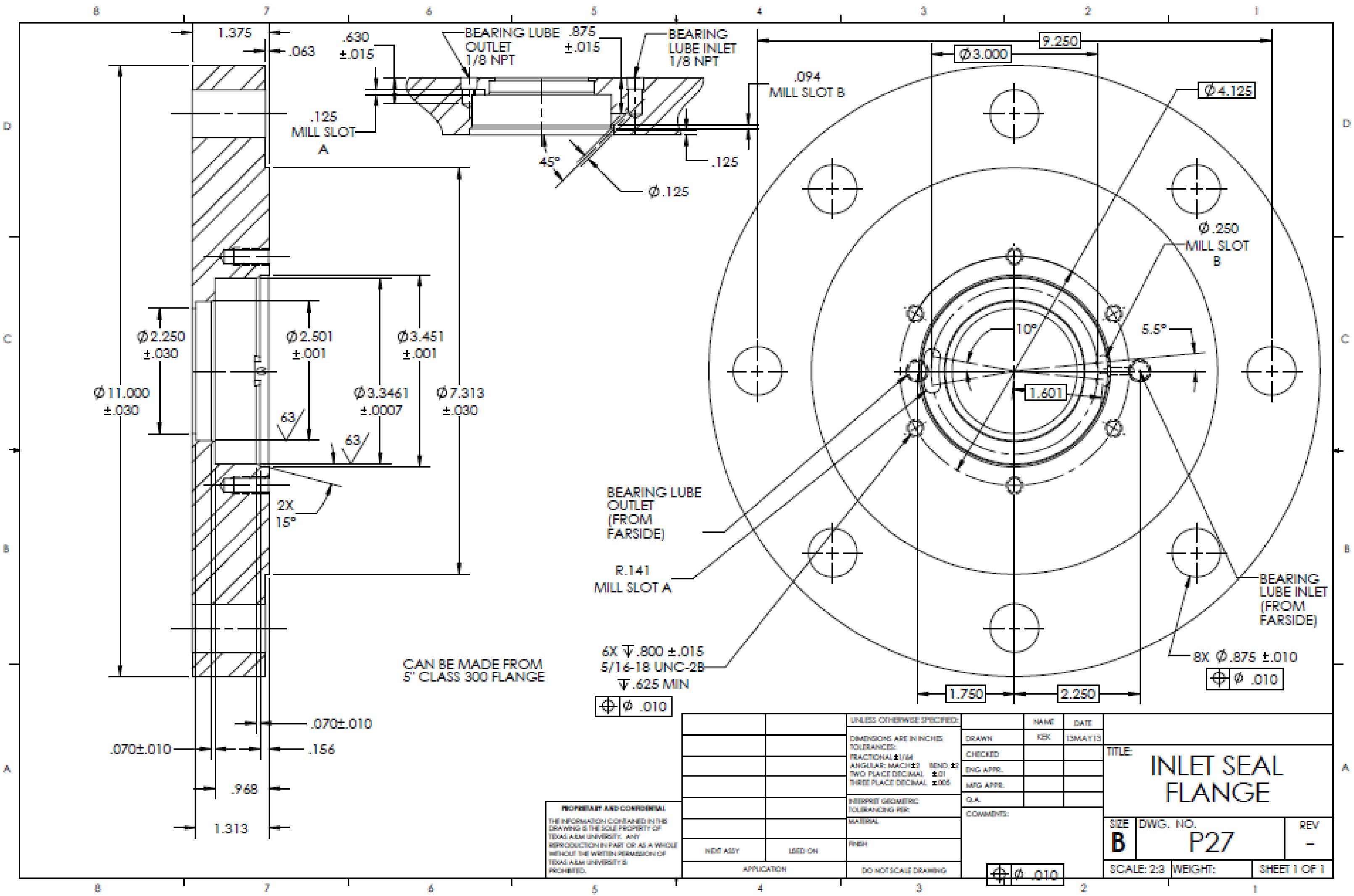

1.375
.063
.630
±.015
BEARING LUBE OUTLET 1/8 NPT
.875 ±.015
BEARING LUBE INLET 1/8 NPT
.094 MILL SLOT B
9.250
Ø3.000
Ø4.125
.125 MILL SLOT A
45°
Ø.125
.125
Ø.250 MILL SLOT B
Ø2.250 ±.030
Ø2.501 ±.001
Ø3.451 ±.001
Ø11.000 ±.030
Ø3.3461 ±.0007
Ø7.313 ±.030
10°
5.5°
1.601
63
2X 15°
BEARING LUBE OUTLET (FROM FARSIDE)
R.141 MILL SLOT A
BEARING LUBE INLET (FROM FARSIDE)
CAN BE MADE FROM 5" CLASS 300 FLANGE
6X ↧.800 ±.015
5/16-18 UNC-2B
↧.625 MIN
Ø .010
1.750
2.250
8X Ø.875 ±.010
Ø .010
.070±.010
.070±.010
.156
.968
1.313
UNLESS OTHERWISE SPECIFIED:
DIMENSIONS ARE IN INCHES
TOLERANCES:
FRACTIONAL ±1/64
ANGULAR: MACH ±2 BEND ±2
TWO PLACE DECIMAL ±.01
THREE PLACE DECIMAL ±.005
INTERPRET GEOMETRIC TOLERANCING PER:
MATERIAL
FINISH
DO NOT SCALE DRAWING
NAME DATE
DRAWN KEK 13MAY13
CHECKED
ENG APPR.
MFG APPR.
Q.A.
COMMENTS:
NEXT ASSY
USED ON
APPLICATION
PROPRIETARY AND CONFIDENTIAL
THE INFORMATION CONTAINED IN THIS DRAWING IS THE SOLE PROPERTY OF TEXAS A&M UNIVERSITY. ANY REPRODUCTION IN PART OR AS A WHOLE WITHOUT THE WRITTEN PERMISSION OF TEXAS A&M UNIVERSITY IS PROHIBITED.
TITLE:
INLET SEAL FLANGE
SIZE B
DWG. NO. P27
REV -
SCALE: 2:3
WEIGHT:
SHEET 1 OF 1
Ø .010

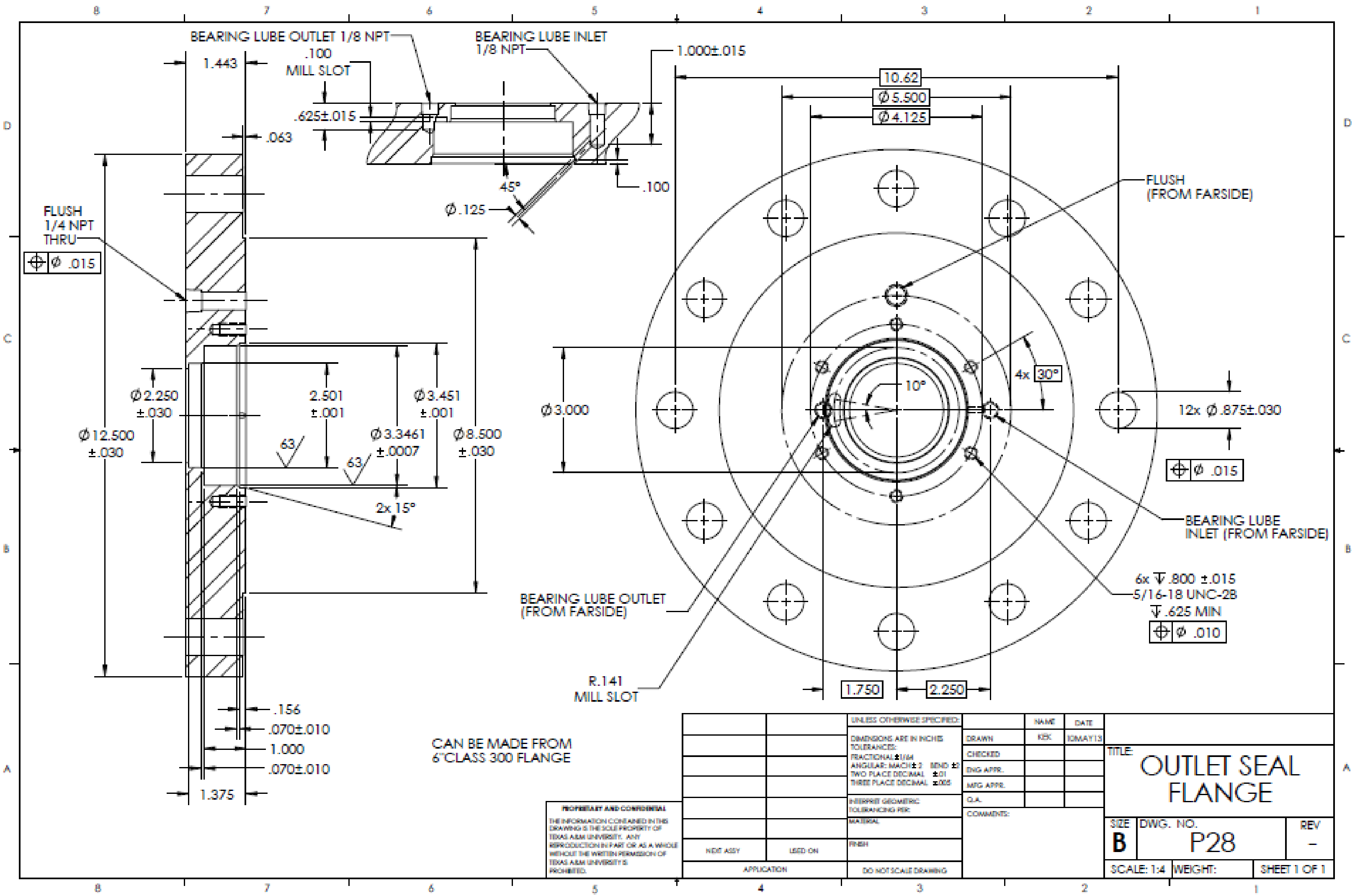

BEARING LUBE OUTLET 1/8 NPT
BEARING LUBE INLET 1/8 NPT
1.443
.100 MILL SLOT
.625±.015
.063
1.000±.015
10.62
Ø 5.500
Ø 4.125
45°
.100
Ø .125
FLUSH 1/4 NPT THRU
Ø .015
FLUSH (FROM FARSIDE)
Ø 2.250 ±.030
2.501 ±.001
Ø 3.451 ±.001
Ø 3.3461 ±.0007
Ø 8.500 ±.030
Ø 12.500 ±.030
Ø 3.000
63
2x 15°
10°
4x 30°
12x Ø .875±.030
Ø .015
BEARING LUBE INLET (FROM FARSIDE)
BEARING LUBE OUTLET (FROM FARSIDE)
6x ↧ .800 ±.015
5/16-18 UNC-2B
↧ .625 MIN
Ø .010
R.141 MILL SLOT
1.750
2.250
.156
.070±.010
1.000
.070±.010
1.375
CAN BE MADE FROM 6"CLASS 300 FLANGE
UNLESS OTHERWISE SPECIFIED:
DIMENSIONS ARE IN INCHES
TOLERANCES:
NAME
DATE
DRAWN
KEK
10MAY13
CHECKED
ENG APPR.
MFG APPR.
Q.A.
COMMENTS:
MATERIAL
FINISH
NEXT ASSY
USED ON
APPLICATION
DO NOT SCALE DRAWING
PROPRIETARY AND CONFIDENTIAL
TITLE:
OUTLET SEAL FLANGE
SIZE B
DWG. NO. P28
REV -
SCALE: 1:4
WEIGHT:
SHEET 1 OF 1

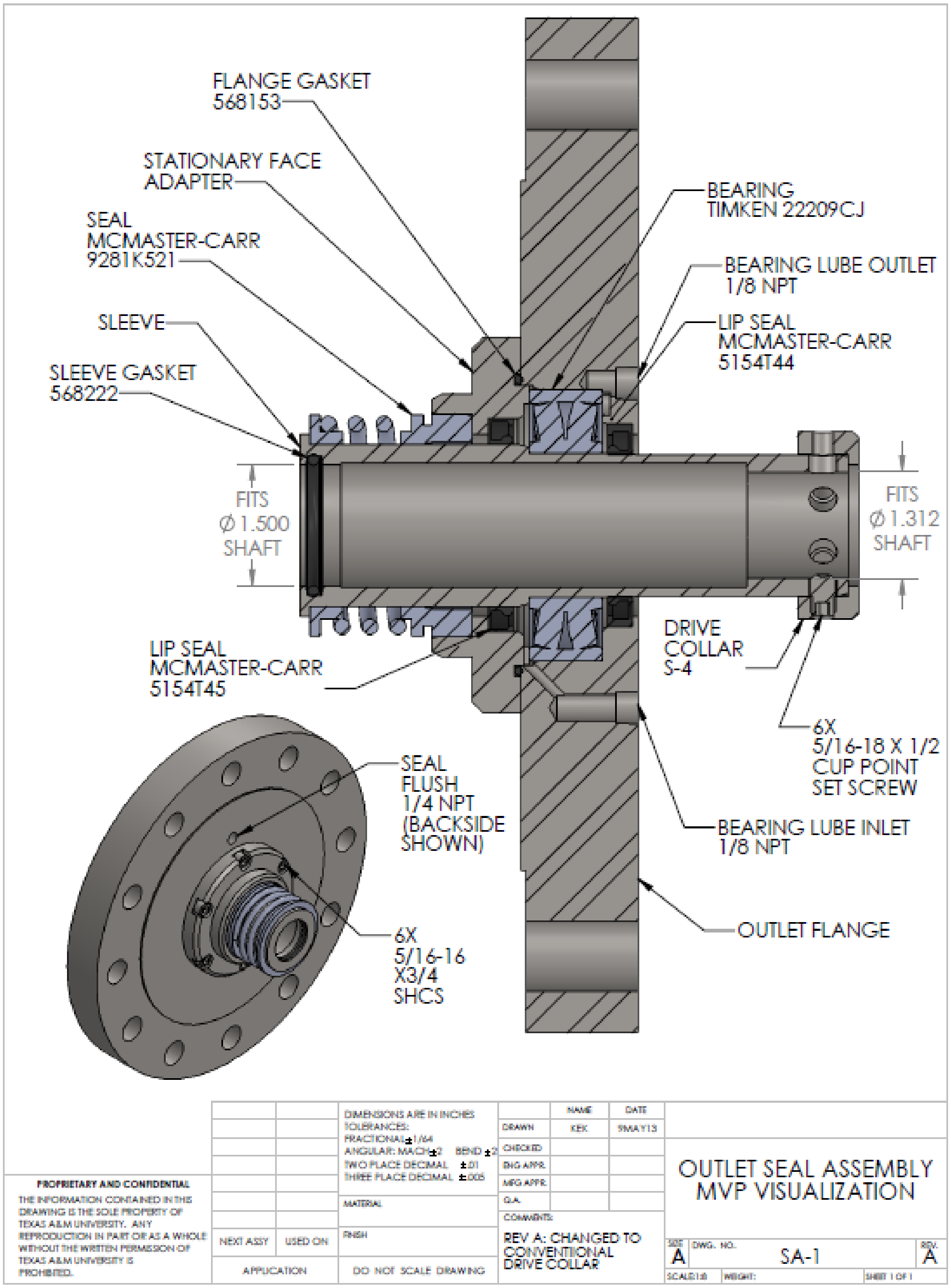
FLANGE GASKET
568153
STATIONARY FACE
ADAPTER
SEAL
MCMASTER-CARR
9281K521
SLEEVE
SLEEVE GASKET
568222
BEARING
TIMKEN 22209CJ
BEARING LUBE OUTLET
1/8 NPT
LIP SEAL
MCMASTER-CARR
5154T44
FITS
Ø 1.500
SHAFT
FITS
Ø 1.312
SHAFT
DRIVE
COLLAR
S-4
LIP SEAL
MCMASTER-CARR
5154T45
6X
5/16-18 X 1/2
CUP POINT
SET SCREW
SEAL
FLUSH
1/4 NPT
(BACKSIDE
SHOWN)
BEARING LUBE INLET
1/8 NPT
OUTLET FLANGE
6X
5/16-16
X3/4
SHCS
DIMENSIONS ARE IN INCHES
TOLERANCES:
FRACTIONAL ±1/64
ANGULAR: MACH ±2 BEND ±2
TWO PLACE DECIMAL ±.01
THREE PLACE DECIMAL ±.005
NAME
DATE
DRAWN
KEK
9MAY13
CHECKED
ENG APPR.
MFG APPR.
Q.A.
COMMENTS:
REV A: CHANGED TO CONVENTIONAL DRIVE COLLAR
MATERIAL
FINISH
NEXT ASSY
USED ON
APPLICATION
DO NOT SCALE DRAWING
PROPRIETARY AND CONFIDENTIAL
THE INFORMATION CONTAINED IN THIS DRAWING IS THE SOLE PROPERTY OF TEXAS A&M UNIVERSITY. ANY REPRODUCTION IN PART OR AS A WHOLE WITHOUT THE WRITTEN PERMISSION OF TEXAS A&M UNIVERSITY IS PROHIBITED.
OUTLET SEAL ASSEMBLY
MVP VISUALIZATION
SIZE
A
DWG. NO.
SA-1
REV.
A
SCALE:1:8
WEIGHT:
SHEET 1 OF 1

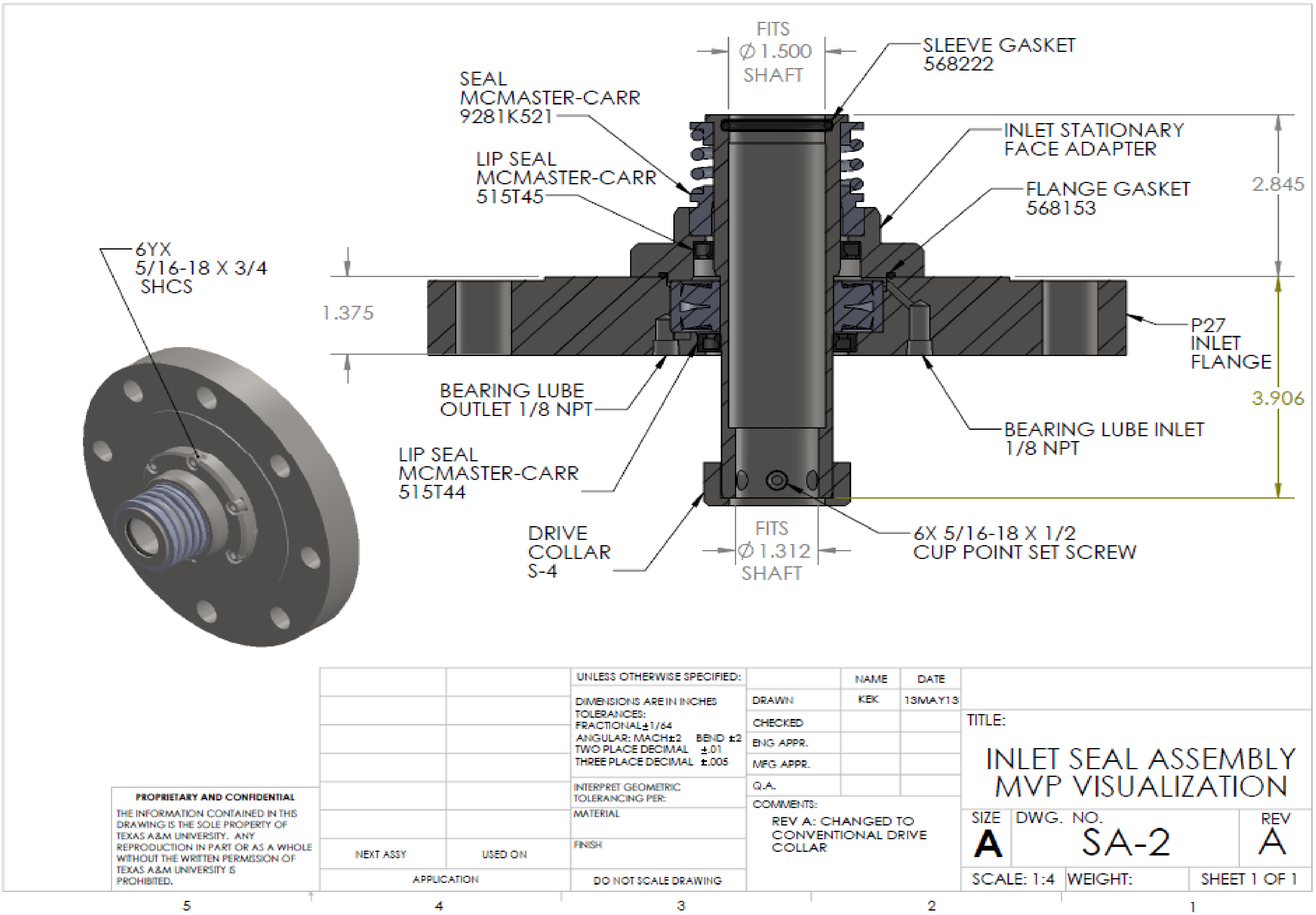
FITS
Ø 1.500
SHAFT
SLEEVE GASKET
568222
SEAL
MCMASTER-CARR
9281K521
INLET STATIONARY
FACE ADAPTER
LIP SEAL
MCMASTER-CARR
515T45
FLANGE GASKET
568153
2.845
6YX
5/16-18 X 3/4
SHCS
1.375
P27
INLET
FLANGE
BEARING LUBE
OUTLET 1/8 NPT
3.906
BEARING LUBE INLET
1/8 NPT
LIP SEAL
MCMASTER-CARR
515T44
DRIVE
COLLAR
S-4
FITS
Ø 1.312
SHAFT
6X 5/16-18 X 1/2
CUP POINT SET SCREW
UNLESS OTHERWISE SPECIFIED:
DIMENSIONS ARE IN INCHES
TOLERANCES:
FRACTIONAL±1/64
ANGULAR: MACH±2 BEND ±2
TWO PLACE DECIMAL ±.01
THREE PLACE DECIMAL ±.005
INTERPRET GEOMETRIC
TOLERANCING PER:
MATERIAL
FINISH
DO NOT SCALE DRAWING
NEXT ASSY
USED ON
APPLICATION
NAME
DATE
DRAWN
KEK
13MAY13
CHECKED
ENG APPR.
MFG APPR.
Q.A.
COMMENTS:
REV A: CHANGED TO
CONVENTIONAL DRIVE
COLLAR
TITLE:
INLET SEAL ASSEMBLY
MVP VISUALIZATION
SIZE
A
DWG. NO.
SA-2
REV
A
SCALE: 1:4
WEIGHT:
SHEET 1 OF 1
PROPRIETARY AND CONFIDENTIAL
THE INFORMATION CONTAINED IN THIS
DRAWING IS THE SOLE PROPERTY OF
TEXAS A&M UNIVERSITY. ANY
REPRODUCTION IN PART OR AS A WHOLE
WITHOUT THE WRITTEN PERMISSION OF
TEXAS A&M UNIVERSITY IS
PROHIBITED.
5
4
3
2
1

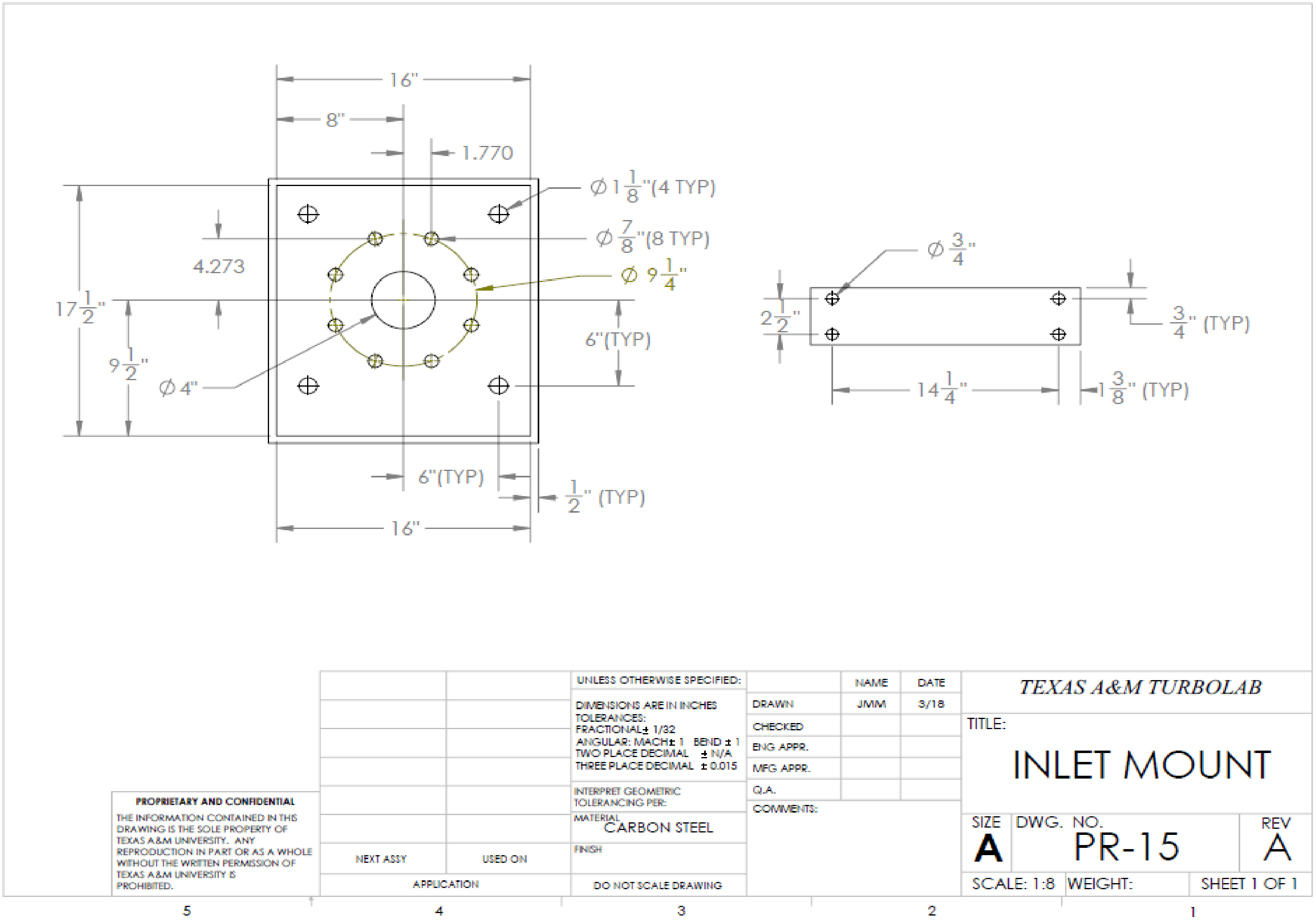
16"
8"
1.770
Ø 1 1/8"(4 TYP)
Ø 7/8"(8 TYP)
Ø 9 1/4"
4.273
17 1/2"
9 1/2"
Ø 4"
6"(TYP)
6"(TYP)
1/2" (TYP)
16"
Ø 3/4"
2 1/2"
3/4" (TYP)
14 1/4"
1 3/8" (TYP)
UNLESS OTHERWISE SPECIFIED:
DIMENSIONS ARE IN INCHES
TOLERANCES:
FRACTIONAL ± 1/32
ANGULAR: MACH ± 1 BEND ± 1
TWO PLACE DECIMAL ± N/A
THREE PLACE DECIMAL ± 0.015
INTERPRET GEOMETRIC TOLERANCING PER:
MATERIAL
CARBON STEEL
FINISH
DO NOT SCALE DRAWING
NEXT ASSY
USED ON
APPLICATION
NAME
DATE
DRAWN
JMM
3/18
CHECKED
ENG APPR.
MFG APPR.
Q.A.
COMMENTS:
TEXAS A&M TURBOLAB
TITLE:
INLET MOUNT
SIZE
A
DWG. NO.
PR-15
REV
A
SCALE: 1:8
WEIGHT:
SHEET 1 OF 1
PROPRIETARY AND CONFIDENTIAL
THE INFORMATION CONTAINED IN THIS DRAWING IS THE SOLE PROPERTY OF TEXAS A&M UNIVERSITY. ANY REPRODUCTION IN PART OR AS A WHOLE WITHOUT THE WRITTEN PERMISSION OF TEXAS A&M UNIVERSITY IS PROHIBITED.
5
4
3
2
1

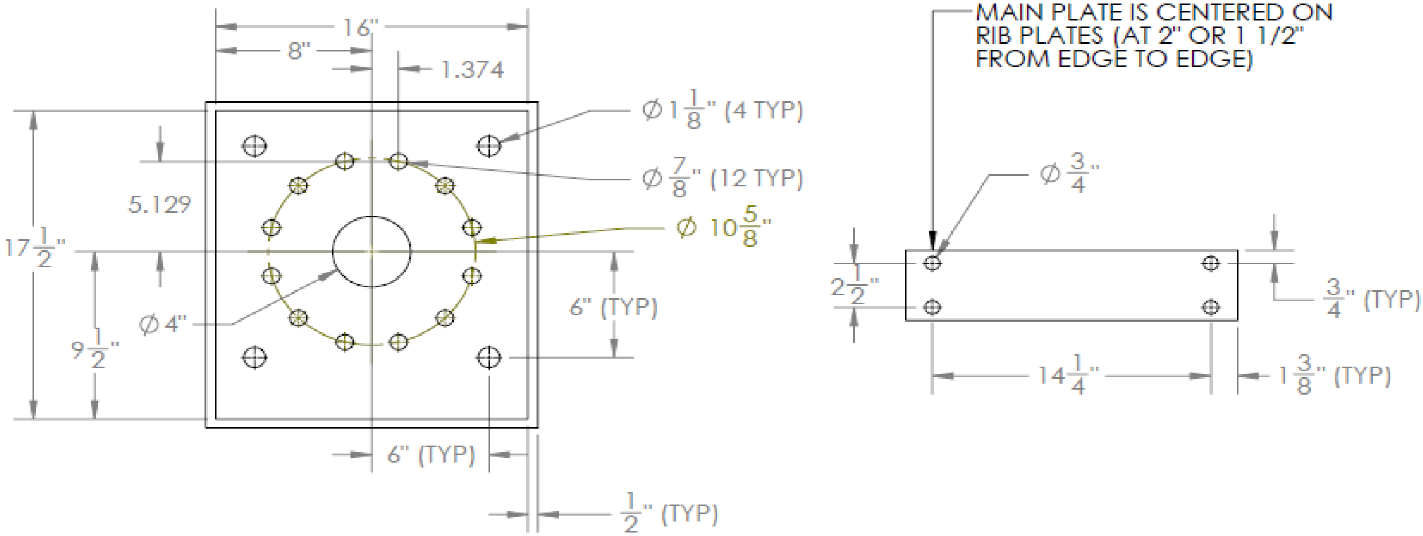

NOTES:
1) WELDS SHOULD BE AT LEAST 3/8" FILLETS FINISHED
2) USE AT LEAST 3/8" CHAMFERS TO WELD MAIN PLATE TO RIBS

UNLESS OTHERWISE SPECIFIED:
DIMENSIONS ARE IN INCHES
TOLERANCES:
FRACTIONAL± 1/32
ANGULAR: MACH± 1 BEND ± 1
TWO PLACE DECIMAL ± N/A
THREE PLACE DECIMAL ± 0.015

INTERPRET GEOMETRIC TOLERANCING PER:

MATERIAL CARBON STEEL

FINISH

DO NOT SCALE DRAWING

NEXT ASSY | USED ON
APPLICATION

	NAME	DATE
DRAWN	JMM	3/18
CHECKED		
ENG APPR.		
MFG APPR.		
Q.A.		

COMMENTS:

TEXAS A&M TURBOLAB

TITLE:

OUTLET MOUNT

SIZE A | DWG. NO. PR-14 | REV A

SCALE: 1:8 | WEIGHT: | SHEET 1 OF 1

PROPRIETARY AND CONFIDENTIAL
THE INFORMATION CONTAINED IN THIS DRAWING IS THE SOLE PROPERTY OF TEXAS A&M UNIVERSITY. ANY REPRODUCTION IN PART OR AS A WHOLE WITHOUT THE WRITTEN PERMISSION OF TEXAS A&M UNIVERSITY IS PROHIBITED.

5 4 3 2 1

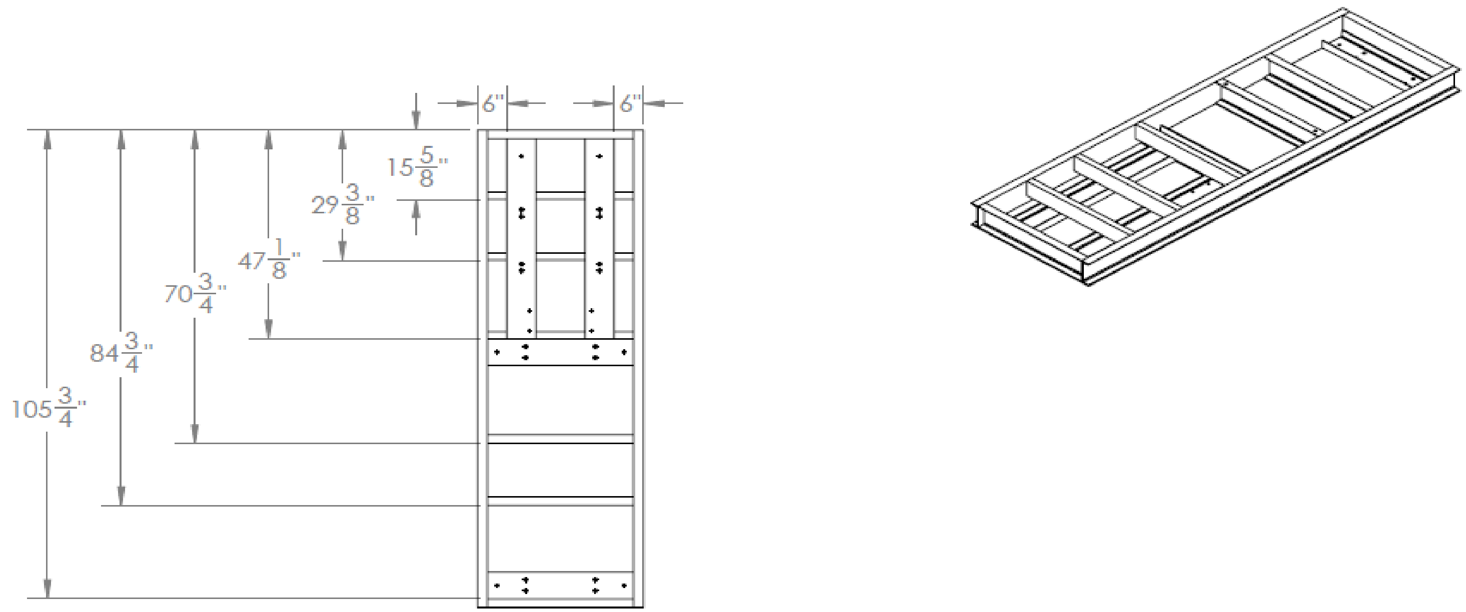

PROPRIETARY AND CONFIDENTIAL

THE INFORMATION CONTAINED IN THIS DRAWING IS THE SOLE PROPERTY OF TEXAS A&M UNIVERSITY. ANY REPRODUCTION IN PART OR AS A WHOLE WITHOUT THE WRITTEN PERMISSION OF TEXAS A&M UNIVERSITY IS PROHIBITED.

NEXT ASSY	USED ON
APPLICATION	

UNLESS OTHERWISE SPECIFIED:

DIMENSIONS ARE IN INCHES
TOLERANCES:
FRACTIONAL± 1/32
ANGULAR: MACH± 1 BEND ± 1
TWO PLACE DECIMAL ± N/A
THREE PLACE DECIMAL ± 0.015

INTERPRET GEOMETRIC TOLERANCING PER:

MATERIAL
CARBON STEEL

FINISH

DO NOT SCALE DRAWING

	NAME	DATE
DRAWN	JMM	4/3
CHECKED		
ENG APPR.		
MFG APPR.		
Q.A.		

COMMENTS:

TEXAS A&M TURBOLAB

TITLE:
SKID FABRICATION

SIZE	DWG. NO.	REV
A	S-1	A

SCALE: 1:32 WEIGHT: SHEET 1 OF 1

5 4 3 2 1

ITEM NO.	PART NUMBER	QTY.
1	S3E_Column_SE_Rev1	1
2	S3D_Column_NE_Rev1	1
3	S3A_SkidSupport_Rev1	1
4	S3B_Column_NW_Rev1	1
5	S3C_Column_SW_Rev1	1
6	S3F_Track_EW_Rev1	1
7	S3G_Header_EW_Rev1	4
8	S3I_Header_NS_W_Rev1	1
9	S3H_Header_NS_Rev1	1
18	S3J_PipeSupport_Rev1	1

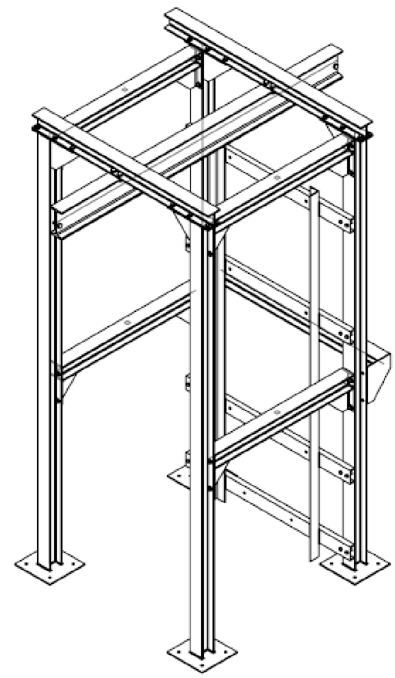

UNLESS OTHERWISE SPECIFIED:
DIMENSIONS ARE IN INCHES
TOLERANCES:
FRACTIONAL ± 1/32
ANGULAR: MACH ± 1 BEND ± 1
TWO PLACE DECIMAL ± 0.06
THREE PLACE DECIMAL ± 0.015
INTERPRET GEOMETRIC TOLERANCING PER:
MATERIAL CARBON STEEL
FINISH N/A
DO NOT SCALE DRAWING

NEXT ASSY | USED ON
APPLICATION

	NAME	DATE
DRAWN	JMM	4/30
CHECKED		
ENG APPR.		
MFG APPR.		
Q.A.		

COMMENTS:

TEXAS A&M TURBOLAB

TITLE: RIG SUPPORT

SIZE B | DWG. NO. S-3M | REV B

SCALE: 1:24 | WEIGHT: | SHEET 1 OF 1

PROPRIETARY AND CONFIDENTIAL
THE INFORMATION CONTAINED IN THIS DRAWING IS THE SOLE PROPERTY OF TEXAS A&M UNIVERSITY. ANY REPRODUCTION IN PART OR AS A WHOLE WITHOUT THE WRITTEN PERMISSION OF TEXAS A&M UNIVERSITY IS PROHIBITED.

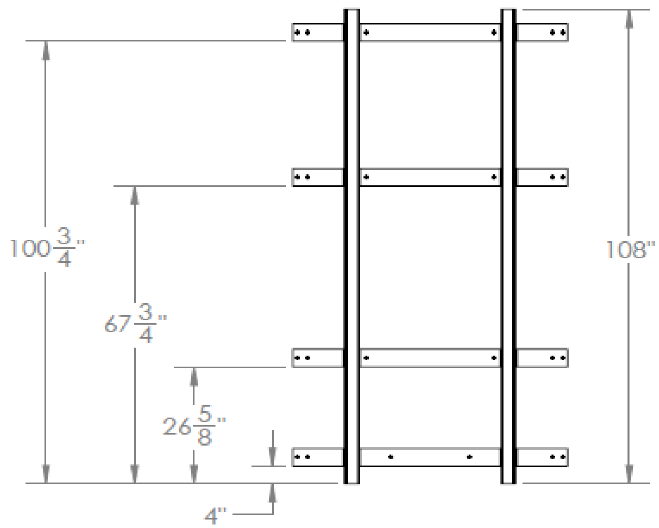

		UNLESS OTHERWISE SPECIFIED:		NAME	DATE	TEXAS A&M TURBOLAB
		DIMENSIONS ARE IN INCHES TOLERANCES: FRACTIONAL± 1/32 ANGULAR: MACH± 1 BEND ± 1 TWO PLACE DECIMAL ± N/A THREE PLACE DECIMAL ± 0.015	DRAWN	JMM	4/3	TITLE: SKID SUPPORT
			CHECKED			
			ENG APPR.			
			MFG APPR.			
		INTERPRET GEOMETRIC TOLERANCING PER:	Q.A.			
		MATERIAL CARBON STEEL	COMMENTS:			SIZE A · DWG. NO. S-3A · REV A
NEXT ASSY	USED ON	FINISH				
APPLICATION		DO NOT SCALE DRAWING				SCALE: 1:32 · WEIGHT: · SHEET 1 OF 1

PROPRIETARY AND CONFIDENTIAL

THE INFORMATION CONTAINED IN THIS DRAWING IS THE SOLE PROPERTY OF TEXAS A&M UNIVERSITY. ANY REPRODUCTION IN PART OR AS A WHOLE WITHOUT THE WRITTEN PERMISSION OF TEXAS A&M UNIVERSITY IS PROHIBITED.

5 4 3 2 1

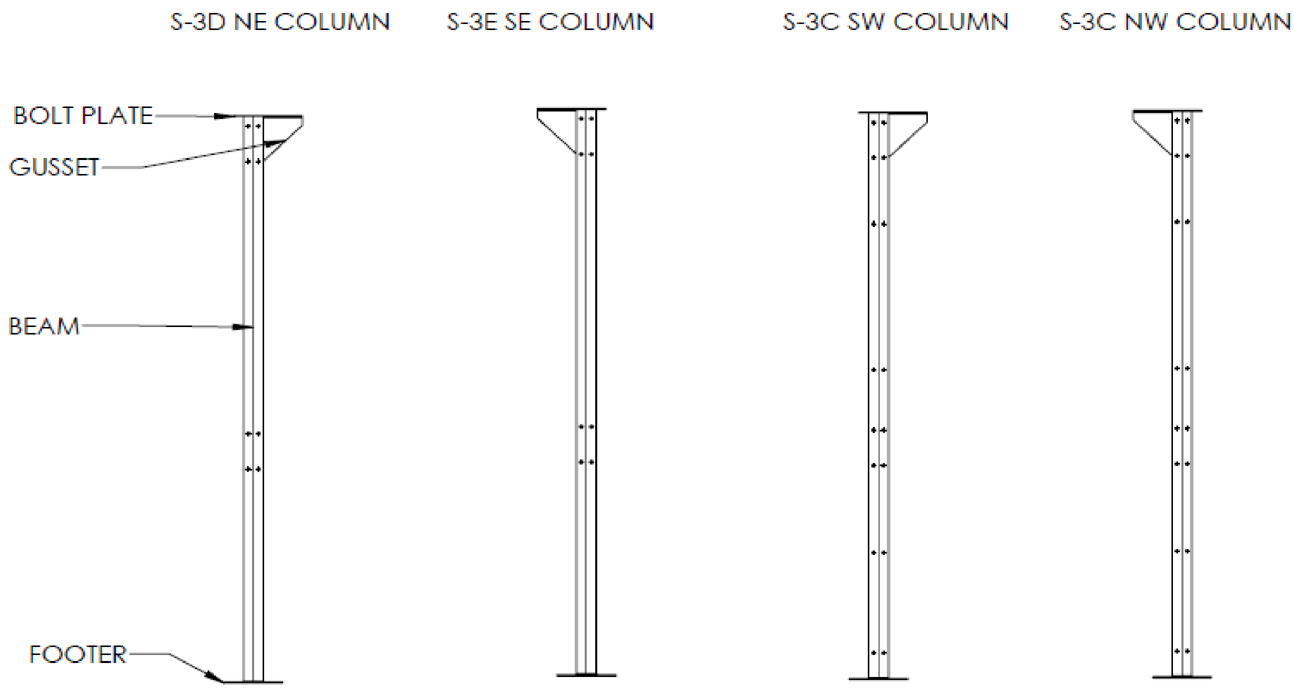

PROPRIETARY AND CONFIDENTIAL

THE INFORMATION CONTAINED IN THIS DRAWING IS THE SOLE PROPERTY OF TEXAS A&M UNIVERSITY. ANY REPRODUCTION IN PART OR AS A WHOLE WITHOUT THE WRITTEN PERMISSION OF TEXAS A&M UNIVERSITY IS PROHIBITED.

NEXT ASSY	USED ON
APPLICATION	

UNLESS OTHERWISE SPECIFIED:

DIMENSIONS ARE IN INCHES
TOLERANCES:
FRACTIONAL ± 1/32
ANGULAR: MACH ± 1 BEND ± 1
TWO PLACE DECIMAL ± 0.06
THREE PLACE DECIMAL ± 0.015

INTERPRET GEOMETRIC TOLERANCING PER:

MATERIAL
CARBON STEEL

FINISH

DO NOT SCALE DRAWING

	NAME	DATE
DRAWN	JMM	5/1
CHECKED		
ENG APPR.		
MFG APPR.		
Q.A.		

COMMENTS:

TEXAS A&M TURBOLAB

TITLE:

COLUMN LAYOUT

SIZE	DWG. NO.	REV
A	S-3	A

SCALE: 1:32 WEIGHT: SHEET 1 OF 1

5 4 3 2 1

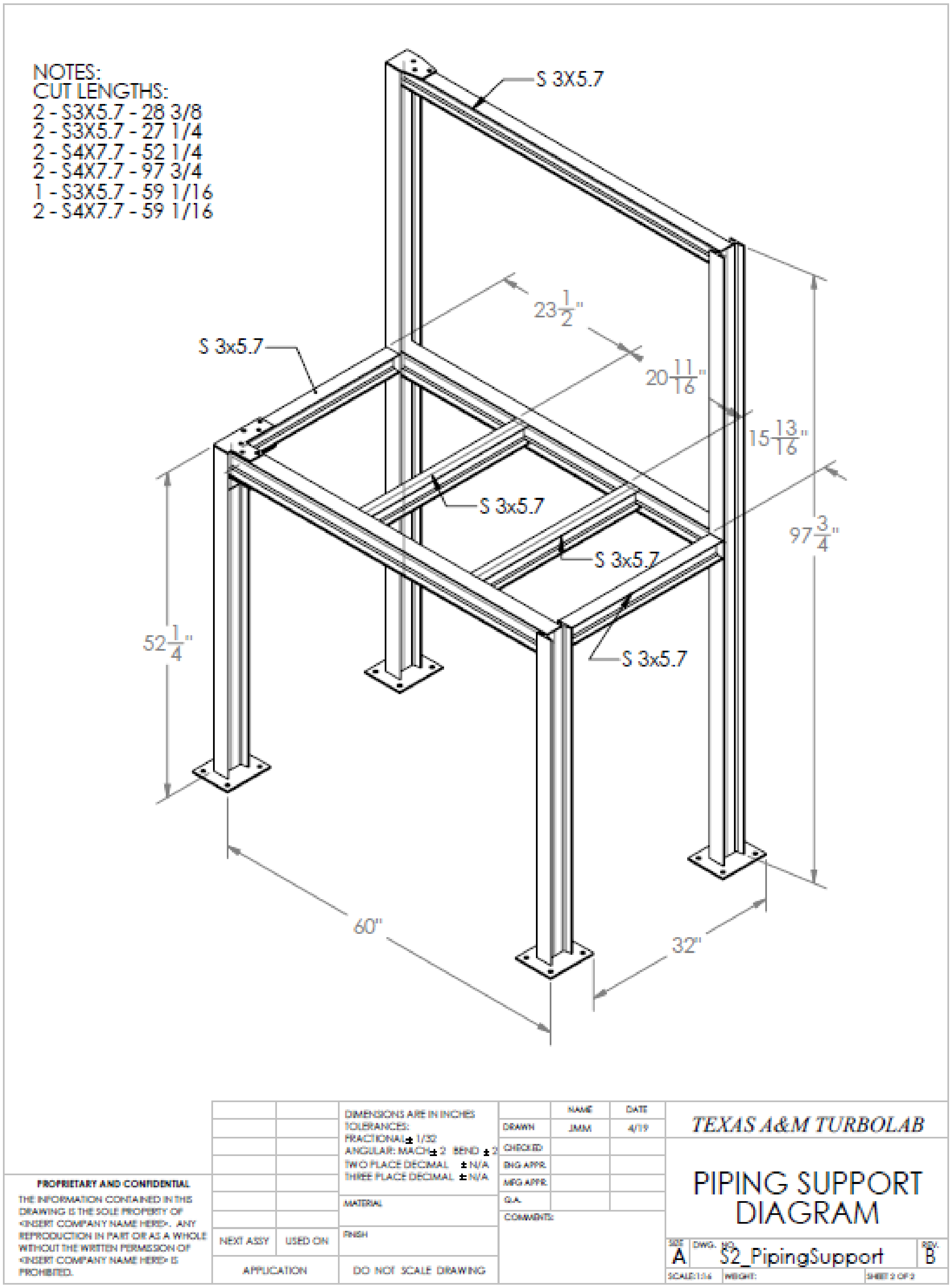
NOTES:
CUT LENGTHS:
2 - S3X5.7 - 28 3/8
2 - S3X5.7 - 27 1/4
2 - S4X7.7 - 52 1/4
2 - S4X7.7 - 97 3/4
1 - S3X5.7 - 59 1/16
2 - S4X7.7 - 59 1/16
S 3X5.7
S 3x5.7
S 3x5.7
S 3x5.7
S 3x5.7
23 1/2"
20 11/16"
15 13/16"
97 3/4"
52 1/4"
60"
32"
DIMENSIONS ARE IN INCHES
TOLERANCES:
FRACTIONAL ± 1/32
ANGULAR: MACH ± 2 BEND ± 2
TWO PLACE DECIMAL ± N/A
THREE PLACE DECIMAL ± N/A
MATERIAL
FINISH
DO NOT SCALE DRAWING
NEXT ASSY
USED ON
APPLICATION
NAME
DATE
DRAWN
JMM
4/19
CHECKED
ENG APPR.
MFG APPR.
Q.A.
COMMENTS:
TEXAS A&M TURBOLAB
PIPING SUPPORT DIAGRAM
SIZE A
DWG. NO. S2_PipingSupport
REV. B
SCALE: 1:16
WEIGHT:
SHEET 2 OF 2
PROPRIETARY AND CONFIDENTIAL
THE INFORMATION CONTAINED IN THIS DRAWING IS THE SOLE PROPERTY OF <INSERT COMPANY NAME HERE>. ANY REPRODUCTION IN PART OR AS A WHOLE WITHOUT THE WRITTEN PERMISSION OF <INSERT COMPANY NAME HERE> IS PROHIBITED.

ITEM NO.	PART NUMBER	STANDARD	MATERIAL	QTY.	Length
1	WNeck Flange 600-NPS6	ASTM A182 F304	UNS S30400	2	
2	Tee Inch 6 Sch40	ASTM A403 WP304	UNS S30400	1	
3	90L LR Inch 6 Sch40	ASTM A403 WP304	UNS S30400	1	
4	6 in, Schedule 40	ASTM A312 TP304	UNS S30400	1	16 1/4"
5	Stub End, Sch. 40	ASTM A403 WP304	UNS S30400	1	
6	Flange, Lap Joint 600-NPS 6	ASTM A182 F304	UNS S30400	1	
7	Ell Weld Eye	Detail B	UNS S30400	1	

NOTES:
1) DIMENSIONS ARE TO FLANGE FACES NOT RAISED GASKET FACE
2) STANDARD 1/8" WELD GAP FOR ROOT PASS OF WELD
3) STANDARD 2 HOLE FLANGE ALIGNMENT ON ALL FLANGES
4) TO BE MARKED: MAWP 575PSIG
5) HYDROTEST TO 750 PSIG PER ASME B31.3 PROCESS PIPING CODE

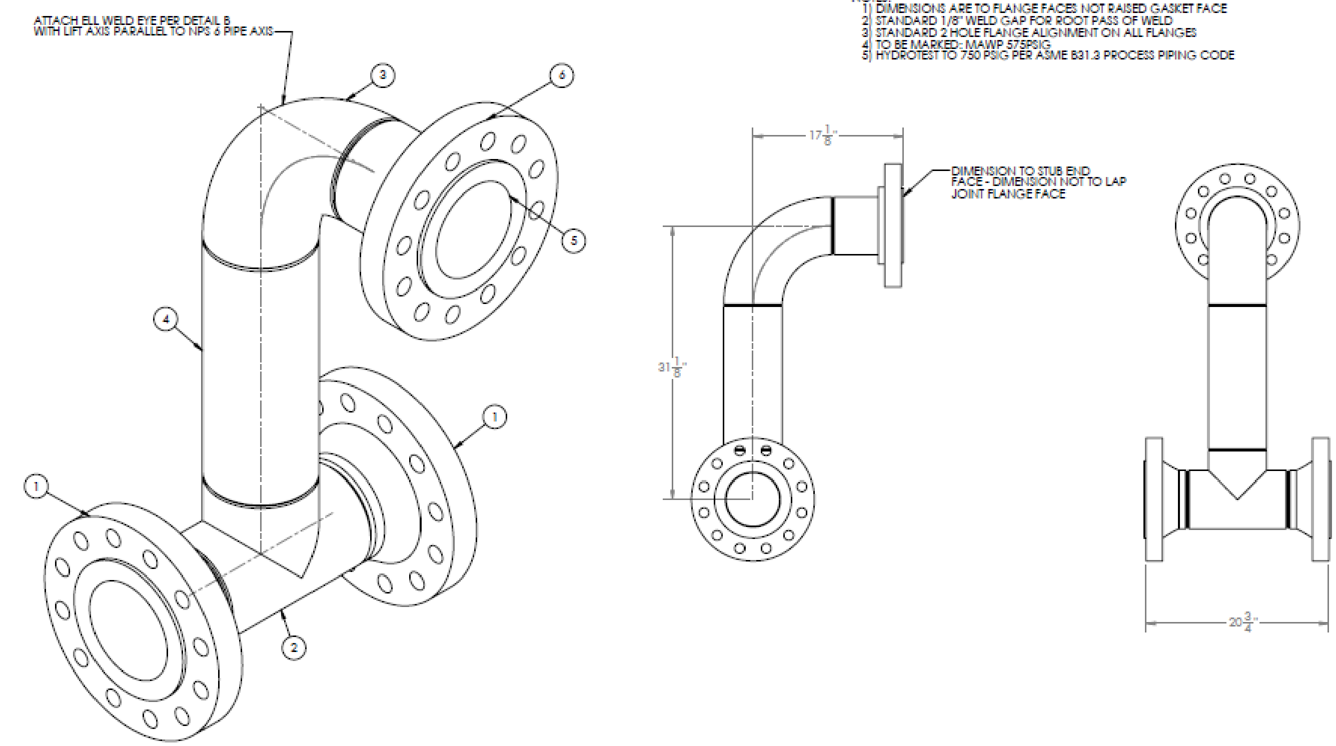

FINISH: N/A

DO NOT SCALE DRAWING | REVISION B

TEXAS A&M TURBOMACHINERY LAB

TITLE: MVP VISUALIZATION

MATERIAL: 304 SS

DWG NO. OUTLET 6" SI12 | A2

ITEM NO.	PART NUMBER	STANDARD	MATERIAL	QTY.	Length
1	WNeck Flange 300-NPS3	ASTM A182 F304	UNS S30400	1	
2	REDUCER 3 x 2 SCH. 40	ASTM A403 WP304	UNS S30400	1	
3	WNeck Flange 300-NPS2	ASTM A182 F304	UNS S30400	1	
4	2 in, Schedule 40	ASTM A312 TP304	UNS S30400	1	42 3/4"

NOTES:
1) DIMENSIONS ARE TO FLANGE FACES NOT RAISED GASKET FACE
2) STANDARD 1/8" WELD GAP FOR ROOT PASS OF WELD
3) STANDARD 2 HOLE FLANGE ALIGNMENT ON ALL FLANGES
4) TO BE MARKED: MAWP 600 PSIG
5) HYDROTEST TO 780 PSIG PER ASME B31.3 PROCESS PIPING CODE

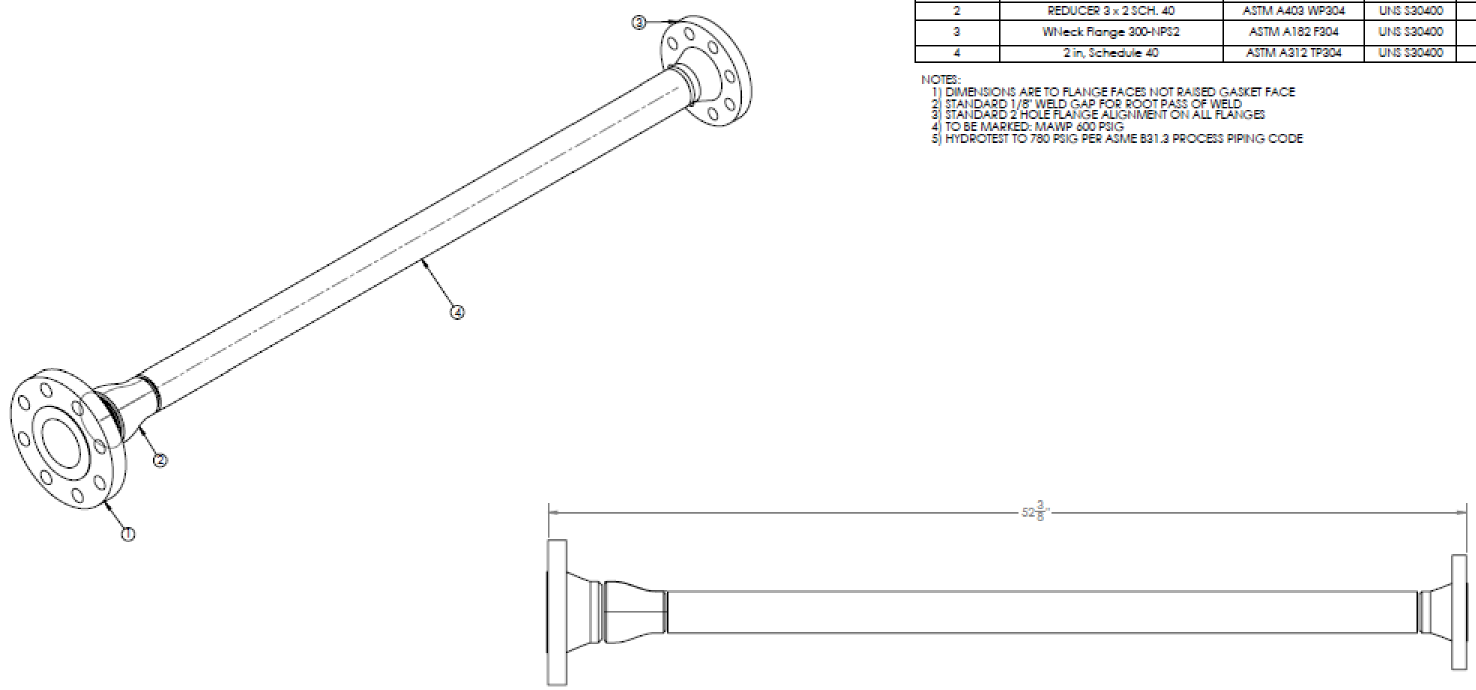

FINISH:	N/A
MATERIAL:	304 SS

TEXAS A&M TURBOMACHINERY LAB

MVP VISUALIZATION

INLET AIR 2" 714

A2

ITEM NO.	PART NUMBER	STANDARD	MATERIAL	QTY.	Length
1	WNeck Flange 600-NPS3	ASTM A182 F304	UNS S30400	2	
2	Tee Inch 3 Sch40	ASTM A403 WP304	UNS S30400	1	
3	WNeck Flange 300-NPS3	ASTM A182 F304	UNS S30400	1	
4	3 in, Schedule 40	ASTM A312 TP304	UNS S30400	1	41 3/8"

NOTES:
1) DIMENSIONS ARE TO FLANGE FACES NOT RAISED GASKET FACE
2) STANDARD 1/8" WELD GAP FOR ROOT PASS OF WELD
3) STANDARD 2 HOLE FLANGE ALIGNMENT ON ALL FLANGES
4) TO BE MARKED: MAWP 600 PSIG
5) HYDROTEST TO 780 PSIG PER ASME B31.3 PROCESS PIPING CODE

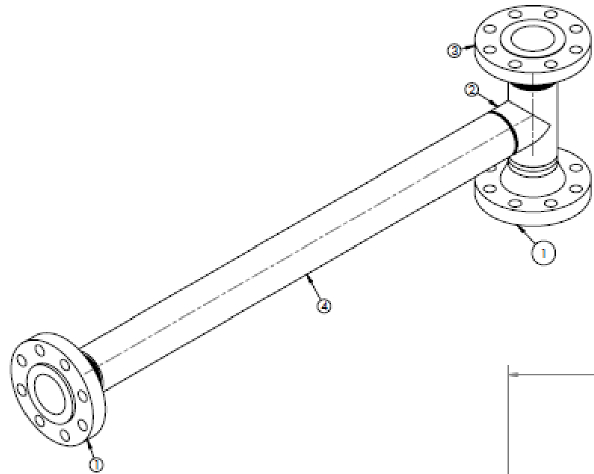

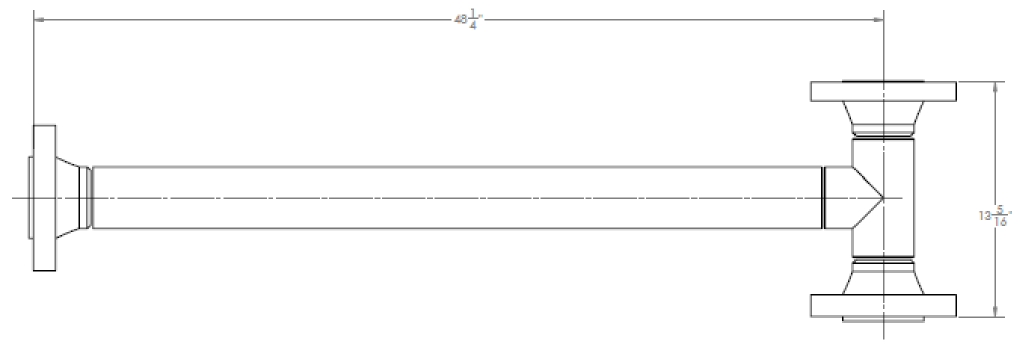

FINISH: N/A

DO NOT SCALE DRAWING — REVISION C

TEXAS A&M TURBOMACHINERY LAB

TITLE: MVP VISUALIZATION

MATERIAL: 304 SS

DWG NO. INLET AIR 3" SI12 — A2

SHEET 1 OF 1

ITEM NO.	PART NUMBER	STANDARD	MATERIAL	QTY.	Length
1	WNeck Flange 300-NPS2	ASTM A182 F304	UNS S30400	2	
2	Tee Inch 2 Sch40	ASTM A403 WP304	UNS S30400	1	
3	90L LR Inch 2 Sch40	ASTM A403 WP304	UNS S30400	2	
4	2 in, Schedule 40			1	29 5/8"
5	Stub End, Sch. 40	ASTM A403 WP304	UNS S30400	1	
6	Flange, Lap Joint 300-NPS 3	ASTM A182 F304	UNS S30400	1	

NOTES:
1) DIMENSIONS ARE TO FLANGE FACES NOT RAISED GASKET FACE
2) STANDARD 1/8" WELD GAP FOR ROOT PASS OF WELD
3) STANDARD 2 HOLE FLANGE ALIGNMENT ON ALL FLANGES
4) TO BE MARKED: MAWP 600 PSIG
5) HYDROTEST TO 780 PSIG PER ASME B31.3 PROCESS PIPING CODE

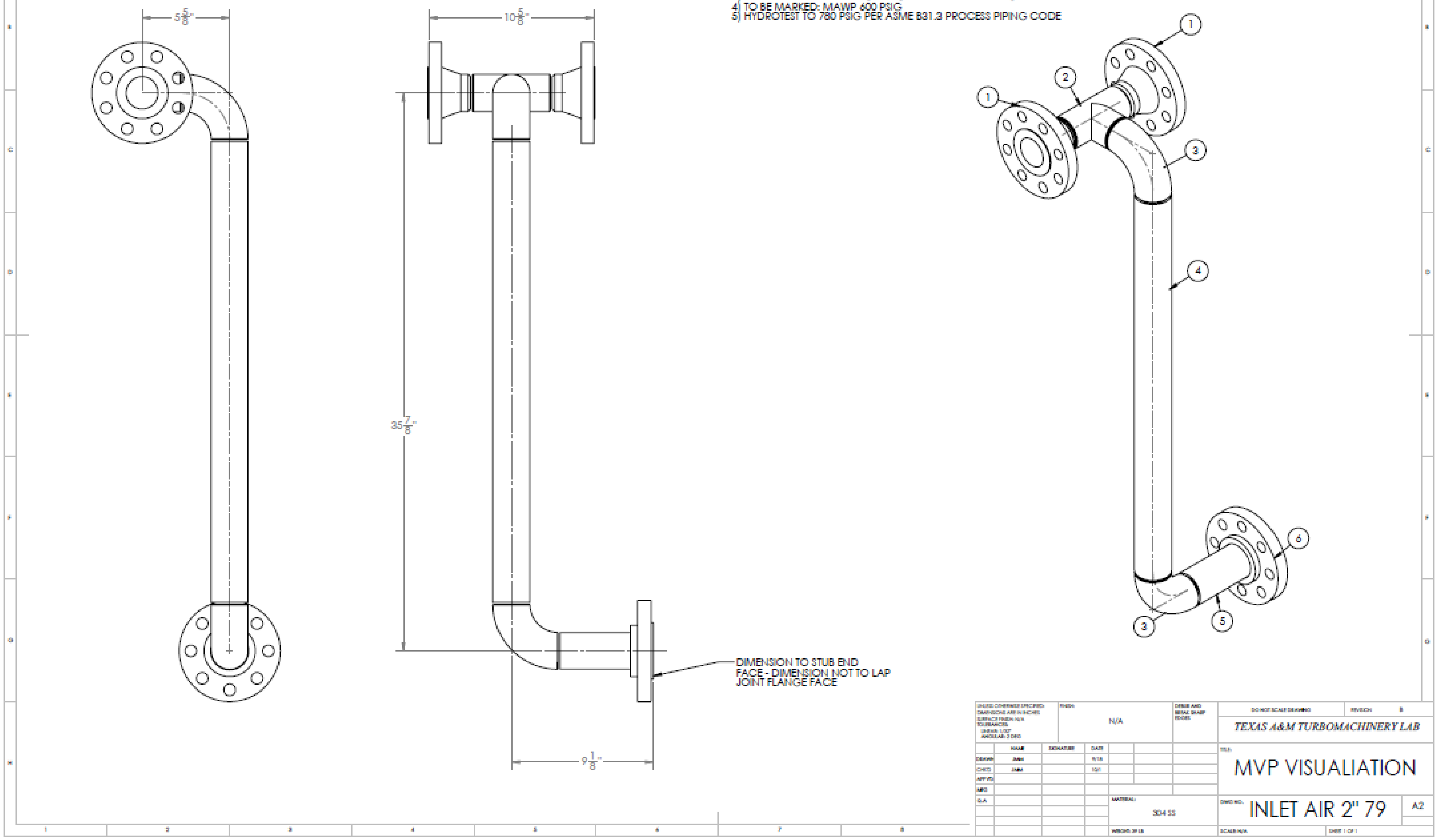

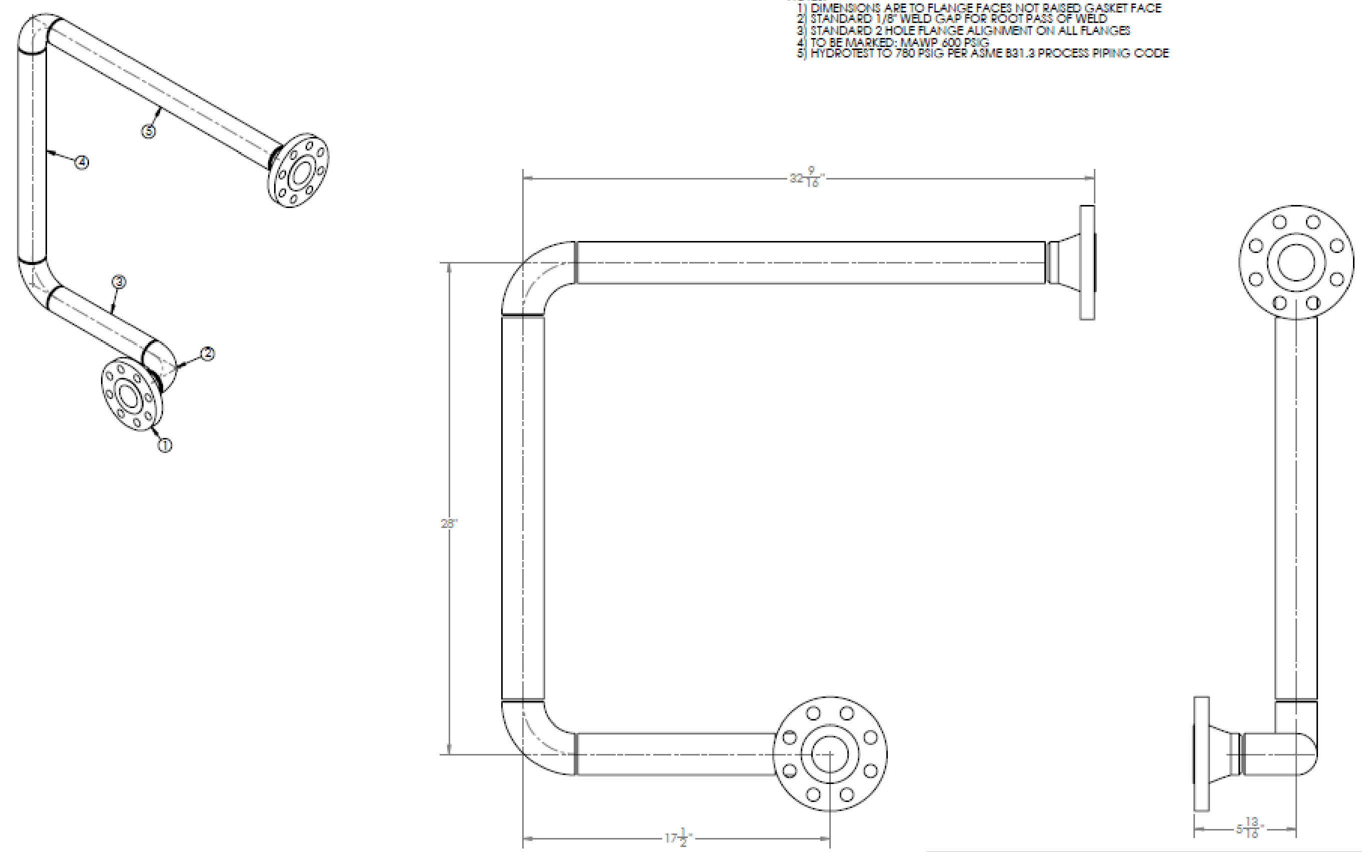

ITEM NO.	PART NUMBER	STANDARD	MATERIAL	QTY.	Length
1	WNeck Flange 300-NPS2	ASTM A182 F304	UNS S30400	2	
2	90L LR Inch 2 Sch40	ASTM A403 WP304	UNS S30400	3	
3	2 in, Schedule 40, 1	ASTM A312 TP304	UNS S30400	1	11 1/4"
4	2 in, Schedule 40, 2	ASTM A312 TP304	UNS S30400	1	21 3/4"
5	2 in, Schedule 40	ASTM A312 TP304	UNS S30400	1	26 5/8"

NOTES:
1) DIMENSIONS ARE TO FLANGE FACES NOT RAISED GASKET FACE
2) STANDARD 1/8" WELD GAP FOR ROOT PASS OF WELD
3) STANDARD 2 HOLE FLANGE ALIGNMENT ON ALL FLANGES
4) TO BE MARKED: MAWP 600 PSIG
5) HYDROTEST TO 780 PSIG PER ASME B31.3 PROCESS PIPING CODE

N/A

TEXAS A&M TURBOMACHINERY LAB

MVP VISUALIZATION

INLET AIR 2" 89

A2

304 SS

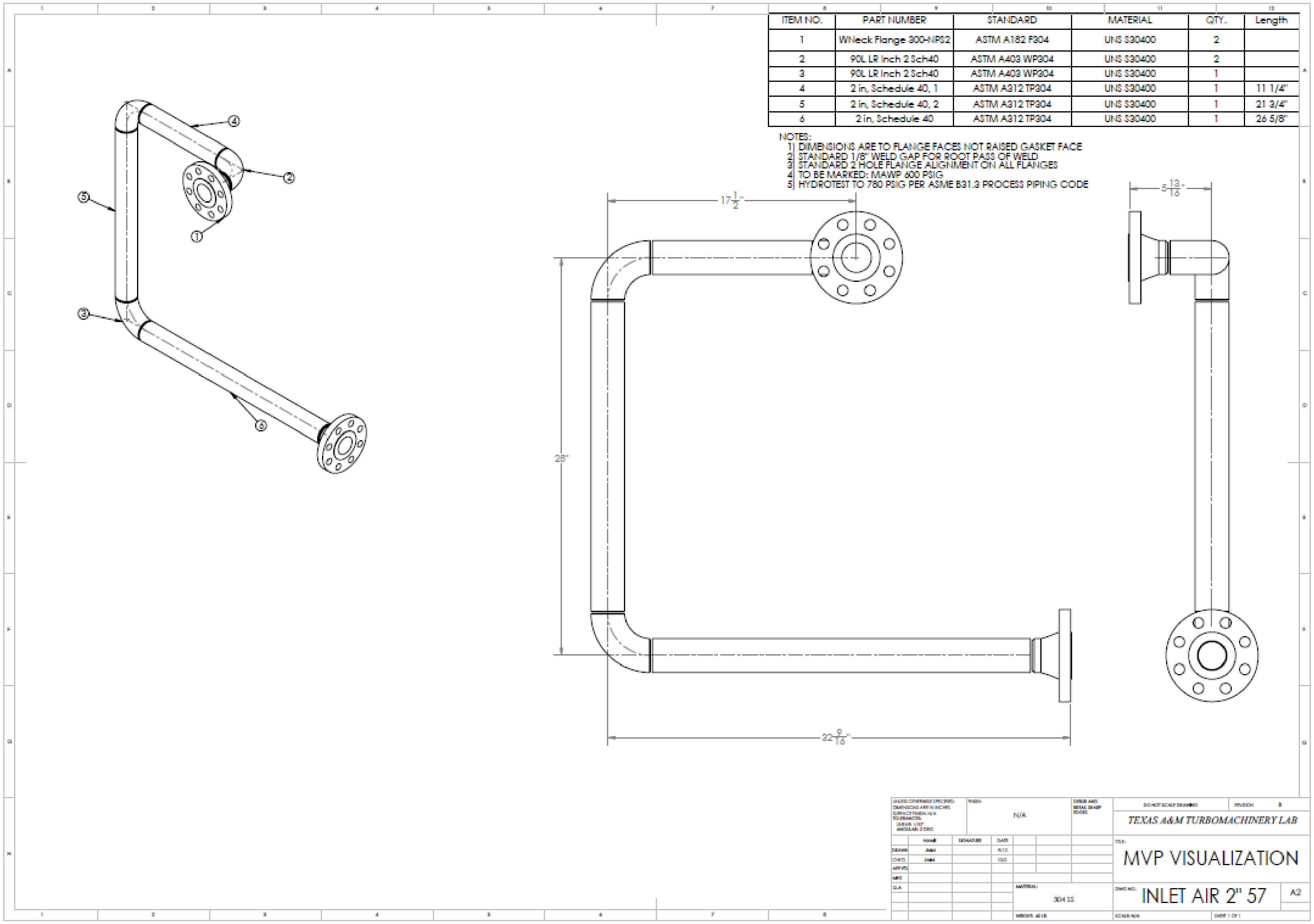

ITEM NO.	PART NUMBER	STANDARD	MATERIAL	QTY.	Length
1	WNeck Flange 300-NPS2	ASTM A182 F304	UNS S30400	2	
2	90L LR Inch 2 Sch40	ASTM A403 WP304	UNS S30400	2	
3	90L LR Inch 2 Sch40	ASTM A403 WP304	UNS S30400	1	
4	2 in, Schedule 40, 1	ASTM A312 TP304	UNS S30400	1	11 1/4"
5	2 in, Schedule 40, 2	ASTM A312 TP304	UNS S30400	1	21 3/4"
6	2 in, Schedule 40	ASTM A312 TP304	UNS S30400	1	26 5/8"

NOTES:
1) DIMENSIONS ARE TO FLANGE FACES NOT RAISED GASKET FACE
2) STANDARD 1/8" WELD GAP FOR ROOT PASS OF WELD
3) STANDARD 2 HOLE FLANGE ALIGNMENT ON ALL FLANGES
4) TO BE MARKED: MAWP 600 PSIG
5) HYDROTEST TO 780 PSIG PER ASME B31.3 PROCESS PIPING CODE

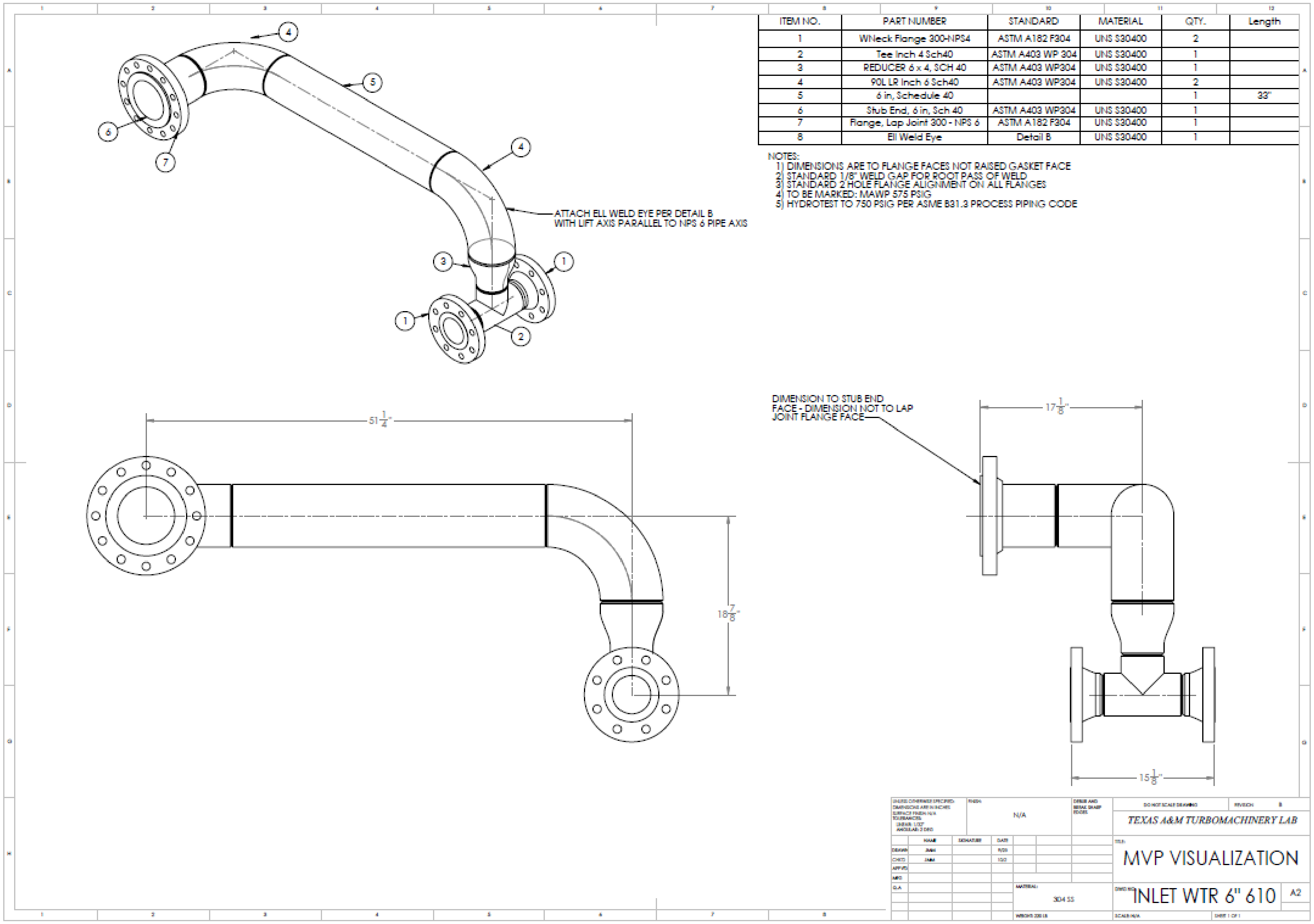

ITEM NO.	PART NUMBER	STANDARD	MATERIAL	QTY.	Length
1	WNeck Flange 300-NPS4	ASTM A182 F304	UNS S30400	2	
2	Tee Inch 4 Sch40	ASTM A403 WP 304	UNS S30400	1	
3	REDUCER 6 x 4, SCH 40	ASTM A403 WP304	UNS S30400	1	
4	90L LR Inch 6 Sch40	ASTM A403 WP304	UNS S30400	2	
5	6 in, Schedule 40			1	33"
6	Stub End, 6 in, Sch 40	ASTM A403 WP304	UNS S30400	1	
7	Flange, Lap Joint 300 - NPS 6	ASTM A182 F304	UNS S30400	1	
8	Ell Weld Eye	Detail B	UNS S30400	1	

NOTES:
1) DIMENSIONS ARE TO FLANGE FACES NOT RAISED GASKET FACE
2) STANDARD 1/8" WELD GAP FOR ROOT PASS OF WELD
3) STANDARD 2 HOLE FLANGE ALIGNMENT ON ALL FLANGES
4) TO BE MARKED: MAWP 575 PSIG
5) HYDROTEST TO 750 PSIG PER ASME B31.3 PROCESS PIPING CODE

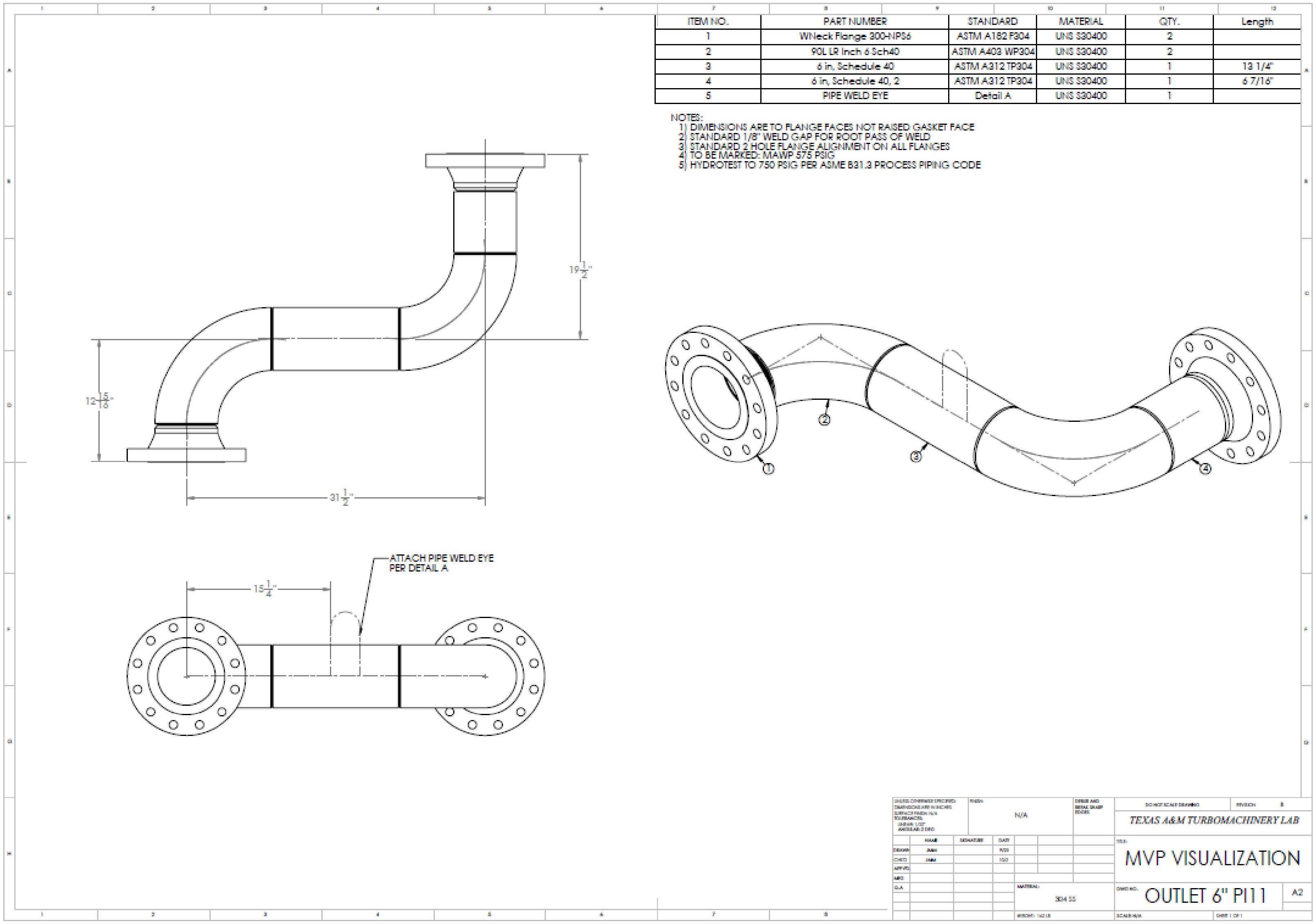

ITEM NO.	PART NUMBER	STANDARD	MATERIAL	QTY.	Length
1	WNeck Flange 300-NPS6	ASTM A182 F304	UNS S30400	2	
2	90L LR Inch 6 Sch40	ASTM A403 WP304	UNS S30400	2	
3	6 in, Schedule 40	ASTM A312 TP304	UNS S30400	1	13 1/4"
4	6 in, Schedule 40, 2	ASTM A312 TP304	UNS S30400	1	6 7/16"
5	PIPE WELD EYE	Detail A	UNS S30400	1	

ITEM NO.	PART NUMBER	STANDARD	MATERIAL	QTY.
1	WNeck Flange 600-NPS6	ASTM A182 F304	UNS S30400	2
2	Tee Inch 6 Sch40	ASTM A403 WP304	UNS S30400	1
3	Stub End, Sch. 40	ASTM A403 WP304	UNS S30400	1
4	Flange, Lap Joint 300-NPS 6	ASTM A182 F304	UNS S30400	1

NOTES:
1) DIMENSIONS ARE TO FLANGE FACES NOT RAISED GASKET FACE
2) STANDARD 1/8" WELD GAP FOR ROOT PASS OF WELD
3) STANDARD 2 HOLE FLANGE ALIGNMENT ON ALL FLANGES
4) TO BE MARKED: MAWP 600 PSIG
5) HYDROTEST TO 780 PSIG PER ASME B31.3 PROCESS PIPING CODE

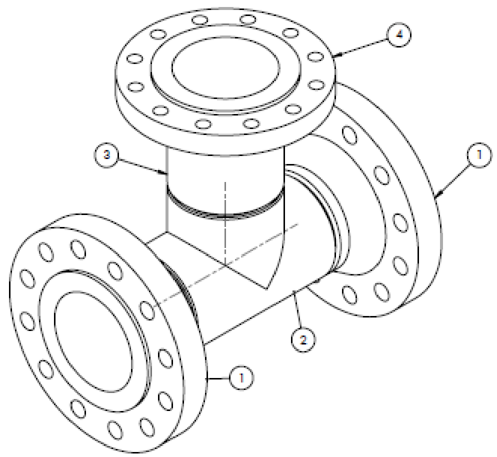

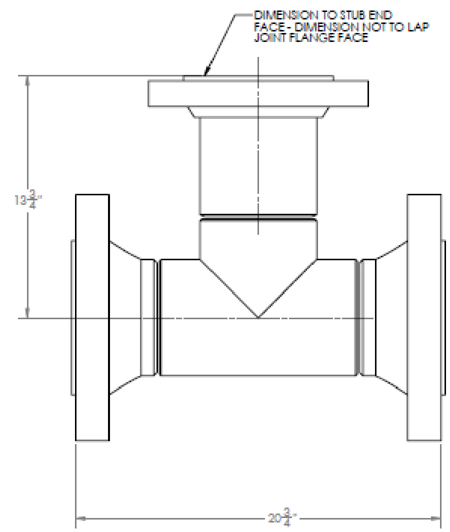

N/A

TEXAS A&M TURBOMACHINERY LAB

MVP VISUALIZATION

INLET WTR TEE

A2

304 SS

ITEM NO.	PART NUMBER	STANDARD	MATERIAL	QTY.	Length
1	RTee Inch4x4x2Sch40	ASTM A403 WP304	UNS S30400	1	
2	WNeck Flange 300-NPS2	ASTM A182 F304	UNS S30400	1	
3	WNeck Flange 300-NPS4	ASTM A182 F304	UNS S30400	1	
4	90L LR Inch 4 Sch40	ASTM A403 WP304	UNS S30400	1	
5	90L LR Inch 4 Sch40	ASTM A403 WP304	UNS S30400	1	
6	4 in, Schedule 40, 3	ASTM A312 TP304	UNS S30400	1	15 3/4"
7	4 in, Schedule 40, 1	ASTM A312 TP304	UNS S30400	1	20 3/4"
8	4 in, Schedule 40, 2			1	7 1/8"
9	Stub End, Sch. 40	ASTM A403 WP304	UNS S30400	1	
10	Flange, Lap Joint 300-NPS 4	ASTM A182 F304	UNS S30400	1	
11	Pipe Weld Eye	Detail A	UNS S30400	2	

NOTES:
1) DIMENSIONS ARE TO FLANGE FACES NOT RAISED GASKET FACE
2) STANDARD 1/8" WELD GAP FOR ROOT PASS OF WELD
3) STANDARD 2 HOLE FLANGE ALIGNMENT ON ALL FLANGES
4) TO BE MARKED: MAWP 600 PSIG
5) HYDROTEST TO 780 PSIG PER ASME B31.3 PROCESS PIPING CODE

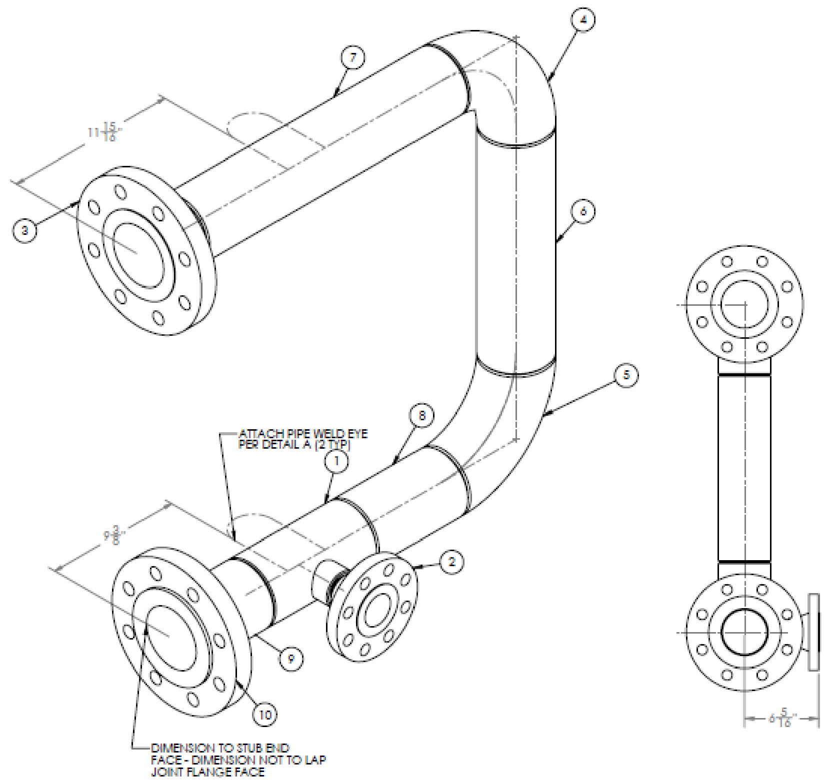

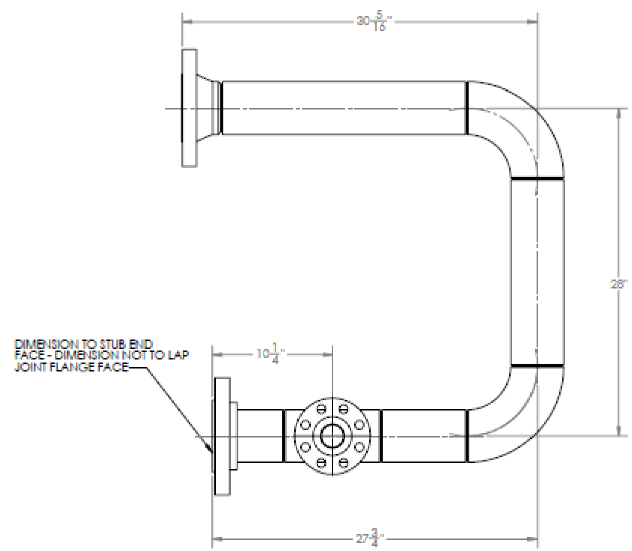

FINISH: N/A

DO NOT SCALE DRAWING | REVISION B

TEXAS A&M TURBOMACHINERY LAB

TITLE: MVP VISUALIZATION

INLET WTR 4" PI810 A2

MATERIAL: 304 SS

ITEM NO.	PART NUMBER	STANDARD	MATERIAL	QTY.	Length
1	WNeck Flange 300-NPS6	ASTM A182 F304	UNS S30400	2	
2	6 in, Schedule 40	ASTM A312 TP304	UNS S30400	1	65 1/2"

NOTES:
1) DIMENSIONS ARE TO FLANGE FACES NOT RAISED GASKET FACE
2) STANDARD 1/8" WELD GAP FOR ROOT PASS OF WELD
3) STANDARD 2 HOLE FLANGE ALIGNMENT ON ALL FLANGES
4) TO BE MARKED: MAWP 575 PSIG
5) HYDROTEST TO 750 PSIG PER ASME B31.3 PROCESS PIPING CODE

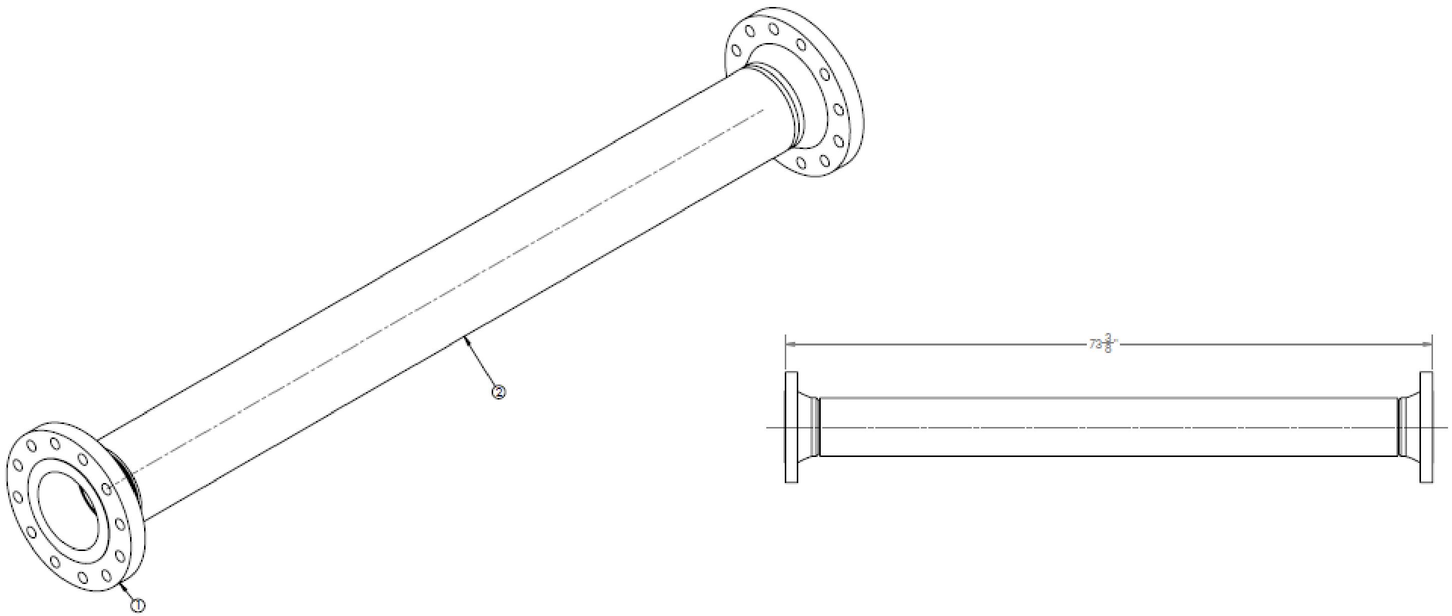

N/A

TEXAS A&M TURBOMACHINERY LAB

MVP VISUALIZATION

INLET WTR 6" 613

A2

304 SS

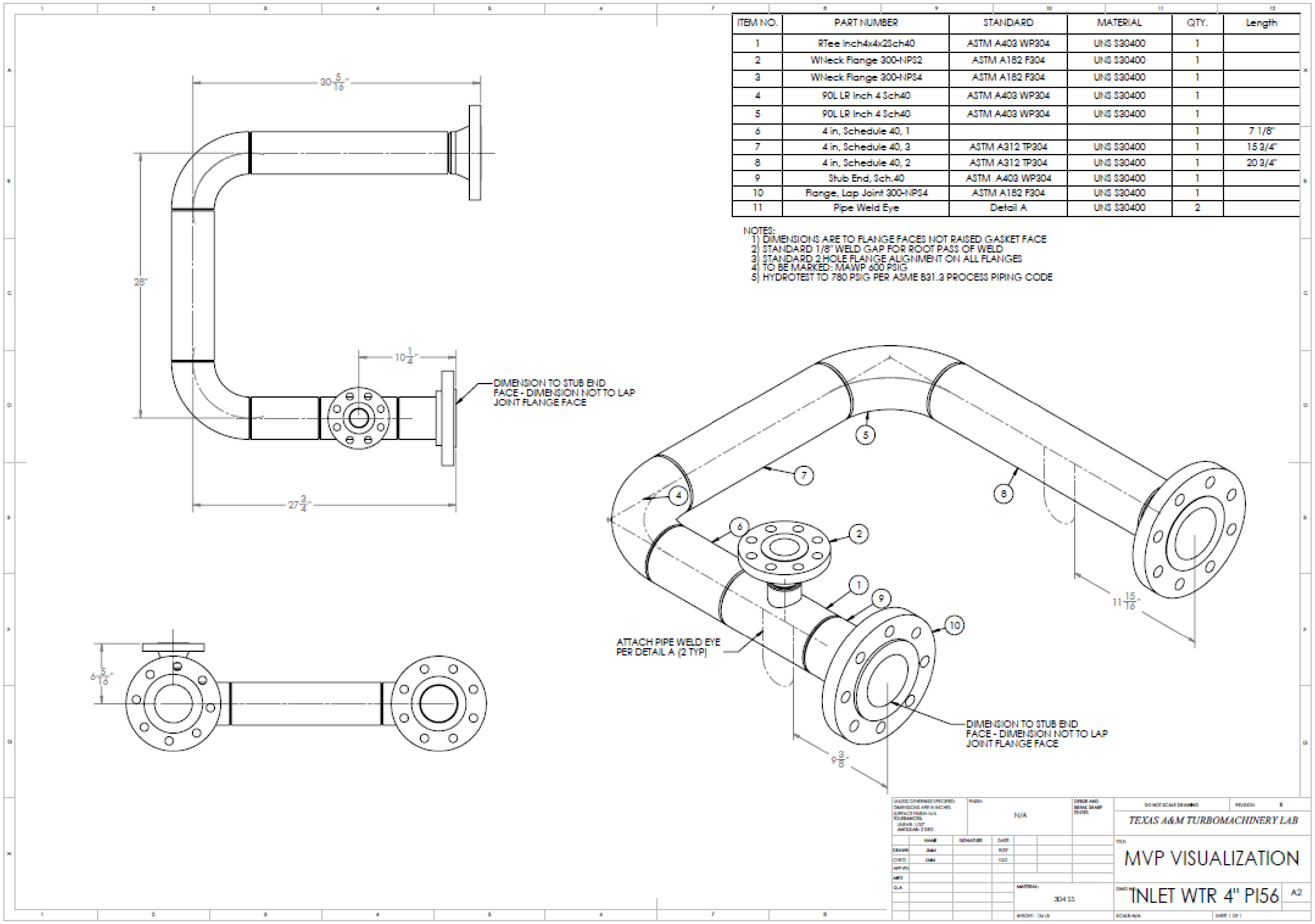

ITEM NO.	PART NUMBER	STANDARD	MATERIAL	QTY.	Length
1	RTee Inch4x4x2Sch40	ASTM A403 WP304	UNS S30400	1	
2	WNeck Flange 300-NPS2	ASTM A182 F304	UNS S30400	1	
3	WNeck Flange 300-NPS4	ASTM A182 F304	UNS S30400	1	
4	90L LR Inch 4 Sch40	ASTM A403 WP304	UNS S30400	1	
5	90L LR Inch 4 Sch40	ASTM A403 WP304	UNS S30400	1	
6	4 in, Schedule 40, 1			1	7 1/8"
7	4 in, Schedule 40, 3	ASTM A312 TP304	UNS S30400	1	15 3/4"
8	4 in, Schedule 40, 2	ASTM A312 TP304	UNS S30400	1	20 3/4"
9	Stub End, Sch.40	ASTM A403 WP304	UNS S30400	1	
10	Flange, Lap Joint 300-NPS4	ASTM A182 F304	UNS S30400	1	
11	Pipe Weld Eye	Detail A	UNS S30400	2	

NOTES:
1) DIMENSIONS ARE TO FLANGE FACES NOT RAISED GASKET FACE
2) STANDARD 1/8" WELD GAP FOR ROOT PASS OF WELD
3) STANDARD 2 HOLE FLANGE ALIGNMENT ON ALL FLANGES
4) TO BE MARKED: MAWP 600 PSIG
5) HYDROTEST TO 780 PSIG PER ASME B31.3 PROCESS PIPING CODE

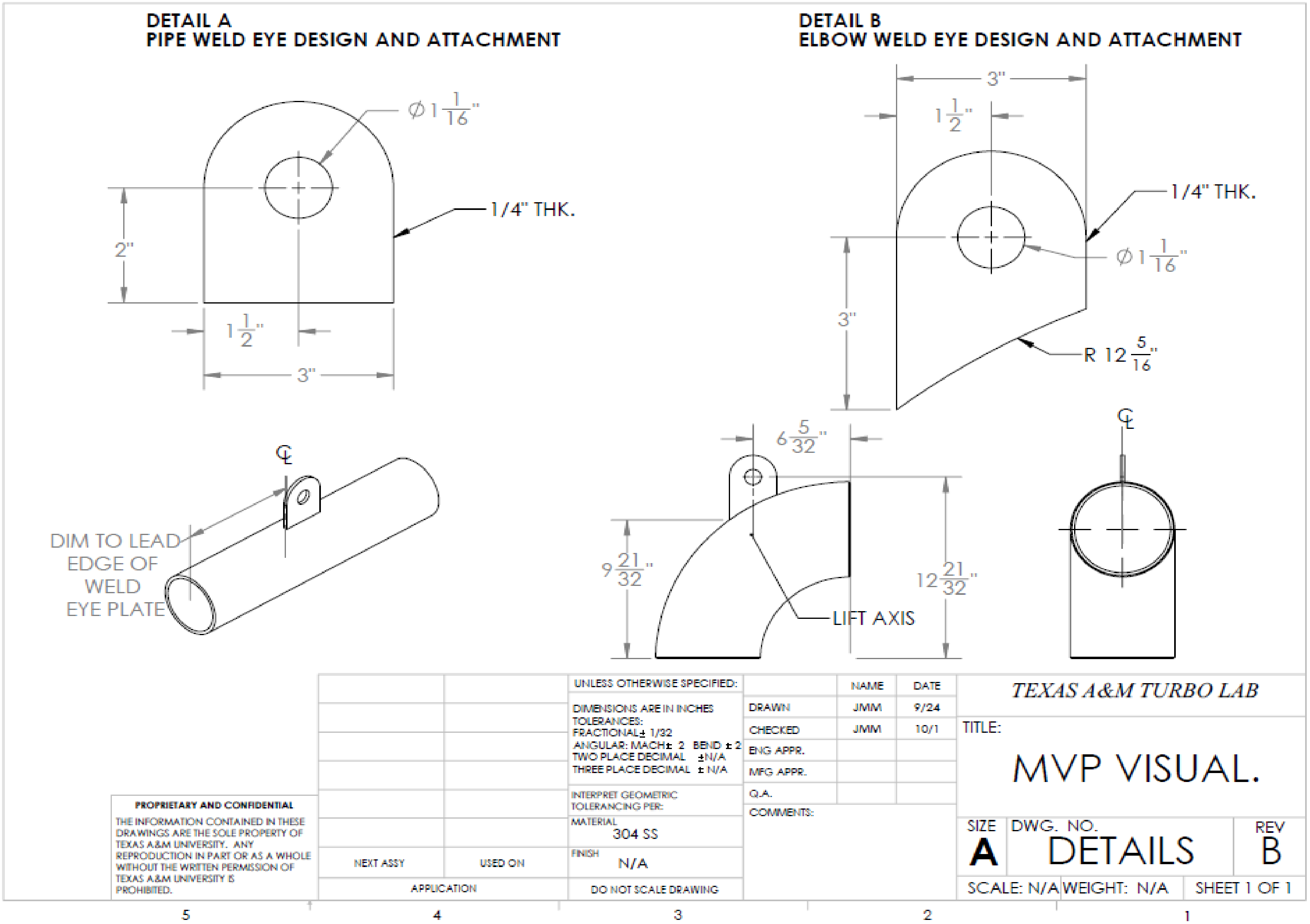
DETAIL A
PIPE WELD EYE DESIGN AND ATTACHMENT
∅ 1 1/16"
1/4" THK.
2"
1 1/2"
3"
DIM TO LEAD EDGE OF WELD EYE PLATE
DETAIL B
ELBOW WELD EYE DESIGN AND ATTACHMENT
3"
1 1/2"
1/4" THK.
∅ 1 1/16"
3"
R 12 5/16"
6 5/32"
9 21/32"
12 21/32"
LIFT AXIS
UNLESS OTHERWISE SPECIFIED:
DIMENSIONS ARE IN INCHES
TOLERANCES:
FRACTIONAL± 1/32
ANGULAR: MACH± 2 BEND ± 2
TWO PLACE DECIMAL ±N/A
THREE PLACE DECIMAL ± N/A
INTERPRET GEOMETRIC TOLERANCING PER:
MATERIAL
304 SS
FINISH
N/A
DO NOT SCALE DRAWING
NEXT ASSY
USED ON
APPLICATION
PROPRIETARY AND CONFIDENTIAL
THE INFORMATION CONTAINED IN THESE DRAWINGS ARE THE SOLE PROPERTY OF TEXAS A&M UNIVERSITY. ANY REPRODUCTION IN PART OR AS A WHOLE WITHOUT THE WRITTEN PERMISSION OF TEXAS A&M UNIVERSITY IS PROHIBITED.
NAME
DATE
DRAWN
JMM
9/24
CHECKED
JMM
10/1
ENG APPR.
MFG APPR.
Q.A.
COMMENTS:
TEXAS A&M TURBO LAB
TITLE:
MVP VISUAL.
SIZE
A
DWG. NO.
DETAILS
REV
B
SCALE: N/A
WEIGHT: N/A
SHEET 1 OF 1
5
4
3
2
1

APPENDIX D

The calibration curve for the FTB-933 air flowmeter is shown in Figure 55.

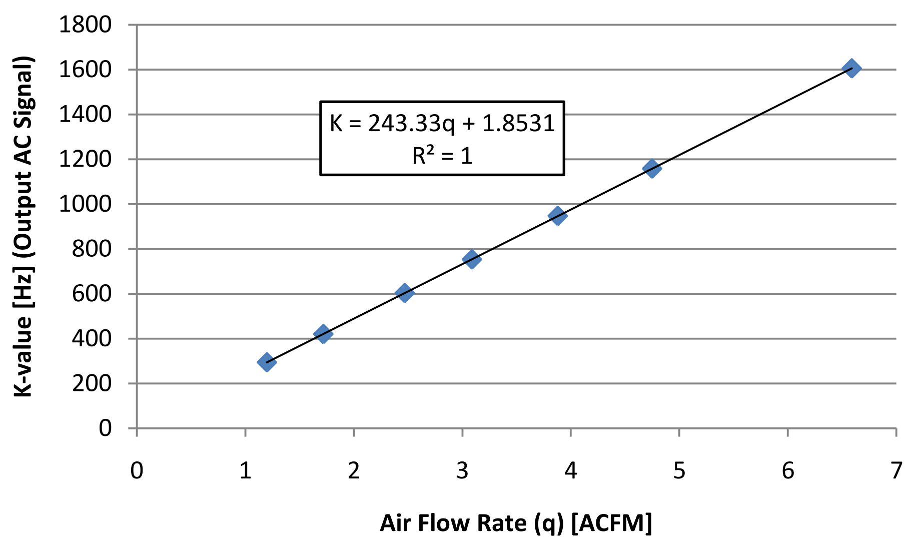

Figure 55 FTB-933 1-10 ACFM air flowmeter calibration curve

The calibration curves for the inlet and outlet pressure transducers are shown in Figure 56. The transducers were connected to power source and return a 4-20 mA signal linearly varying with pressure. To acquire the signal with the cRIO chassis and a voltage input module in conjunction with LabVIEW, the powered loop was run through a resistor. The voltage drop across the resistor was acquired by the module and cRIO chassis and this calibration curve was used to accurately obtain pressure measurements.

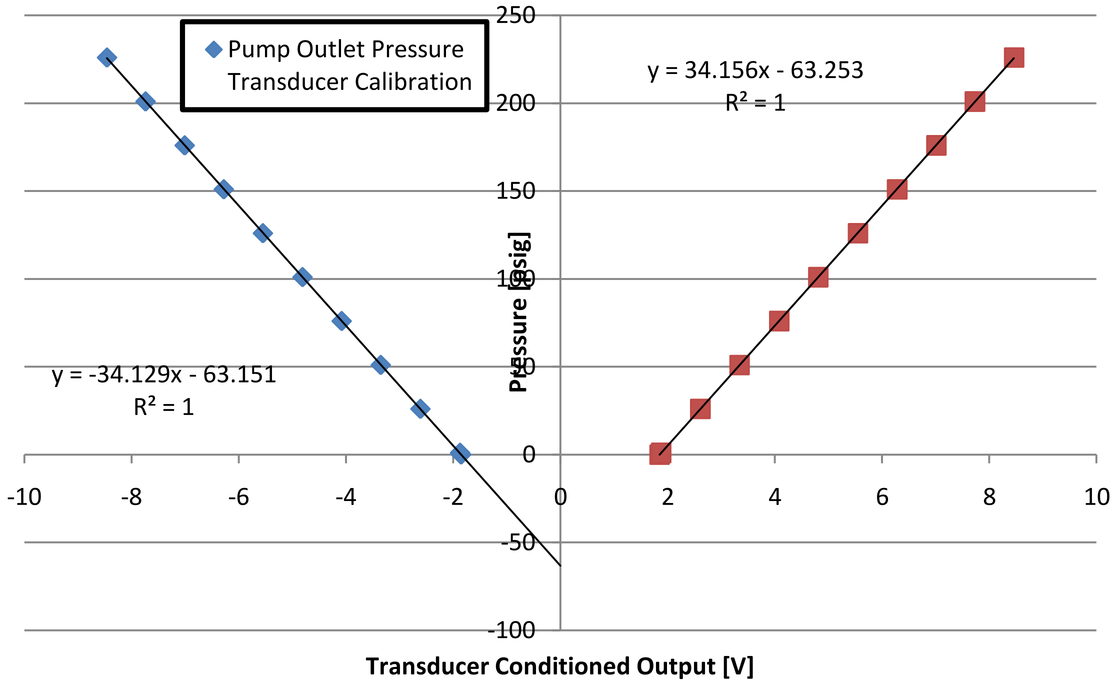

Figure 56 Inlet and outlet pressure transducer calibration curves

APPENDIX E

Embedded here are videos taken from the MVP Visualization rig during testing at 2% GVF, 1800 rpm, and 66-70 psig inlet pressures. The videos are ordered by flow rate and region of the diffuser. The flow visualization for the inlet and outlet of the diffuser at 10,000 bpd of liquid flow will be shown first followed by paired videos of the inlet and outlet of the diffuser at incrementally larger flow rates to 17,000 bpd flow rates.

The clips of the inlet and outlet of the diffuser are shown in Figure 57 and Figure 58 for liquid flow rates of 10,000 bpd.

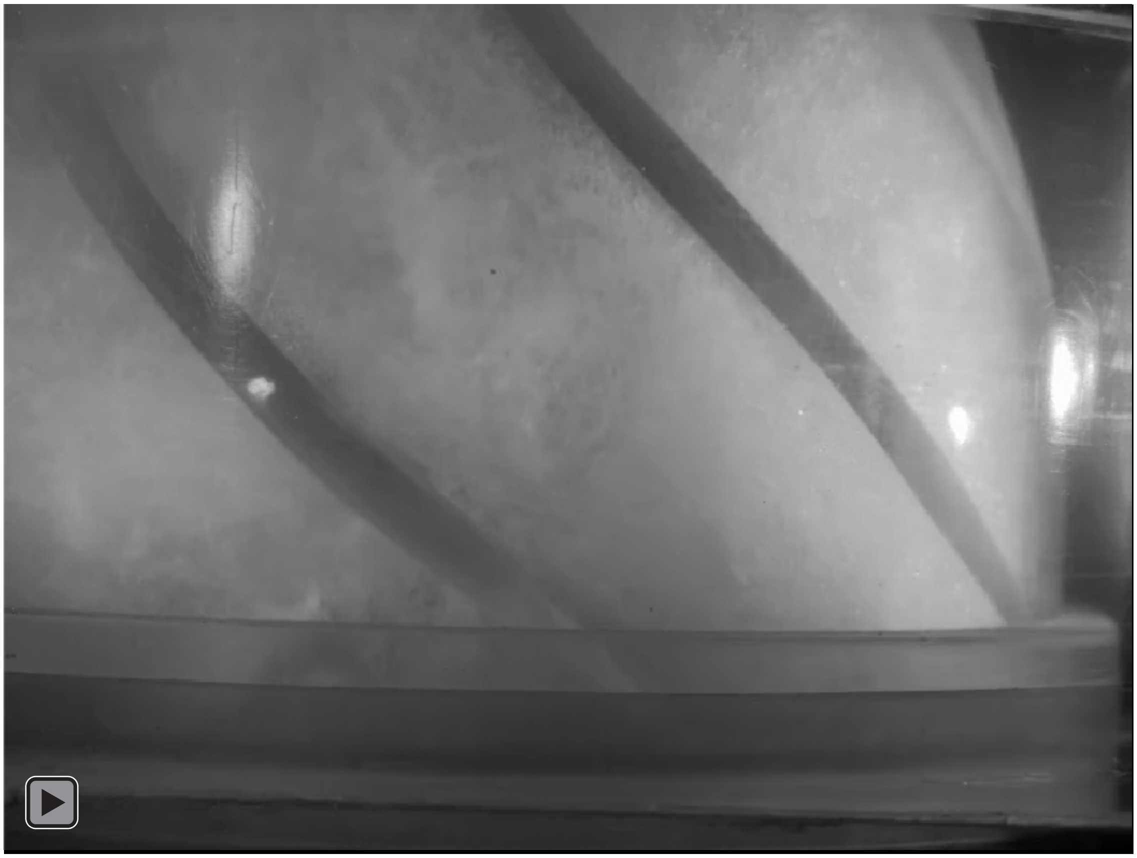

Figure 57 10,800 fps clip of diffuser inlet at 10,000 bpd flow rate and 2% GVF

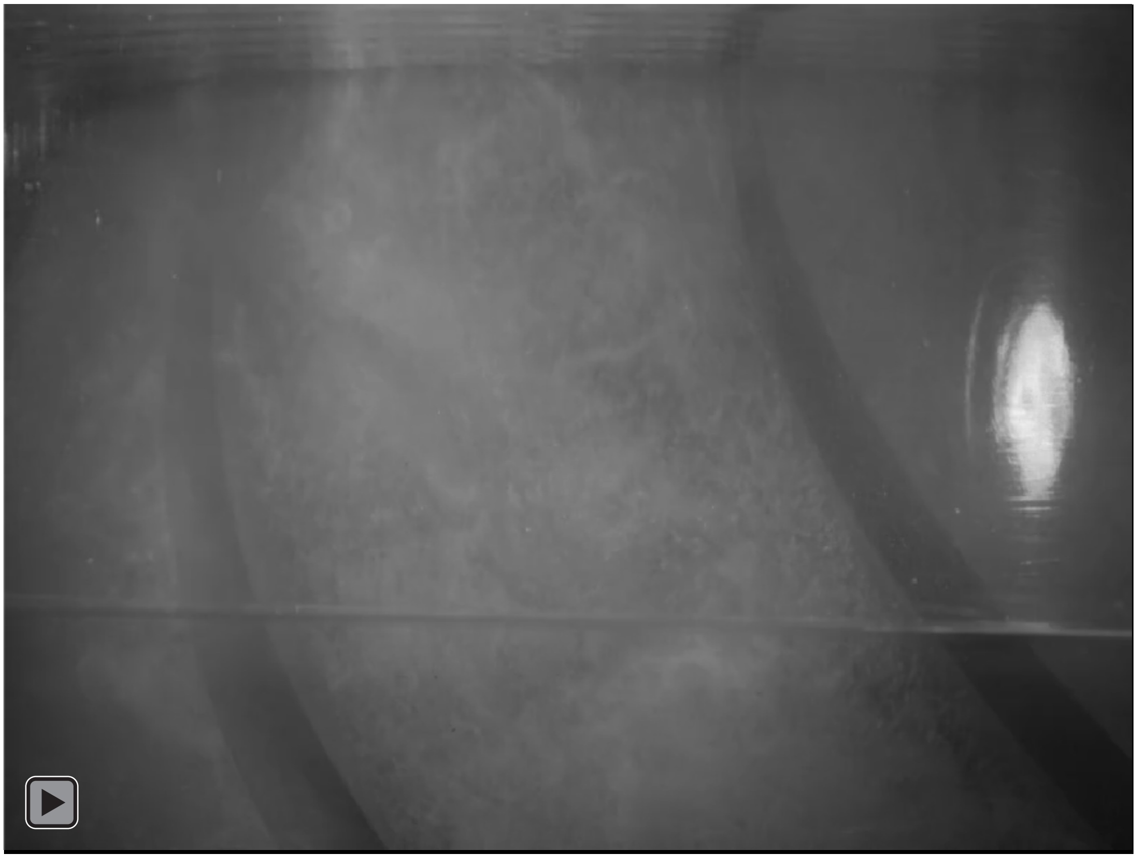

Figure 58 10,800 fps clip of diffuser outlet at 10,000 bpd flow rate and 2% GVF

The clips of the inlet and outlet of the diffuser are shown in Figure 59 and Figure 60 for liquid flow rates of 12,000 bpd.

Figure 59 10,800 fps clip of diffuser inlet at 12,000 bpd flow rate and 2% GVF

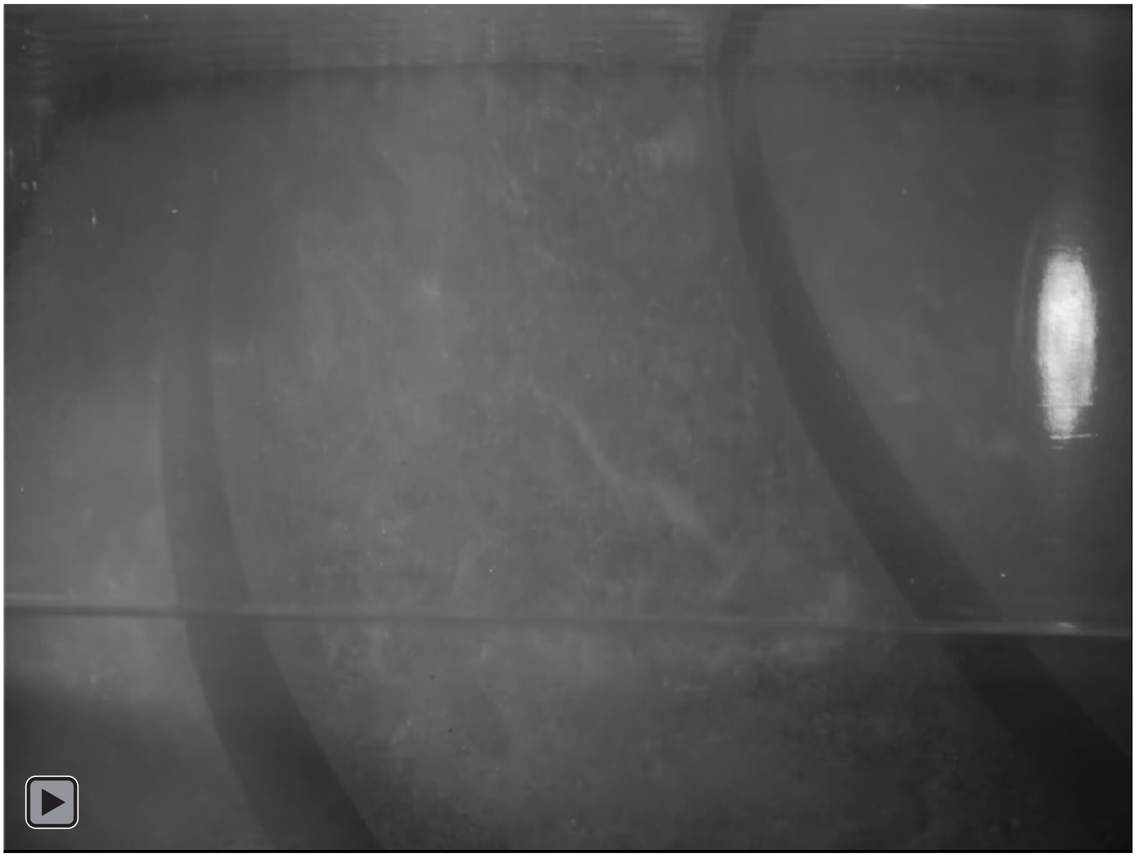

Figure 60 10,800 fps clip of diffuser outlet at 12,000 bpd flow rate and 2% GVF

The clips of the inlet and outlet of the diffuser are shown in Figure 61 and Figure 62 for liquid flow rates of 14,000 bpd.

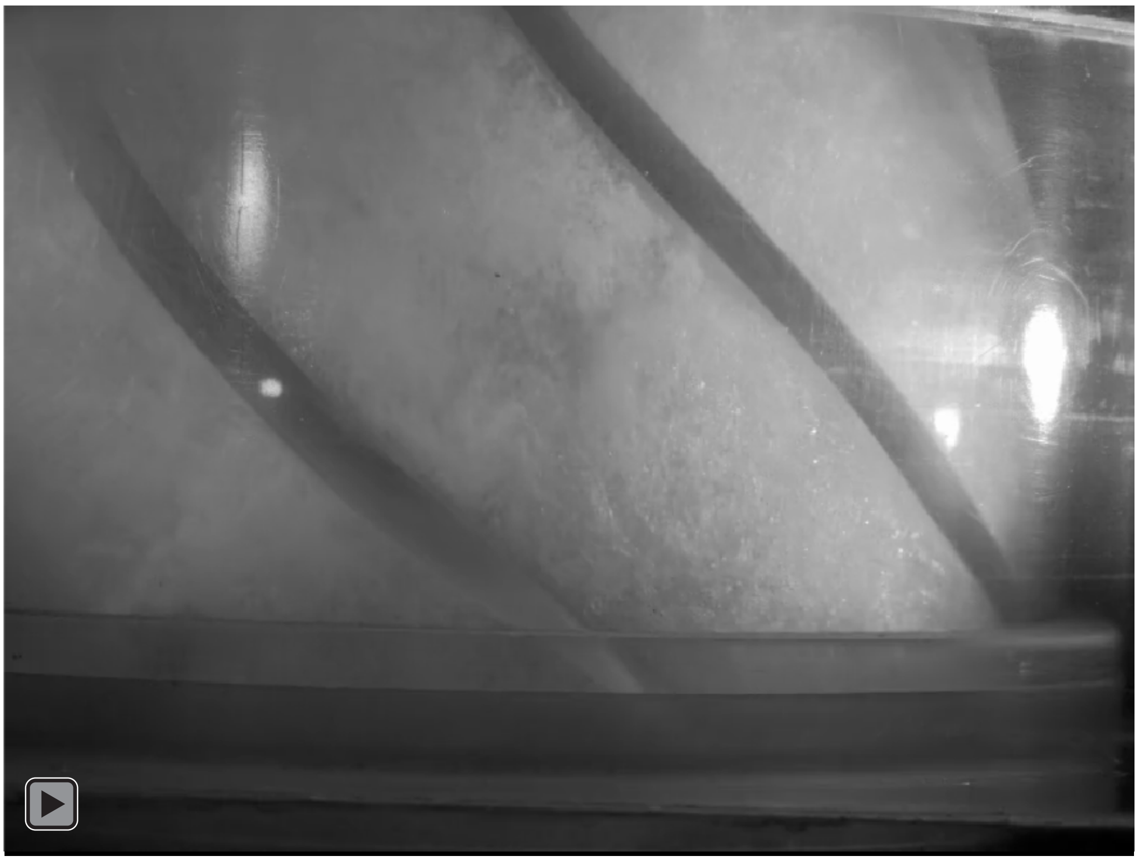

Figure 61 10,800 fps clip of diffuser inlet at 14,000 bpd flow rate and 2% GVF

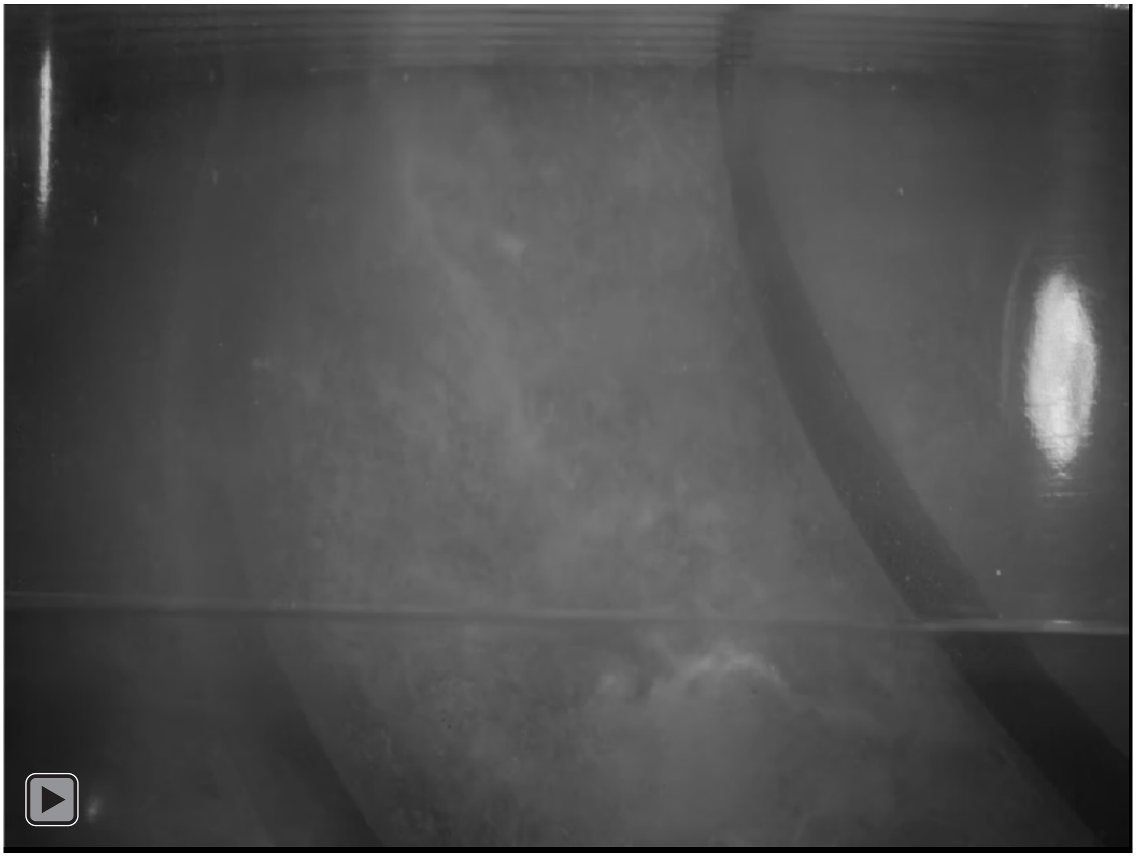

Figure 62 10,800 fps clip of diffuser outlet at 14,000 bpd flow rate and 2% GVF

The clips of the inlet and outlet of the diffuser are shown in Figure 63 and Figure 64 for liquid flow rates of 16,000 bpd.

Figure 63 10,800 fps clip of diffuser inlet at 16,000 bpd flow rate and 2% GVF

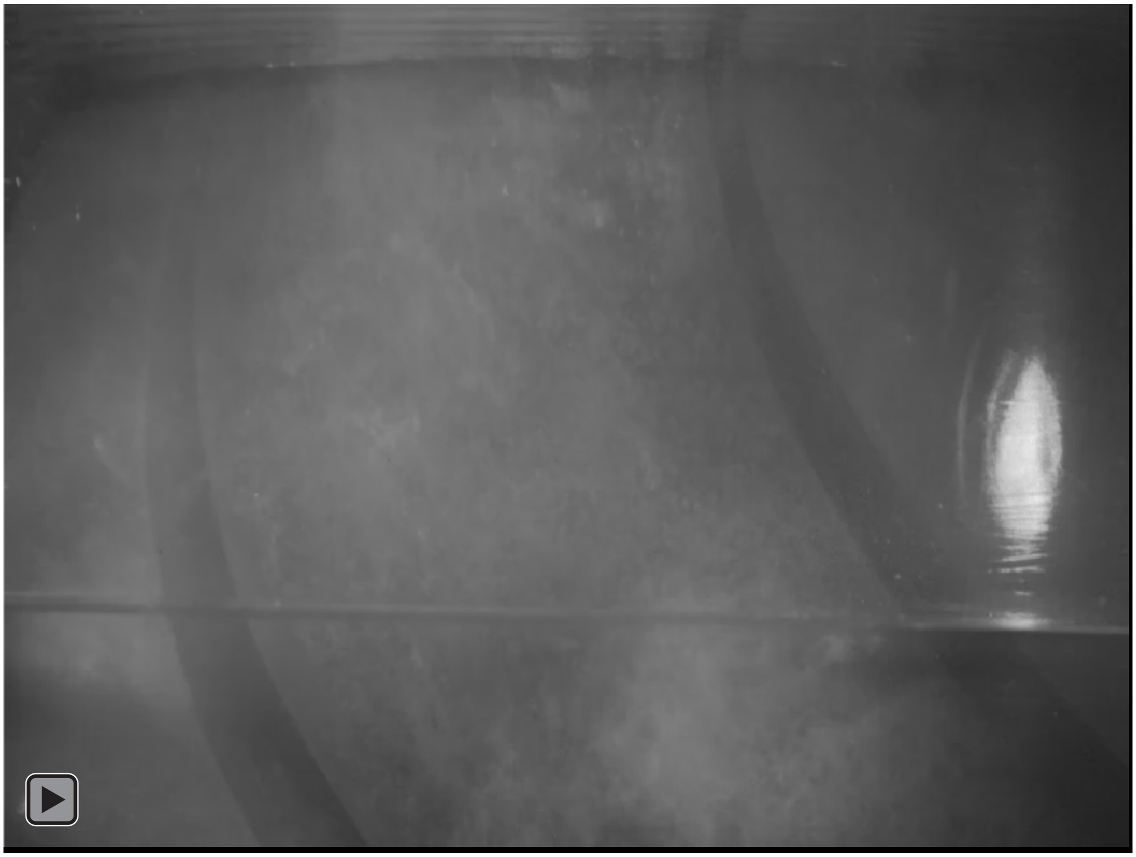

Figure 64 10,800 fps clip of diffuser outlet at 16,000 bpd flow rate and 2% GVF

The clips of the inlet and outlet of the diffuser are shown in Figure 65 and Figure 66 for liquid flow rates of 17,000 bpd.

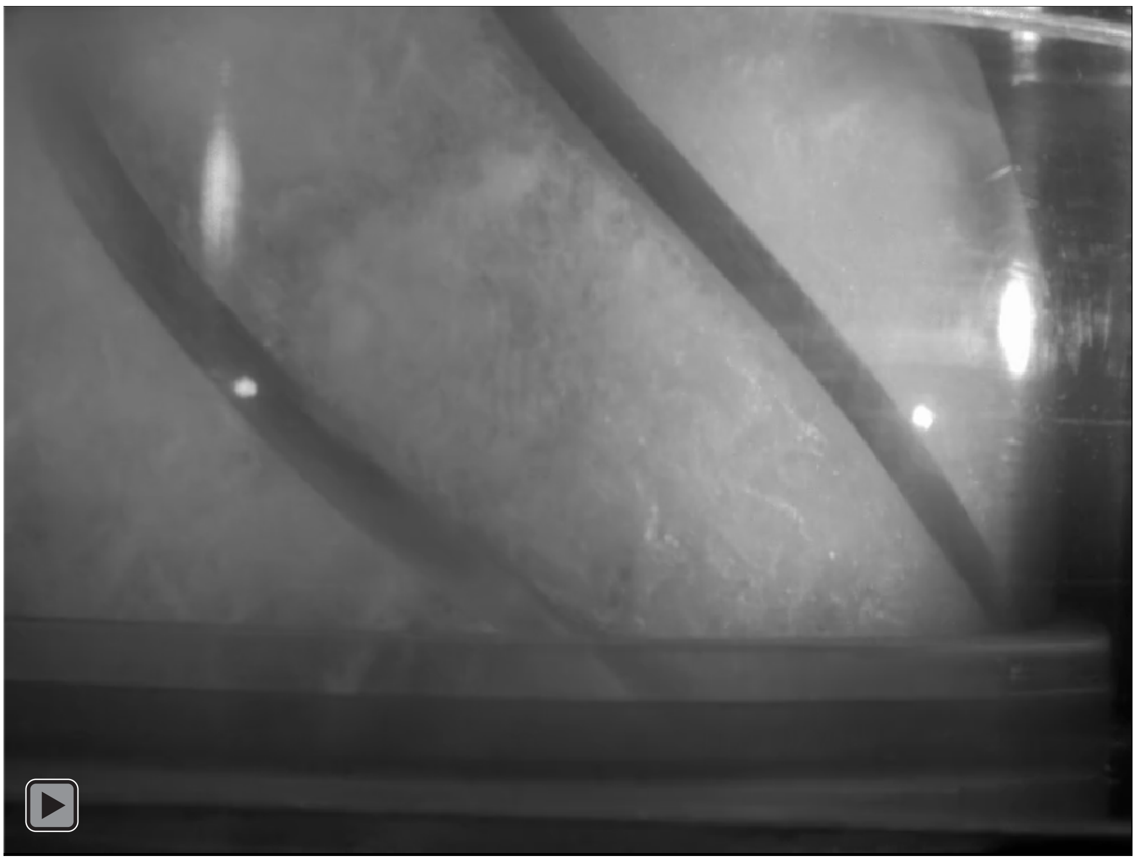

Figure 65 10,800 fps clip of diffuser inlet at 17,000 bpd flow rate and 2% GVF

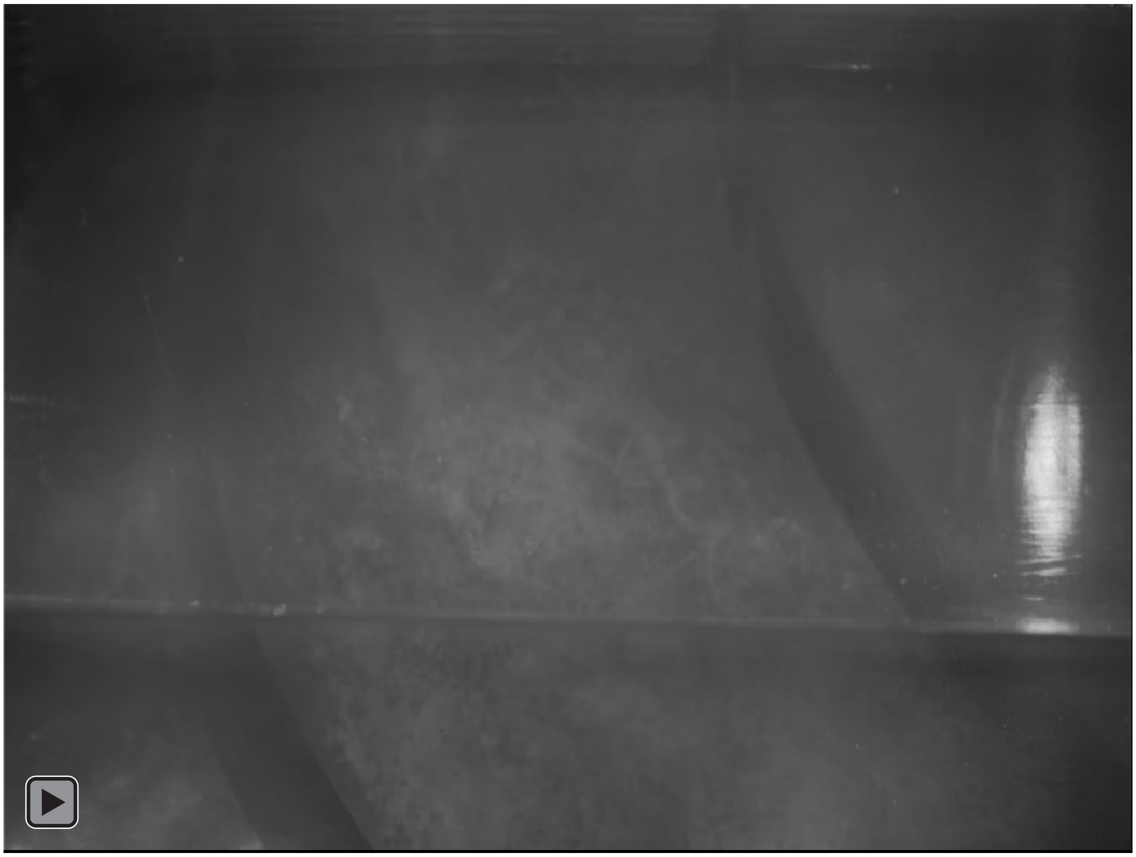

Figure 66 10,800 fps clip of diffuser outlet at 17,000 bpd flow rate and 2% GVF